Journal Information

Maejo International Journal of Science and Technology (ISSN 1905-7873 © 2013), the international journal for preliminary communications in Science and Technology is the first peer-refereed scientific journal of Maejo University (www.mju.ac.th). Intended as a medium for communication, discussion, and rapid dissemination of important issues in Science and Technology, articles are published online in an open access format, which thereby gives authors the chance to communicate with a wide range of readers in an international community.

Publication Information

MIJST is published triannually. Articles are available online and can be accessed free of charge at http://www.mijst.mju.ac.th. Printed and bound copies of each volume are produced and distributed to selected groups or individuals.

Abstracting/Indexing Information

MIJST is covered and cited by Science Citation Index Expanded, SCOPUS, Journal Citation Reports/Science Edition, Zoological Record, Directory of Open Access Journals (DOAJ), CAB Abstracts, ProQuest, Google Scholar and EBSCO.

Contact Information

Editorial office: Maejo International Journal of Science and Technology (MIJST), 1st floor, Orchid Building, Maejo University, San Sai, Chiang Mai 50290, Thailand

Tel: +66-53-87-3880
E-mail: duang@mju.ac.th

MAEJO INTERNATIONAL JOURNAL OF SCIENCE AND TECHNOLOGY

MAEJO INTERNATIONAL JOURNAL OF SCIENCE AND TECHNOLOGY

The International Journal for the Publication of Preliminary Communications in Science and Technology

http://www.mijst.mju.ac.th
ISSN 1905-7873

MAEJO INTERNATIONAL JOURNAL OF SCIENCE AND TECHNOLOGY

Volume 7, Issue 1 (January - April 2013)

CONTENTS

http://www.mijst.mju.ac.th
ISSN 1905-7873

http://www.mijst.mju.ac.th

MAEJO INTERNATIONAL JOURNAL
OF SCIENCE AND TECHNOLOGY

Volume 7, Issue 1 (January-April 2013)

Author Index

Instructions for Authors

A proper introductory e-mail page containing the title of the submitted article and certifying its originality should be sent to the editor (Duang Buddhasukh, e-mail: duang@mju.ac.th). The manuscript proper together with a list of suggested referees should be attached in separate files. The list should contain at least 5 referees with appropriate expertise. Three referees should be non-native from 3 different countries. Each referee's academic/professional position, scientific expertise, affiliation and e-mail address must be given. The referees should not be affiliated to the same university/institution as any of the authors, nor should any two referees come from the same university/institution. The editorial team, however, retain the sole right to decide whether or not the suggested referees are approached.

Failure to conform to the above instructions will result in non-consideration of the submission.

Please also ensure that English and style is properly edited before submission. UK style of spelling should be used. Authors who would like to consult a professional service can visit www.proof-reading-service.com, www.editage.com, www.bioedit.co.uk (bioscience and medical papers), www.bioscienceeditingsolutions.com, www.scribendi.com, www.letpub.com, www.papersconsulting.com, www.sticklerediting.com, Cambridge Proofreading (http://proofreading.org/) or www.proofreadingservices.com.

Important : Manuscript with substandard English and style will not be considered.

Warning : Plagiarism (including self-plagiarism) may be checked for at the last stage of processing and, if detected, will result in a rejection and blacklisting.

Manuscript Preparation

Manuscripts must be prepared in English using a word processor. MS Word for Macintosh or Windows, and .doc or .rtf files are preferred. Manuscripts may be prepared with other software provided that the full document (with figures, schemes and tables inserted into the text) is exported to a MS Word format for submission. Times or Times New Roman font is preferred. The font size should be 12 pt and the line spacing 'at least 17 pt'. A4 paper size is used and margins must be 1.5 cm on top, 2.0 cm at the bottom and 2.0 cm on both left and right sides of the paper. Although our final output is in .pdf format, authors are asked NOT to send manuscripts in this format as editing them is much more complicated. Under the above settings, a manuscript submitted should not be longer than **15 pages** for a full paper or **20 pages for** a review paper.

A template file may be downloaded from the Maejo *Int. J. Sci.* Technol. homepage. (DOWNLOAD HERE)

Authors' full mailing addresses, homepage addresses, phone and fax numbers, and e-mail addresses homepages can be included in the title page and these will be published in the manuscripts and the Table of Contents. The corresponding author should be clearly identified. It is the corresponding author's responsibility to ensure that all co-authors are aware of and approve of the contents of a submitted manuscript.

A brief (200 word maximum) Abstract should be provided. The use in the Abstract of numbers to identify compounds should be avoided unless these compounds are also identified by names.

A list of three to five keywords must be given and placed after the Abstract. Keywords may be single words or very short phrases.

Although variations in accord with contents of a manuscript are permissible, in general all papers should have the following sections: Introduction, Materials and Methods, Results and Discussion, Conclusions, Acknowledgments (if applicable) and References.

Authors are encouraged to prepare Figures and Schemes in colour. Full colour graphics will be published free of charge.

Tables and Figures should be inserted into the main text, and numbers and titles supplied for all Tables and Figures. All table columns should have an explanatory heading. To facilitate layout of large tables, smaller fonts may be used, but in no case should these be less than 10 pt in size. Authors should use the Table option of MS Word to create tables, rather than tabs, as tab-delimited columns are often difficult to format in .pdf for final output.

Figures, tables and schemes should also be placed in numerical order in the appropriate place within the main text. Numbers, titles and legends should be provided for all tables, schemes and figures. Chemical structures and reaction schemes should be drawn using an appropriate software package designed for this purpose. As a guideline, these should be drawn to a scale such that all the details and text are clearly legible when placed in the manuscript (i.e. text should be no smaller than 8-9 pt).

For bibliographic citations, the reference numbers should be placed in square brackets, i.e. [ ], and placed before the punctuation, for example [4] or [1-3], and all the references should be listed separately and as the last section at the end of the manuscript.

Format for References

Journal :

1. D. Buddhasukh, J. R. Cannon, B. W. Metcalf and A. J. Power, "Synthesis of 5-n-alkylresorcinol dimethyl ethers and related compounds via substituted thiophens", *Aust. J. Chem*., **1971**, 24, 2655-2664.

Text :

2. A. I. Vogel, "A Textbook of Practical Organic Chemistry", 3rd Edn., Longmans, London, **1956**, pp. 130-132.

Chapter in an edited text :

3. W. Leistritz, "Methods of bacterial reduction in spices", in "Spices: Flavor Chemistry and Antioxidant Porperties" (Ed. S. J. Risch and C-T. Ito), American Chemical Society, Washington, DC, **1997**, Ch. 2.

Thesis / Dissertation :

4. W. phutdhawong, "Isolation of glycosides by electrolytic decolourisation and synthesis of pentinomycin", PhD Thesis, **2002**, Chiang Mai University, Thailand.

Patent :

5. K. Miwa, S. Maeda and Y. Murata, "Purification of stevioside by electrolysis", *Jpn. Kokai Tokkyo Koho 79 89,066* (**1979**).

Proceedings :

6. P. M. Sears, J. Peele, M. Lassauzet and P. Blackburn, "Use of antimicrobial proteins in the treatment of bovine mastitis", Proceedings of the 3rd International Mastitis Seminars, **1995**, Tel-Aviv, Israel, pp. 17-18.

Websites :

7. S. Simon, "What is an odds ratio?", **2008**, http://www.childrensmercy.org/stats/definitions/or.htm (Accessed: October 2011).

Manuscript Revision Time

Authors who are instructed to revise their manuscript should do so within **45** days. Otherwise the revised manuscript will be regarded as a new submission.

Manuscript Processing Time

As a result of a large number of submissions, there may be a long delay in the evaluation or publication of a paper. A duration of at least 6-8 mouths between submission and acceptance (or rejection) can normally be expected.

Maejo International
Journal of Science and Technology

ISSN 1905-7873
Available online at www.mijst.mju.ac.th

Editor's Note

Questions have been raised every now and again about the refereeing system of our journal. Many authors have complained that their papers are still rejected or delayed even though all the referees have given the green light to them. We would therefore like to point out that although the comments of the external referees suggested by the authors themselves are taken into serious consideration, we do not entirely rely on them. Thus, when in doubt, a second opinion from other reviewers is often sought by us to make sure that all the articles appeared online are acceptable with respect to standard quality of the content.

Then again the content of a submitted paper may be excellent, whereas the language and writing style used still leaves much to be desired, and although we used to provide a free overhaul of it earlier, the ever increasing submissions have prevented us from doing so. Refereeing is thus only one of the screening processes used by our journal, and the editorial team reserves the right to the final decision regarding acceptance of a paper for publication.

11 January 2013

Duang Buddhasukh
Editor-in-Chief

Maejo Int. J. Sci. Technol. **2013**, *7*(01), 1-15

Maejo International
Journal of Science and Technology

ISSN 1905-7873
Available online at www.mijst.mju.ac.th

Review

Current STR-based techniques in forensic science

Phuvadol Thanakiatkrai* **and Thitika Kitpipit**

Department of Applied Science, Faculty of Science, Prince of Songkla University, Thailand

* Corresponding author, e-mail: pthanakiatkrai@gmail.com; phuvadol.t@psu.ac.th

Received: 30 April 2012 / Accepted: 28 December 2012 / Published: 2 January 2013

Abstract: DNA analysis in forensic science is mainly based on short tandem repeat (STR) genotyping. The conventional analysis is a three-step process of DNA extraction, amplification and detection. An overview of various techniques that are currently in use and are being actively researched for STR typing is presented. The techniques are separated into STR amplification and detection. New techniques for forensic STR analysis focus on increasing sensitivity, resolution and discrimination power for suboptimal samples. These are achieved by shifting primer-binding sites, using high-fidelity and tolerant polymerases and applying novel methods to STR detection. Examples in which STRs are used in criminal investigations are provided and future research directions are discussed.

Keywords: forensic science, DNA, STRs, STR amplification, STR detection

---

INTRODUCTION

Since the beginning of forensic DNA in 1985, the non-coding regions of DNA have been used for forensic identification due to the variation between individuals found in these regions [1]. Four things contribute to making DNA an excellent source of information that aids individualisation in forensic science: (1) almost no difference in DNA between cell types, (2) individual's DNA do not generally change throughout his or her lifetime, (3) resistance of DNA to degradation as compared to proteins and (4) high variations among individuals and between species [2-5].

The variations mainly used in forensic science are microsatellites or short tandem repeats (STRs). They occupy about three per cent of the human genome and occur on every 10,000 nucleotides [6]. STRs selected for forensic purposes have been shown to have minimal linkages with diseases and are mainly in non-coding regions [7]. Other conditions include high heterozygosity, distinguishable alleles and the ability to be robustly amplified. The current forensic STRs are a combination of traditionally selected ones and the ones recommended by national and international organisations through a more detailed study of the STRs for favourable characteristics [8].

The aim of this review is to provide an overview of the techniques that are currently available for STR typing in forensic science as well as the applications of STR typing to actual casework. Techniques for STR typing are divided into two parts – amplification and detection. Although there is an overlap in some techniques, the ultimate goal of a forensic STR analysis is a rapid, robust, cheap and portable amplification with simple interpretation. The polymerase chain reaction (PCR) is the vital support for all amplification techniques, from low copy number to rapid and direct amplification. Regarding detection, sequencing techniques such as pyrosequencing, next-generation sequencing and mass spectrometry have become increasingly cheaper by the year and could replace fragment length analysis, which is the current standard, in the future. The applications of STR typing are also highlighted.

TECHNIQUES FOR FORENSIC STR TYPING

STR Amplification

PCR is a technique that enzymatically multiplies a target region of the DNA template, generating millions or more copies of a particular DNA sequence [9]. PCR consists of cycles of repeated heating and cooling for DNA melting and enzymatic replication of the DNA, leading to an exponential increase of the target region. This targeting is achieved by specific primers which are single-stranded oligonucleotides designed to bind to the complementary DNA sequence on template DNA.

The success of PCR amplification depends on both DNA template quantity and quality. Degraded DNA samples, such as those exposed to the environment, give a distinctive allele and/or locus dropout at the larger loci [10, 11]. A mixture of repair enzymes, e.g. ligase, could theoretically repair these DNA damages. Westen and Sijen [12] evaluated two commercial repair mixes and reported minimal improvements, but modifications by Diegoli et al. resulted in a two to three times increase in peak heights and recovery of lost alleles [13].

Another inevitable problem faced by forensic scientists during the PCR process is the presence of PCR inhibitors such as heme in blood, humic acid from soil and calcium from bones [14-16]. These inhibitors are usually removed from DNA samples during the purification process, although they can be carried over into subsequent reactions. The mechanisms of inhibition have only been characterised recently [15, 16]; for example, humic acid binds DNA and produces sequence-specific inhibition, while calcium interferes with the binding of magnesium by the *Taq* polymerase.

Another problem associated with PCR amplification is stutter formation – an artefact peak usually seen at one unit shorter in length than the true allele. Even though stutters are well known and documented [10, 17, 18], the factors that influence their formation have not been studied until recently. Brookes et al. [19] found that increased repeat number and A-T content of synthetic oligomers are correlated with increased stutter formations, while interruption to the repeat units decrease stutters. As one can see, forensic scientists are not only pushing the technology but also trying to explain the mechanisms of the phenomena associated with the STR typing process.

Low Copy Number (LCN) / Low Template DNA (LT-DNA)

Low copy number (LCN) analysis, first proposed by Gill et al. [17], involves using 34 PCR cycles instead of the manufacturer's recommendation of 28 cycles (SGM Plus kit, Applied Biosystems, USA). Optimally 0.5 to 2 ng of DNA is needed for a full STR profile but with LCN techniques suboptimal amounts (<0.1 ng) can be analysed. Nevertheless, there are many caveats associated with the utilisation of this technique [20]. The most common problems tied to LCN analysis are increased stutters, allelic and locus dropout, and allelic dropin and complexity in interpretation of the results [17, 21]. Other techniques such as whole genome amplification [22] and post-PCR purification [23, 24] have been tried to overcome these problems, although they also suffer from the same analytical difficulties. In addition, Thanakiatkrai and Welch [25, 26] explored the possibility of nucleosome protection on forensic STRs as an alternative to LCN, but they did not find any significant difference between the protected and unprotected STR loci.

There is also much confusion about the term LCN analysis among reporting scientists, judicial personnel and the media whether it refers to a specific technique (34 cycles), specific interpretation criterion or the stochastic effect observed [27]. Due to these issues, the UK court questioned the reliability, reproducibility and lack of validation of LCN method in the landmark Omagh trial [28], sparking a review of the LCN method [29]. The forensic science community has responded feverishly to these issues [30, 31]. A wider term called "low template DNA" (LT-DNA) has been proposed when referring to samples with low amount of DNA, in which a stochastic effect is expected and seen regardless of the method used to generate STR profiles [29, 31].

Recent attempts have been made to clarify ambiguous terms and to introduce statistics-based interpretation criteria [10, 31, 32]. Gill and Buckleton [33] have suggested that a single universal interpretation rule be accepted and used without referring to the term LCN. However, a few forensic scientists believe 'general acceptance' has not been reached and implementation of the proposed statistical frameworks is not widely carried out [34]. Currently, there is no indication of the debate abating [35-37]. Even though some scientists oppose the use of LCN, the general consensus among prominent forensic scientists is acceptance of the technique but care must be taken in interpreting the results. The judicial system is also in favour of LCN analysis in recent years [38, 39].

Mini-STRs

Conventional STR kits fail to yield desirable results in the case of highly degraded samples such as those from burnt human remains, stains or remains exposed to the environment and DNA samples co-mingled with environmental contaminants [40-44]. In order to amplify successfully, the DNA sequence targeted must be intact [45]. Reducing the size of the PCR products by redesigning the primers to bind as close to the repeat sequence as possible has shown an improvement with these types of samples [42, 44, 46, 47]. This is due to the fact that the amount of flanking region in the target sequence that must be intact is kept to a minimum and thus is less prone to random degradation. The minimum size limit of a mini-STR is therefore the repeat units themselves plus the forward and reverse primers. Nonetheless, the regions closer to the repeat units are more prone to mutation (base polymorphism, partial repeat, mononucleotide stretches and insertion/deletion [41, 48]). Therefore, concordance and validation studies are necessary with new mini-STRs.

Larger STR multiplexes (e.g. PowerPlex® 16) move the primers away from the repeat regions in order to avoid overlapping sizes and thus one dye can be used for many loci. This allows more than ten loci to be amplified and detected simultaneously for a very low match probability of less than one in a billion. Mini-STR multiplexes – generating products in the regions of 100-200 bp – sacrifice discrimination power for higher success rates in amplifying inhibited or degraded DNA samples [6]. Because most of the amplicons are the same size, only one to two loci can be tagged with one of the five dyes available. This means that a maximum of about ten loci can be amplified and detected simultaneously with conventional capillary electrophoresis. Table 1 shows the discrimination power and number of loci for mini-STR and STR commercial kits.

Table 1. The number of loci (excluding amelogenin), the number of fluorescent dyes used, the size standard, the longest amplicon and the discrimination power (for US Caucasian) of some commercial STR and mini-STR kits

Kit	STR loci	Dyes	Size standard	Max amplicon size	Discrimination power
S5	4	3	ROX 600	260 bp	1 in 1.9 x 10^{5}
MF	8	5	LIZ 500	260 bp	1 in 1.2 x 10^{10}
SGM+	9	4	ROX 500	353 bp	1 in 3.3 x 10^{12}
NGM	15	5	LIZ 500	352 bp	1 in 4.5 x 10^{18}
ESI	15	5	LIZ 500	383 bp	1 in 1 x 10^{18}
ESX	15	5	LIZ 500	410 bp	1 in 1 x 10^{18}
Q-ESS	15	5	BTO 550	440 bp	1 in 6.25 x 10^{18}
PP-16	15	4	CXR 600	474 bp	1 in 1.8 x 10^{17}

Note: S5 = PowerPlex® S5, MF = ABI MiniFiler™, SGM+ = ABI SGM Plus®, NGM = ABI NGM™, ESI/ESX = PowerPlex® ESI/ESX, Q-ESS = Qiagen Investigator ESSplex Plus and PP-16 = PowerPlex® 16 (information from each kit's manual)

Rapid Thermal Cycler and Direct PCR

In order to lessen the amount of time required for a DNA profile to be generated, recent shifts have been made towards fast (rapid) thermal cycler. Without any backlog, a DNA profile can be obtained in about 8-12 hours using conventional method. The major part of this is taken by PCR amplification (usually about 3-4 hours) while Vallone et al. [49] could complete it in about 36 minutes. This protocol did not significantly affect intra- and inter-locus balance but there was a decrease in sensitivity and increase in incomplete adenylation products (-A). Verheij et al. [50] have shown that the whole STR typing process can be completed in two to three hours by employing direct PCR with a fast PCR protocol in combination with regulating sample input through mini-tape. They have validated the technique and it is currently available to the police [50].

These rapid processes would not have been successful without the change in the polymerase enzyme. Many alternatives to AmpliTaq Gold, the current standard in forensic genetics, have been proposed by various researchers. For example, Vallone et al. [49] used PyroStart and SpeedSTAR, while Verheij et al. [50] favoured Phusion® Flash polymerase. Other mutant polymerases have been shown to overcome PCR inhibitors better than wildtype *Taq* [51] and AmpliTaq Gold [52, 53].

All these involve the use of direct amplification, in which samples are added directly to the PCR process without prior purification. Widely used in microbiology, direct amplification has only recently found its way to forensic samples due to alternative polymerases and buffer [54]. Blood on FTA papers as well as DNA deposited on various substrates (glass, plastic, ceramic and stainless steel) have been successfully amplified and profiled using direct PCR [55, 56]. The reason why direct PCR works well for trace samples is the inefficiency of the extraction process, in which only 16% of DNA presented in the pre-extracted sample is recovered [56-58]. With the aid of inhibitor resistant polymerases and enhanced buffer, it will not be surprising to find more direct PCR commercial kits replacing the current ones, at least with reference samples [59].

STR detection

Fluorescent-based fragment analysis

Primers in STR kits are labelled with dyes of different colours. These dyes are excited by laser and the emission spectra are detected via a sensor in an automated gel analyser such as the ABI 3130. The passing of fluorescent dye-labelled products through the capillary depends on the size of the PCR products, with smaller products moving quicker through the polymer in the capillary than larger ones. Size separation of mini-STRs can be aided by the addition of non-nucleotide linkers (NNL), oligomeric hexaethyleneoxide (HEO) molecules that change the mobility characteristics of PCR products [60]. As a consequence, similar-size mini-STR products can be visualised in an electropherogram as if they had different sizes [6]. The MiniFiler™ and the NGM™ kit from Applied Biosystems utilise NNLs in order to amplify and visualise many mini-STR loci using five dyes [61]. Fragment analysis, peak heights in particular, has been shown to be dependent upon the genetic analysers used [62].

Pyrosequencing

Pyrosequencing is a real-time sequencing method for a short strand of DNA based on the synthesis of its complementary strand [63]. It is achieved by the combination of a sequencing primer, four deoxynucleotide triphosphates (dNTPs), adenosine 5’ phosphosulfate (APS), luciferin, four enzymes DNA polymerase, ATP sulfurylase, luciferase and apyrase. First, the four deoxyribonucleotide triphosphates (dNTPs) are added to the reaction one base at a time. The correct complementary dNTP is incorporated with the DNA template by the DNA polymerase and produces pyrophosphate (PPi) as a by-product. ATP sulfurylase then converts PPi to ATP, which is then used to change luciferin to oxyluciferin. This generates a chemiluminescent signal (visible light) proportional to the amount of ATP. The light is detected by camera and interpreted as a peak on the pyrogram. Apyrase is added to degrade excess dNTPs and the reaction can start again with a new dNTP. Pyrosequencing has been used to genotype 10 STRs of 114 Swedish individuals [64]. The advantage over current capillary detection system is the ability to detect the actual sequence and variant alleles [64].

Mass spectrometry

Mass spectrometry (MS) was first used to separate STR alleles but the size limitation (100 bp) of the instrument at that time made the analysis difficult [65]. Using electrospray ionisation (ESI) instead of matrix-assisted laser desorption-ionisation (MALDI) has allowed up to 250 bp of products to be injected [66]. In mass spectrometry, the mass-to-charge ratios (determined via time of flight) of

PCR products that have been heated into gas phase and ionised by ESI or MALDI are measured in a vacuum. Because this detection is carried out using mass rather than size, there is better separation of STR alleles with internal sequence polymorphisms [66]. An automated ESI-MS system that is backward compatible with capillary electrophoresis and capable of analysing all 13 CODIS loci has been developed recently [67].

Microchip device

The ultimate goal for DNA analysis is to achieve a rapid result using a portable device. Recently this goal is being realised via the use of rapid PCR and a microfluidic system, in which all the steps of a conventional DNA analysis is performed in a small microchip [68-70]. These systems use miniaturised circuitry to automate the extraction and PCR cycling in their dedicated chambers [71]. These devices have been shown to work with whole blood and semen, both of which are complex samples, and with commercial STR kits [70].

APPLICATIONS

Commercial STR typing kits are available from companies such as Promega Corporation (WI, USA) and Applied Biosystems (CA, USA) [72-74]. The kits currently in use include PowerPlex® 16, PowerPlex® Y, AmpF*l*STR® Identifiler®, AmpF*l*STR® SEfiler™ and AmpF*l*STR® SGM Plus® (SGM+). These kits are different in the STR loci that they amplify (Table 2). They have been validated to be very sensitive and are capable of STR typing from aged and degraded samples [75, 76].

In the past few years, commercial manufacturers worked closely with the forensic DNA community to develop two next-generation kits, viz. AmpF*l*STR® Next Generation Multiplex™ (Applied Biosystems) and PowerPlex® ESX/ESI (Promega Corporation), both of which utilise mini-STR technology and have been validated for casework [75, 76]. Tvedebrink et al. [77] compared the performance of the two kits and found no substantial differences.

The intended purpose of the kit should be considered when selecting and adopting an STR kit. For instance, if extra discrimination power is required, the NGM™, ESX and ESI kits should be the first choices [78]. Nonetheless, the MiniFiler™ kit works well as an adjunct kit for degraded samples, as the loci in the kit are mini-STRs of the largest loci in the SGM+ and Identifiler® kits, plus additional CODIS loci. In the case of cross-border data sharing in Europe, the NGM™, ESX, ESI and ESSplex kits are most appropriate because they all amplify the same loci, all of which overlap with both CODIS and ENFSI recommendations (Table 2). In contrast, the S5 kit, which is the least discriminatory but at the same time the cheapest, is perfect for screening samples to exclude individuals in casework scenarios, in preliminary mass screenings and mass disaster screenings.

Table 2. The markers of each next-generation and mini-STR kit compared to two current standard kits (SGM Plus® and PowerPlex® 16) and two recommendations (COD = CODIS and ENF = ENFSI). A tick mark (✓) indicates inclusion in the set. Plus (+) is optional inclusion. Chr = chromosome

Chr	Marker	S5	MF	SGM+	NGM	ESI/ESX	Q-ESS	PP-16	COD	ENF
1	D1S1656				✓	✓	✓			✓
2	D2S1338		✓	✓	✓	✓	✓			
	TPOX							✓	✓	
	D2S441				✓	✓	✓			✓
3	D3S1358			✓	✓	✓	✓	✓	✓	✓
4	FGA	✓	✓	✓	✓	✓	✓	✓	✓	✓
5	D5S818							✓	✓	
	CSF1PO		✓					✓	✓	
6	SE33				+	+	+			
7	D7S820		✓					✓	✓	
8	D8S1179	✓		✓	✓	✓	✓	✓	✓	✓
10	D10S1248				✓	✓	✓			✓
11	TH01	✓		✓	✓	✓	✓	✓	✓	✓
12	vWA			✓	✓	✓	✓	✓	✓	✓
	D12S391				✓	✓	✓			✓
13	D13S317		✓					✓	✓	
15	PENTA E							✓		
16	D16S539		✓	✓	✓	✓	✓	✓	✓	
18	D18S51	✓	✓	✓	✓	✓	✓	✓	✓	✓
19	D19S433			✓	✓	✓	✓			
21	D21S11		✓	✓	✓	✓	✓	✓	✓	✓
	PENTA D							✓		
22	D22S1045				✓	✓	✓			✓
X/Y	AMEL	✓	✓	✓	✓	✓	✓	✓	✓	

The Innocence Project, a non-profit law clinic whose main objective is to exonerate wrongfully convicted individuals, has used STR and mini-STR kits. As of January 31, 2012, there have been 289 post-conviction DNA exonerations, with an average of 13.5 years served by the exonerees [65]. Mini-STRs mainly feature in mass disasters and cases where DNA is limited. They have been used for identification of 19,963 human remains from the World Trade Centre incident [66, 79]. There have been over 10 mass disasters, both natural and man-made, where STRs have played a major role [66]. A staggering 20,000 remains have been analysed and the number is rapidly increasing with each passing year [66]. Other difficult sample types successfully amplified include charred femur [80], buried and exposed femurs and a tibia [81], severely degraded skeletons [82], and human telogen hairs [47].

An alternative to autosomal STRs, especially in the case of paternity testing, are Y-STRs and X-STRs. Numerous population studies have been carried out, for example in China, Brazil, Italy, Spanish-Portuguese speaking countries, Japan and the United States [83-85]. A reference database for Y-STR haplotypes was established in 2000 and currently houses nearly 100,000 haplotypes from all over the world [86]. Y-STRs are useful for separating the male component from a mixed stain and also in paternity testing [87, 88]. Commercial kits that type the minimal Y haplotype (minHt), SWGDAM recommended loci, and other highly polymorphic markers are currently available [89]. X-STRs have been demonstrated that they can be used in degraded DNA found in real casework [84].

In addition to human applications, STRs of other organisms have aided criminal investigations. Fifteen canine STRs were used to assess 52 cases of canine bites [90]. Another ten canine STRs were used in a case involving the death of a 7-year-old by dog attack [91]. Similarly, the death of a 3-month-old baby by a miniature dachshund was aided by the use of STRs [92]. A very recent panel of 16 bovine STRs, as well as 17 equine STRs, have been recommended for use in forensic identification (e.g. paternity testing and breed identification) and a population study subsequently carried out [93, 94]. Another study demonstrated that equine STRs can be typed from blood, urine and hair for controlling doping of racehorses [95]. *Cannabis sativa*, an important plant in forensic science, has its STRs characterised and an STR kit developed validated [96]. An Australian DNA database for tracking *C. sativa* specimens is even available [97].

CONCLUSIONS

Forensic DNA analysis has come a long way since its inception by Sir Alec Jeffreys. With the advent of PCR, miniscule amounts of body fluid and even skin flakes can now be used to link crimes and individuals. STRs are the de facto standard due to their being established in national DNA databases worldwide; thus, they are here to stay. Methodologies from other fields of science have made their way to the forensic community, resulting in an ever better method for STR genotyping. Undoubtedly, some of the techniques described here will find their way to mainstream uses while others will fall out of favour. With the current focus on quicker analysis time and portability, we envision that STR typing will be developed in three areas: (1) a portable system for on-scene analysis, (2) high-throughput analysis of reference samples using direct PCR, and (3) more sensitive and inhibitor tolerant protocols for use with casework samples.

REFERENCES

1. A. Jeffreys, V. Wilson and S. Thein, "Hypervariable minisatellite regions in human DNA", *Nature*, **1985**, *314*, 67-73.
2. A. Linacre, "Forensic Science in Wildlife Investigations", 1st Edn., CRC Press, Boca Raton, **2009**, p. 178.
3. A. M. T. Linacre, "Application of mitochondrial DNA technologies in wildlife investigations–species identification", *Forensic. Sci. Rev.*, **2006**, *18*, 1-8.
4. G. J. Adcock, E. S. Dennis, S. Easteal, G. A. Huttley, L. S. Jermiin, W. J. Peacock and A. Thorne, "Mitochondrial DNA sequences in ancient Australians: Implications for modern human origins", *Proc. Natl. Acad. Sci. U. S. A.*, **2001**, *98*, 537-542.

5. I. V. Ovchinnikov, A. Gotherstrom, G. P. Romanova, V. M. Kharitonov, K. Liden and W. Goodwin, "Molecular analysis of Neanderthal DNA from the northern Caucasus", *Nature*, **2000**, *404*, 490-493.
6. J. Butler, "Forensic DNA Typing: Biology, Technology, and Genetics of STR Markers", 2nd Edn., Elsevier, Burlington, **2005**, p. 660.
7. M. Klintschar, U. D. Immela, M. Kleiber and P. Wiegand, "Physical location and linked genes of common forensic STR markers", *Int. Congr.*, **2006**, *1288*, 801-803.
8. P. Gill, L. Fereday, N. Morling and P. M. Schneider, "The evolution of DNA databases--recommendations for new European STR loci", *Forensic Sci. Int.*, **2006**, *156*, 242-244.
9. K. Mullis, F. Ferre and R. Gibbs, "PCR: The Polymerase Chain Reaction", Birkhäuser Boston Inc., Cambridge (MA), **1994**, p. 480.
10. D. Balding and J. Buckleton, "Interpreting low template DNA profiles", *Forensic Sci. Int. Genet.*, **2009**, *4*, 1-10.
11. T. Tvedebrink, P. S. Eriksen, H. S. Mogensen and N. Morling, "Statistical model for degraded DNA samples and adjusted probabilities for allelic drop-out", *Forensic Sci. Int. Genet.*, **2012**, *6*, 97-101.
12. A. A. Westen and T. Sijen, "Degraded DNA sample analysis using DNA repair enzymes, mini-STRs and (tri-allelic) SNPs", *Forensic Sci. Int. Genet. Suppl.*, **2009**, *2*, 505-507.
13. T. M. Diegoli, M. Farr, C. Cromartie, M. D. Coble and T. W. Bille, "An optimized protocol for forensic application of the PreCR™ Repair Mix to multiplex STR amplification of UV-damaged DNA", *Forensic Sci. Int. Genet.*, **2012**, *6*, 498-503.
14. A. Akane, K. Matsubara, H. Nakamura, S. Takahashi and K. Kimura, "Identification of the heme compound copurified with deoxyribonucleic acid (DNA) from bloodstains, a major inhibitor of polymerase chain reaction (PCR) amplification", *J. Forensic Sci.*, **1994**, *39*, 362-372.
15. S. B. Seo, H. Y. Lee, A. H. Zhang, H. Y. Kim, D. H. Shin and S. D. Lee, "Effects of humic acid on DNA quantification with Quantifiler® Human DNA quantification kit and short tandem repeat amplification efficiency", *Int. J. Legal Med.*, **2012**, *126*, 961-968.
16. M. E. Funes-Huacca, K. Opel, R. Thompson and B. R. McCord, "A comparison of the effects of PCR inhibition in quantitative PCR and forensic STR analysis", *Electrophoresis*, **2011**, *32*, 1084-1089.
17. P. Gill, J. Whitaker, C. Flaxman, N. Brown and J. Buckleton, "An investigation of the rigor of interpretation rules for STRs derived from less than 100 pg of DNA", *Forensic Sci. Int.*, **2000**, *112*, 17-40.
18. P. S. Walsh, N. J. Fildes and R. Reynolds, "Sequence analysis and characterization of stutter products at the tetranucleotide repeat locus vWA", *Nucleic Acids Res.*, **1996**, *24*, 2807-2812.
19. C. Brookes, J.-A. Bright, S. Harbison and J. Buckleton, "Characterising stutter in forensic STR multiplexes", *Forensic Sci. Int. Genet.*, **2012**, *6*, 58-63.
20. P. Gill, "Application of low copy number DNA profiling", *Croat. Med. J.*, **2001**, *42*, 229-232.
21. M. A. Jobling and P. Gill, "Encoded evidence: DNA in forensic analysis", *Nat. Rev. Genet.*, **2004**, *5*, 739-751.

22. K. N. Ballantyne, R. A. H. van Oorschot, I. Muharam, A. van Daal and R. John Mitchell, "Decreasing amplification bias associated with multiple displacement amplification and short tandem repeat genotyping", *Anal. Biochem.*, **2007**, *368*, 222-229.
23. P. J. Smith and J. Ballantyne, "Simplified low-copy-number DNA analysis by post-PCR purification", *J. Forensic Sci.*, **2007**, *52*, 820-829.
24. L. Forster, J. Thomson and S. Kutranov, "Direct comparison of post-28-cycle PCR purification and modified capillary electrophoresis methods with the 34-cycle "low copy number" (LCN) method for analysis of trace forensic DNA samples", *Forensic Sci. Int. Genet.*, **2008**, *2*, 318-328.
25. P. Thanakiatkrai and L. Welch, "Evaluation of nucleosome forming potentials (NFPs) of forensically important STRs", *Forensic Sci. Int. Genet.*, **2011**, *5*, 285-290.
26. P. Thanakiatkrai and L. Welch, "An investigation into the protective capabilities of nucleosomes on forensic STRs", *Forensic Sci. Int. Genet. Suppl.*, **2011**, *3*, e417-e418.
27. P. Gill, R. Brown, M. Fairley, L. Lee, M. Smyth, N. Simpson, B. Irwin, J. Dunlop, M. Greenhalgh, K. Way, E. Westacott, S. Ferguson, L. Ford, T. Clayton and J. Guiness, "National recommendations of the Technical UK DNA working group on mixture interpretation for the NDNAD and for court going purposes", *Forensic Sci. Int. Genet.*, **2008**, *2*, 76-82.
28. H. Orde, "DNA test halted after Omagh case", BBC News, **2007**, http://news.bbc.co.uk/2/hi/uk_news/7156051.stm, (Accessed: 25 November 2011).
29. B. Caddy, G. R. Taylor and A. M. T. Linacre, "A review of the science of low template DNA analysis", Police Home Office, United Kingdom, **2008**, p. 1-35.
30. S. Petricevic, J. Whitaker, J. Buckleton, S. Vintiner, J. Patel, P. Simon, H. Ferraby, W. Hermiz and A. Russell, "Validation and development of interpretation guidelines for low copy number (LCN) DNA profiling in New Zealand using the AmpFlSTR SGM Plus multiplex", *Forensic Sci. Int. Genet.*, **2010**, *4*, 305-310.
31. J. Buckleton, "Validation issues around DNA typing of low level DNA", *Forensic Sci. Int. Genet.*, **2009**, *3*, 255-260.
32. T. Tvedebrink, P. Eriksen, H. Mogensen and N. Morling, "Estimating the probability of allelic drop-out of STR alleles in forensic genetics", *Forensic Sci. Int. Genet.*, **2009**, *3*, 222-226.
33. P. Gill and J. Buckleton, "A universal strategy to interpret DNA profiles that does not require a definition of low-copy-number", *Forensic Sci. Int. Genet.*, **2010**, *4*, 221-227.
34. B. Budowle, A. J. Eisenberg and A. van Daal, "Low copy number typing has yet to achieve 'general acceptance'", *Forensic Sci. Int. Genet.*, **2009**, *2*, 551-552.
35. J. Buckleton and P. Gill, "Further comment on 'Low copy number typing has yet to achieve general acceptance' by Budowle, B., et al, 2009. Forensic Sci. Int. Genetics: Supplement Series 2, 551–552", *Forensic Sci. Int. Genet.*, **2011**, *5*, 7-11.
36. B. Budowle, A. J. Eisenberg and A. van Daal, "Comment on 'A universal strategy to interpret DNA profiles that does not require a definition of low copy number' by Peter Gill and John Buckleton, 2010, Forensic Sci. Int. Genetics 4, 221-227", *Forensic Sci. Int. Genet.*, **2011**, *5*, 15.
37. T. Caragine and M. Prinz, "Comment on 'Low copy number typing has yet to achieve general acceptance' by Budowle, B., et al., 2009. Forensic Sci. Int. Genetics: Supplement Series 2, 551-552", *Forensic Sci. Int. Genet.*, **2011**, *5*, 3-4.

38. H. Glazebrook and E. France, "Michael Scott Wallace vs. the Queen", Hearing before Court of Appeal of New Zealand, **2010**.
39. R. J. Hanophy, "The People of the State of New York vs. Hemant Megnath", Hearing before Supreme Court - State of New York, **2010**.
40. L. A. Dixon, C. M. Murray, E. J. Archer, A. E. Dobbins, P. Koumi and P. Gill, "Validation of a 21-locus autosomal SNP multiplex for forensic identification purposes", *Forensic Sci. Int.*, **2005**, *154*, 62-77.
41. J. M. Butler, Y. Shen and B. R. McCord, "The development of reduced size STR amplicons as tools for analysis of degraded DNA", *J. Forensic Sci.*, **2003**, *48*, 1054-1064.
42. K. Opel, D. Chung, J. Drabek, J. Butler and B. McCord, "Developmental validation of reduced-size STR Miniplex primer sets", *J. Forensic Sci.*, **2007**, *52*, 1263-1271.
43. K. Tsukada, K. Takayanagi, H. Asamura, M. Ota and H. Fukushima, "Multiplex short tandem repeat typing in degraded samples using newly designed primers for the TH01, TPOX, CSF1PO, and vWA loci", *Leg. Med.*, **2002**, *4*, 239-245.
44. P. Wiegand and M. Kleiber, "Less is more–length reduction of STR amplicons using redesigned primers", *Int. J. Legal Med.*, **2001**, *114*, 285-287.
45. J. Watterson, V. Blackman and D. Bagby, "Considerations for the analysis of forensic samples following extended exposure to the environment", *The Forensic Examiner*, **2006**, *15*, 19-25.
46. M. D. Coble and J. M. Butler, "Characterization of new miniSTR loci to aid analysis of degraded DNA", *J. Forensic Sci.*, **2005**, *50*, 43-53.
47. A. Hellmann, U. Rohleder, H. Schmitter and M. Wittig, "STR typing of human telogen hairs–a new approach", *Int. J. Legal Med.*, **2001**, *114*, 269-273.
48. B. Rolf, N. Bulander and P. Wiegand, "Insertion-/deletion polymorphisms close to the repeat region of STR loci can cause discordant genotypes with different STR kits", *Forensic Sci. Int. Genet.*, **2011**, *5*, 339-341.
49. P. Vallone, C. Hill and J. Butler, "Demonstration of rapid multiplex PCR amplification involving 16 genetic loci", *Forensic Sci. Int. Genet.*, **2008**, *3*, 42-45.
50. S. Verheij, J. Harteveld and T. Sijen, "A protocol for direct and rapid multiplex PCR amplification on forensically relevant samples", *Forensic Sci. Int. Genet.*, **2011**, *6*, 167-175.
51. Z. Zhang, M. B. Kermekchiev and W. M. Barnes, "Direct DNA amplification from crude clinical samples using a PCR enhancer cocktail and novel mutants of Taq", *J. Mol. Diagn.*, **2010**, *12*, 152-161.
52. J. Hedman, A. Nordgaard, B. Rasmusson, R. Ansell and P. Rådström, "Improved forensic DNA analysis through the use of alternative DNA polymerases and statistical modeling of DNA profiles", *Biotechniques*, **2009**, *47*, 951-958.
53. M. B. Kermekchiev, L. I. Kirilova, E. E. Vail and W. M. Barnes, "Mutants of Taq DNA polymerase resistant to PCR inhibitors allow DNA amplification from whole blood and crude soil samples", *Nucleic Acids Res.*, **2009**, *37*, e40.
54. S. J. Park, J. Y. Kim, Y. G. Yang and S. H. Lee, "Direct STR amplification from whole blood and blood- or saliva-spotted FTA without DNA purification", *J. Forensic Sci.*, **2008**, *53*, 335-341.

55. D. Y. Wang, C.-W. Chang, R. E. Lagacé, N. J. Oldroyd and L. K. Hennessy, "Development and validation of the AmpFℓ STR® Identifiler® Direct PCR Amplification Kit: a multiplex assay for the direct amplification of single-source samples", *J. Forensic Sci.*, **2011**, *56*, 835-845.
56. Y. C. Swaran and L. Welch, "A comparison between direct PCR and extraction to generate DNA profiles from samples retrieved from various substrates", *Forensic Sci. Int. Genet.*, **2012**, *6*, 407-412.
57. A. Colussi, M. Viegas, J. Beltramo and M. Lojo, "Efficiency of DNA IQ System® in recovering semen DNA from cotton swabs", *Forensic Sci. Int. Genet. Suppl.*, **2009**, *2*, 87-88.
58. R. Kishore, W. Reef Hardy, V. J. Anderson, N. A. Sanchez and M. R. Buoncristiani, "Optimization of DNA extraction from low-yield and degraded samples using the BioRobot EZ1 and BioRobot M48", *J. Forensic Sci.*, **2006**, *51*, 1055-1061.
59. B. A. Myers, J. L. King and B. Budowle, "Evaluation and comparative analysis of direct amplification of STRs using PowerPlex® 18D and Identifiler® Direct systems", *Forensic Sci. Int. Genet.*, **2012**, *6*, 640-645.
60. P. D. Grossman, W. Bloch, E. Brinson, C. C. Chang, F. A. Eggerding, S. Fung, D. M. Iovannisci, S. Woo, E. S. Winn-Deen and D. A. Iovannisci, "High-density multiplex detection of nucleic acid sequences: Oligonucleotide ligation assay and sequence-coded separation", *Nucleic Acids Res.*, **1994**, *22*, 4527-4534.
61. R. A. van Oorschot, K. N. Ballantyne and R. J. Mitchell, "Forensic trace DNA: A review", *Invest. Genet.*, **2010**, *1*, 14.
62. A. Debernardi, E. Suzanne, A. Formant, L. Pène, A. B. Dufour and J. R. Lobry, "One year variability of peak heights, heterozygous balance and inter-locus balance for the DNA positive control of AmpFℓ STR© Identifiler© STR kit", *Forensic Sci. Int. Genet.*, **2011**, *5*, 43-49.
63. M. Ronaghi, S. Karamohamed, B. Pettersson, M. Uhlén and P. Nyrén, "Real-time DNA sequencing using detection of pyrophosphate release", *Anal. Biochem.*, **1996**, *242*, 84-89.
64. A.-M. Divne, H. Edlund and M. Allen, "Forensic analysis of autosomal STR markers using pyrosequencing", *Forensic Sci. Int. Genet.*, **2010**, *4*, 122-129.
65. The Innocence Project, "Facts on post-conviction DNA exonerations", Benjamin N. Cardozo School of Law at Yeshiva University, **2012**, http://www.innocenceproject.org/Content/Facts_on_PostConviction_DNA_Exonerations.php, (Accessed: January 2012).
66. A. Alonso, P. Martin, C. Albarrán, P. Garcia, L. Fernandez de Simon, M. Jesús Iturralde, A. Fernández-Rodriguez, I. Atienza, J. Capilla, J. García-Hirschfeld, P. Martinez, G. Vallejo, O. García, E. García, P. Real, D. Alvarez, A. León and M. Sancho, "Challenges of DNA profiling in mass disaster investigations", *Croat. Med. J.*, **2005**, *46*, 540-548.
67. J. V. Planz, K. Sannes-Lowery, D. D. Duncan, S. Manalili, B. Budowle, R. Chakraborty, S. Hofstadler and T. Hall, "Automated analysis of sequence polymorphism in STR alleles by PCR and direct electrospray ionization mass spectrometry", *Forensic Sci. Int. Genet.*, **2012**, 594-606.
68. P. Liu, S. H. I. Yeung, K. A. Crenshaw, C. A. Crouse, J. R. Scherer and R. A. Mathies, "Real-time forensic DNA analysis at a crime scene using a portable microchip analyzer", *Forensic Sci. Int. Genet.*, **2008**, *2*, 301-309.
69. K. M. Horsman, J. M. Bienvenue, K. R. Blasier and J. P. Landers, "Forensic DNA analysis on microfluidic devices: a review", *J. Forensic Sci.*, **2007**, *52*, 784-799.

70. J. M. Bienvenue, L. a. Legendre, J. P. Ferrance and J. P. Landers, "An integrated microfluidic device for DNA purification and PCR amplification of STR fragments", *Forensic Sci. Int. Genet.*, **2010**, *4*, 178-186.
71. K. J. Shaw, D. A. Joyce, P. T. Docker, C. E. Dyer, G. M. Greenway, J. Greenman and S. J. Haswell, "Development of a real-world direct interface for integrated DNA extraction and amplification in a microfluidic device", *Lab. Chip*, **2011**, *11*, 443-448.
72. E. A. Cotton, R. F. Allsop, J. L. Guest, R. R. E. Frazier, P. Koumi, I. P. Callow, A. Seager and R. L. Sparkes, "Validation of the AMPFlSTR SGM Plus™ system for use in forensic casework", *Forensic Sci. Int.*, **2000**, *112*, 151-161.
73. P. J. Collins, L. K. Hennessy, C. S. Leibelt, R. K. Roby, D. J. Reeder and P. A. Foxall, "Developmental validation of a single-tube amplification of the 13 CODIS STR loci, D2S1338, D19S433, and amelogenin: the AmpFlSTR Identifiler PCR Amplification Kit", *J. Forensic Sci.*, **2004**, *49*, 1265-1277.
74. S. Greenspoon, J. Ban, L. Pablo, C. Crouse, F. Kist, C. Tomsey, A. Glessner, L. Mihalacki, T. Long, B. Heidebrecht, C. Braunstein, D. Freeman, C. Soberalski, B. Nathan, A. Amin, E. Douglas and J. Schumm, "Validation and implementation of the PowerPlex 16 BIO System STR multiplex for forensic casework", *J. Forensic Sci.*, **2004**, *49*, 71-80.
75. V. C. Tucker, A. J. Hopwood, C. J. Sprecher, R. S. McLaren, D. R. Rabbach, M. G. Ensenberger, J. M. Thompson and D. R. Storts, "Developmental validation of the PowerPlex((R)) ESI 16 and PowerPlex((R)) ESI 17 Systems: STR multiplexes for the new European standard", *Forensic Sci Int Genet*, **2011**, *5*, 436-448.
76. A. Barbaro, P. Cormaci and A. Agostino, "Validation of AmpFLSTR NGM SElect™ PCR amplification kit on forensic samples", *Forensic Sci. Int. Genet. Suppl.*, **2011**, *3*, e67-e68.
77. T. Tvedebrink, H. S. Mogensen, M. C. Stene and N. Morling, "Performance of two 17 locus forensic identification STR kits–Applied Biosystems's AmpFℓ STR® NGMSElect™ and Promega's PowerPlex® ESI17 kits", *Forensic Sci. Int. Genet.*, **2012**, *6*, 523-531.
78. Forensic News, "The AmpFlSTR NGM™ PCR amplification kit: The perfect union of data quality and data sharing", Applied Biosystems, **2009**, http://marketing.appliedbiosystems.com/ images/Product_Microsites/NGM/downloads/PCRAmplificationKit_SS_v2.pdf, (Accessed: October 2012).
79. L. G. Biesecker, J. E. Bailey-Wilson, J. Ballantyne, H. Baum, F. R. Bieber, C. Brenner, B. Budowle, J. M. Butler, G. Carmody, P. M. Conneally, B. Duceman, A. Eisenberg, L. Forman, K. K. Kidd, B. Leclair, S. Niezgoda, T. J. Parsons, E. Pugh, R. Shaler, S. T. Sherry, A. Sozer and A. Walsh, "Epidemiology. DNA identifications after the 9/11 World Trade Center attack", *Science*, **2005**, *310*, 1122-1123.
80. M. Fondevila, C. Phillips, N. Naveran, L. Fernandez, M. Cerezo, A. Salas, A. Carracedo and M. V. Lareu, "Case report: identification of skeletal remains using short-amplicon marker analysis of severely degraded DNA extracted from a decomposed and charred femur", *Forensic Sci. Int. Genet.*, **2008**, *2*, 212-218.
81. K. L. Opel, D. T. Chung, J. Drábek, N. E. Tatarek, L. M. Jantz and B. R. McCord, "The application of miniplex primer sets in the analysis of degraded DNA from human skeletal remains", *J. Forensic Sci.*, **2006**, *51*, 351-356.

82. J. A. Irwin, R. S. Just, O. M. Loreille and T. J. Parsons, "Characterization of a modified amplification approach for improved STR recovery from severely degraded skeletal elements", *Forensic Sci. Int. Genet.*, **2012**, *6*, 578-587.
83. L. Gusmão, P. Sánchez-Diz, C. Alves, I. Gomes, M. T. Zarrabeitia, M. Abovich, I. Atmetlla, C. Bobillo, L. Bravo, J. Builes, L. Cainé, R. Calvo, E. Carvalho, M. Carvalho, R. Cicarelli, L. Catelli, D. Corach, M. Espinoza, O. García, M. Malaghini, J. Martins, F. Pinheiro, M. João Porto, E. Raimondi, J. A. Riancho, A. Rodríguez, A. Rodríguez, B. Rodríguez Cardozo, V. Schneider, S. Silva, C. Tavares, U. Toscanini, C. Vullo, M. Whittle, I. Yurrebaso, A. Carracedo and A. Amorim, "A GEP-ISFG collaborative study on the optimization of an X-STR decaplex: data on 15 Iberian and Latin American populations", *Int. J. Legal Med.*, **2009**, *123*, 227-234.
84. H. Asamura, H. Sakai, K. Kobayashi, M. Ota and H. Fukushima, "MiniX-STR multiplex system population study in Japan and application to degraded DNA analysis", *Int. J. Legal Med.*, **2006**, *120*, 174-181.
85. I. Gomes, M. Prinz, R. Pereira, C. Meyers, R. S. Mikulasovich, A. Amorim, A. Carracedo and L. Gusmão, "Genetic analysis of three US population groups using an X-chromosomal STR decaplex", *Int. J. Legal Med.*, **2007**, *121*, 198-203.
86. S. Willuweit and L. Roewer, "Y chromosome haplotype reference database (YHRD): Update", *Forensic Sci. Int. Genet.*, **2007**, *1*, 83-87.
87. B. Rolf, W. Keil, B. Brinkmann, L. Roewer and R. Fimmers, "Paternity testing using Y-STR haplotypes: assigning a probability for paternity in cases of mutations", *Int. J. Legal Med.*, **2001**, *115*, 12-15.
88. D. Corach, L. Filgueira Risso, M. Marino, G. Penacino and a. Sala, "Routine Y-STR typing in forensic casework", *Forensic Sci. Int.*, **2001**, *118*, 131-135.
89. J. J. Mulero, C. W. Chang, L. M. Calandro, R. L. Green, Y. Li, C. L. Johnson and L. K. Hennessy, "Development and validation of the AmpFlSTR Yfiler PCR amplification kit: a male specific, single amplification 17 Y-STR multiplex system", *J. Forensic Sci.*, **2006**, *51*, 64-75.
90. C. Eichmann, B. Berger, M. Reinhold, M. Lutz and W. Parson, "Canine-specific STR typing of saliva traces on dog bite wounds", *Int. J. Legal Med.*, **2004**, *118*, 337-342.
91. Z. Pádár, B. Egyed, K. Kontadakis, S. Füredi, J. Woller, L. Zöldág and S. Fekete, "Canine STR analyses in forensic practice. Observation of a possible mutation in a dog hair", *Int. J. Legal Med.*, **2002**, *116*, 286-288.
92. A. Tsuji, A. Ishiko, H. Kimura, M. Nurimoto, K. Kudo and N. Ikeda, "Unusual death of a baby: a dog attack and confirmation using human and canine STRs", *Int. J. Legal Med.*, **2008**, *122*, 59-62.
93. L. H. P. van de Goor, M. T. Koskinen and W. A. van Haeringen, "Population studies of 16 bovine STR loci for forensic purposes", *Int. J. Legal Med.*, **2011**, *125*, 111-119.
94. L. H. P. van de Goor, W. A. van Haeringen and J. A. Lenstra, "Population studies of 17 equine STR for forensic and phylogenetic analysis", *Anim. Genet.*, **2011**, *42*, 627-633.
95. J.-W. Chen, C. E. Uboh, L. R. Soma, X. Li, F. Guan, Y. You and Y. Liu, "Identification of racehorse and sample contamination by novel 24-plex STR system", *Forensic Sci. Int. Genet.*, **2010**, *4*, 158-167.
96. C. Howard, S. Gilmore, J. Robertson and R. Peakall, "Developmental validation of a *Cannabis sativa* STR multiplex system for forensic analysis", *J. Forensic Sci.*, **2008**, *53*, 1061-1067.

97. C. Howard, S. Gilmore, J. Robertson and R. Peakall, "A *Cannabis sativa* STR genotype database for Australian seizures: forensic applications and limitations", *J. Forensic Sci.*, **2009**, *54*, 556-563.

Maejo Int. J. Sci. Technol. **2013**, *7*(01), 16-25

Maejo International Journal of Science and Technology

ISSN 1905-7873
Available online at www.mijst.mju.ac.th

Full Paper

Voltage controlled resistor using quasi-floating-gate MOSFETs

Rockey Gupta and Susheel Sharma*

Department of Physics and Electronics, University of Jammu, Jammu-180006, India

* Corresponding author, e-mail: susheelksharma@gmail.com

Received: 20 January 2012 / Accepted: 7 January 2013 / Published: 9 January 2013

Abstract: A voltage controlled resistor (VCR) using quasi-floating-gate MOSFETs (QFGMOS) suitable for low voltage applications is presented. The performance of the VCR implemented with QFGMOS is compared with its floating-gate MOSFET (FGMOS) version. It was found that QFGMOS offers better performance than FGMOS in terms of frequency response, offsets and chip area. The VCR using QFGMOS offers high bandwidth and low power dissipation and yields high value of resistance as compared to its FGMOS counterpart. The workability of the presented circuits was tested by PSpice simulations using level 3 parameters of 0.5µm CMOS technology with supply voltage of ± 0.75V. The simulations results were found to be in accordance with the theoretical predictions.

Keywords: voltage controlled resistor, floating- gate MOSFET, quasi-floating-gate MOSFET

INTRODUCTION

Implementation of active resistors in integrated circuits is desired for minimal chip area and high accuracy. An MOS transistor operating below saturation region can implement a voltage controlled resistor (VCR) but with a limited range. These VCRs are useful in the design of tunable analog circuits such as voltage controlled oscillators, automatic gain controllers, voltage controlled filters, current-mode dividers and trans-resistance amplifiers [1-4]. The design of analog circuits operating with low voltage and dissipating low power is significant for mixed-mode implementation of systems on chip which comprises both digital and analog components. For scaled-down analog circuits, the threshold voltage of the MOS transistor poses a limitation for low voltage design and it is not expected to be too low in sub-micron technologies [5, 6]. A floating-gate MOSFET (FGMOS) is a possible solution to this problem, which offers tunability of threshold voltage with a bias voltage without the need of actually lowering the threshold voltage. However, FGMOS has certain limitations like isolated floating-gate, which may accumulate static charge, give low frequency response and need large chip area [7, 8]. These limitations can be further overcome by quasi-floating-gate MOSFET (QFGMOS). In QFGMOS, the gate is not floating like in FGMOS but is weakly connected to one of the supply rails through a high value resistor. Besides, lowering the supply voltage requirements, QFGMOS offers better frequency response and needs less chip area [9]. It is therefore expected that the QFGMOS based VCR would exhibit better characteristics as compared to its FGMOS version.

In this paper, we have implemented a QFGMOS-based VCR and compared its performance with its FGMOS version. It is observed through both the mathematical equations and PSpice simulations that for a given value of control voltage (V_C = 0.3V) QFGMOS-based VCR exhibits a higher value of resistance (R_{eq} =1.48 kΩ) and larger bandwidth (3.61 GHz), whereas FGMOS-based VCR simulates a resistance value of 1.30 kΩ with a bandwidth of 490 MHz.

METHODS

Quasi-Floating-Gate Transistor

The equivalent circuit of the n-input N-type QFGMOS is shown in Figure 1. The input terminals are capacitively coupled to the quasi-floating gate (QFG) and its gate voltage (V_{QFG}) is set to V_{DD} through a pull-up resistor which can be implemented by using the large leakage resistance of the reverse biased p-n junction of a PMOS transistor operating in cut-off region.

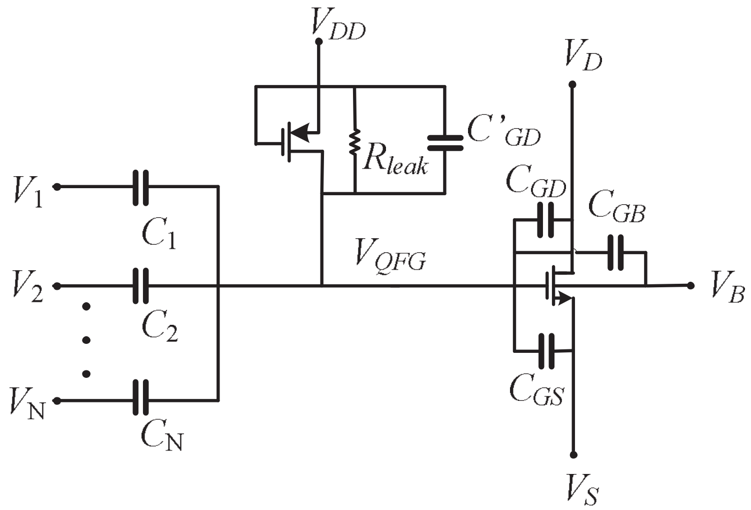

Figure 1. Equivalent circuit of QFGMOS

The quasi-floating gate voltage (V_{QFG}) in Figure 1 can be expressed as

$$V_{QFG} = V_{in} \frac{sR_{leak}C_{Total}}{1 + sR_{leak}C_{Total}} \tag{1}$$

where

$$C_{Total} = \sum_{i=1}^{N} C_i + C_{GS} + C_{GD} + C_{GB} + C'_{GD} \tag{2}$$

and

$$V_{in} = \frac{1}{C_{Total}} \left(\sum_{i=1}^{N} C_i V_i + C_{GS}V_S + C_{GD}V_D + C_{GB}V_B \right) \tag{3}$$

On substituting Equation (3) in Equation (1), V_{QFG} becomes

$$V_{QFG} = \frac{1}{C_{Total}}\left(\sum_{i=1}^{N} C_iV_i + C_{GS}V_S + C_{GD}V_D + C_{GB}V_B\right)\left(\frac{sR_{leak}C_{Total}}{1 + sR_{leak}C_{Total}}\right) \tag{4}$$

We observe from Equation (4) that input signals encounter a high-pass filter with a cut-off frequency of $(2\pi R_{leak}C_{Total})^{-1}$, which is very low due to large value of R_{leak}. Therefore, even for very low frequencies, Equation (4) becomes a weighted average of the AC input voltages determined by capacitance ratios plus some parasitic terms. The pull-up resistor R_{leak} sets a DC voltage equal to V_{DD} on the quasi-floating gate upon which an AC voltage given in Equation (4) is superimposed. Hence, the gate voltage can become larger than V_{DD}. Similarly for P-type QFGMOS, a pull-down resistor sets the DC gate voltage to V_{SS}, which is implemented by a reverse biased p-n junction of an NMOS transistor in the cut-off region [10-18].

Voltage Controlled Resistor

The circuit of a simple MOS-based VCR is shown in Figure 2 where MOSFETs M1 and M2 are biased in the triode region and M2 acts as resistor whose resistance can be controlled by its gate voltage (V_C). The N-type current mirror formed by M3-M4 and P-type current mirror formed by M5-M6 ensure the same drain current in both M1 and M2. The transistors M1 and M2 are assumed to be perfectly matched transistors with the same drain currents I_1 and I_2 in the absence of input current (I_{in}) and M1 is biased in the ohmic region. This arrangement makes M2 operate in the ohmic region whose conductivity can be further varied by I_{in}. Thus, M2 acts as a variable resistor whose resistance value is controlled by V_C [19].

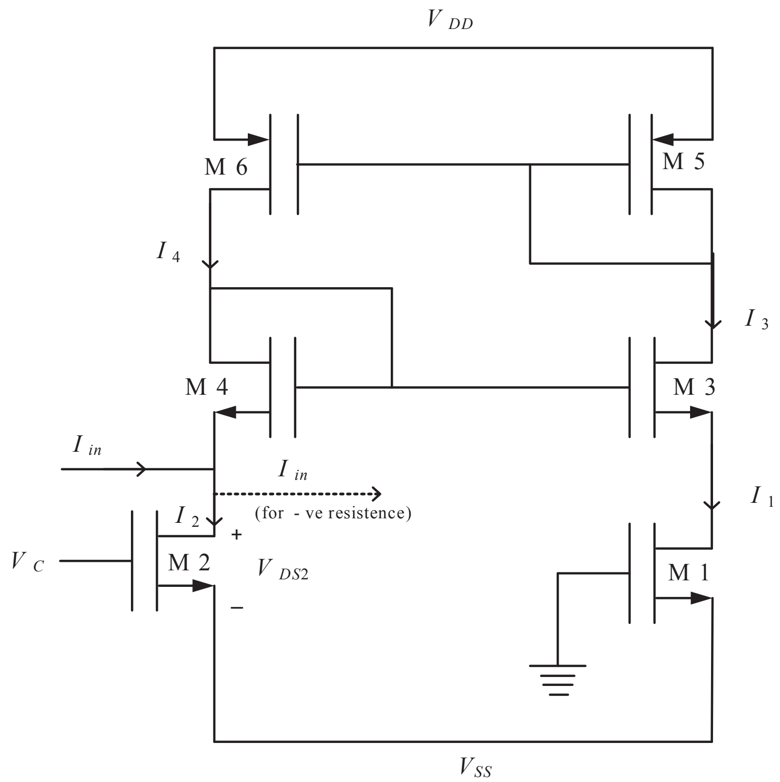

Figure 2. MOS-based VCR

The equivalent resistance of the MOS-based VCR [3] is given by:

$$R_{eq} = \frac{V_{DS2}}{I_{in}} = \frac{1}{K_n V_C} \tag{5}$$

To ascertain the workability of the circuit shown in Figure 2, PSpice simulation was used by selecting *W/L* as 10µm/1µm for M1 and M2, 50µm/1µm for M3 and M4, 20µm/0.5µm for M5 and 40µm/1µm for M6 with a supply voltage of ±0.75V. The simulated resistance (R_{eq}) varied with control voltage (V_C) in accordance with Equation (5) as shown in Figure 3 where the resistance varies from 2 kΩ to 1.11 kΩ as control voltage varies from 0.3 V to 0.75 V.

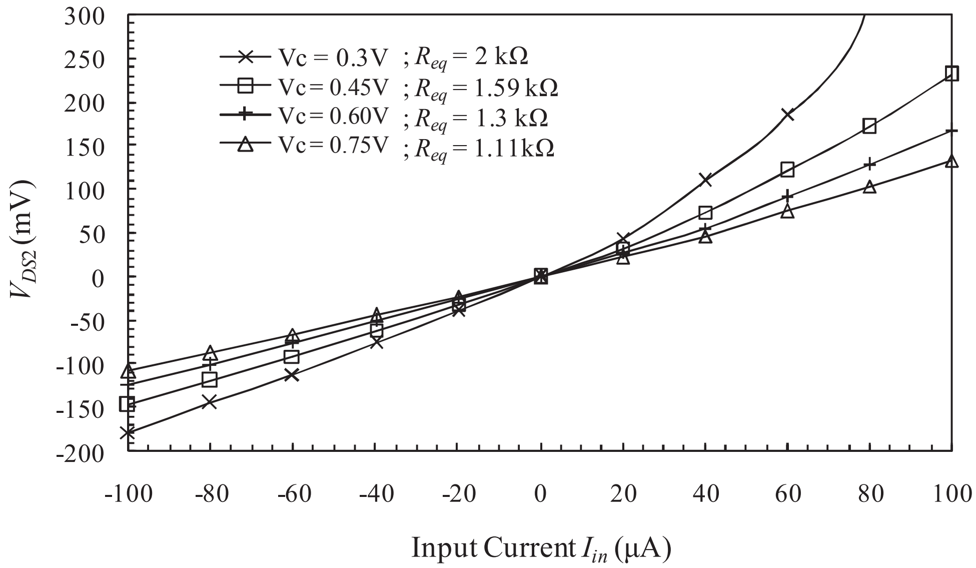

Figure 3. Resistance simulation using MOS-based VCR

QFGMOS-based Voltage Controlled Resistor

The QFGMOS-based VCR is shown in Figure 4. It differs from the FGMOS-based VCR presented [2] in that the gates of FGMOS are connected to a biased voltage through a large value capacitor ($C_2 >> C_1$) whereas the gates of QFGMOS are connected to the supply rails through reverse biased MOSFETs M8-M11.

The drain currents of M1 and M2, biased in the ohmic region are given by:

$$I_1 = K_n\left[\left\{\left(\frac{C_1}{C_{Total}}(-V_{SS}) + \frac{C'_{GD}}{C_{Total}}V_{DD} - \frac{C_{GS}}{C_{Total}}V_{SS}\right) - V_{Tn1}\right\} - \frac{V_{DS1}}{2}\right]V_{DS1} \tag{6}$$

where

$$K_n = \frac{\mu_0 C_{OX} W}{L}$$

and

$$I_2 = I_{in} + I_4 = K_n\left[\left\{\left(\frac{C_1}{C_{Total}}(V_C - V_{SS}) + \frac{C'_{GD}}{C_{Total}}V_{DD} - \frac{C_{GS}}{C_{Total}}V_{SS}\right) - V_{Tn2}\right\} - \frac{V_{DS2}}{2}\right]V_{DS2} \tag{7}$$

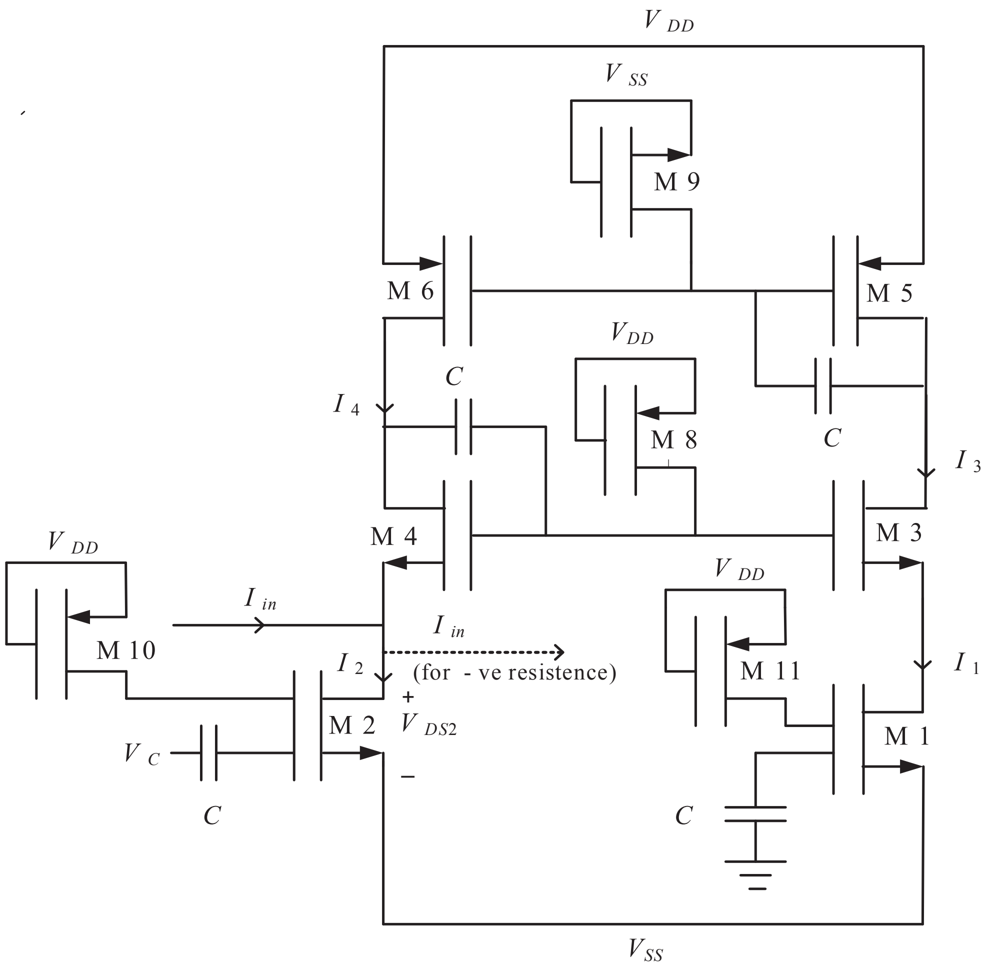

Figure 4. QFGMOS-based VCR

The current mirror arrangement of transistors M5 and M6 generates a current I_3 such that $I_3 = I_4 = I_1$. Since transistors M3 and M4 are assumed to be perfectly matched and are biased in saturation region, their drain currents are given by:

$$I_3 = \frac{K_n}{2}\left(V_{GS3} - V_{Tn3}\right)^2 \tag{8}$$

$$I_4 = \frac{K_n}{2}\left(V_{GS4} - V_{Tn4}\right)^2 \tag{9}$$

which gives

$$I_{in} = K_n\left(K_1 V_{DD} + K_2 V_C\right)V_{DS2} \tag{10}$$

From Equation (10), the equivalent resistance (R_{eq}) is given by:

$$R_{eq} = \frac{V_{DS2}}{I_{in}} = \frac{1}{K_n\left(K_1 V_{DD} + K_2 V_C\right)} \tag{11}$$

where $K_1 = \dfrac{C'_{GD}}{C_{Total}}$ & $K_2 = \dfrac{C_1}{C_{Total}}$ (12)

Equation (11) reveals that the circuit in Figure 4 implements a VCR whose resistance value depends on the control voltage (V_C). The corresponding equation for R_{eq} using FGMOS [2] is given by:

$$R_{eq} = \frac{1}{K_n\left(K_1 V_b + K_2 V_C\right)} \tag{13}$$

where K_2 is the same as in Equation (11) for VCR using QFGMOS and $K_1 = \dfrac{C_2}{C_{Total}}$. Since $C_2 >> C'_{GD}$, the resistance value for QFGMOS-based VCR will be larger than FGMOS-based VCR at a given value of control voltage. It also results in a better frequency response of QFGMOS- based VCR than its FGMOS counterpart [8, 9].

RESULTS AND DISCUSSION

The circuit of Figure 4 was simulated using PSpice level 3 parameters with supply voltage of ± 0.75V and by selecting *W/L* of 10μm/1μm for M1 and M2, 50μm/1μm for M3 and M4, 20μm/0.5μm for M5, 40μm/1μm for M6 and 50μm/0.5μm for M8-M11. The variation of resistance with different control voltages is shown in Figure 5. It is observed that the value of the simulated resistance varies inversely with the control voltage as shown by Equation (11).

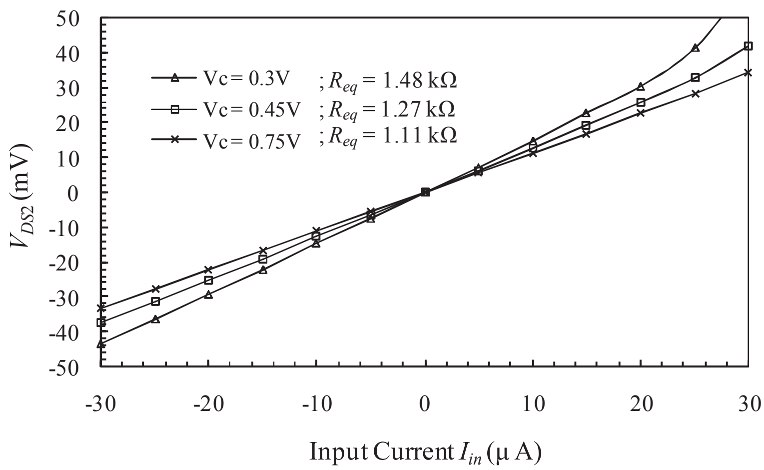

Figure 5. Resistance simulation with QFGMOS VCR

The circuit of VCR was also implemented using FGMOS and its performance compared with its QFGMOS counterpart. The performance of QFGMOS-based VCR was found to be better than that of its FGMOS version due to the inherent advantages of QFGMOS over FGMOS. The values of the equivalent resistance realised using QFGMOS vis-a-vis FGMOS for different values of V_C are given in Table 1.

It can be seen that R_{eq} decreases from 1.48 kΩ to 1.11 kΩ for QFGMOS-based VCR and from 1.3 kΩ to 1.11 kΩ for FGMOS-based VCR with the increase in V_C from 0.3 V to 0.75 V. A large value of the resistance of the order of kΩs or more can be obtained for smaller dimensions of transistors, which may lead to non-linearity.

Table 1. Variation of R_{eq} with V_C

V_C (V)	R_{eq} with QFGMOS (kΩ)	R_{eq} with FGMOS (kΩ)
0.3	1.48	1.30
0.45	1.27	1.23
0.6	1.19	1.17
0.75	1.11	1.11

It was also found that for control voltage (V_C) of the order of supply voltage, both QFGMOS and FGMOS topology of VCR yield the same value of resistance. This can be attributed to the fact that Equations (11) and (13) approximately become identical and resemble Equation (5). when V_C approaches positive supply voltage. The frequency response of QFGMOS-based VCR at different control voltages is shown in Figure 6. It can be observed that as control voltage increases from 0.3V to 0.75V, the bandwidth of QFGMOS-based VCR increases from 3.61 GHz to 4.9 GHz with the corresponding decrease in the value of simulated resistance. The same trend has also been observed in FGMOS-based VCR [2]. When control voltage in FGMOS-based VCR increases from 0.3V to 0.75V, the bandwidth increases from 490 MHz to 576 MHz and the corresponding value of simulated resistance decreases from 1.30 kΩ to 1.11 kΩ. This is due to the fact that with an increase in control voltage, the drain current of the transistors increases, which results in higher bandwidth and lower resistance.

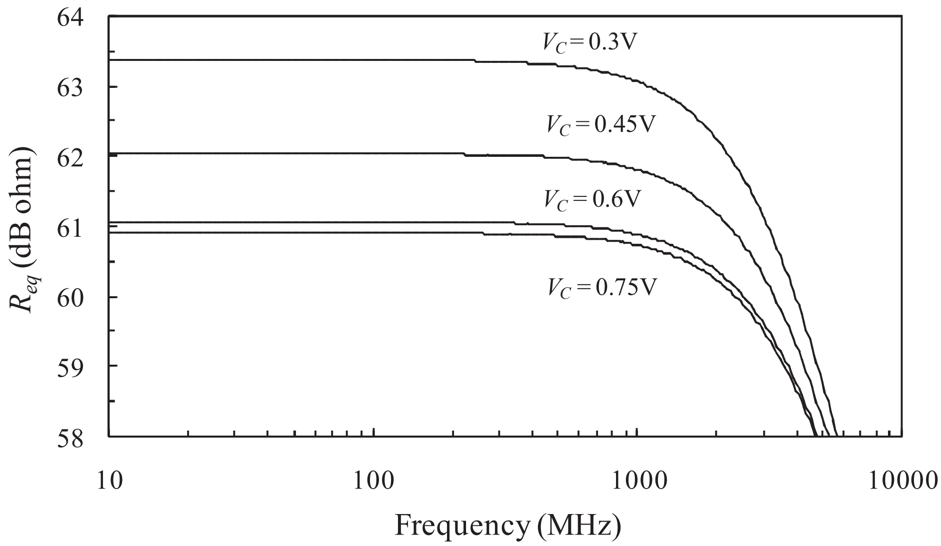

Figure 6. Frequency response of QFGMOS-based VCR

The comparative resistance simulation characteristics of VCR based on FGMOS and QFGMOS are shown in Figure 7. For the same value of control voltage (V_C = 0.3 V), R_{eq} for FGMOS is 1.30 kΩ whereas it is 1.48 kΩ for QFGMOS-based VCR. The power dissipation of QFGMOS-based VCR (0.04 μW) is less than that of its FGMOS version (0.7 μW).

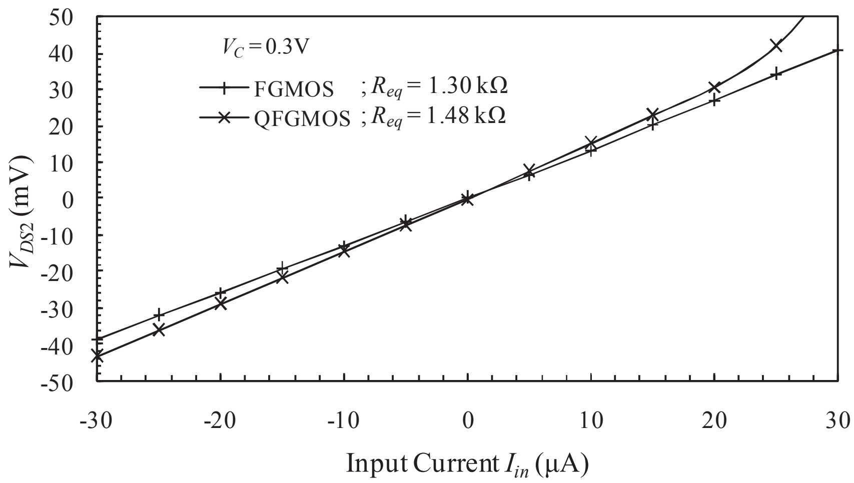

Figure 7. Comparative resistance simulation characteristics

The comparative frequency response of QFGMOS- and FGMOS-based VCRs is shown in Figure 8. The bandwidth of QFGMOS-based VCR is found to be 3.61 GHz, which is greater than that of FGMOS based VCR (490 MHz) due to the absence of large capacitance (C_2).

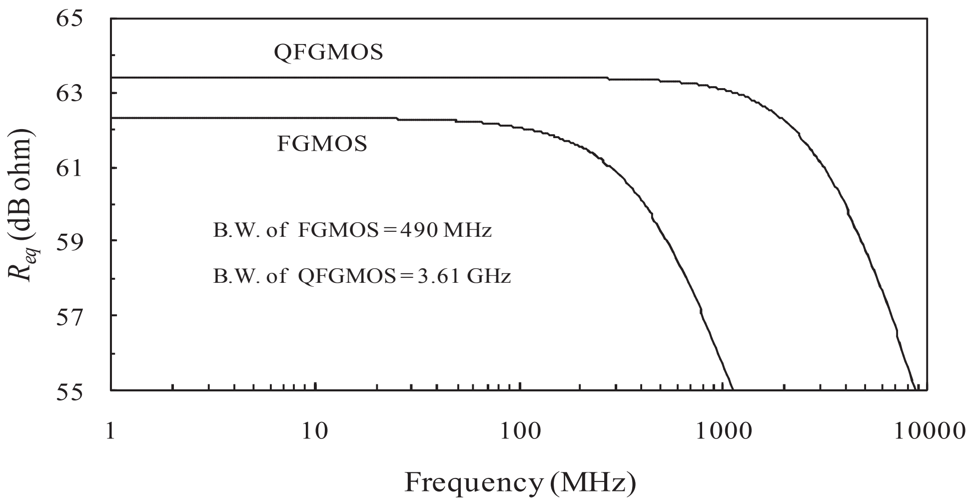

Figure 8. Comparative frequency response of QFGMOS- and FGMOS-based VCRs

CONCLUSIONS

In this paper, we have briefly described QFGMOS and used it to implement a voltage controlled resistor (VCR). The characteristics of QFGMOS-based VCR were compared with those of its FGMOS counterpart. It was found that for a given value of controlling voltage, the QFGMOS-based VCR simulates a higher value of resistance and offers a larger bandwidth as compared to its FGMOS version due to its inherent advantages and consumption of less power. The PSpice simulation results were found to be in conformity with the theory.

REFERENCES

1. I. L. S. Han and S. B. Park, "Voltage-controlled linear resistor by two MOS transistors and its application to active *RC* filter MOS integration", *Proc. IEEE,* **1984,** *72*, 1655-1657.
2. M. Gupta and R. Pandey, "FGMOS based voltage-controlled resistor and its applications", *Microelectron. J.,* **2010**, *41*, 25-32.
3. W. Liu and S. I. Liu, "CMOS tunable 1/x circuit and its applications", *IEICE Trans. Fundam. Electron. Commun. Comput. Sci.*, **2003**, *E86-A*, 1896-1899.
4. W. Liu, S. I. Liu and S. K. Wei, "CMOS current-mode divider and its applications", *IEEE Trans. Circuits Syst. II, Express Briefs,* **2005**, *52*, 145-148.
5. E. Sanchez-Sinencio and A. G. Andreou, "Low Voltage/Low Power Integrated Circuits and Systems: Low-Voltage Mixed-Signal Circuits", Wiley-IEEE Press, New York, **1999**, p. 562.
6. S. Yan and E. Sanchez-Sinencio, "Low voltage analog circuit design techniques: A tutorial", *IEICE Trans. Analog Integr. Circuits Syst.*, **2000**, *E00-A*, 179-196.
7. J. Ramirez-Angulo, S. C. Choi and G. G. Altamirano, "Low-voltage circuits building blocks using multiple-input floating-gate transistors", *IEEE Trans. Circuits Syst. I,* **1995,** *42*, 971-974.
8. S. Sharma, S. S. Rajput, L. K. Mangotra and S. S. Jamuar, "FGMOS current mirror: Behaviour and bandwidth enhancement", *Analog Integr. Circuits Signal Process.,* **2006**, *46*, 281-286.
9. J. Ramirez-Angulo, C. A. Urquidi, R. Gonzalez-Carvajal, A. Torralba and A. Lopez-Martin, "A new family of very low-voltage analog circuits based on quasi-floating-gate transistors", *IEEE Trans. Circuits Syst. II,* **2003**, *50*, 214-220.
10. J. Ramirez-Angulo, A. J. Lopez-Martin, R. G. Carvajal and F. M. Chavero, "Very low-voltage analog signal processing based on quasi-floating-gate transistors", *IEEE J. Solid State Circuits,* **2004,** *39*, 434-442.
11. C. Urquidi, J. Ramirez-Angulo, R Gonzalez-Carvajal and A. Torralba, "A new family of low-voltage circuits based on quasi-floating-gate transistors", The 2002 45th Midwest Symposium on Circuits and Systems, **2002**, Tulsa, USA, Vol.2, pp.93-96.
12. I. Seo and R. M. Fox, "Comparison of quasi-/ pseudo-floating gate techniques and low-voltage applications", *Analog Integr. Circuits Signal Process.,* **2006,** *47*, 183-192.
13. K. A. Townsend, J. W. Haslett and K. Ineiwski, "Design and optimization of low-voltage low-power quasi-floating gate digital circuits", Proceedings of 5th International Workshop on System-on-Chip for Real-Time Applications, **2005**, Washington, DC, USA, pp.132-136.
14. L. Ren, Z. Zhu and Y. Yang, "Design of ultra-low voltage op amp based on quasi-floating gate transistors", Proceedings of 7th International Conference on Solid-State and Integrated Circuits Technology, **2004**, Beijing, China, Vol.2, pp.1465-1468.
15. J. Alfredsson and B. Oelmann, "Influence of refresh circuits connected to low power digital quasi-floating gate designs", Proceedings of 13th IEEE International Conference on Electronics, Circuits and Systems, **2006**, Nice, France, pp.1296-1299.
16. A. Torralba, J. Galan, C. Lujan-Martinez, R. G. Carvajal, J. Ramirez-Angulo and A. Lopez-Martin, "Comparison of programmable linear resistors based on quasi-floating gate MOSFETs", Proceedings of IEEE International Symposium on Circuits and Systems, **2008,** Washington, USA , pp.1712-1715.

17. A. Torralba, C. Lujan-Martinez, R. G. Carvajal, J. Galan, M. Pennisi, J. Ramirez-Angulo and A. Lopez-Martin, "Tunable linear MOS resistors using quasi-floating-gate techniques", *IEEE Trans. Circuit Syst.-II: Express Briefs,* **2009**, *56*, 41-45.
18. R. Gupta, S. Sharma and S. S. Jamuar, "A low voltage current mirror based on quasi-floating gate MOSFETs", Proceedings of IEEE Asia Pacific Conference on Circuits and Systems, **2010**, Kuala Lumpur, Malaysia, pp.580-583.
19. H. Barthelemy, S. Meillere and E. Kussener, "CMOS sinusoidal oscillator based on current-controlled current conveyors", *Electron. Lett.,* **2002***, 38*, 1254-1256.

Maejo Int. J. Sci. Technol. **2013**, *7*(01), 26-41

Maejo International Journal of Science and Technology

ISSN 1905-7873
Available online at www.mijst.mju.ac.th

Full Paper

Synthesis, characterisation and antimicrobial activities of vic-dioxime derivatives containing heteroaromatic hydrazone groups and their metal complexes

Ilknur Babahan[1], Esin Poyrazoglu Coban[2] and Halil Biyik[2,*]

[1]Department of Chemistry, Adnan Menderes University, 09010, Aydin, Turkey
[2]Department of Biology, Adnan Menderes University, 09010, Aydin, Turkey

* Corresponding author, e-mail: hhalilb@gmail.com; tel: +902562182000; fax: +902562135379

Received: 7 April 2011 / Accepted: 9 January 2013 / Published: 9 January 2013

Abstract: Three novel heteroaromatic hydrazone derivatives bearing vic-dioxime groups (L^1H_2: 5-methyl-2-furfural hydrazone glyoxime, L^2H_2: 3-acetylpyridine hydrazone glyoxime and L^3H_2: 4-acetylpyridine hydrazone glyoxime) and their Ni(II), Cu(II) and Co(II) complexes were prepared. They were characterised by elemental analysis, gel permeation chromatography (GPC), FT-IR, UV, ^{1}H NMR and ^{13}C NMR. The antimicrobial activities of compounds L^1H_2, L^2H_2, L^3H_2 and their Ni(II), Cu(II) and Co(II) complexes were evaluated using the disc diffusion method against 13 bacteria and 5 yeasts. The minimal inhibitory concentrations (MICs) against 3 bacteria and 3 yeasts were also determined. Among the test compounds attempted, L^1H_2, $[Co(L^1H)_2(H_2O)_2]$, $[Ni(L^2H)_2]$, $[Cu(L^2H)_2]$, L^3H_2, $[Ni(L^3H)_2$ and $[Co(L^3H)_2(H_2O)_2]$ showed some activities against certain Gram-positive bacteria and some of the yeasts tested.

Key Words: vic-dioximes, hydrazone glyoximes, metal complexes, antimicrobial activity

---

INTRODUCTION

Schiff base ligands are well known for their wide range of applications in pharmaceutical and industrial fields [1-3]. Moreover, the hydrazone group plays an important role of the antimicrobial and possesses interesting antibacterial, antifungal [4-6] and anti-tubercular activities [7-12]. In addition, their varied coordinating behaviour makes them interesting candidates for metal-based drugs. Generally, the ligands act synergistically with metals towards their biological activity [11, 12].

Hydrazones possessing an azomethine proton (-NHN=CH-) constitute an important class of compounds for new drug development. Many researchers have synthesised these compounds as well as their metal complexes as target structures and evaluated their biological activities. These observations have guided the development of new hydrazones with varied biological activities [13]. The biological activity of complexes derived from hydrazones have been studied and contrasted with regard to their antibacterial, antitumoral, antiviral, antimalarial and antitubercular properties [14]. It has also been shown that the azomethine N, which has a lone pair of electrons in an sp^2 hybridised orbital, is biologically important [15].

Oximes are becoming increasingly important as analytical, biochemical and antimicrobial reagents and they have received attention due to their use as liquid crystals and dyes [16]. Coordination compounds of oximes also receive considerable attention due to their structural features. A large amount of work has been accumulated in areas such as structural stability and reactivity, biochemical modelling and synthesis of molecules with unusual electronic properties [e.g. 17, 18]. However, detailed literature survey reveals that there is only a little investigation made so far on the synthesis of metal hydrazone-oxime chelates. In continuation of our interest in the chemistry and biology of transition metal hydrazone-oxime chelates [19], we now carry out another systematic study of their synthesis and biological activity. Herein, the synthesis of the novel 5-methyl-2-furfural hydrazone glyoxime (L^1H_2), 3-acetylpyridine hydrazone glyoxime (L^2H_2) and 4-acetylpyridine hydrazone glyoxime (L^3H_2) as well as their complexes with Ni(II), Cu(II) and Co(II) ions are described and their antimicrobial properties are evaluated.

EXPERIMENTAL

The ^1H and ^{13}C NMR spectra were recorded in DMSO-d^6 on a Bruker-400 MHz spectrophotometer using tetramethylsilane as an internal reference. The apparent resonance multiplicity was described as: s (singlet), br s (broad singlet), d (doublet), dd (doublet of doublets), t (triplet), q (quartet) and m (multiplet). Infrared spectra were recorded in the range 400-4000 cm^{-1} on Spectrum 900 by Varian. Electronic spectra were recorded on a Shimadzu UV1601 spectrophotometer. Elemental analysis was carried out using PerkinElmer CHNS/O 2400. Room temperature magnetic susceptibility measurements were carried out using a Sherwood-Scientific Gouy magnetic balance (Calibrant: $Hg[Co(SCN)_4]$).

Cobalt(II) chloride hexahydrate (Merck), nickel(II) chloride hexahydrate (Merck), copper(II) chloride dihydrate (Merck), 5-methyl-2-furfuraldehyde (Merck), 3-acetylpyridine (Merck) and 4-acetylpyridine (Merck) were used as received for the sythesis of ligands and complexes. *Anti*-glyoximehydrazine (GH_2) was prepared according to a reported procedure [20]. Commercially available pure grade solvents, dried and purified by conventional procedure were used.

Synthesis

General procedure for the synthesis of ligands

L^1H_2, L^2H_2 and L^3H_2 were synthesised from the starting materials, namely *anti*-glyoximehydrazine (GH_2) [20] (Scheme 1), 5-methyl-2-furfuraldehyde (for L^1H_2), 3-acetylpyridine (for L^2H_2) and 4-acetylpyridine (for L^3H_2), using glacial acetic acid as a catalyst (Schemes 2 and 3). A cooled (5°C) solution of ketone or aldehyde (1 mmol) in ethanol was added dropwise into a cooled solution (5°C) containing 1 mmol (0.118 g) of *anti*-glyoximehydrazine (GH_2) and 3-5 drops of acetic acid with constant stirring. After the addition of aldehyde or ketone was completed, the solution was stirred for 2-4 hours at room temperature. The resulting solid compounds were filtered off, washed with water and ethanol and dried at room temperature in a vacuum oven. The results of the spectroscopic and composition analyses are as follows.

L^1H_2: yield 70 %; m.p. 118°C; colour yellow; IR (KBr, cm^{-1}) 3256 (N-H), 3124 (O-H), 3068 ($C\text{-}H_{arom.}$), 1608 ($C{=}N_{oxime}$), 1644 ($C{=}N_{hydr.}$), 953 (N-O); ^1H-NMR (DMSO, ppm) 10.18 s, 1H (NH), 11.50–10.65 s, 2H (OH), 6.70 s, 1H (C$\underline{H}$=NOH), 6.60 d (J 4.66 Hz), 2H (Ar-H), 7.80 s, 2H (-CH=N-NH), 2.20 s, 3H ($-CH_3$); ^{13}C-NMR (DMSO, ppm) 158.80 (-$\underline{C}$H=N-NH-), 154.64 (N-NH-$\underline{C}$=N-OH), 150.34 (C-$\underline{C}$H=N-OH), 148.48, 147.67, 141.13, 126.33 (Ar-C), 14.14 ($-CH_3$); UV-Vis (DMSO, λ_{max}/nm) 262, 394. For $C_8H_{10}O_3N_4$ (210.190 $g.mol^{-1}$), calculated: 45.71 % C, 4.80 % H, 26.66 % N; found: 45.65 % C, 4.46 % H, 26.24 % N.

L^2H_2: yield 60 %; m.p. 146.5°C; colour yellow; IR (KBr, cm^{-1}) 3364 (N-H), 3180 (O-H), 3066 ($C\text{-}H_{arom.}$), 1605 ($C{=}N_{oxime}$), 1656 ($C{=}N_{hydr.}$), 962 (N-O); ^1H-NMR (DMSO, ppm): 8.82 s, 1H (NH), 11.50–10.70 s, 2H (OH), 7.82 s, 1H (C$\underline{H}$=NOH), 8.70 s, 1H (Ar-H), 8.50 d (J 6.0 Hz), 1H, 7.94 d (J 7.0 Hz), 1H, 7.53 t (J 7.6 Hz), 1H (Ar-H), 2.13 s, 3H ($-CH_3$); ^{13}C-NMR (DMSO, ppm) 154.06 (-$\underline{C}$Me=N-NH-), 149.83 (N-NH-$\underline{C}$=N-OH), 147.58 (C-$\underline{C}$H=N-OH), 146.47, 141.86, 134.45, 133.60, 124.08 (Ar-C), 12.69 ($-CH_3$); UV-Vis (DMSO, λ_{max}/nm) 260. For $C_9H_{11}O_2N_5$ (221.216 $g.mol^{-1}$), calculated: 48.86 % C, 5.01 % H, 31.66 % N; found: 48.68 % C, 5.52 % H, 30.98 % N.

L^3H_2: yield 60 %; m.p. 136°C; colour yellow; IR (KBr, cm^{-1}) 3340 (N-H), 3161 (O-H), 3073 ($C\text{-}H_{arom.}$), 1605 ($C{=}N_{oxime}$), 1640 ($C{=}N_{hydr.}$), 960 (N-O); ^1H-NMR (DMSO, ppm) 8.92 s, 1H (NH), 11.60–10.87 s, 2H (OH), 7.61 s, 1H (C$\underline{H}$=NOH), 8.27 d (J 6.8 Hz) 4H (Ar-H), 2.19 s, 3H ($-CH_3$); ^{13}C-NMR (DMSO, ppm) 151.45 (-$\underline{C}$Me=N-NH-), 150.50 (N-NH-$\underline{C}$=N-OH), 146.17 (C-$\underline{C}$H=N-OH), 143.34, 141.68, 121.96 (Ar-C), 12.20 ($-CH_3$); UV-Vis (DMSO, λ_{max}/nm) 262. For $C_9H_{11}O_2N_5$ (221.216 $g.mol^{-1}$), calculated: 48.86 % C, 5.01 % H, 31.66 % N; found: 48.69 % C, 5.34 % H, 31.37 % N.

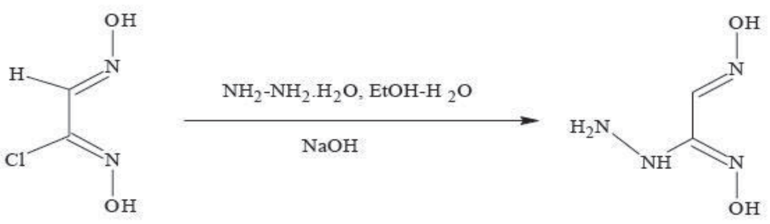

Scheme 1. Synthesis of *anti*-glyoximehydrazine [20]

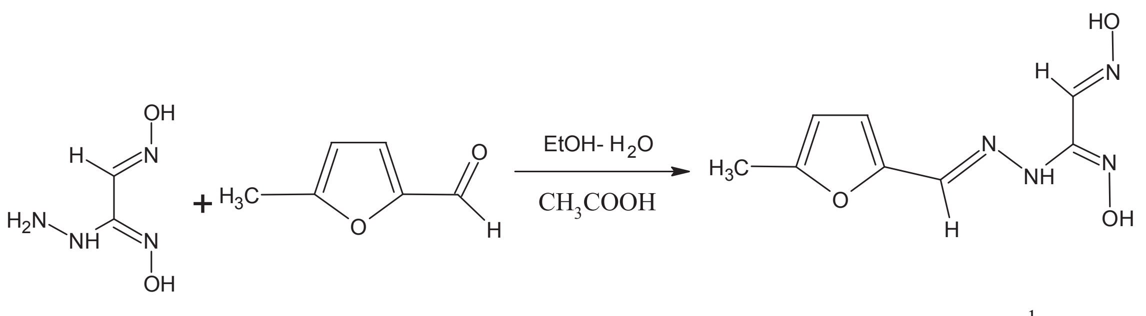

Scheme 2. Synthesis of 5-methyl-2-furfuraldehyde hydrazone glyoxime (L^1H_2)

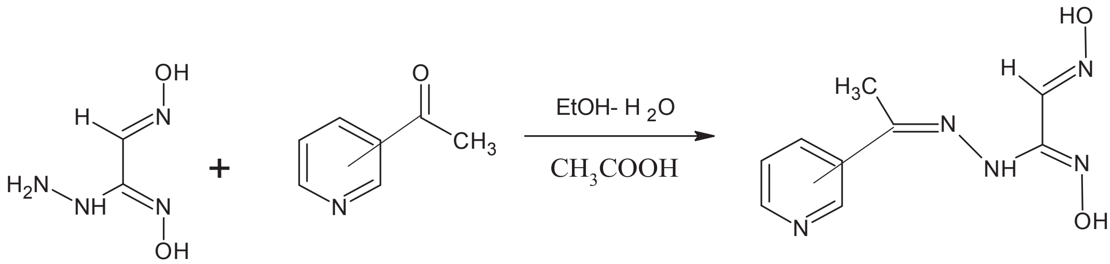

Scheme 3. Synthesis of 3-acetylpyridine hydrazone glyoxime (L^2H_2) and 4-acetylpyridine hydrazone glyoxime (L^3H_2)

Synthesis of the Ni(II), Cu(II) and Co(II) complexes of ligands

A solution of a metal salt (1 mmol: 0.237 g of $NiCl_2.6H_2O$, 0.170 g of $CuCl_2.2H_2O$ or 0.237 g of $CoCl_2.6H_2O$ in 20 mL of water) was added to 2 mmol of the ligand solution (0.420 g of L^1H_2, 0.442 g of L^2H_2 or 0.442 g of L^3H_2 in 15 mL of ethanol) with stirring. An initial sharp decrease in the pH of the solution from 5.5 to 3-3.5 was observed. After raising the pH to 5-5.5 using a 1% aqueous NaOH solution, the reaction mixture was kept in a hot water bath (60°C) for 2 hours to complete the precipitation. Then the precipitated complexes were filtered, washed with water and dried at room temperature in a vacuum oven. Results of the spectroscopic and composition analyses are shown as follows. Proposed structures of complexes are shown in Figures 1 and 2.

$[Ni(L^1H)_2]$: yield 60 %; m.p. >400°C; colour red; IR (KBr, cm^{-1}) 3437 (N-H), 3105 ($C\text{-}H_{arom.}$), 1578 ($C{=}N_{oxime}$), 1633 ($C{=}N_{hydr.}$), 1882 (H...OH), 947 (N-O); UV-Vis (DMSO, λ_{max}/nm) 221, 350, 490. For $C_{16}H_{18}O_6N_8Ni$ (477.058 $g.mol^{-1}$), calculated: 40.28 % C, 3.80 % H, 23.49 % N; found: 40.48 % C, 3.66 % H, 23.36 % N.

$[Cu(L^1H)_2]$: yield 60 %; m.p. >400°C; colour brown; IR (KBr, cm^{-1}) 3433 (N- H), 3120 ($C\text{-}H_{arom.}$), 1567 ($C{=}N_{oxime}$), 1622 ($C{=}N_{hydr.}$), 1735 (H...OH), 956 (N-O); UV-Vis (DMSO, λ_{max}/nm) 266, 322, 390. For $C_{16}H_{18}O_6N_8Cu$ (481.910 $g.mol^{-1}$), calculated: 39.88 % C, 3.76 % H, 23.25 % N; found: 39.03 % C, 3.87 % H, 23.68 % N.

$[Co(L^1H)_2(H_2O)_2]$: yield 60 %; m.p. >400°C; colour brown; IR (KBr, cm^{-1}) 3398 (N-H), 3121 (OH/H_2O), 3109 ($C\text{-}H_{arom.}$), 1573 ($C{=}N_{oxime}$), 1623 ($C{=}N_{hydr.}$), 1762 (H...OH), 949 (N-O); UV-Vis (DMSO, λ_{max}/nm) 255, 310, 390. For $C_{16}H_{22}O_8N_8Co$ (513.328 $g.mol^{-1}$), calculated: 37.44 % C, 4.32 % H, 21.83 % N; found: 37.20 % C, 3.94 % H, 22.32 % N.

$[Ni(L^2H)_2]$: yield 60 %; m.p. >400°C; colour red; IR (KBr, cm^{-1}) 3444 (N-H), 3109 ($C\text{-}H_{arom.}$), 1578 ($C{=}N_{oxime}$), 1652 ($C{=}N_{hydr.}$), 1782 (H...OH), 942 (N-O); UV-Vis (DMSO, λ_{max}/nm) 273, 388, 482. For $C_{18}H_{20}O_4N_{10}Ni$ (499.110 $g.mol^{-1}$), calculated: 43.32 % C, 4.04 % H, 28.06 % N; found: 43.08 % C, 4.34 % H, 27.44 % N.

$[Cu(L^2H)_2]$: yield 60 %; m.p. >400°C; colour brown; IR (KBr, cm^{-1}) 3393 (N-H), 3066 ($C\text{-}H_{arom.}$), 1574 ($C{=}N_{oxime}$), 1648 ($C{=}N_{hydr.}$), 1782 (H...OH), 941 (N-O); UV-Vis (DMSO, λ_{max}/nm) 267, 300, 390. For $C_{18}H_{20}O_4N_{10}Cu$ (503.962 $g.mol^{-1}$), calculated: 42.90 % C, 4.00 % H, 27.79 % N; found: 43.58 % C, 4.51 % H, 27.68 % N.

$[Co(L^2H)_2(H_2O)_2]$: yield (60 %); m.p. >400°C; colour brown; IR (KBr, cm^{-1}) 3380 (N-H), 3194 (OH/H_2O), 3072 ($C\text{-}H_{arom.}$), 1562 ($C{=}N_{oxime}$), 1636 ($C{=}N_{hydr.}$), 1749 (H...OH), 941 (N-O);

UV-Vis (DMSO, λ_{max}/nm) 264, 294, 404. For $C_{18}H_{24}O_6N_{10}Co$ (535.380 g.mol^{-1}), calculated: 40.38 % C, 4.52 % H, 26.16 % N; found: 40.54 % C, 4.51 % H, 26.86 % N.

[Ni($L^3H)_2$]: yield 60 %; m.p. >400°C; colour red; IR (KBr, cm^{-1}) 3437 (N-H), 3047 (C-$H_{arom.}$), 1588 (C=N_{oxime}), 1629 (C=$N_{hydr.}$), 1855 (H...OH), 950 (N-O); UV-Vis (DMSO, λ_{max}/nm) 270, 335, 498. For $C_{18}H_{20}O_4N_{10}Ni$ (499.110 g.mol^{-1}), calculated: 43.32 % C, 4.04 % H, 28.06 % N; found: 43.62 % C, 4.34 % H, 27.38 % N.

[Cu($L^3H)_2$]: yield 60 %; m.p. >400°C; colour brown; IR (KBr, cm^{-1}) 3422 (-NH), 3086 (C-$H_{arom.}$), 1562 (C=N_{oxime}), 1634 (C=$N_{hydr.}$), 1782 (H...OH), 949 (N-O); UV-Vis (DMSO, λ_{max}/nm) 258, 270, 394. For $C_{18}H_{20}O_4N_{10}Cu$ (503.962 g.mol^{-1}), calculated: 42.90 % C, 4.00 % H, 27.79 % N; found: 42.64 % C, 3.58 % H, 27.35 % N.

[Co($L^3H)_2(H_2O)_2$]: yield 60 %; m.p. >400°C; colour brown; IR (KBr, cm^{-1}) 3397 (N-H), 3225 (OH/H_2O), 3050 (C-$H_{arom.}$), 1589 (C=N_{oxime}), 1616 (C=$N_{hydr.}$), 1776 (H...OH), 946 (N-O); UV-Vis (DMSO, λ_{max}/nm) 258, 279, 395. For $C_{18}H_{24}O_6N_{10}Co$ (535.380 g.mol^{-1}), calculated: 40.38 % C, 4.52 % H, 26.16 % N; found: 40.85 % C, 5.05 % H, 25.94 % N.

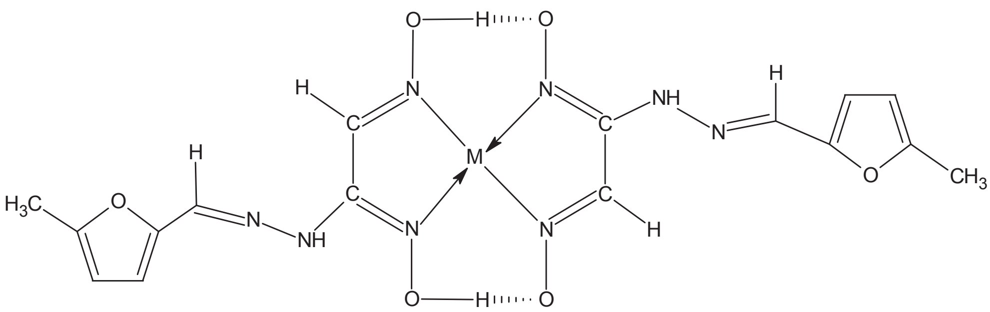

Figure 1. Suggested structure of Co(II)·2H_2O, Ni(II) and Cu(II) complexes of 5-methyl-2-furfuraldehyde hydrazone glyoxime

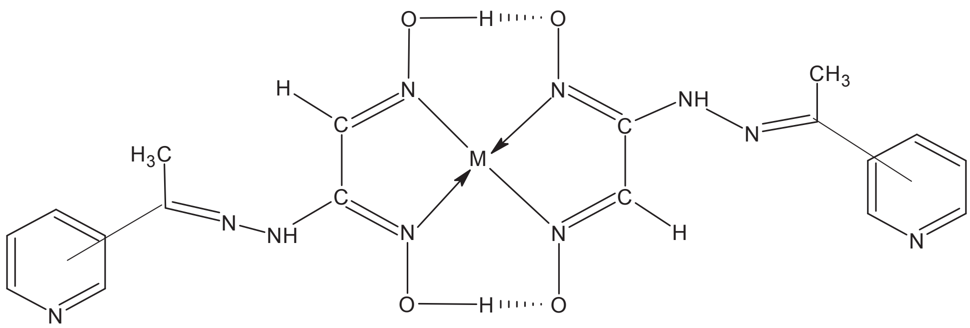

Figure 2. Suggested structure of the Co(II)·2H_2O, Ni(II) and Cu(II) complexes of L^2H_2 and L^3H_2 (3-acetylpyridine for L^2H_2 and 4-acetlypyridine for L^3H_2)

Biological Studies

Eight bacterial strains and one yeast strain were obtained from the American Type Culture Collection (ATCC, Rockville, MD, USA). Other strains were obtained from Faculty of Medicine, Adnan Menderes University. The Gram-negative (G-) were: *Escherichia coli* ATCC 25922, *Salmonella typhimurium* ATCC 14028, *Proteus sp.*, *Serratia marcescens* and *Enterobacter sp.*, and the Gram-positive (G+) were: *Micrococcus luteus* ATCC 9341, *Staphylococcus aureus* ATCC 25923, *Staphylococcus epidermidis* ATCC 12228, *Bacilllus cereus* ATCC 11778, *Bacillus thuringiensis*, *Enterococcus faecalis* ATCC 29212, *Streptococcus pneumoniae* ATCC 49617 and *Listeria sp*. The following five yeast strains, i.e. *Candida utilis*, *C. albicans*, *C. glabrata*, *C. Tropicalis* and *Saccharomyces cerevisiae* ATCC 9763, were also tested using disc diffusion method [21, 22] and the minumum inhitory concentration (MIC) was determined by broth dilution method [23].

Disc diffusion method

Screening for antibacterial and antifungal activities were carried out using sterile antibiotic discs (6 mm), following the standard procedure of Antimicrobial Disc Susceptibility Tests outlined by the National Committee for Clinical Laboratory Standards-NCCLS [21, 22]. Fresh stock solutions (30 $\mu g.mL^{-1}$) of the ligands were prepared in DMSO according to the needed concentrations for the experiments.

The inoculum suspensions of the tested bacteria and yeasts were prepared from the broth cultures (18-24 hr) and the turbidity equivalent adjusted to 0.5 McFarland standard tube to give a concentration of $1x10^8$ bacterial cells and $1x10^6$ yeast cells/mL. To test the antimicrobial activity of each aromatic hydrazone derivative bearing vic-dioxime group or its complex, a Mueller Hinton agar plate was inoculated with 0.1 mL broth culture of bacteria or yeast. Then a hole of 6 mm in diameter and depth was made on top with a sterile stick and filled with 10 µL of the hydrazone derivative or its complex containing vic-dioxime group.

Plates inoculated with *E. coli* ATCC 25922, *S. typhimurium* ATCC 14028, *S. aureus* ATCC 25923, *S. epidermidis* ATCC 12228, *E. faecalis* ATCC 29212*, S. pneumoniae* ATCC 49617, *Listeria sp., Proteus sp., S. Marcescens* and *Enterobacter sp*. were incubated at $37^{\circ}C$ for 24 hr and those inoculated with *M. luteus* ATCC 9341, *B. cereus* ATCC 11778, *B. thuringiensis, S. cerevisiae* ATCC 9763, *C. albicans* ATCC 90028, *C. glabata*, *C. utilis* and *C. tropicalis* were incubated at $30^{\circ}C$ for 24 hr. The diameter of the inhibition zone was then measured. Discs of chloramphenicol (C30, Oxoid), gentamycin (GN10 Oxoid), nystatin (NS100 Oxoid) were used as positive controls. The inhibition zones were compared with those of the reference discs.

Dilution method

Screening for antibacterial and antifungal activities were carried out by preparing a micro-dilution broth, following the procedure outlined in Manual of Clinical Microbiology [23]. All the bacteria were inoculated in the nutrient broth and incubated at 30-37°C for 24 hr while the yeasts were inoculated in malt extract broth and incubated at 30°C for 48 hr. The compounds were dissolved in DMSO (2 mg mL^{-1}) and then diluted in Mueller Hinton broth. Twofold serial dilution of the compounds were employed to determine the MIC ranging from 256 to 1.0 µg mL^{-1}. Cultures were grown at 30-37°C (18-20 hr) and the final inoculum was approximately 10^6 cfu mL^{-1}. Test cultures were incubated at 37°C (24 hr). The lowest concentration of antimicrobial agent that resulted in complete inhibition of the microorganisms was represented as MIC (µg mL^{-1}). As positive controls, streptomycin (I. E. Ulagay) for bacteria and nystatin (NS100, Oxoid) for yeast were used in the dilution method. In each case, the test was performed in triplicate and the results were expressed as means.

RESULTS AND DISCUSSION

Some physical properties, elemental analysis results and magnetic susceptibility data of the ligands and complexes are summarised in Table 1. FT-IR data of the ligands and their complexes are given in Table 2. ^{1}H-NMR and ^{13}C-NMR data of the ligands are given in Table 3. Attempts to isolate crystals suitable for X-ray diffraction were unsuccessful for the ligands and complexes. ^{1}H-NMR and ^{13}C-NMR spectra of these complexes could not be taken because of their very low solubility in organic solvents. FT-IR, UV, elemental analysis and magnetic susceptibility techniques were employed in order to determine the structural characteristics of the complexes. Antimicrobial activities of the ligands and their metal complexes are given Tables 4 and 5.

IR Spectra

The IR spectra of the new hydrazone-oxime compounds (L^1H_2, L^2H_2 and L^3H_2) were in accord with the previously reported oxime derivatives [16, 20, 24-27]. In the IR spectra of Co(II) complexes, the weak deformation vibration band assigned to the intramolecular hydrogen bond O-H....O bending vibration was observed around 1749-1776 cm^{-1} [16, 20, 27]. The C=N_{oxime} stretch decreased from 1608-1605 cm^{-1} in the free ligands to 1589-1562 cm^{-1} in the Co(II) complexes [22, 25, 28]. The coordinated H_2O molecules of $(L^1H)_2Co(H_2O)_2$ and $(L^2H)_2Co(H_2O)_2$ were identified by a broad OH absorption around 3225-3194 cm^{-1} with constant intensities after heating above 110°C for 24 hr. The IR spectra of Ni(II) and Cu(II) complexes exhibited a C=N_{oxime} stretching vibration around 1588-1562 cm^{-1}. These vibrations were at a lower frequency than for the free ligands, which were attributed to N,N- chelation [16, 20, 26-31].

A weak band around 1882-1735 cm^{-1} can be assigned to the intramolecular hydrogen bond O-H....O bending vibration [16-20, 31]. The intensity of the characteristic stretching and bending vibrations of the free ligands shifted and lowered on complex formation and new vibrational bands characteristic of the Ni(II) and Cu(II) complexes were observed.

The dioxime ligand, a neutral compound, forms, when complexed, a monoanion by the loss of an oxime proton with concomitant formation of an intra-molecular hydrogen bond. The cobalt ion coordinates with the ligand through its nitrogen donors in the equatorial positions [31]. The band O-H...O is absent in the ligand but appears in the spectrum of the complexes, showing that the Ni(II) and Cu(II) complexes have a square-planar structure (Figure 1).

NMR Spectra

The signals in the ^{1}H-NMR spectra of the ligands were in accord with the previously reported oxime derivatives [24, 31]. Two peaks were observed for the O-H protons of the oxime groups. These two deuterium-exchangeable singlets correspond to two inequivalent O-H protons that also indicate the *anti*-configuration of the O-H groups relative to each other [29-32].

In the ^{13}C-NMR spectra of the ligands, different signals which were observed at 154.64 ppm for L^1H_2, 149.83 ppm for L^2H_2 and 150.50 ppm for L^3H_2 (HN$\underline{C}$=N-OH), together with 150.34 ppm for L^1H_2, 147.58 ppm for L^2H_2 and 146.17 ppm for L^3H_2 (H-$\underline{C}$=N-OH) showed that the vic-dioximes are asymetrically substituted [25, 33]. The two different frequencies in each case also indicate that the vic-dioxime has *anti* structure [25].

Table 1. Physical properties and elemental analyses of the ligands and complexes

Compound Formula	m.p. (ºC)	(%) Yield	Colour	μ_{eff} [a] (BM)	Calculated (Found) % C	H	N
L^1H_2	118	65	Yellow	-	45.71(45.65)	4.80 (4.46)	26.66 (26.24)
$[Ni(L^1H)_2]$	> 400	60	Red	Dia.	40.28 (40.48)	3.80 (3.66)	23.49 (23.36)
$[Cu(L^1H)_2]$	> 400	47	Brown	1.75	39.88 (39.03)	3.76 (3.87)	23.25 (23.68)
$[Co(L^1H)_2(H_2O)_2]$	> 400	60	Brown	4.40	37.44 (37.20)	4.32 (3.94)	21.83(22.32)
L^2H_2	146.5	64	Yellow	-	48.86 (48.65)	5.01 (4.46)	31.66 (31.24)
$[Ni(L^2H)_2]$	> 400	60	Red	Dia.	43.32 (43.08)	4.04 (4.34)	28.06 (27.44)
$[Cu(L^2H)_2]$	> 400	55	Brown	1.75	42.90 (43.58)	4.00 (4.51)	27.79 (27.68)
$[Co(L^2H)_2(H_2O)_2]$	> 400	57	Brown	4.10	40.38 (40.54)	4.52 (4.51)	26.16 (26.86)
L^3H_2	136	68	Yellow	-	48.86 (48.69)	5.01 (5.34)	31.66 (31.37)
$[Ni(L^3H)_2]$	> 400	60	Red	Dia.	43.32 (43.62)	4.04 (4.34)	28.06 (27.38)
$[Cu(L^3H)_2]$	> 400	57	Brown	1.73	42.90 (42.64)	4.00 (3.58)	27.79 (27.35)
$[Co(L^3H)_2(H_2O)_2]$	> 400	50	Brown	4.21	40.38 (40.85)	4.52 (5.05)	26.16 (25.94)

[a] magnetic moment (Dia. = diamagnetic)

Table 2. Characteristic IR bands (cm^{-1}) of the vic-dioxime ligands and their metal complexes

Compound	(N-H)	(O-H) (OH/H_2O)	$(C{=}N)_{oxime}$	$(C{=}N)_{hydr.}$	$(C\text{-}H)_{arom.}$	$(C\text{-}H)_{aliph.}$	(N-O)	(OH...O)
L^1H_2	3256 (b)	3124 (b)	1608 (s)	1644 (s)	3068 (w)	2935-2820 (w)	953 (m)	-
$[Ni(L^1H)_2]$	3437 (b)	-	1578 (s)	1633 (s)	3105 (w)	2920- 2898 (w)	947 (m)	1882 (w)
$[Cu(L^1H)_2]$	3433 (b)	-	1567 (s)	1622 (s)	3120 (w)	2912-2850 (w)	956 (m)	1735 (w)
$[Co(L^1H)_2(H_2O)_2]$	3398 (b)	3121 (b)	1573 (s)	1623 (s)	3109 (w)	2916-2835 (w)	949 (m)	1762 (w)
L^2H_2	3364 (b)	3180 (b)	1605 (s)	1656 (s)	3066 (w)	2942-2808 (w)	962 (m)	-
$[Ni(L^2H)_2]$	3444 (b)	-	1578 (s)	1652 (s)	3109 (w)	2912-2850 (w)	942 (m)	1782 (w)
$[Cu(L^2H)_2]$	3393 (b)	-	1574 (s)	1648 (s)	3066 (w)	2908-2850 (w)	942 (m)	1782 (w)
$[Co(L^2H)_2(H_2O)_2]$	3380 (b)	3194 (b)	1562 (s)	1636 (s)	3072 (w)	2919-2851 (w)	941 (m)	1749 (w)
L^3H_2	3340 (b)	3161 (b)	1605 (s)	1640 (s)	3073 (w)	2957-2844(w)	960 (m)	-
$[Ni(L^3H)_2]$	3437 (b)	-	1588 (s)	1629 (s)	3047 (w)	2920-2843 (w)	950 (m)	1855 (w)
$[Cu(L^3H)_2]$	3422 (b)	-	1562 (s)	1634 (s)	3086 (w)	2924-2850 (w)	949 (m)	1782 (w)
$[Co(L^3H)_2(H_2O)_2]$	3397 (b)	3225 (b)	1589 (s)	1616 (s)	3050 (w)	2912-2858 (w)	946 (m)	1776 (w)

Note: s = strong, m = medium, w = weak, b = broad

Table 3. Important ^{1}H-NMR and ^{13}C-NMR signals (ppm) of ligands in DMSO-d_6

	^{1}H-NMR					
	-OH[a]	-NH[a]	Ar-H	CH=NOH	CH=NNH	$-CH_3$
L^1H_2	11.50-10.65, s, 2H	10.18, s, 1H	7.00, 6.20, d, 2H	6.70, s, 1H	7.80, s, 1H	2.20, s, 3H
L^2H_2	11.50-10.70, s, 2H	8.82, s, 1H	8.50, 7.94, d, 2H 8.70 s, 1H, 7.53, t, 1H	7.82, s, 1H	-	2.13, s, 3H
L^3H_2	11.60-10.87, s, 2H	8.92, s, 1H	8.54, 7.99, d, 4H	7.61, s, 1H	-	2.19, s, 3H

	^{13}C-NMR				
	HNC=NOH	HC=NOH	Me(H)C=NNH	Ar-C	$-CH_3$
L^1H_2	154.64	150.34	158.80	148.48-126.33	14.14
L^2H_2	149.83	147.58	154.06	146.47-124.08	12.69
L^3H_2	150.50	146.17	151.45	143.34-121.96	12.20

[a] Disappears on D_2O exchange.

Table 4. Antimicrobial activities of ligands and their metal complexes (Inhibition zone in mm)

Test Microorganism	1	2	3	4	5	6	7	8	9	10	11	12	GN10	C30	NS100
Escherichia coli ATCC 25922	-	-	-	-	-	-	-	-	-	-	-	-	21	24	NT
Salmonella typhimurium ATCC 14028	-	-	-	-	-	-	-	-	-	-	-	-	16	17	NT
*Proteus sp.**	-	-	-	-	-	-	-	-	-	-	-	-	24	17	NT
*Serratia marcescens**	-	-	-	-	-	-	-	-	-	-	-	-	19	23	NT
Micrococcus luteus, ATCC 9341	-	-	-	-	-	-	-	-	-	-	-	-	15	25	NT
*Enterobacter sp.**	-	-	-	-	-	-	-	-	-	-	-	-	20	19	NT
Staphylococcus aureus ATCC 25923	-	-	-	-	-	-	-	-	-	-	-	12	20	23	NT
Staphylococcus epidermidis ATCC 12228	-	-	-	-	-	-	-	-	-	-	-	11	17	22	NT
Bacilllus cereus ATCC 11778	10	-	-	-	-	11	12	-	-	11	11	18	24	23	NT
*Bacillus thuringiensis**	-	-	-	13	-	-	-	-	13	-	-	12	21	26	NT

Table 4. (Continued)

Test Microorganism	1	2	3	4	5	6	7	8	9	10	11	12	GN10	C30	NS100
Enterococcus faecalis 29212	-	-	-	-	-	-	-	-	-	-	-	-	11	16	NT
Streptococcus pneumoniae ATCC 49617	9	-	-	-	-	-	-	-	-	-	-	13	20	24	NT
*Listeria sp**	-	-	-	-	-	-	-	-	-	-	-	-	11	16	NT
*Candida utilis**	-	-	-	10	-	-	-	-	-	-	-	17	NT	NT	21
*Candida albicans**	-	-	-	-	-	-	-	-	-	-	-	-	NT	NT	21
*Candida glabata**	-	-	-	-	-	-	-	-	-	-	-	-	NT	NT	15
*Candida tropicalis**	-	-	-	-	13	-	-	-	14	12	-	-	NT	NT	15
Saccharomyces cerevisiae ATCC 9763	11	-	-	-	-	11	10	-	10	-	-	-	NT	NT	15

Note: 1= L^1H_2, 2= $[Ni(L^1H)_2]$, 3= $[Cu(L^1H)_2]$, 4= $[Co(L^1H)_2(H_2O)_2]$, 5= L^2H_2, 6= $[Ni(L^2H)_2]$, 7= $[Cu(L^2H)_2]$, 8= $[Co(L^2H)_2(H_2O)_2]$, 9= L^3H_2, 10= $[Ni(L^3H)_2]$, 11= $[Cu(L^3H)_2]$, 12= $[Co(L^3H)_2(H_2O)_2]$
C30= chloramphenicol, GN10= gentamycin, NS100= nystatin
(-)= No zone, NT= Not tested
* from Faculty of Medicine, Adnan Menderes University

Table 5. Antimicrobial activities of ligands and their metal complexes (MIC, $\mu g.mL^{-1}$)

Test Microorganism	1	4	5	6	7	9	10	11	12	Str	NS100
Bacilllus cereus ATCC 11778	8	–	–	8	16	–	128	8	–	64	–
*Bacillus thuringiensis**	–	16	–	–	–	64	–	–	32	64	–
Streptococcus pneumoniae ATCC 49617	16	–	–	–	–	–	–	–	128	128	–
*Candida utilis**	–	4	–	–	–	–	–	–	4	–	64
*Candida tropicalis**	–	–	8	–	–	16	8	–	–	–	64
Saccharomyces cerevisiae ATCC 9763	16	–	–	16	–	32	–	–	–	–	128

Note: 1= L^1H_2, 2= $[Ni(L^1H)_2]$, 3= $[Cu(L^1H)_2]$, 4= $[Co(L^1H)_2(H_2O)_2]$, 5= L^2H_2, 6= $[Ni(L^2H)_2]$, 7= $[Cu(L^2H)_2]$, 8= $[Co(L^2H)_2(H_2O)_2]$, 9= L^3H_2, 10= $[Ni(L^3H)_2]$, 11= $[Cu(L^3H)_2]$, 12= $[Co(L^3H)_2(H_2O)_2]$
Compounds 2,3,8 did not show antibacterial activity.
Str= streptomycin, NS100= nystatin
(-)= no effect
* from Faculty of Medicine, Adnan Menderes University

Magnetic Susceptibility

The magnetic susceptibility measurements of the Ni(II) complexes indicate that these complexes are diamagnetic while the Co(II) and Cu(II) complexes are paramagnetic. The copper complexes showed 1.75 BM for L^1H_2, 1.75 BM for L^2H_2 and 1.73 BM for L^3H_2. These results indicate square-planar structures for the Cu(II) complexes [20, 25, 33-36]. The cobalt complexes showed 4.40 BM for L^1H_2, 4.10 BM for L^2H_2 and 4.21 BM for L^3H_2. The microanalysis shows that the complexes of Co(II) can be octahedral [20, 25, 33]. Therefore, square-planar geometry for the Ni(II) and Cu(II) complexes and octahedral geometry for the Co(II) complexes are proposed (Figures 1 and 2).

UV Spectra

The bands in the electronic spectra of the Ni(II), Cu(II) and Co(II) complexes were assigned to both a charge transfer transition from the metal to the anti-bonding orbital of the ligand and to a spin-allowed transition of the ligand. The general character of the spectra was very similar to that of the corresponding complexes of symmetrically disubstituted dioximate ligands. The d^8 metal ion, Ni(II), exhibited a preference for square planar geometry with the dioxime complexes. The decrease in the intensities of the transitions indicates coordination with the nitrogen atoms [37, 38].

Antimicrobial Assays

The three novel aromatic hydrazone derivatives containing vic-dioxime groups and their Ni(II), Cu(II) and Co(II) complexes exhibited moderate antimicrobial activity (Tables 4 and 5). Among the test compounds attempted, compounds 1, 4, 6, 7, 9, 10 and 12 showed slightly higher activity against some bacteria and yeasts (Table 4). The MIC values (Table 5) also indicate that some of the compounds tested exhibited moderate antimicrobial activity. Compounds 1, 4, 6, 7, 9, 10 and 12 showed stronger activity against some bacteria (*B. thuringiensis*, *B. cereus* ATCC 11778 and *Streptococcus pneumoniae* ATCC 49617) compared with streptomycin. These compounds also had strong activity against the yeasts (*Saccharomyces cerevisiae* ATCC 9763, *Candida utilis* and *Candida tropicalis*) compared with nystatin.

All the ligands and their metal complexes studied had no effect on the Gram-negative bacteria. In general, the ligands and their metal complexes have antimicrobial activities against Gram-positive bacteria, especially *B. cereus* ATCC 11778, *B. thuringiensis*, *S. pneumoniae* ATCC 49617 and yeasts, *S. cerevisiae* ATCC 9763 and *C. tropicalis C. utilis*.

Members of the genus *Bacillus* are aerobic spore-forming rods which are ubiquitous in nature [39]. Despite their widespread distribution, even as normal skin flora, *Bacillus* spp. rarely cause infections. An exception is *Bacillus cereus*, which is a well-known cause of food poisoning and dreaded post-traumatic endophthalmitis [39]. *B. cereus* can also cause opportunistic infections, mainly in the immuno-compromised host [39, 40]. Although *B. anthracis* and *B. cereus* behave as human pathogens and *B. thuringiensis* is a common insect pathogen, genetic evidence indicates that these microorganisms should be regarded as unique species [41]. *B. thuringiensis* has been used worldwide as a biopesticide in forestry and agriculture [41, 42], being non-pathogenic to humans and able to produce potent species-specific insecticidal activities. More recently, however, repeated observations are documenting the association of this microorganism with various infectious diseases in humans such as food-poisoning associated diarrhoea [43], corneal ulcer [44], periodontitis [39], and burn [45] and wound [46] infections.

The term candidiasis is often used to describe an infection caused by a yeast-like fungus *Candida albicans*. Species of *Candida* other than *C. albicans*, however, have the potential to cause infection, particularly in patients who are immunologically or physiologically compromised [44, 45]. *Candida tropicalis* has emerged as a potentially dangerous opportunistic fungus. This may be due both to an increased awareness and specific identification of *C. tropicalis* as an etiologic agent of infection and to an increase in the number of compromised patients susceptible to opportunistic fungi. *C. tropicalis* has been shown to be the most frequent opportunistic fungus isolated from specimens from patients in a critical care unit [45, 46]. *C. tropicalis* has also been reported to be a frequent opportunistic pathogen in a cancer hospital [47] and has been identified as the etiologic agent in a variety of infections including pyelonephritis [48], lower urinary tract infection, thrombophlebitis, arthritis, bursitis, meningitis, multiple organ infection, pericarditis and candida vulvovaginitis [47, 49].

Suggestions are made that the negative inductive effect plays a significant role. Dimerisation of oxime involves the formation of a pair of H bonds [19, 50]. This feature causes a decrease in electronic density of oximes compared with phenylhydrazones, thereby facilitating entry of the oxime into the cell. This is likely to increase the antibacterial potency [19, 50].

A comparative study of the ligands and their complexes as antibacterial agents indicates that the metal complexes are more active than the free ligands [19, 50]. Such increased activity of the metal chelates can be explained by the reduced polarity of the ligand due to the overlap of the ligand orbital and partial sharing of the positive charge of the metal ion with electron releasing groups. It is obvious that reducing the total electron density on free ligands makes the diffusion proceed faster through the bacterial cells [51].

It is generally observed that metal chelates have higher antibacterial activity than the free ligand due to an increase in cell permeability. The lipid membrane which surrounds the cell favours only the passage of lipid soluble materials and it is known that liposolubility is an important factor controlling antimicrobial activity [52-54]. Such screening of various organic compounds and identifying the active agents are essential because the successful prediction of a lead molecule and the drug-like properties at the onset of drug design will pay off later in drug development.

CONCLUSIONS

Three novel vic-dioxime derivatives containing hydrazone side groups and their transition metal complexes with Ni(II), Cu(II) and Co(II) were synthesised. The antimicrobial activities of compounds (L^1H_2, L^2H_2, L^3H_2 and their Ni(II), Cu(II) and Co(II) complexes) were evaluated using disc diffusion method against 13 bacteria and 5 yeasts. Minimal inhibitory concentration (MIC) dilution against 3 bacteria and 3 yeasts were also determined. Among the test compounds attempted, L^1H_2, $[Co(L^1H)_2(H_2O)_2]$, $[Ni(L^2H)_2]$, $[Cu(L^2H)_2]$, L^3H_2, $Ni(L^3H)_2$ and $[Co(L^3H)_2(H_2O)_2]$ showed activities against certain Gram-positive bacteria and certain yeasts. Some of them were comparatively higher or equipotent to the antibiotic and antifungal agents in the comparison tests. These compounds appeared to have moderate antibacterial and antifungal activity.

ACKNOWLEDGEMENTS

We thank the Research Fund of Adnan Menderes University-Turkey (FEF-08005).

REFERENCES

1. C. M. Metzler, A. Cahil and D. E. Metzler, "Equilibria and absorption spectra of Schiff bases", *J. Am. Chem. Soc.,* **1980**, *102,* 6075-6082.
2. J. W. Pyrz, A. L. Roe, L. J. Stern and L. Que Jr.*,* "Model studies of iron-tyrosinate proteins", *J. Am. Chem. Soc.*, **1985**, *107*, 614-620.
3. D. Chen and A. E. Martell, "Dioxygen affinities of synthetic cobalt schiff base complexes", *Inorg. Chem*., **1987**, *26*, 1026-1030.
4. C. Loncle, J. M. Brunel, N. Vidal, M. Dherbomez and Y. Letourneux, "Synthesis and antifungal activity of cholesterol-hydrazone derivatives", *Eur. J. Med. Chem.*, **2004***, 39*, 1067-1071.
5. S. Papakonstantinou-Garoufalias, N. Pouli, P. Marakos and A. Chytyroglou-Ladas, "Synthesis antimicrobial and antifungal activity of some new 3 substituted derivatives of 4-(2,4-dichlorophenyl)-5-adamantyl-1*H*-1,2,4-triazole", *Farmaco*, **2002***, 57*, 973-977.
6. B. K. Kaymakcioglu and S. Rollas, "Synthesis, characterization and evalution of antibuberculosis activity of some hydrazones", *Farmaco*, **2002**, *57*, 595-599.
7. R. Maccari, R. Ottana and M. G. Vigorita, "In vitro advanced antimycobacterial screening of isoniazid-related hydrazones, hydrazides and cyanoboranes: Part 14", *Bioorg. Med. Chem. Lett.,* **2005**, *15*, 2509-2513.
8. M. T. Cocco, C. Congiu, V. Onnis, M. C. Pusceddu, M. L. Schivo and A. De Logu, "Synthesis and antimycobacterial activity of some isonicotinoylhydrazones", *Eur. J. Med. Chem*., **1999**, *34*, 1071-1076.
9. D. G. Rando, D. N. Sato, L. Siqueira, A. Malvezzi, C. Q. F. Leite, A. T. de Amaral, E. I. Ferreira and L.C. Tavares, "Potential tuberculostatic agents. Topliss application on benzoic acid [(5-Nitro-thiophen-2-yl)-methylene]-hydrazide series", *Bioorg. Med. Chem*., **2002,** *10,* 557-560.
10. J. Patole, D. Shingnapurkar, S. Padhye and C. Ratledge, "Schiff base conjugates of *p*-aminosalicylic acid as antimycobacterial agents", *Bioorg. Med. Chem. Lett.,* **2006**, *16*, 1514-1517.
11. A. Maiti and S. Ghosh, "Synthesis and reactivity of the oxovanadium(IV) complexes of two N-O donors and potentiation of the antituberculosis activity of one of them on chelation to metal ions: Part IV"**,** *J. Inorg. Biochem.,* **1989**, *36*, 131-139.
12. D. S. Badiger, R. S. Hunoor, B. R. Patil, R. S. Vadavi, C. V. Mangannavar, I. S. Muchchandi, Y. P. Patil, M. Nethaji and K. B. Gudasi, "Synthesis, spectroscopic properties and biological evaluation of transition metal complexes of salicylhydrazone of anthranilhydrazide: X-ray crystal structure of copper complex", *Inorganica Chim. Acta*, **2012**, *384*, 197-203.
13. S. Rollas and S. G. Kucukguzel, "Biological activities of hydrazone derivatives", *Molecules*, **2007**, *12*, 1910-1939.
14. P. B. Sreeja, M. R. P. Kurup, A. Kishore and C. Jasmin, "Spectral characterizatıon, X-ray structure and biological investigations of copper(II) ternary complexes of 2-hydroxyacetophenone 4-hydroxybenzoic acid hydrazone and heterocyclic bases", *Polyhedron*, **2004**, *23*, 575-581.

15. S. Patai, "The Chemistry of Carbon–Nitrogen Double Bond", Interscience, NewYork, **1970**, pp.149-180.
16. F. Karapcin and F. Arabali, "Synthesis and characterization of 4-arylaminobi- phenylglyoximes and their complexes", *J. Chil. Chem. Soc.*, **2006**, *51*, 982-985.
17. P. Chaudhuri, "Homo- and hetero-polymetallic exchange coupled metal-oximates", *Coord. Chem. Rev.*, **2003**, *243*, 143-190.
18. M. Kurtoglu and S. A. Baydemir, "Studies on mononuclear transition metal chelates derived from a novel (*E*,*E*)-dioxime: Synthesis, characterization and biological activity", *J. Coord. Chem.*, **2007**, *60*, 655-665.
19. I. Babahan, E. Poyrazoglu, A. Özmen, H. Biyik and B. Isman, "Synthesis, characterization and biological activity of *vic*-dioxime derivatives containing benzaldehydehydrazone groups and their metal complexes", *African J. Microbiol. Res.*, **2011**, *5*, 271-283.
20. N. Sarıkavakli and G. Irez, "Synthesis and complex formation of some novel *vic*-dioxime derivatives of hydrazones", *Turk. J. Chem.*, **2005**, *29*, 107-115.
21. National Committee for Clinical Laboratory Standards, "Performance standards for antimicrobial disc susceptibility tests", Approved Standard NCCLS Publication, Villanova (PA), **1993**, pp.32-51.
22. C. H. Collins, P. M. Lyre and J. M. Grange, "Microbiological Methods", 6th Edn., Butterworths Co. Ltd., London, **1989**.
23. R. N. Jones, A. L. Barry, T. L. Gaven and J. A. Washington, "Manual of Clinical Microbiology", 4th Edn., American Society for Microbiology, Washington DC, **1984**, pp. 972-977.
24. I. Babahan, H. Anil and N. Sarikavakli, "Synthesis of novel tetraoxime derivative with hydrazone side groups and its metal complexes", *Turk. J. Chem.*, **2011**, *35*, 613-624.
25. I. Babahan, H. Anil and N. Sarikavakli, "Synthesis of *vic*-dioxime derivatives with hydrazone side groups and their metal complexes", *Turk. J. Chem.*, **2006**, *30*, 563-571.
26. M. Macit, H. Bati and B. Bati, "Synthesis of 4-benzyl-1-piperazineglyoxime and its use in the spectrophotometric determination of nickel", *Turk. J. Chem.*, **2000**, *24*, 81-88.
27. A. Kilic, E. Tas, B. Gumgum and A.Yılmaz, "Synthesis, spectroscopic and electrochemical investigations of two novel *vic*-dioximes and their mononuclear Ni^{II}, Cu^{II} and Co^{II} metal complexes containing morpholine group", *Chin. J. Chem.*, **2006**, *24*, 1599-1604.
28. E. Canpolat and M. Kaya, "Synthesis and formation of a new *vic*-dioxime complexes", *J. Coord. Chem.*, **2005**, *58*, 1217-1224.
29. E. Canpolat and M. Kaya, "Synthesis and characterization of a *vic*-dioxime derivative and investigation of its complexes with Ni(II), Co(II), Cu(II) and UO_2(VI) metals", *J. Coord. Chem.*, **2002**, *55*, 961-968.
30. E. Ozcan, E. Karapinar and B. Demirtas, "Synthesis of four new *vic*-dioximes and their nickel(II), cobalt(II), copper(II) and cadmium(II) complexes", *Transit. Metal Chem.*, **2002**, *27*, 557-561.

31. A. Bilgin and Y. Gok, "Synthesis and characterization of a new dioxime and its cobalt(III) complexes as vitamin B_{12} models", *Synth. React. Inorg. Met.-Org. Chem.*, **2001**, *31*, 1717-1730.
32. M. Dolaz, M. Tumer and A. Golcu, "Synthesis and spectrophotometric investigation of a new *vic*-dioxime ligand and its transition metal complexes", *Turk. J. Chem.*, **2001**, *25*, 491-500.
33. S. Serin, "New transition metal complexes *vic*-dioximes", *Transit. Metal Chem.*, **2001**, *26*, 300-306.
34. E. Tas, M. Ulusoy and M. Guler, "Synthesis of a novel oxime ligand: Characterization and investigation of its complexes with some metal ions", *Synth. React. Inorg. Metal-Org. Chem.*, **2004**, *34*, 1211- 1221.
35. S. Y. Ucan and B. Mercimek, "Synthesis and characterization of tetradentate N_2O_2 Schiff base ligands and their transition metal complexes", *Synth. React. Inorg. Met.-Org. Nano- Met. Chem.*, **2005**, *35*, 197-201.
36. M. Durmuş, V. Ahsen, D. Luneau and J. Pecaut, "Synthesis and structures of morpholine and its Ni(II) complexes", *Inorg. Chim. Acta*, **2004**, *357*, 588-594.
37. E. Canpolat, M. Kaya and A. Yazici, "Synthesis and characterization of Co(II), Ni(II), Cu(II), and Zn(II) complexes with a new *vic*-dioxime (E,E)- N′-hydroxy-2-(hydroxyimino)-N-(4-{[(2-phenyl-1,3-dioxolan-4yl)methyl]amino}butyl)ethanimidamide", *Russian J. Coord. Chem.*, **2004**, *30*, 87-93.
38. M. Kurtoglu, E. Ispir, N. Kurtoglu and S. Serin, "Novel *vic*-dioximes: Synthesis, complexation with transition metal ions, spectral studies and biological activity", *Dyes Pigments*, **2008**, *77*, 75-80.
39. C. U. Tuazon, "Other *Bacillus* species", in "Principles and Practice of Infectious Diseases" (Ed. G. E. Mandell, J. E. Bennett and R. Dolin), 4th Edn., Churchill Livingstone, Edinburgh, **1995**, pp. 1890-1894.
40. F. A. Drobniewski, "*Bacillus cereus* and related species", *Clin. Microbiol. Rev.*, **1993**, *6*, 324-338.
41. E. Helgason, D. A. Caugant, I. Olsen and A. B. Kolstø, "Genetic structure of population of *Bacillus cereus* and *B. thuringiensis* isolates associated with periodontitis and other human infections", *J. Clin. Microbiol.*, **2000**, *38*, 1615-1622.
42. E. Schnepf, N. Crickmore, J. Van Rie, D. Lereclus, J. Baum, J. Feitelson, D. R. Zeigler and D. H. Dean, "*Bacillus thuringiensis* and its pesticidal crystal proteins", *Microbiol. Mol. Biol. Rev.*, **1998**, *62*, 775-806.
43. S. G. Jackson, R. B. Goodbrand, R. Ahmed and S. Kasatiya, "*Bacillus cereus* and *Bacillus thuringiensis* isolated in a gastroenteritis outbreak investigation", *Lett. Appl. Microbiol.*, **1995**, *21*, 103-105.
44. J. W. Rippon, "Medical Mycology: The Pathogenic Fungi and the Pathogenic Actinomycetes", 2nd Edn., W. B. Saunders Co., Philadelphia, **1982**, pp.615-640.
45. J. R. Wingard, W. G. Merz and R. Saral, "*Candida tropicalis*: A major pathogen in immunocompromised patients", *Ann. Int. Med.*, **1979**, *91*, 539-543.

46. L. G. Morganti, M. P. Delogu, Tampieri, G. R. Gristina, R. Dominici and G. De Ritis, "Spread of opportunistic fungi at a critical care unit: A study of 55 patients", *Acta Anaesthesiol. Ital.*, **1982**, *33*, 605-610.
47. R. Horn, B. Wong, T. E. Kiehn and D. Armstrong, "Fungemia in a cancer hospital: Changing frequency, earlier onset, and results of therapy", *Rev. Infect. Dis.*, **1985**, *7*, 646-655.
48. S. M. Seidenfeld, C. F. Lemaistre, H. Setiawan and R. S. Munford, "Emphysematous pyelonephritis caused by *Candida tropicalis*", *J. Infect. Dis*., **1982**, *146*, 569.
49. G. N. Ling, "The role of inductive effect in the determination of protein structure", *Physiol. Chem. Phys. Med. NMR*, **1986**, *18*, 3-16.
50. M. M. Hania, "Synthesis and antibacterial activity of some transition metal complexes of oxime, semicarbazone and phenylhydrazone", *E- J. Chem.*, **2009**, *6*, 508-514.
51. N. Raman, A. Kulandaisamy and K. Jeyasubramanian, "Synthesis, spectral, redox and biological activities of schiff base transition metal(II) complexes derived from 4-aminoantipyrine and Benzil", *Synth. React. Inorg. Met-Org. Nano-Met. Chem.* **2002,** *32,* 1583-1610.
52. R. Nair, A. Shah, S. Baluja and S. Chanda, "Synthesis and antibacterial activity of some Schiff base complexes", *J. Serb. Chem. Soc.*, **2006**, *71*, 733-744.
53. J. Parekh, P. Inamdhar, R. Nair, S. Baluja and S. Chanda, "Synthesis and antibacterial activity of some schiff bases derived from 4-aminobenzoic acid", *J. Serb. Chem. Soc.*, **2005**, *70***,** 1155-1161.
54. Y. K. Vaghasia, R. Nair, M. Soni, S. Baluja and S. Chanda, "Synthesis, structural determination and antibacterial activity of compounds derived from vanillin and 4-aminoantipyrine", *J. Serb. Chem. Soc.*, **2004**, *69*, 991-998.

Maejo Int. J. Sci. Technol. **2013**, *7*(01), 42-47

Maejo International Journal of Science and Technology

ISSN 1905-7873
Available online at www.mijst.mju.ac.th

Short Communication

Mixed cropping of annual feed legumes with barley improves feed quantity and crude protein content under dry-land conditions

Khoshnood Alizadeh[1,]* and Jaime A. Teixeira da Silva[2]

[1] Dry-land Agricultural Research Institute, P. O. Box 119, Maragheh, Iran
[2] Faculty of Agriculture and Graduate School of Agriculture, Kagawa University, Miki cho, Kita gun, Ikenobe, 761-0795, Japan
* Corresponding author, e-mail: khoshnod2000@yahoo.com; tel: +98-421-2228078; fax: +98-421-2222069

Received: 20 July 2011 / Accepted: 16 January 2013 / Published: 18 January 2013

Abstract: The objective of this research is to determine a suitable mixture of annual feed legumes and barley as a winter crop under dry-land conditions. Seeds of Hungarian vetch (cv. 2670), smooth vetch (cv. Maragheh), and local varieties of grass pea and field pea were mixed with barley (cv. Abidar) in a 1:1 ratio and were tested, along with related monoculture. All legumes in the mixture survived winter while legumes alone, except Hungarian vetch, did not survive in the cold areas. The maximum fresh and dry forage yields (56 and 15 ton ha^{-1} respectively) were obtained from a mixture of smooth vetch and barley in provinces with mild winter and more than 400 mm of rainfall. The mixture of barley and smooth vetch resulted in the highest mean crude protein content (17%). Autumn seeding of smooth vetch and barley in a 1:1 ratio produced more than 2 ton ha^{-1} of dry biomass with good quality in all studied areas and thus could serve as an alternative cropping system after wheat/barley in cold and semi-cold dry land.

Keywords: mixed cropping, field pea, grass pea, Hungarian vetch, smooth vetch, barley

INTRODUCTION

Dry land occupies about 6.2 million ha across Iran. It is mainly used for wheat and food legume production while about 2-3 million ha of arable land is left fallow each year, mainly due to the lack of suitable cold-tolerant varieties in rotation with cereals [1]. The resource base of dry-land agriculture is experiencing increasing pressure due to rapidly growing human population and demands for livestock. Considerable variation in herbage and grain yields of improved vetches (*Vicia* spp.) and grass pea (*Lathyrus* spp.) under rainfed conditions in different environments has been reported. Rainfall and temperature dictate the relative importance of feed legume species. Introduction of annual feed legumes in dry-land cropping systems that are dominated by cereals could reduce the risk of pests and diseases and increase sustainable productivity [2]. Mixed cropping of cereals with forage legumes can improve the quantity and quality of fodder compared to a pure cereal crop [3, 4].

Lithourgidis et al. [5] evaluated the forage yield of common vetch mixed with oat and triticale in Greece and reported that mixtures of annual feed legumes and winter cereals have great potential for forage production in rainfed conditions and a mixture of common vetch and oat at a ratio of 2:1 gave the highest forage yield. In highlands with harsh winter conditions there are more limitations. Pure stands of most feed legumes in autumn planting under cold dry-land conditions of Iran are damaged because of freezing temperature during winter [6]. The problem becomes more serious when monoculture of feed legumes as a spring crop does not provide remarkable results for forage production in highlands because of a short growing season. On the other hand, winter cereals provide high yields in terms of dry weight but they produce forage with low protein. Moreover, the forage quality is generally lower than that required to meet production goals for many classes of livestock [2]. In a legume-cereal mixture, the companion cereal provides structural support for the legume, improve light interception and facilitate mechanical harvest while the legume in mixture improves forage quality [3]. Other benefits of the mixture include greater uptake of water and nutrients, enhanced weed suppression and increased soil conservation [7].

Competition between component species in a mixture may affect the yield and quality of forage produced [8]. Competition normally reduces yield of the mixture compared with cereal monoculture [9], although higher yields have been reported when competition between the two species of a mixture is lower than competition within the same species [2]. Cereal and legume species that are used in a mixture have different levels of competition and interaction. Caballero and Goicoechea [9] and Thomson et al. [10] reported that the most suitable cereal for a mixture with common vetch is oat (*Avena sativa* L.), whereas Thomson et al. [11] and Roberts et al. [8] reported that barley (*Hordeum vulgare* L.) and wheat (*Triticum aestivum* L.) are the most suitable cereals for mixtures. Seeding ratio is another factor that affects the competition between two species of a mixture [12]. Although competition is a factor that can affect forage yield and quality, there have been no reports on the effect of different cereals and different seeding ratios on the growth rate of legume-cereal mixtures. Competition can also have a significant effect on the growth rate of different species used in a mixture [5].

The objective of the present work is to evaluate biomass yield and protein content in mixtures of barley and different varieties of annual feed legumes, viz. Hungarian vetch, smooth vetch, grass pea and field pea at 1:1 seeding ratio. Barley serves as the winter crop under rainfed conditions.

MATERIALS AND METHODS

Seeds of Hungarian vetch (*Vicia panonica* L., cv. 2671), smooth vetch (*Vicia dasycarpa* L., cv. Maragheh), grass pea (*Lathyrus sativus* L., cv. Naghadeh) and local field pea (*Pisum sativum* L., cv. Zanjan) were mixed with barley (*Hordeum vulgare* L., cv. Abidar) at 1:1 ratio. Since seeding rate for the mixture was proportional to the pure stand seeding rate, we used 125 legume seeds and 200 barley seeds to make 1:1 mixture for each square metre. Experimental fields were prepared by chisel-ploughing followed by surface cultivation at the end of September. Appropriate N-P fertiliser (40 kg ha^{-1} N + 20 kg ha^{-1} P_2O_5) was applied uniformly to the soil just before seeding. Five different mixtures of barley and feed legumes, along with related monoculture, were planted in a randomised complete block design with three replications in mid-October under rainfed condition. The same experiment was performed in Golestan province in the north and Kermanshah province in the west, considered to be typical semi-cold areas, and in the north-west (East Azarbaijan, Zanjan and Kurdestan provinces), considered to be typical cold highlands of Iran. Each plot size was 10 m^2. Hay was harvested when the legumes initiated pod formation, which coincided with the milky stage of barley. At that time, samples from a randomly selected 1-m^2 area of each plot were cut to the ground level. Sub-samples (0.3 kg biomass from each plot) were dried at 70°C for 48 hr to determine dry matter yield. Crude protein, crude fibre and crude ash were then determined. The nitrogen content of hay was determined by the micro-Kjeldahl procedure described by Nelson and Sommers [13] while the crude protein concentration was calculated as N×6.25. AOAC [14] methods were used to determine crude fibre and crude ash.

SPSS (version 10) software [15] was used for analysis of variance (ANOVA). Treatment mean differences were separated by the least significant difference (LSD) test at 0.05 probability level.

RESULTS AND DISCUSSION

All legumes in the mixtures survived winter successfully. However, pure stands of feed legumes except Hungarian vetch were damaged by severe frost (-20°C or lower) in the cold north-west areas. Low rainfall in early fall and rapidly decreasing temperature along with severe cold in winter restrict the planting of many crops in the Iranian cold drylands [6]. Planting legumes as monoculture is possible as a spring crop in cold dry land but optimal plant growth is hampered by many problems such as short growth season in the highlands, difficulty in soil preparation, missing early spring precipitation and soil compaction [6]. Mixed cropping makes use of environmental resources better than monoculture and competition between component crops is not high [16, 17].

The ANOVAs for forage yield indicate that there were significant differences among treatments and location interactions ($P \leq 0.01$). A mixture of smooth vetch and barley produced more biomass at all sites since the climbing nature of smooth vetch produced more condensed forage. Precipitation and temperature during the vegetative growth period were higher in Golestan province than in other areas, resulting in higher yields. Maximum fresh (56.9 ton ha^{-1}) and dry (15 ton ha^{-1}) forage yields were obtained from a mixture of smooth vetch and barley in Golestan and Kermanshah provinces with a mild winter and high rainfall. Results in East Azarbaijan (harsh winter with more than 90 days of freezing temperature) show that a mixed cultivation of smooth vetch and Hungarian vetch with barley was superior, with a mean of 9 ton ha^{-1} of fresh forage yield. The mixture of barley and field pea was superior in Kurdestan and Zanjan provinces, although significant differences ($P \leq 0.05$) of the mixture of barley and smooth vetch were lacking (Table 1). Differences may have arisen from environmental conditions such as favourable precipitation and temperature during the vegetative growth phase of each location. Karadag and Buyukburc [18] recommended 50% Hungarian vetch and 50% triticale mixture for optimal dry matter yield in the rainfed condition of north-east Turkey.

Table 1. Mean fresh and dry biomass yield (ton ha^{-1}) of different mixtures of feed legumes and barley (1:1 ratio)

	Smooth vetch + barley		Field pea+ barley		Hungarian vetch + barley		Grass pea + barley		Pure Hungarian vetch		Pure barley		LSD 5%	
	Fresh	Dry	Fresh	Dry	Fresh	Dry	Fresh	Dry	Fresh	Dry	Fresh	Dry	Fresh	Dry
Maragheh	9.1	4.4	8.7	4.7	9.1	5.1	8.6	4.3	7.3	3.4	10.1	5.2	0.5	0.4
Golestan	56.9	15.4	51.1	13.1	45.1	12.7	44.8	10.6	29.5	9.21	55.3	15.4	3.2	1.9
Kurdestan	8.1	2.1	9.8	3.1	4	1.1	3.9	1.2	3.5	0.97	5.5	2.53	2.1	1.6
Kermanshah	13.7	4.4	13.6	6.4	13.1	4.2	14.3	7.4	11.2	5.7	13.1	3.9	0.6	0.5
Zanjan	5.8	1.8	6.8	1.9	5.5	1.8	5.3	1.8	4.7	0.9	7.5	2.6	1.1	0.6

Nutritional analysis shows that the mixture of barley and smooth vetch had the highest crude protein content (17%) followed by Hungarian vetch and barley (15%) (Table 2). In contrast, barley monoculture had the lowest crude protein content (11%). The crude protein content of forage is one of the most important criteria for evaluating forage quality [19]. In all mixtures, the crude protein content was at least 20% more than that of the barley monoculture (Table 2). These results are in agreement with those reported by Giacomini et al. [20]. In addition, Jannink et al. [21] found that a vetch mixture had much higher crude protein content than pea and oat alone.

Table 2. Mean protein and other quality indices of different mixtures of feed legumes and barley (1:1 ratio)

Mix	Crude protein (%)	Fibre (%)	Ash (%)
Smooth vetch + barley	16.87	24.27	12.85
Hungarian vetch + barley	15.38	24.09	10.25
Field pea+ barley	13.63	24.88	11.54
Grass pea + barley	13.88	27.65	10.55
Pure Hungarian vetch	24.32	7.10	3.20
Pure barley	11.25	28.83	12.97

CONCLUSIONS

Autumn seeding of smooth vetch (cv. Maragheh) and barley (cv. Abidar) in 1:1 ratio produces considerable forage in terms of quantity and quality. The mixture could thus be a suitable alternative crop after wheat or barley in cold and semi-cold dry land.

ACKNOWLEDGEMENTS

We would like to thank Dr. N. Ariamanesh from the University of Western Australia for his kind assistance with English writing in an earlier version of the manuscript. The collaboration of Mr. M. Dorri, Mr. J. Lamei, Mr. A. Shabani and Mr. S. Bahrami at different Research Stations of Iran are greatly appreciated.

REFERENCES

1. K. Alizadeh, “Performance of Hungarian vetch as a winter crop in cold drylands”, Proceedings of 9th International Conference on Dryland Development, **2008**, Alexandria, Egypt, pp.543-544.
2. A. Clark, “Managing Cover Crops Profitably”, 3rd Edn., Sustainable Agriculture Research and Education, National Agricultural Laboratory, Beltsville (MD), **2007**.
3. D. R. Mpairwe, E. N. Sabiti, N. N. Umuna, A. Tegegne and P. Osuji, “Integration of forage legumes with cereal crops. I. Effects of supplementation with graded levels of lablab hay on voluntary food intake, digestibility, milk yield and milk composition of crossbred cows fed maize-lablab stover or oats-vetch hay ad libitum”, *Livest. Prod. Sci.*, **2003**, *79*, 193-212.
4. N. N. Umuna, P. O. Osuji, H. Khalili, I. V. Nsahlai and S. Cross, “Comparative feeding value of forages from two cereal-legume based cropping systems for beef production of crossbred (*Bos taurus* X *Bos indicus*) steers and subsequent performance of underfed and realimented steers”, *Anim. Sci.*, **1995**, *61*, 35-42.
5. A. S. Lithourgidis, I. B. Vasilakoglou, K. V. Dhima, C. A. Dordas and M. D. Yiakoulaki, “Forage yield and quality of common vetch mixtures with oat and triticale in two seeding ratios”, *Field Crops Res.*, **2006**, *99*, 106-113.
6. K. Alizadeh, “Feed legumes status in drylands of Iran - limitations and opportunities”, Proceedings of 5th International Food Legumes Research Conference, **2010**, Antalya, Turkey, pp.214-215.
7. I. B. Vasilakoglou, A. S. Lithourgidis and K. V. Dhima, “Assessing common vetch: Cereal intercrops for suppression of wild oat”, Proceedings of 13th International Symposium, European Weed Research Society, **2005**, Bari, Italy, pp.289-290.
8. C. A. Roberts, K. J. Moore and K. D. Johnson, “Forage quality and yield of wheat-vetch at different stages of maturity and vetch seeding rates”, *Agron. J.*, **1989**, *81*, 57-60.
9. R. Caballero and E. L. Goicoechea, “Utilization of winter cereals as companion crops for common vetch and hairy vetch”, Proceedings of 11th General Meeting of the European Grassland Federation, **1986**, Setuba, Portugal, pp.379-384.
10. D. J. Thompson, D. G. Stout and T. Moore, “Forage production by four annual cropping sequences emphasizing barley under irrigation in southern interior British Columbia”, *Can. J. Plant Sci.*, **1992**, *72*, 181-185.
11. E. F. Thomson, S. Rihawi and N. Nersoyan, "Nutritive value and yields of some forage legumes and barley harvested as immature herbage, hay and straw in North-West Syria", *Exp. Agric.*, **1990**, *26*, 49-56.

12. R. Caballero, E. L. Goicoechea and P. J. Hernaiz, “Forage yields and quality of common vetch and oat sown at varying seeding ratios and seeding rates of vetch”, *Field Crops Res.*, **1995**, *41*, 135-140.
13. D. W. Nelson and L. E. Sommers, “Total nitrogen analysis for soil and plant tissues”, *J. Assoc. Offic. Anal. Chem.*, **1980**, *63*, 770-778.
14. Association of Official Analytical Chemists (AOAC), “Official Methods of Analysis”, 11rd Edn., AOAC, Washington, DC, **1980**, p.125.
15. SPSS, “SPSS Base 8.0 User’s Guide and SPSS Applications Guide”, SPSS, Chicago, **1998**, p. 256.
16. K. V. Dhima, A. S. Lithourgidis, I. B. Vasilakoglou and C. A. Dordas, “Competition indices of common vetch and cereal intercrops in two seeding ratio”, *Field Crops Res.*, **2007**, *100*, 249-256.
17. R. Hatipoglu and T. Tukel, “Competition among plants in agricultural ecosystems”, *J. Agric. Col. Adana*, **1997**, *12*, 177-186.
18. Y. Karadag and U. Buyukburc, “Forage qualities, forage yields and seed yields of some legume-triticale mixtures under rainfed conditions”, *Acta Agric. Scand. B*, **2004**, *54*, 140-148.
19. G. Assefa and I. Ledin, “Effect of variety, soil type and fertilizer on the establishment, growth, forage yield, quality and voluntary intake by cattle of oats and vetches cultivated in pure stands and mixtures”, *Anim. Feed Sci. Technol.*, **2001**, *92*, 95-111.
20. S. J. Giacomini, E. R. O. Vendruscolo, M. Cubilla, R. S. Nicoloso and M. R. Fries, “Dry matter, C/N ratio and nitrogen, phosphorus and potassium accumulation in mixed soil cover crops in Southern Brazil”, *Rev. Bras. Ciencia Solo*, **2003**, *27*, 325-334.
21. J. L. Jannink, M. Leibman and L. C. Merrick, “Biomass production and nitrogen accumulation in pea, oat, and vetch green manure mixtures”, *Agron. J.*, **1996**, *88*, 231-240.

Maejo International
Journal of Science and Technology

ISSN 1905-7873
Available online at www.mijst.mju.ac.th

Full Paper

Influence of laser beam's image-plane position on geometry of through-holes in percussion-drilled glass using excimer laser

Ales Babnik*, Rok Petkovsek and Janez Mozina

University of Ljubljana, Faculty of Mechanical Engineering, Askerceva 6, SI-1000 Ljubljana, Slovenia

*Corresponding author, e-mail: ales.babnik@fs.uni-lj.si

Received: 19 August 2011 / Accepted: 22 January 2013 / Published: 25 January 2013

Abstract: We study the influence of a laser beam's image-plane position relative to the processed surface for the deep-hole, laser-microdrilling of soda-lime glass with an excimer 308-nm laser and mask-projection technique. It is demonstrated that the image-plane position has a significant influence on the hole's tapering and final depth. Holes with exit diameters up to 10 times smaller than the mask-image diameter are produced in the case of perforation during the appropriate process phase determined by the formation of the plasma plume.

Keywords: laser processing, excimer laser, mask-projection technique, glass micro-drilling, hole geometry

---

INTRODUCTION

Lasers with wavelengths in the UV region are convenient for processing different types of glass due to their high absorption coefficient. Percussion laser drilling is a method for the production of holes with diameter in the micrometre range [1, 2]. For this purpose a small focal diameter beam is needed, which can only be achieved using a high-quality, laser-beam source. Since the beam quality of the excimer laser is rather poor, a single-lens focusing scheme on its own cannot be used [3]. Instead, a special beam treatment should be used to achieve the required properties of the processing beam. Beam homogenisation in combination with a mask-projection technique is a well-known procedure for the processing treatment of the beam [4]. Such an optical system in combination with an excimer laser source is a useful tool for the production of precisely defined holes with diameter down to a few micrometres. However, the hole's definition is only maintained for a low aspect ratio (shallow hole depth compared to diameter). In this case, the physical properties of the laser light (energy and pulse duration) are predominant. The same processing system can also be used for drilling deep holes with a high aspect ratio when the geometrical properties (focus location and numerical aperture) are as important as the physical properties of the processing beam.

High-aspect-ratio holes drilled with a laser are tapered in most cases. The amount of deviation from the cylindrical shape primarily depends on the geometrical properties of the processing beam. Nearly cylindrical holes can be drilled using a high-quality beam (Gaussian intensity distribution) and a focusing system with a low numerical aperture (NA) [5]. The same processing conditions cannot be achieved when a mask-projection technique is used [2, 6]. Here, the beam diameter at the image plane is defined by the optical system's demagnification and the circular-aperture-mask diameter. It is to be expected that decreasing the image diameter reduces the deep-hole drilling efficiency due to an increase in NA of the focusing optics, which leads to an increased light absorption on the hole's wall. It should be noted that the intensity distribution at the processing point is a flat (top-hat) intensity profile. Consequently, it is probable that the shape of the hole becomes extremely conical or even horn-shaped and the hole's aspect ratio is expected to be small [6]. This deviation from the ideal cylindrical geometry can be prevented by both reducing the NA of the objective lens and properly adjusting the beam's processing point (i.e. mask image or focal point position) with respect to the sample surface. When considering the geometry of the laser micro-drilled hole, two further phenomena occurring inside the microhole need to be considered, i.e. refocusing [7, 8] and the wave-guide effect [9, 10]. These effects may maintain a high light intensity inside the hole, which leads to a cylindrically shaped microhole with a high aspect ratio. So a prediction of the maximum hole depth, calculated with respect to the beam-intensity reduction due to an increase of the beam radius while the beam penetrates into the bulk [11], cannot be confirmed in practice. An interesting calculation was also presented by Paterson et al. [12]. They showed that the hole's taper depends on the energy of the laser beam in such a way that the taper angle can even be negative, i.e. the hole's diameter increases with depth, at higher energy. However, their experiments were performed on a photoresist material and not on a glass-like material. Another model was presented by Tokarev at al. [1], who showed a similar hole-geometry behaviour at processing fluence up to 6 times higher than the threshold fluence. Their model was tested on polymers employed as the processing material. The results of a test ablation of polyimide with regard to the image-plane shift were presented by Gerlach at al. [4].

In general, laser-percussion deep microdrilling is characterised by three process phases according to the three different types of plasma-plume formation when the processing beam with a fluence higher than the threshold value is used. The three phases are related to the removal rate or the hole depth versus the laser pulse number [13, 14] and in a special situation can be clearly visible in the hole's cross section [9]. Knowledge of the beam-material interaction including the plasma formation in each of the three phases is helpful when through holes with the desired exit diameter are processed. Typically, perforation during the second phase results in an exit diameter slightly smaller than the beam focus diameter. When an exit hole diameter much smaller than the focus diameter is required, perforation should be performed during the third process phase. By using this approach an exit hole with a very small diameter, several times smaller than the focus diameter of the beam, can be achieved. Expertise in the production of small-diameter holes is important for some specific applications [6].

So far, research in the laser drilling of high-aspect-ratio holes was devoted mainly to process efficiency, viz. maximisation of the removal rate and the final depth of the hole. Only a few papers deal with an investigation of deep hole's geometry when processed with a mask-projection system, but none of them deals with the processing of glass material. In this paper we characterise the influence of the high-fluence beam's image-plane position relative to the sample surface on the hole's geometry in percussion-drilled glass. We present the results of some typical combinations of the pulse energy and the NA of the objective-lenses assembly.

EXPERIMENTAL SET-UP

A scheme of our experimental set-up for the mask-projection drilling technique is shown in Figure 1. For the processing laser-beam source, an excimer laser is used with the following characteristics: wavelength $\lambda = 308$ nm, pulse duration = 20 ns, repetition rate = 20 Hz and beam energy up to 100 mJ. The excimer laser is a typical source with a low-quality beam. In our case, a beam with a rectangular profile (5 x 40 mm) and non-uniform beam intensity is emitted from the source. Therefore, a special treatment—homogenisation and spatial filtering—is involved to improve the beam quality at the processing point.

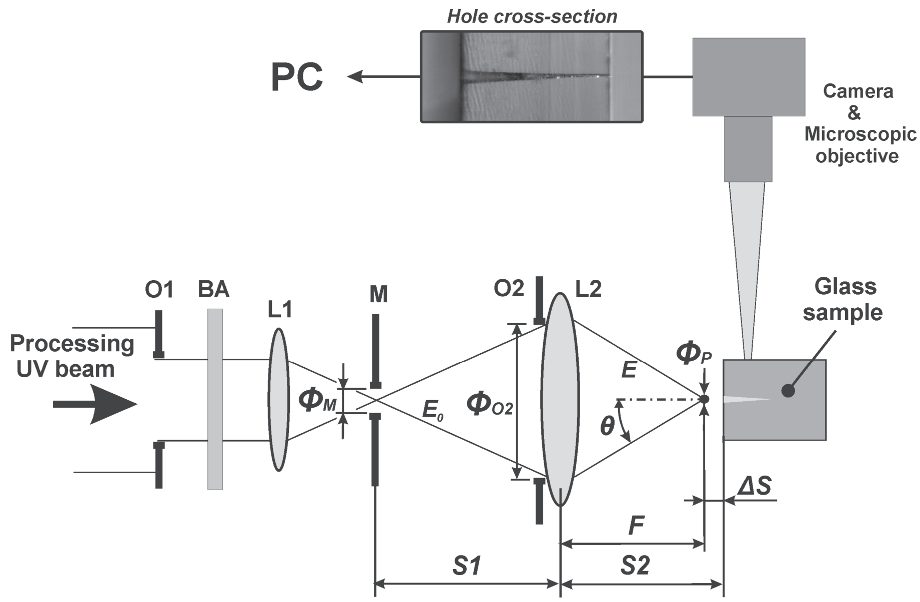

Figure 1. The experimental set-up: O1 and O2 = circular apertures, L1 = focusing lens, L2 = objective assembly, BA = beam attenuator, M = mask, *S1* = distance from mask to objective lenses, *S2* = distance between L2 and sample, *F* = image-plane distance, ΔS = image-plane position shift, $Ø_M$ = mask diameter, $Ø_{O2}$ = adjustable objective aperture diameter, $Ø_P$ = image-plane beam diameter. E_0 and E denote beam energy in front of and after aperture O2

The optical set-up is divided into two sections. The aim of the first section is to homogenise the processing beam. This section consists of a cylindrical beam expander: Kepler telescope (not shown in Figure 1), a circular aperture O1, a focusing lens L1 and a pinhole M. With this optical system, a laser beam with a rectangular profile is expanded in the narrower direction to give a square beam profile. Furthermore, the beam is spatially limited and spatially filtered by focusing through the pinhole. The same pinhole is employed as a mask in the second section. An objective lens system L2 projects the image of the mask M onto the sample surface. With a 1-mm mask diameter $Ø_M$ and an objective magnification of 1/20 (distance *S1/F* ratio, where $S1 = 400$ mm and $F = 20$ mm), a beam diameter $\O_P$ of approximately 60 μm is achieved at the image plane (F). Since the projection technique is used, where the laser beam is first focused through the pinhole M and then directed through the objective optics, the focus location coincides with the image plane at the processing point. A similar beam-treatment system has already been used by Buerhop et al. [15] because it successfully improves the beam quality without using an expensive optical homogeniser. It should be noted that in ordinary projection systems the focus position does not coincide with the position of the image [1]. In our case the beam has an almost uniform intensity profile (top-hat profile) at the place of the image, while the intensity profile at the focus has a nearly Gaussian shape. A circular aperture O2 with an adjustable diameter $\O_{O2}$ is used as an iris to control the diameter of the beam passing through the objective lens. In this way we define the NA of the processing beam, which can be expressed as NA = $\sin\theta$, where θ is the angle of the outermost ray in the focused beam.

By reducing the O2 diameter, not only is the NA adjusted but also the processing energy is changed. To compare some test results the increase in the processing energy due to an enlargement of the O2 diameter is corrected by inserting an appropriate attenuator BA into the beam path.

The processing laser-pulse energy E is varied between 0.2-4.7 mJ by the BA attenuation and O2 diameter adjustment. The beam attenuator is placed between the aperture O1 and the lens L1 to keep the beam's geometrical properties unaffected. The values of E are measured on the exiting side of the objective optics L2 with a calibrated bolometer (Gentec SOLO). Using these data we obtain a beam fluence in the range of 7-165 J/cm^2 (beam intensity: 0.34-8 GW/cm^2) at the image plane.

Plain soda-lime glass samples with a thickness of 0.7 mm are mounted normal to the incident processing beam on the translation stage in order to shift the surface distance $S2$ by the distance ΔS relative to the image-plane distance F. Through the fluorescence of the glass due to UV beam excitation, the image plane location where the laser beam is narrower, can be precisely located within the glass. Knowing the image-plane position in the glass, the image-plane position in the air F can be calculated by taking into account the refractive index of the glass. The experimentally determined ablation threshold was 0.2 mJ and the calculated threshold fluence was ≈3.5 J/cm^2. All the experiments were performed without gas assistance.

The drilling was performed near the sample's upper edge, which was polished to enable real-time, hole-growth observation and imaging of the hole's final cross section. For this purpose, a PC-controlled digital video BW camera, mounted on a microscope objective with a magnification of 110, was used.

OSLO-EDU (Lambda Research) software for optics design and optimisation was used to model the assembly of the L2 objective lenses. The objective construction is shown in Figure 2, where the ray traces are also shown for the largest diameter of aperture O2 used in our experiments.

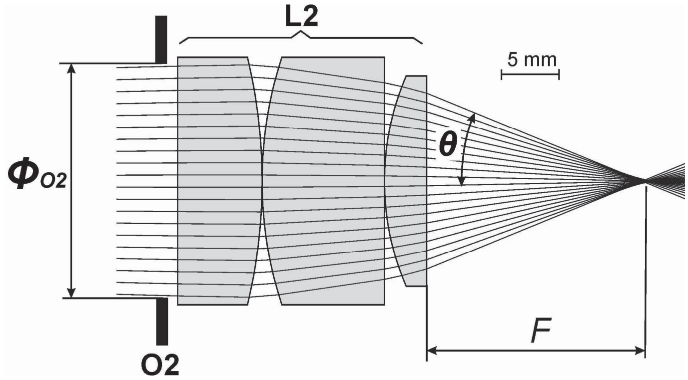

Figure 2. Objective lenses assembly

RESULTS AND DISCUSSION

Drilling tests were performed to analyse the effect of the image-plane position on the hole's geometry at process energy up to 10 times higher than the ablating threshold energy. Experiments were performed at five different combinations of pulse-energy/NA that lead to the most interesting results, presented in Figure 3, where the subfigure columns marked with letters from a) to e) show the drilling results for selected pulse-energy/NA combinations. The image-plane position was shifted along the beam axis (ΔS in Figure 1) with a step of 0.1 mm by moving the sample towards or away from the objective lens. The corresponding plane position shift is marked on each subfigure. During the drilling process, the sample remained at rest. The reference snap-shots, marked with $\Delta S = 0$, denote the sample position where the locus of the image plane coincides with the sample's front surface. Snapshots placed above and under the reference ones in each column show holes processed with the image plane shifted away from the sample's surface and into the bulk respectively. Each drilling test was completed when the hole's growth stopped or the sample was perforated.

The three characteristic drilling phases can be discerned in the photographs of the holes' cross sections. Each phase is associated with a unique hole shape as a consequence of the plasma expansion.

A horn-shaped hole is typical for the first phase when the surface ablation takes place. Ablation in the bulk material in the shape of a half-sphere appears and a cracked-material region is manifested at the place of the laser beam's interaction due to reduced heat transfer and consequent temperature increase. The diameter of this region is large compared to the beam diameter and the ablation rate is much higher in this first phase than in the subsequent phases. Also, it should be noted that the fluence at the processing point is several times higher than the threshold value. By analysing the sample-hole geometry, we can conclude that the taper and the initial diameter of the hole depend heavily on the image-plane position. When the image plane coincides with the sample's front surface, these two properties are at a minimum and increase as the image plane is shifted in both directions.

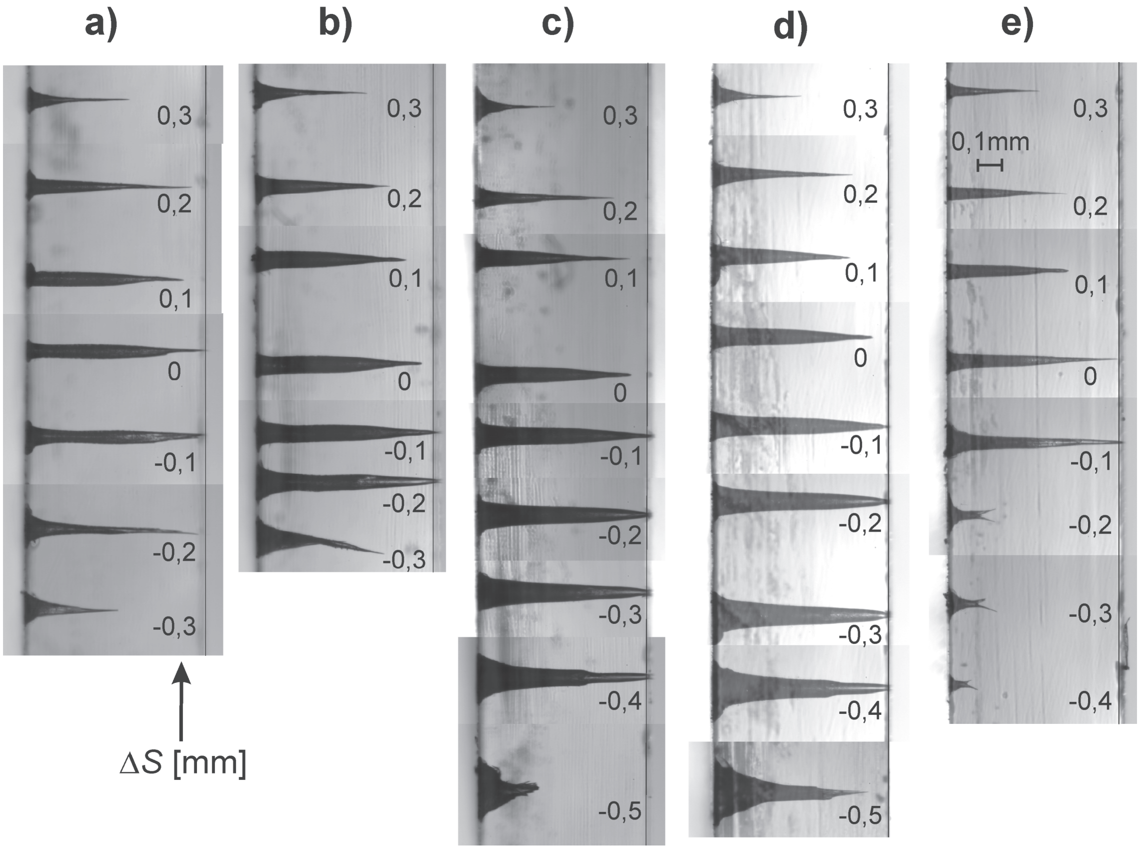

Figure 3. The hole geometry for different processing-beam image-plane positions and typical combinations of pulse-energy and NA values. The image-plane position coincides with the sample surface at the null offset ΔS. The indicated negative image-plane offsets ΔS meet the physical image-plane positions within the glass sample. The image-plane shift ΔS was incremented in 0.1-mm steps. The glass sample thickness was 0.73 mm.

a) $Ø_{O2}$ = 7.5 mm, NA = 0.15, E_0 = 8.2 mJ, E = 0.6 mJ
b) $Ø_{O2}$ = 10 mm, NA = 0.19, E_0 = 8.2 mJ, E = 1 mJ
c) $Ø_{O2}$ = 15 mm, NA = 0.29, E_0 = 8.2 mJ, E = 2.3 mJ
d) $Ø_{O2}$ = 20 mm, NA = 0.38, E_0 = 8.2 mJ, E = 4.1 mJ
e) $Ø_{O2}$ = 20 mm, NA = 0.38, E_0 = 4,1 mJ, E = 2.1 mJ

The process passes over to the second phase when the hole shape becomes conical with a small taper angle. Here, a portion of the processing light reflects from the walls and concentrates at the hole tip [10]. For this reason and because of screening by the hole's wall, the plasma starts to expand in one dimension, i.e. in the direction of the hole's longitudinal axis. The ablation is concentrated at the hole tip and a small portion of light energy ablates the wall. The ratio between the tip and wall ablation is defined by the NA and the influence of this ratio on the hole's geometry can be determined from Figure 3. It seems that the tapered shape is more pronounced for high values of NA (Figure 3d) than for low values (Figure 3a), but a more precise description cannot be made because the beam fluences were not equal for all the tests. The hole diameter depends on the beam energy and is almost identical to the focus diameter when this energy approaches the damage threshold value. Employing the unique feature of this phase, i.e. that the removal rate is constant [16, 17, 18], a precise hole depth can be achieved by applying a certain number of laser pulses. With a particular choice of the beam parameters (Figures 3a and 3b) and when the NA is low and the image plane has been shifted by about 0.1 mm into the bulk material, nearly cylindrical holes can be produced during the second phase with the best aspect ratio and with no effect on the process efficiency. In this case the maximum hole depth is achieved. It is interesting that these findings do not match the theoretical model [1], probably because of the employment of a different test material or different projection system.

The characteristics of the third process phase include sharply tapered holes caused by an increased beam absorption on the side walls of deep holes due to the apex geometry and the presence of re-solidified material. The process terminates when the ablation threshold energy is achieved at the hole's apex. Many beam and material properties define the processing conditions, so drilling results in this phase cannot be precisely predicted. Even small anomalies in the material structure or beam-delivery conditions may lead to unexpected hole geometry such as apex branching (Figure 3e) or a bent apex (Figure 3b). Despite these effects, the hole exit diameter can be as small as a few micrometres when the sample is perforated during the third process phase.

For the evaluation of the holes' geometry we chose a group of characteristic dimensions described in Figure 4. The criterion for the separate phase determination is also seen from the figure. We used the second process-phase dimensions to determine the criteria for the hole-geometry evaluation because the second phase dimension shows the best repeatability.

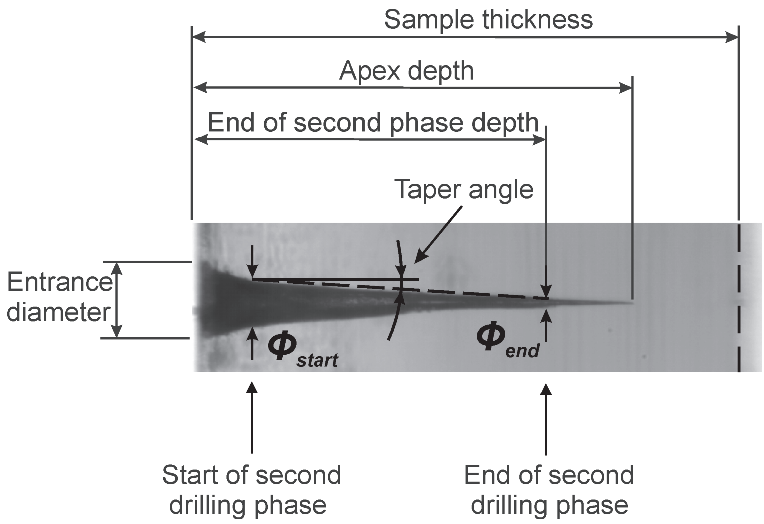

Figure 4. Characteristic dimensions of the hole. Its depth and average diameter are taken from the second drilling-phase geometry

The beam diameter at the image plane $Ø_P$ can be theoretically predicted using equations of geometrical optics:

$$\phi_P = \frac{\phi_M \cdot F}{S1}, \tag{1}$$

and should be 50 μm wide in our case. Considering the theory of Gaussian beam propagation the approximate beam diameter $Ø_P$ can be expressed as:

$$\phi_P \approx \frac{2 \cdot \lambda}{\pi \cdot \arctan\left(\frac{\phi_{O2}}{2F}\right)}, \tag{2}$$

where λ is the wavelength of the beam. In the case of the smallest diameter of the aperture $Ø_{O2}$, the increase in the beam diameter $Ø_P$ is the largest and is about 1 µm; therefore, this effect can be neglected. So the real diameter (60 µm), measured as the diameter of the ablated region after the first laser pulse, is wider mainly due to optical system aberration. To explain this effect, a model of the objective-lenses assembly is used to evaluate the image distortion. Figure 5 shows the calculated intersection of the border rays for various experimental $Ø_{O2}$. As has already been mentioned, we located the image plane at the place where the focused beam was the narrowest when the largest O2 aperture was used. This position is marked with the dash vertical line in Figure 5. It should be noted that all the rays between the border ones are omitted from the figure for better clarity, but must be considered for further explanation. When the diameter of the O2 aperture is small, only the rays near the optical axis propagate through the objective and intersect at a certain point, i.e. the theoretical focus. When increasing the O2 diameter the number of marginal rays increases and their intersections move toward the objective, so the real focus of the beam spreads in the same direction. Furthermore, the energy distribution perpendicular to the optical axis becomes non-uniform, with a changeable profile depending on the shift of the observation plane and with higher values of the energy near the optical axes. Another interesting feature can be observed: the divergence of the focused beam in front of the focus is smaller than the divergence on the opposite side.

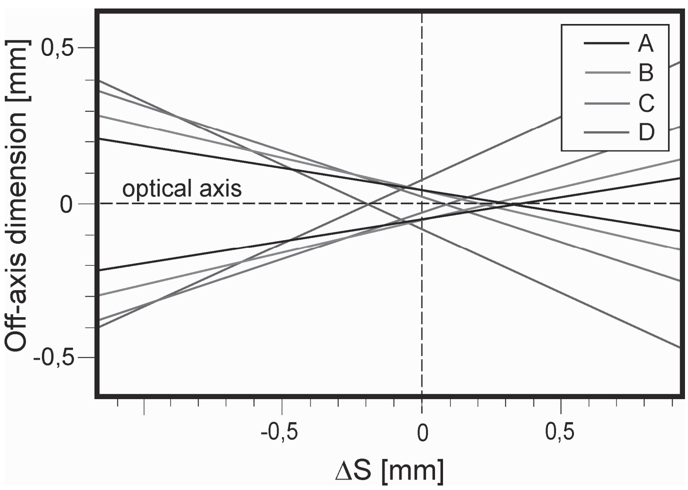

Figure 5. Theoretical ray propagation near the focal point performed by OSLA-EDU software. The lines show the border rays at different O2 diameters:

A) $Ø_{O2}$ = 7.5 mm, NA = 0.15
B) $Ø_{O2}$ = 10 mm, NA = 0.19
C) $Ø_{O2}$ = 15 mm, NA = 0.29
D) $Ø_{O2}$ = 20 mm, NA = 0.38

Figure 6 presents the characteristic dimensions of the holes in Figure 3 and graphically demonstrates the influence of a typical pulse-energy/NA combination and the image-plane offset. The dimensions were determined from photographs of the holes' cross sections (Figure 3), where the plate's thickness (0.73 mm) was taken as the reference dimension. Accordingly, labels A to E in the legend of each figure correspond to the processing beam's properties. Furthermore, the data shown in each diagram at the null image-plane offset were taken from a snapshot marked with ΔS = 0 in Figure 3.

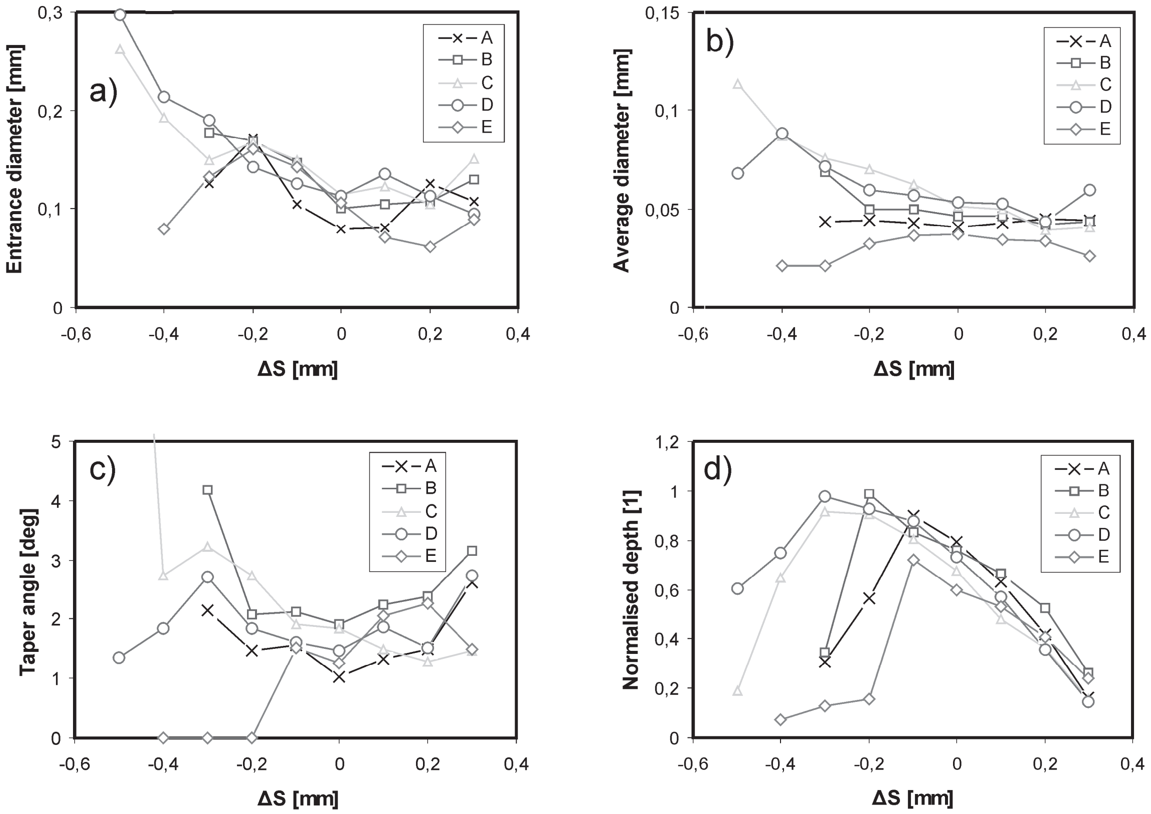

Figure 6. Characteristic dimensions of the holes' dependence on the image-plane offset ΔS. Graphs A to E in all the figures represent the results of different combinations of pulse-energy/NA.

A) $Ø_{O2}$=7.5mm, NA=0.15, E_0=8.2 mJ, E=0.6mJ
B) $Ø_{O2}$=10mm, NA=0.19, E_0=8.2 mJ, E=1mJ
C) $Ø_{O2}$=15mm, NA=0.29, E_0=8.2 mJ, E=2.3mJ
D) $Ø_{O2}$=20mm, NA=0.38, E_0=8.2 mJ, E=4.1mJ
E) $Ø_{O2}$=20mm, NA=0.38, E_0=4,1 mJ, E=2.1mJ

Figures 6a and 6b present the characteristic hole diameters. Based on the graphs, it can be concluded that the entrance hole diameter (Figure 6a) and the average hole diameter (Figure 6b), the latter being defined by ($Ø_{start}$+$Ø_{end}$)/2, respond equally to the processing-beam parameters. The figures show the increase in diameter when the image plane is shifted towards the sample, which can be explained by the beam-diameter enlargement on the surface due to its divergence presented in Figure 5. Assuming that each ray contains the same portion of energy, a beam with a nearly uniform fluence profile hits the surface so the entrance-hole diameter corresponds to the beam diameter, i.e. the hole diameter increases with the surface shift. When the image plane is shifted away from the sample surface, the central rays start to concentrate near the optical axis while the marginal rays start to fade with the surface shift. Therefore, the fluence becomes lower approaching the beam's margin.

The effect of plasma shielding also takes place so the hole diameter maintains its minimal value at a null image plane offset. In this case, the hole diameter depends mainly on the beam energy while the image-plane shift is less influential, although the beam diameter increases. Similar behaviour can be noticed for the entrance and average diameters of a hole. Overall, the holes have a smaller diameter than could be expected according to the results of the modelled objective assembly. The reason is probably the energy profile, which is not perfectly uniform. The incident angle of each ray also decreases when the ray travels closer to the optical axis. Both factors decrease the impinging fluence as the rays approach the beam's border. Because of the different plasma formation and consequently the different ablation direction, the entrance-hole diameter, established out of the second-phase hole geometry, is more than two times greater than the average diameter, while the latter is equal to or slightly smaller than the image diameter at the image plane.

Figure 6c shows the change of the taper angle with the image-plane shift for different typical pulse-energy/NA combinations. The variation of the taper angle is almost insensitive to the beam's NA and energy. Only a small increase can be detected when the NA and the corresponding energy are increased and when the image plane is shifted from its central position in both directions. At this point it should be noted that the taper angle was evaluated according to the hole dimensions in the second process phase.

In contrast to the taper-angle behaviour, the hole's depth shows a stronger dependence on the image-plane offset (Figure 6d). Deeper holes can be produced with an image-plane shift into the bulk. A shift in the opposite direction leads to a significant decrease in hole depth. In all cases, the greatest depth is obtained with the image-plane position shifted into the sample by 0.1-0.3 mm. A less than 20% hole-depth reduction occurs when the image plane is located on the sample surface. The normalised hole depths in Figure 6d are defined as a ratio of the depth of a particular hole to the depth of the deepest one.

The third phase hole geometry is not as repeatable as the second phase, so we did not make any further dimensional evaluation. However, the third process phase is very important from the view of applicability. The hole diameter in this phase drastically decreases to a few micrometres and the hole starts to grow in the shape of a capillary. This hole geometry permits only a one-dimensional plasma expansion with a very low transverse dimension and a large longitudinal length. Plasma shielding becomes an increasingly predominant drilling parameter, which leads to a spontaneous termination of the process. The random nature of the plasma-formation phenomena is a key factor for the low geometrical repeatability of the process in its third phase. With the performed drilling tests we confirm that the depth of the third-phase hole cannot be precisely predicted. For that reason, through-hole microdrilling can only be performed with a reliable control of the second-phase hole geometry.

In general, laser-percussion deep microdrilling is characterised by three process phases according to the three different types of plasma-plume formation when the processing beam with a fluence higher than the threshold value is used. The three phases are related to the removal rate or the hole depth versus the laser-pulse number [13, 14].

CONCLUSIONS

We have presented the results of microdrilling in soda-lime glass samples based on a UV excimer laser beam and a modified mask-projection technique. We analysed the effects of the laser beam's image-plane position shift at different pulse-energy/NA combinations on the hole's geometry. The process consists of three consecutive phases according to the plasma-plume formation. We show that each phase is characterised by the geometrical properties of the holes. The beam geometry has a unique effect for each processing phase, so knowledge of the phase presented during the perforation in combination with the beam's geometrical properties is important for achieving the desired drilling results. The explanation of the hole's diameter dependence on the NA and the image-plane shift can be found by considering the focusing optical system model when holes are drilled within the first and the second drilling-process phases.

The processing image-plane position with respect to the sample's front surface significantly affects the drilling efficiency. Cylindrical holes with the highest aspect ratio and the highest depth were obtained by shifting the image-plane position into the processing sample. It was also shown that the processing beam with a low numerical aperture and energy slightly above the threshold values should be used for processing cylindrically shaped holes with the smallest diameter. Holes with exit diameter up to 10 times smaller than the beam focus diameter were produced in the case where perforation occurs during the third process phase, where the hole tip is in the form of a thin capillary.

REFERENCES

1. V. N. Tokarev, J. Lopez and S. Lazare, "Modelling of high-aspect ratio microdrilling of polymers with UV laser ablation", *Appl. Surf. Sci.*, **2000**, *168*, 75-78.
2. B. Keiper, H. Exner, U. Loschner and T. Kuntze, "Drilling of glass by excimer laser mask projection technique", *J. Laser Appl.*, **2000**, *12*, 189-193.
3. W. Yuan and B. Ma, "Micro-machinability of monocrystal silicon by direct etching using excimer laser", *J. Mater. Process. Technol.*, **2008**, *200*, 390-397.
4. K. H. Gerlach, J. Jersch, K. Dickmann and L. J. Hildenhagen, "Design and performance of an excimer-laser based optical system for high precision microstructuring", *Optics Laser Technol.*, **1998**, *29*, 439-447.
5. R. Pini, R. Salimbeni, G. Toci and M. Vannini, "High-quality drilling with copper vapour lasers", *Opt. Quant. Electron.*, **1995**, *27*, 1243-1256.
6. R. Petkovšek, A. Babnik and J. Diaci, "Optodynamic monitoring of the laser drilling of through-holes in glass ampoules", *Meas. Sci. Technol.*, **2006**, *17*, 1-7.
7. A. Feldman, D. Horowitz and R. M. Waxler, "Mechanisms for self-focusing in optical glasses", *IEEE J. Quant. Electron.*, **1973**, *9*, 1054-1061.
8. C. Y. Ho and M. Y. Wen, "Distribution of the intensity absorbed by the keyhole wall in laser processing", *J. Mater. Process. Technol.*, **2004**, *145*, 303-310.
9. K. H. Chen, W. Wu, B. H. Chu, C. Y. Chang, J. Lin, S. J. Pearton, D. P. Norton and F. Ren, "UV excimer laser drilled high aspect ratio submicron via hole", *Appl. Surf. Sci.*, **2009**, *256*, 183-186.
10. K. H. Chen, W. Wu, B. H. Chu, C. F. Lo, J. Lin, Y. L. Wang, C. Y. Chang, S. J. Pearton and F. Ren, "190 nm excimer laser drilling of glass slices: Dependence of drilling rate and via hole shape on the diameter of the via hole", *J. Vac. Sci. Technol. B*, **2009**, *27*, L42-L46.
11. W. S. Lau, T. M. Yue, T. C. Lee and W. B. Lee, "Un-conventional machining of composite materials", *J. Mater. Process. Technol.*, **1995**, *48*, 199-205.

12. C. Paterson, A. S. Holmes and R. W. Smith, "Excimer laser ablation of microstructures: A numerical model", *J. Appl. Phys.*, **1999**, *86*, 6538-6546.
13. V. N. Tokarev, J. Lopez, S. Lazare and F. Weisbuch, "High-aspect-ratio microdrilling of polymers with UV laser ablation: Experiment with analytical model", *Appl. Phys. A*, **2003**, *76*, 385-396.
14. L. Shah, J. Tawney, M. Richardson and K. Richardson, "Self-focusing during femtosecond micromachining of silicate glasses", *IEEE J. Quant. Electron.*, **2004**, *40*, 57-68.
15. C. Buerhop, N. Lutz, R. Weismann and G. Tomandl, "Surface treatment of glass and ceramics using XeCl excimer laser radiation", *Glastech. Ber.*, **1993**, *66*, 61-67.
16. J. Ihlemann, "Excimer laser ablation of fused silica", *Appl. Surf. Sci.*, **1992**, *54*, 193-200.
17. P. E. Dyer, R. J. Farley, R. Giedl and D. M. Karnakis, "Excimer laser ablation of polymers and glasses for grating fabrication", *Appl. Surf. Sci.*, **1996**, *96-98*, 537-549.
18. R. Petkovšek, A. Babnik, J. Diaci and J. Možina, "Optodynamic monitoring of laser micro-drilling of glass by using a laser probe", *Appl. Phys. A*, **2008**, *93*, 141-145.

Maejo International Journal of Science and Technology

ISSN 1905-7873
Available online at www.mijst.mju.ac.th

Full Paper

Effects of nutrient media on vegetative growth of *Lemna minor* and *Landoltia punctata* during in vitro and ex vitro cultivation

Chokchai Kittiwongwattana[1,*] and Supachai Vuttipongchaikij[2]

[1]Department of Applied Biology, Faculty of Science, King Mongkut's Institute of Technology Ladkrabang, Chalongkrung Rd., Ladkrabang, Bangkok, 10520, Thailand

[2]Department of Genetics, Faculty of Science, Kasetsart University, 50 Ngamwongwan, Chattuchak, Bangkok, 10900, Thailand

*Corresponding Author, e-mail: kkchokch@kmitl.ac.th

Received: 21 December 2011 / Accepted: 28 January 2013 / Published: 30 January 2013

Abstract: Lemnaceous plants, namely *Lemna minor* and *Landoltia punctata*, have been used in various types of biological research. The effects of Murashige and Skoog (MS) and Hoagland media on vegetative growth rate of both species during in vitro and ex vitro cultivation were investigated. Under axenic conditions, frond proliferation of *L. minor* and *Lan. punctata* in Hoagland medium are 8 and 11.5% respectively faster than that in MS medium. Biomass production in Hoagland medium also increases 2.2-fold (*L. minor*) and 1.4-fold (*Lan. punctata*) compared to MS medium. The roots of both species in MS medium are distinctly shorter than those in Hoagland medium. In contrast, ex vitro regeneration of frond colonies in MS medium is 22.2% (for *L. minor*) and 17.1% (for *Lan. punctata*) faster than in Hoagland medium. Similarly, ex vitro biomass production of both species in MS increases 1.8-fold (for *L. minor*) and 1.3-fold (for *Lan. punctata*) compared to that in Hoagland medium. Root elongation of the frond colonies in MS and Hoagland media is comparable. The distinct effects of MS and Hoagland media on vegetative growth of both species and the pre-determination of ex vitro growth rates in each medium are demonstrated.

Keywords: *Lemna minor*, *Landoltia punctata*, effects of nutrient media, in vitro cultivation, ex vitro cultivation, frond proliferation, biomass production, root elongation

---

INTRODUCTION

The Family Lemnaceae, generally recognised as duckweeds, comprises 38 different species in 5 genera, i.e. *Lemna, Landoltia, Spirodela, Wolffia* and *Wolffiella.* Duckweeds are small, free-floating, aquatic flowering plants that are widely distributed around the globe ranging from temperate to tropical regions [1, 2]. Duckweed plants lack true stems and leaves. The plant body generally consists of expanded, flat, leaf-like structures called fronds [2]. Each plant contains leaf-like fronds that float on the water surface or are slightly submerged. Fronds are primarily involved in photosynthesis and reproduction. The roots attach themselves on the lower surface of the fronds. The maximum root number is species specific [1, 3]. Generally, duckweeds reproduce vegetatively by generating daughter fronds from the meristematic tissue on the pocket cleft towards the base of the mother frond. Daughter fronds stay attached to the mother frond to form a colony and dissociate upon maturation. Alternatively, at low-temperature many duckweed species produce specialised fronds called turions that are starch-enriched and serve as an overwintering form. Duckweeds may also undergo sexual reproduction by forming flowers and setting fertile seeds [4]. Because of their relatively simple life cycle and rapid growth, lesser duckweed (*Lemna minor*)*,* fat duckweed (*L. gibba*)*,* dotted duckweed (*Landoltia punctata*), and greater duckweed (*Spirodela polyrhiza*) have been extensively used in biochemical and physiological research [3]. Previous studies have demonstrated that several species of duckweeds can be used to remove toxic heavy metals and organic compounds from waste water [5-9]. *L. minor* is currently used as a monitor for water quality according to the ISO 20079 protocol because of its high sensitivity to water pollutants [10]. The guideline for the substance toxicity test provided by the Organisation for Economic Cooperation and Development (OECD) also employs *L. minor* as well as other species in the same genus as test species [11]. *L. minor* chloroplast genome has been fully sequenced for public use and applied for molecular identification of lemnaceous species [2].

Axenic cultures of duckweeds are often used for biological research and stock-culture maintenance. Currently, axenic cultures of *L. minor* are used as the manufacturing platform for bioproduction of some pharmaceutical proteins [12]. Duckweeds can be grown on various types of media consisting of basic inorganic salts. Addition of 1% sucrose as the carbon source also supports frond growth [3]. Murashige and Skoog (MS) [13] and Hoagland [14] media are examples of nutrient solutions that have been widely used in plant tissue culture including duckweeds [15-18]. The aim of this study is to compare the effects of MS and Hoagland media on the vegetative growth of *L. minor* and *Lan. punctata* during in vitro and ex vitro cultivation.

MATERIALS AND METHODS

Preparation of Plant Materials and Culture Conditions

L. minor and *Lan. punctata* were collected from natural ponds in the northern and western regions of Thailand. Fronds were surface-sterilised using 10% chlorox solution supplied with a few drops of Tween-20. They were then thoroughly washed with sterile water three times to remove excess chlorox solution. Each frond was then placed separately on solid MS medium [13] containing 0.7% agar, pH 5.7, to allow frond regeneration. Daughter fronds of both species derived from a single mother frond were kept and maintained as stock cultures, which were grown under 16hr-light/8hr-dark photoperiod with 50 µmol $m^{-2}s^{-1}$ light intensity from fluorescent light tubes (36W/840) at 24 ± 2^oC.

Effects of Media on In Vitro Growth and Subsequent Ex Vitro Growth

Two-frond colonies of *L. minor* and *Lan. punctata* from the stock cultures were transferred onto fresh solid MS medium and grown for 14 days. Newly generated colonies of each species consisting of two fronds were pretreated with 0.7% solid agar without nutrients for 24 hours before being transferred to liquid MS and Hoagland media [14] with 1% sucrose, pH 5.7. The composition of MS and Hoagland media used in this study is shown in Table 1.

Table 1. Composition of MS and Hoagland media used in this study [13, 14]

Nutrient	Concentration (mg/L)	
	MS	Hoagland
KNO_3	1900	505.5
$MgSO_4.7H_2O$	370	492.74
KH_2PO_4	170	136.09
NH_4NO_3	1650	-
$CaCl_2.2H_2O$	440	-
$Ca(NO_3)_2$	-	820.45
H_3BO_3	6.2	2.86
$Na_2MoO_4.2H_2O$	0.25	0.025
$MnSO_4.H_2O$	16.9	-
$ZnSO_4.7H_2O$	8.6	-
$CuSO_4.5H_2O$	0.025	-
$CoCl_2.6H_2O$	0.025	-
$FeSO_4.7H_2O$	27.8	-
$CuCl_2.2H_2O$	-	0.05
$MnCl_2.4H_2O$	-	1.81
$ZnCl_2$	-	0.11
$FeCl_3.6H_2O$	-	27
KI	0.83	-
Na_2EDTA	37.2	44.8
Myo-inositol	100	-
Nicotinic acid	0.5	-
Pyridoxine.HCl	0.5	-
Glysine	2	-
Thiamine	0.1	-

The experiment was performed in six replicates for each medium. Each replicate contained 15 randomly chosen, pretreated fronds which were aseptically grown in closed cylindrical crystal-clear bottles (8 cm high, 4 cm in diameter) containing 40 mL of liquid medium. Growth conditions were similar to those of the stock cultures described above. To observe frond proliferation and biomass production, pictures of each culture were taken from atop with a digital camera on day 0, 1, 4, 7, 10 and 13 along with a standard rectangle of 25 mm^2. Frond proliferation was determined based on doubling time of the frond number (T_d) on day 4. T_d was calculated by the following equation: $T_d = \ln 2/\mu$. The parameter μ (day^{-1}) is the average growth rate that is obtained as follows:

$$\mu_{ij} = (\ln N_j - \ln N_i) / (t_j - t_i)$$

where $i = 0$, $j = 4$, N = total frond number, and t = time (day) of cultivation [11].

The rate of biomass production is indicated by the growth index calculated by using total frond area as follows:

$$\text{Growth index} = T_{(i)} / T_{(0)}$$

where $T_{(i)}$ is the total frond area measured on different days of the cultivation (day 1, 4, 7, 10 and 13) and T_0 is the total frond area measured at the beginning of the test (day 0) [7]. The total frond area was measured by using the Adobe Photoshop CS3 program (Adobe Systems Inc.). Briefly, the frond area is selected by using the 'colour range' command that distinguishes the green colour of fronds from the background. The selected area is then determined as the number of pixel. This number is used to obtain the total frond area in mm^2 by comparing to the number of pixel representing the area of the standard rectangle (25 mm^2). Student's *t*-test was used to determine statistically significant differences ($P < 0.05$) between growth indices of samples in MS and Hoagland media on the same day of cultivation. After 13 days of cultivation, pictures of roots produced in both media were taken at the side of the bottles.

The in vitro pre-cultured frond colonies from each medium formula were then used to observe the vegetative growth rate after seven days of ex vitro cultivation in diluted pond water. The test was done in triplicate in the crystal-clear bottles similar to those for axenic cultures. Each replicate contained 10 randomly chosen three- or four-frond colonies grown in 40 mL of one-third-diluted pond water (distilled water: pond water = 1:3). The bottles were covered with glass plates to prevent evaporation. The growth conditions were 16 hr-light/ 8 hr-dark photoperiod with 50 µmol $m^{-2}s^{-1}$ light intensity from fluorescent light tubes (36W/840) and $28\pm2^{o}C$. Pictures of all fronds in each bottle were taken on day 0, 4 and 7 with a standard rectangle of 25 mm^2. T_d, total frond area, growth index and root elongation of the frond colonies were determined as described above.

RESULTS AND DISCUSSION

In Vitro Cultivation

Different effects of MS and Hoagland nutrient solutions on the vegetative growth of *L. minor* and *Lan. punctata* during in vitro and subsequent ex vitro cultivation are demonstrated. Because of their simple preparation, MS and Hoagland media have been used for growing axenic cultures of various duckweed species for stock-culture maintenance and callus production [15-18]. However, the effects of these two media on frond proliferation, biomass production and root elongation of the two duckweed species have never been described. Selection of a medium suitable for research is very important. For example, robust bioproduction of recombinant protein molecules using the duckweed platform requires optimal biomass production that may be optimised through environmental conditions and growing medium [3]. Many constituents are commonly present in MS and Hoagland media at different concentrations, including KNO_3, $MgSO_4$, KH_2PO_4, H_3BO_3, $NaMoO_4$ and Na_2EDTA. Micronutrients are sulphate and chloride salts in MS and Hoagland media respectively. Nine additional constituents are in MS medium but not in Hoagland medium. They are NH_4NO_3, $CaCl_2.2H_2O$, $CoCl_2.2H_2O$, KI, myo-inositol, nicotinic acid, pyridoxine-HCl, glycine and thymine. Various carbon sources are available for axenic culture of duckweeds depending on the purpose of a particular study. Glucose, fructose and mannitol support regeneration of *L. minor* intact plants while galactose and sorbitol are more efficiently utilised by *L. minor* calli [16, 19]. Sucrose is generally used as carbon source in plant tissue culture because of its nature as a native product from the carbon assimilation process. Sucrose at 1% is suggested as the optimal concentration for duckweed tissue culture [3] and thus is used in this study.

After four days of cultivation, the effects of MS and Hoagland media on the rates of frond proliferation of axenically grown *L. minor* and *Lan. punctata* are determined based on the frond doubling time (T_d). Under experimental conditions, *L. minor* cultivated in MS medium displays T_d of 2.5 days while in Hoagland medium it exhibits T_d of 2.3 days. Similarly, frond proliferation of *Lan. punctata* is relatively slow in MS medium (T_d = 2.6 days) compared to Hoagland medium (T_d = 2.3 days). This indicates that Hoagland medium produces a faster proliferation rate than MS medium by 8% and 11.5% for *L. minor* and *Lan. punctata* respectively.

The rate of biomass production of *L. minor* and *Lan. punctata* is determined by using the growth index, which is relatively similar for *L. minor* grown on MS and Hoagland media up to four days of cultivation (Figure 1a). However, the growth index of *L. minor* in Hoagland medium is significantly higher than in MS medium after that. From day 10 to 13, a 1.4-fold and 2-fold increase in growth index are observed in MS and Hoagland media respectively. At the end of the test, the growth index of *L. minor* cultured in Hoagland medium (growth index = 24.03) is 2.2 times higher than in MS medium (growth index = 10.85). In contrast, the growth index of *Lan. punctata* in both media remains relatively similar up to 10 days of cultivation (Figure 1b). From day 10 to 13, a 1.5-fold and a 2-fold increase in the growth index are observed in MS and Hoagland media respectively. This results in a 1.4-fold difference between the growth indices of *Lan. punctata* in MS (growth index = 13.78) and Hoagland media (growth index = 19.66) after 13 days of cultivation. Similar to frond proliferation, the rate of biomass production of the two duckweed species is elevated in Hoagland medium compared to that in MS medium.

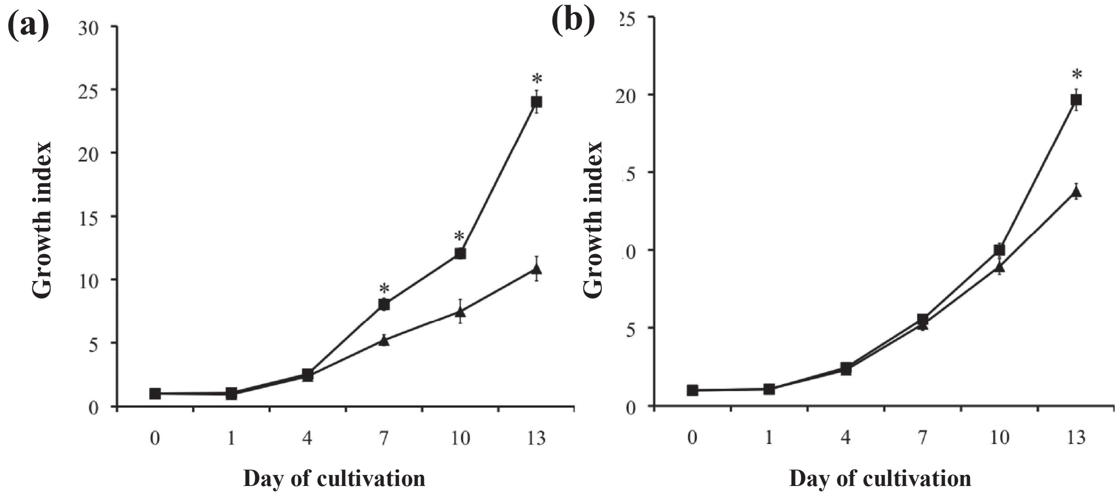

Figure 1. Biomass production of *L. minor* (a) and *Lan. punctata* (b) in MS (▲) and Hoagland (■) media on day 0, 1, 4, 7, 10 and 13 as determined by the growth index. *Vertical bars* represent standard error of the mean (n = 6). Asterisks indicate the statistically significant difference of the growth index of the plants in Hoagland and MS medium on the same day of cultivation (P<0.05)

The root growth from the lower surface of fronds is also examined. After 13 days of cultivation, roots of *L. minor* grown in MS medium are obviously shorter than those in Hoagland medium (Figure 2a-b). A similar effect is observed in *Lan. Punctata*, which displays a substantial

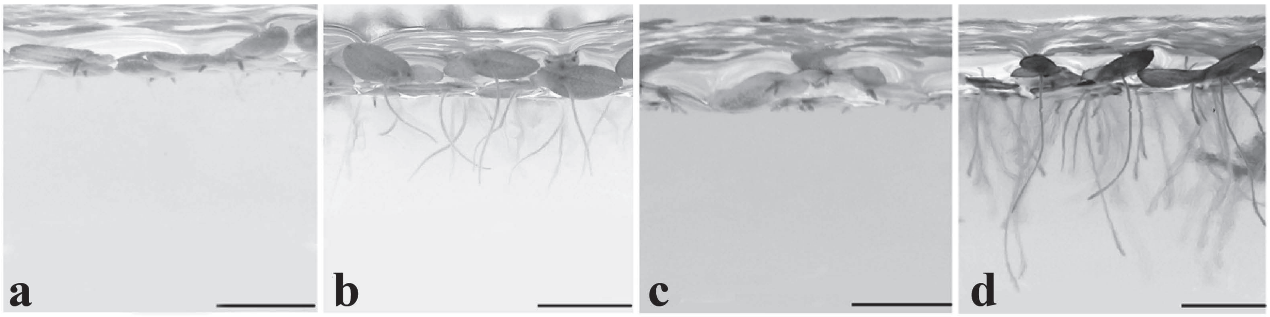

Figure 2. Effects of MS (a, c) and Hoagland (b, d) media on root growth of *L. minor* (a, b) and *Lan. punctata* (c, d) in axenic cultures (bar = 0.5 cm)

reduction in root elongation in MS medium compared to that in Hoagland medium (Figure 2c-d). This indicates an inhibitory effect of MS medium on root elongation in both species. The apparent effects of MS and Hoagland media on root elongation may be related to endogenous phytohormones. Gibberellin has been implicated in contributing to root growth in *L. minor* [20]. Exogenous application of uniconazole P, a gibberellin biosynthesis inhibitor, causes a significant reduction in both the root length and diameter. This inhibition is reversible upon addition of giberellic acid (GA_3) [20]. Another study has reported the effect of abscisic acid (ABA) on root growth. The application of exogenous ABA inhibits root growth of *L. minor* and induces starch accumulation in root cortical cells [21]. Auxin and ethylene are also plant hormones that regulate root elongation. Despite the lack of reports on root inhibition in lemnaceous plants, previous studies showed that auxin and ethylene affect root growth by synergistically reducing cell expansion in the central domain of the region of elongation of Arabidopsis [22, 23]. Further analyses are needed to better understand the effect of medium on root elongation of *L. minor* and *Lan. punctata*,. A comparative study on gibberellins, ABA and auxin levels in both plant species grown in MS and Hoagland media may confirm whether the reduction of root elongation in MS medium is related to these phytohormones.

Several previous studies showed distinct effects of the media on growth and physiological responses of other duckweed species. The rate of frond multiplication of *Lemna paucicostata* grown in a medium described by Boss et al. [24] is slower than in Hutner's medium [25]. The presence of EDTA, a chelating agent, in Hoagland medium prevents flowering of *Lemna perpusilla* but stimulates flowering of *L. gibba* under long-day conditions [26]. Frond proliferation and callus induction in *L. gibba* require different medium formula. While Nitsch-Nitsch, Schenk-Hildebrant and Gamborg media are efficient in frond proliferation, MS medium is more suitable for callus induction [27]. It was shown that Lemnaceae medium [28] is efficient for induction of turion formation as opposed to Hoagland medium, which promotes regeneration of daughter fronds [29]. According to our results, the rates of frond proliferation, biomass production and root elongation of *L. minor* and *Lan. punctata* in Hoagland medium are higher than those in MS medium. This indicates that Hoagland medium may be efficiently used for growing duckweeds when high biomass production and root elongation are needed. In contrast, slower growth rate can be obtained by using MS medium. Additionally, the effects of media on plant growth may also be a determining factor for the selection of medium that can be used in certain studies. In the Organisation for Economic Cooperation and Development (OECD) guideline, it requires T_d of the *Lemna* species to be less than 2.5 days for the substance toxicity test [11]. Based on our observation, Hoagland medium may be more preferable than MS medium for this particular toxicity test with *L. minor*.

Ex Vitro Cultivation

To examine the growth rates of pre-in-vitro cultured duckweeds during ex vitro cultivation, independent *L. minor* and *Lan. punctata* frond colonies in MS and Hoagland media are randomly selected and transferred to diluted pond water. Frond proliferation and biomass production are determined on day 4 and day 7 respectively after the transfer. It is found that the rates of vegetative growth of frond colonies in MS medium are generally higher than those obtained from Hoagland medium. While *L. minor* transferred from MS medium displays an observed T_d of 2.8 days, those from Hoagland medium exhibits a T_d of 3.6 days. *Lan. punctata* frond colonies from MS medium also show a faster frond proliferation (T_d = 3.4 days) compared to that from Hoagland medium (T_d = 4.1 days). For biomass production, the growth index of *L. minor* frond colonies from MS medium (growth index = 5.5) is 1.8 times higher than that from Hoagland medium (growth index = 3.07) (Figure 3). Similarly, *Lan. punctata* from MS medium exhibits a growth index (3.31) that is 1.3 times higher than that from Hoagland medium (growth index = 2.61) (Figure 3). Additionally, the root growth of *L. minor* and *Lan. punctata* frond colonies transferred from MS medium resumes and becomes comparable to what is observed in those from Hoagland medium after seven days of cultivation (Figure 4a-d).

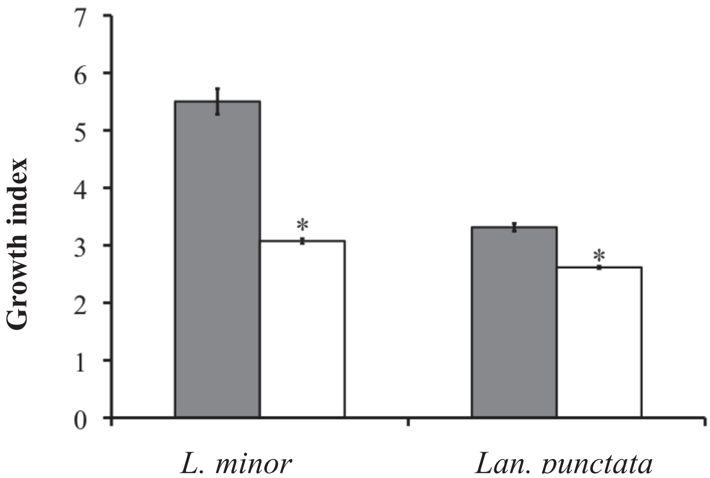

Figure 3. Biomass production of *L. minor* and *Lan. punctata* frond colonies from MS (gray bars) and Hoagland (white bars) media grown ex vitro in diluted pond water for seven days as determined by the growth index. Vertical bars represent standard error of the mean (n = 3). Asterisks indicate statistically significant difference of the growth index of the plants from Hoagland medium compared to MS medium ($P<0.05$).

In contrast to the observation during in vitro cultivation, the vegetative growth during ex vitro cultivation indicates the positive effects of MS medium on *L. minor* and *Lan. punctata* frond colonies in diluted pond water, which is strikingly different from the elevation of growth rates of axenic cultures by Hoagland medium compared to MS medium. This result shows that the growth rate of ex vitro cultures can be pre-determined by the previous medium formula. It also suggests that one may need to consider or investigate the effect of medium formula on plant growth before

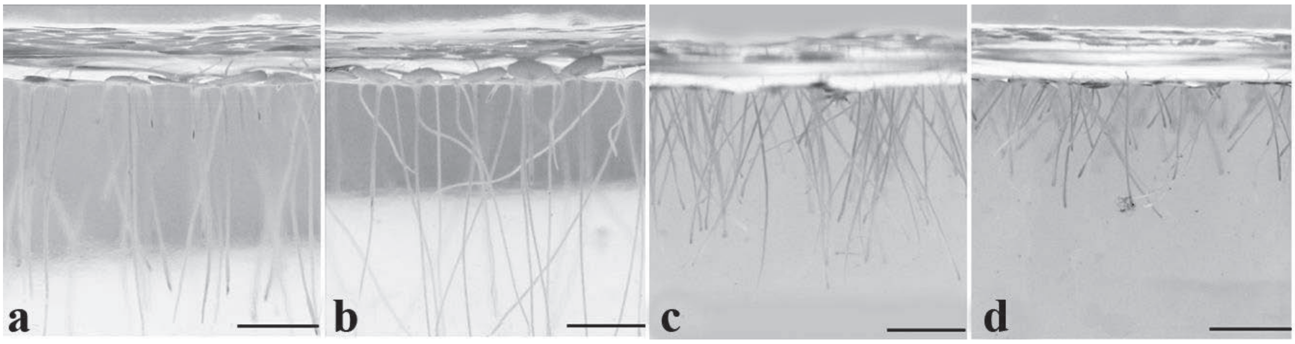

Figure 4. Root growth of *L. minor* (a, b) and *Lan. punctata* (c, d) after ex vitro cultivation for seven days in diluted pond water: frond colonies derived from MS (a, c) and from Hoagland (b, d) medium (bar = 0.5 cm)

planning a subsequent ex vitro toxicity test using axenic cultures of Lemnaceous plants. It is speculated that the MS medium may induce food storage which causes slower vegetative growth during in vitro cultivation. This reserved food then becomes readily available to support the growth during ex vitro cultivation in diluted pond water where nutrients are more limited. In contrast, Hoagland medium may stimulate a higher level of food consumption to sustain rapid frond and root growth in axenic cultures. This may result in a low level of food stored in the fronds and in turn cause a slower growth rate of the frond colonies in diluted pond water. Our speculation is partly supported by a previous study on the induction of turion formation in *S. polyrhiza*. Turions are the over-wintering form of several lemnaceous species that accumulate starch and sink to the bottom of the pond [26]. The use of Lemnaceae medium is more efficient to induce *S. polyrhiza* fronds to accumulate starch and transform into turions as opposed to Hoagland medium that stimulates daughter-frond regeneration [26]. Taken together, our results and the previous report implicate the medium relevance in starch or food-reserve accumulation. Further analysis of starch levels in the frond colonies of *L. minor* and *Lan. punctata* axenic cultures in MS and Hoagland media may confirm this speculation.

CONCLUSIONS

It has been shown that the rates of frond proliferation, biomass production and root elongation of *L. minor* and *Lan. punctata* are similarly dependent on the medium formula. This indicates the influence of the medium on the growth of both species. Plant responses to Hoagland medium are rapid frond proliferation and biomass production. The medium also supports root elongation and consequently is appropriate for further studies regarding root morphology and physiology of both duckweed species. In contrast, the growth rates are relatively low in MS medium. Thus, MS medium can be used to maintain a large collection of stock cultures where slower growth is preferred to reduce the amount of labour required for subculturing. It has also been found that *L. minor* and *Lan. punctata* frond colonies obtained from Hoagland medium grow slower than those from MS medium during ex vitro cultivation. This indicates the impact of medium formula on the use of axenic cultures under ex vitro conditions for standardised toxicity tests, etc., with lemnaceous species.

REFERENCES

1. D. H. Les, E. Landolt and D. J. Crawford, "Systematics of the Lemnaceae (duckweeds): Inferences from micromolecular and morphological data", *Plant Syst. Evol.*, **1997**, *204,* 161-177.
2. W. Wang, Y. Wu, Y. Yan, M. Ermakova, R. Kerstetter and J. Messing, "DNA barcoding of the *Lemnaceae*, a family of aquatic monocots", *BMC Plant Biol.*, **2010**, *10,* 205.
3. A. M. Stomp, "The duckweeds: A valuable plant for biomanufacturing", *Biotechnol. Annu. Rev.*, **2005**, *11,* 69-99.
4. W. S. Hillman, "The *Lemnaceae*, or Duckweeds: A review of the descriptive and experimental literature", *Bot. Rev.*, **1961**, *27,* 221-287.
5. K. J. Appenroth, K. Krech, A. Keresztes, W. Fischer and H. Koloczek, "Effects of nickel on the chloroplasts of the duckweeds *Spirodela polyrhiza* and *Lemna minor* and their possible use in biomonitoring and phytoremediation", *Chemosphere*, **2010**, *78,* 216-223.
6. N. R. Axtell, S. P. Sternberg and K. Claussen, "Lead and nickel removal using *Microspora* and *Lemna minor*", *Bioresour. Technol.*, **2003**, *89,* 41-48.
7. N. Khellaf and M. Zerdaoui, "Growth response of the duckweed *Lemna gibba* L. to copper and nickel phytoaccumulation", *Ecotoxicology*, **2010**, *19*, 1363-1368.
8. E. Obek and A. Sasmaz, "Bioaccumulation of aluminum by *Lemna gibba* L. from secondary treated municipal wastewater effluents", *Bull. Environ. Contam. Toxicol.*, **2011**, *86*, 217-220.
9. J. J. Cheng and A. M. Stomp, "Growing duckweed to recover nutrients from wastewaters and for production of fuel ethanol and animal feed", *Clean Soil Air Water*, **2009**, *37*, 17-26.
10. British Standards Institute Staff, "Determination of the Toxic Effect of Water Constituents and Waste Water on Duckweed (*Lemna minor*). Duckweed Growth Inhibition Test", B S I Standards, London, **2006**.
11. OECD, "*Lemna sp.* growth inhibition test", in "OECD Guidelines for the Testing of Chemicals, Section 2", OECD Publishing, Paris, **2002**, Test No. 221.
12. R. Fischer, E. Stoger, S. Schillberg, P. Christou and R. M. Twyman, "Plant-based production of biopharmaceuticals", *Curr. Opin. Plant Biol.*, **2004**, *7*, 152-158.
13. T. Murashige and F. Skoog, "A revised medium for rapid growth and bio assays with tobacco tissue cultures", *Physiol. Plant.*, **1962**, *15*, 473-497.
14. J. B. Jones, "Hydroponics: Its history and use in plant nutrition studies", *J. Plant Nutr.*, **1982,** *5,* 1003-1030.
15. P. Langlois, S. Bourassa, G. G. Poirier and C. Beaulieu, "Identification of *Streptomyces coelicolor* proteins that are differentially expressed in the presence of plant material", *Appl. Environ. Microbiol.*, **2003**, *69*, 1884-1889.
16. J. Li, M. Jain, R. Vunsh, J. Vishnevetsky, U. Hanania, M. Flaishman, A. Perl and M. Edelman, "Callus induction and regeneration in *Spirodela* and *Lemna*", *Plant Cell Reports*, **2004**, *22*, 457-464.
17. H. Matsuzawa, Y. Tanaka, H. Tamaki, Y. Kamagata and K. Mori, "Culture-dependent and independent analyses of the microbial communities inhabiting the giant duckweed (*Spirodela polyrrhiza*) rhizoplane and isolation of a variety of rarely cultivated organisms within the Phylum Verrucomicrobia", *Microbes Environ.*, **2010**, *25*, 302-308.

18. Y. Yamamoto, N. Rajbhandari, X. Lin, B. Bergmann, Y. Nishimura and A. M. Stomp, "Genetic transformation of duckweed *Lemna gibba* and *Lemna minor*", *In Vitro Cell. Dev. Biol. Plant*, **2001**, *37*, 349-353.
19. H. Frick, "Callogenesis and carbohydrate utilization in *Lemna minor*", *J. Plant Physiol.*, **1991**, *137*, 397-401.
20. S. Inada, M. Tominaga and T. Shimmen, "Regulation of root growth by gibberellin in *Lemna minor*", *Plant Cell Physiol.*, **2000**, *41*, 657-665.
21. R. J. Newton, "Abscisic acid effects on growth and metabolism in the roots of *Lemna minor*", *Physiol. Plantarum*, **1974**, *30*, 108-112.
22. A. Rahman, A. Bannigan, W. Sulaman, P. Pechter, E. B. Blancaflor and T. I. Baskin, "Auxin actin and growth of the *Arabidopsis thaliana* primary root", *Plant J.*, **2007**, *50*, 514-528.
23. R. Swarup, P. Perry, D. Hagenbeek, D. Van Der Straeten, G. T. Beemster, G. Sandberg, R. Bhalerao, K. Ljung and M. J. Bennett, "Ethylene upregulates auxin biosynthesis in Arabidopsis seedlings to enhance inhibition of root cell elongation", *Plant Cell*, **2007**, *19*, 2186-2196.
24. M. L. Boss, M. J. Dukman and E. Russell, "Standardized culture of some Lemnaceae", *Quart. J. Florida Acad. Sci.*, **1964**, *26*, 335-346.
25. A. H. Datko, S. H. Mudd and J. Giovanelli, "*Lemna paucicostata* Hegelm. 6746: Development of standardized growth conditions suitable for biochemical experimentation", *Plant Physiol.*, **1980**, *65*, 906-912.
26. W. S. Hillman, "Experimental control of flowering in Lemna. III. A relationship between medium composition and the opposite photoperiodic responses of *L. perpusilla* 6746 and *L. gibba* G3", *Amer. J. Bot.*, **1961**, *48*, 413-419.
27. H. K. Moon and A. M. Stomp, "Effects of medium components and light on callus induction, growth, and frond regeneration in *Lemna gibba* (duckweed)", *In Vitro Cell. Dev. Biol. Plant*, **1997**, *33*, 20-25.
28. K. J. Appenroth, S. Teller and M. Horn, "Photophysiology of turion formation and germination in *Spirodela polyrhiza*", *Biol. Plantarum*, **1996,** *38*, 95-106.
29. K. J. Appenroth, "No photoperiodic control of the formation of turions in eight clones of *Spirodela polyrhiza*", *J. Plant Physiol.*, **2003**, *160,* 1329-1334.

Maejo Int. J. Sci. Technol. **2013**, *7*(01), 70-82

Maejo International Journal of Science and Technology

ISSN 1905-7873
Available online at www.mijst.mju.ac.th

Full Paper

Identification and biocellulose production of *Gluconacetobacter* strains isolated from tropical fruits in Thailand

Amornrat Suwanposri[1], Pattaraporn Yukphan[2], Yuzo Yamada[3] and Daungjai Ochaikul[1,*]

[1] Department of Biology, Faculty of Science, King Mongkut's Institute of Technology Ladkrabang, Chalongkrung Rd. Ladkrabang, Bangkok, 10520, Thailand
[2] BIOTEC Culture Collection (BCC), Bioresources Technology Unit, National Centre for Genetic Engineering and Biotechnology, National Science and Technology Development Agency, 113 Thailand Science Park, Phaholyothin Road, Klong 1, Klong Luang, Pathumthani 12120, Thailand
[3] Shizuoka University, 836 Ohya, Suruga-ku, Shizuoka 422-8529, Japan

* Corresponding author, e-mail: kodaungj@kmitl.ac.th

Received: 28 January 2012 / Accepted: 19 January 2013 / Published: 1 February 2013

Abstract: Two hundred and four strains of biocellulose (BC)-producing *Gluconacetobacter* strains were isolated from 48 rotten tropical fruits collected in Thailand. Twenty-nine representative isolates were selected from each of the 16 isolation sources and identified by morphological, physiological and biochemical characteristics and 16S rRNA gene sequence analysis. The selected 29 isolates were divided into seven subgroups within the *Gluconacetobacter xylinus* group of the genus *Gluconacetobacter* and identified as *Gluconacetobacter oboediens* (subgroup I, five isolates), *Gluconacetobacter rhaeticus* (subgroup II, one isolate), *Gluconacetobacter hansenii* (subgroup III, seven isolates), *Gluconacetobacter swingsii* (subgroup IV, two isolates) and *Gluconacetobacter sucrofermentans* (subgroup V, two isolates). The remaining isolates were grouped into subgroups VIa (three isolates) and VIb (nine isolates). All the isolates were cultured in Hestrin-Schramm (HS) medium statically at 30°C for 7 days to determine cellulose production capability. Of the 29 isolates, isolate PAP1 (subgroup VIb, unidentified) gave the highest yield (1.15 g/L) of BC. However, the BC yield increased threefold (3.5 g/L) when D-glucose in HS medium was replaced by D-mannitol.

Keywords: biocellulose-producing bacteria, *Gluconacetobacter*, tropical fruit, 16S rRNA gene sequence analysis

---

INTRODUCTION

Bacterial cellulose or biocellulose (BC) is an extracellular cellulose naturally produced by many species of microorganisms. BC has been considered as an alternative biomaterial since it possesses superior qualities to other cellulose. BC exhibits many unique characteristics which are different from those of other plant celluloses, such as high water-holding capacity (over 100 times of its weight), high degree of crystallinity, great elasticity, high tensile strength, non-drying state, excellent biocompatibility and high purity, because it is free from other contaminating components such as hemicelluloses, lignins or waxy aromatic substances [1-3]. These distinct physical and mechanical qualities have made BC more attractive than other materials well known as alternative materials in food, biomedical and other industries. For food applications, BC has been used as raw materials for nata de coco, which is a popular dessert in Philippines and other countries, and a dietary drink called Kombucha or Manchurian tea. In biomedical applications, BC is ideal for wound-healing dressing, micro blood vessels and scaffolds for tissue engineering of cartilage and bone [4-5]. In other applications, BC has potential for producing banknote and Bible paper, high performance speaker diaphragms, electronic paper displays, flexible display screens, paint thickeners, make-up pads and anti-aging cosmetics [2, 6-8].

Members of the genus *Gluconacetobacter* are divided into two groups, viz. the *Gluconacetobacter liquefaciens* group and the *Gluconacetobacter xylinus* group [9]. The former group consists of the non-nitrogen fixers such as *G. liquefaciens* and *G. sacchari* and the nitrogen fixers such as *G. diazotrophicus*, *G. azotocaptans* and *G. johannae*. The latter group consists of the non-BC producers such as *G. hansenii* and *G. europaeus*, and the BC producers such as *G. xylinus*, *G. nataicola* and *G. rhaeticus*. *G. xylinus* (formerly *Acetobacter xylinum*) are the most common species, many strains of which are high cellulose producers. These cellulose-producing bacteria are commonly found in natural sources such as flowers, vegetables, nuts, sugar cane and, in particular, rotten fruits [10-12]. Industrial production of BC using these bacteria is traditionally achieved by using a static cultivation method. BC is produced as white pellicle at the air-liquid interface of a liquid medium. However, this method requires a long cultivation time and large area while in shaking or agitated culture, non-BC producing mutants are produced [13]. Therefore, the improvement of static fermentation process, optimisation of culture condition and isolation of highly effective BC-producing strains are desirable.

Thailand is a country with relatively high humidity and high temperature and has a range of indigenous fruits that might be a rich source of BC-producing bacteria. This study is aimed at the isolation, identification and production of cellulose from *Gluconacetobacter* strains isolated from tropical fruits in Thailand.

MATERIALS AND METHODS

Isolation of *Gluconacetobacter* Strains

BC-producing *Gluconacetobacter* isolates in this study were isolated from 48 rotten tropical fruits collected in Thailand using the modification method described by Park et al. [12]. Firstly, 10 g of each rotten fruit was transferred into 90 mL of a modified Hestrin-Schramm (HS) medium in a 250-mL flask containing 2.0% D-glucose (w/v), 0.5% peptone (w/v), 0.5% yeast extract (w/v), 0.27% Na_2HPO_4 (w/v), 0.12% citric acid (w/v), 0.2% acetic acid (v/v), 0.5% ethanol (v/v) and 0.01% cycloheximide (w/v) [14]. The flask with rotten fruit and liquid medium was then incubated statically at 30°C for 7 days. After incubation, the flask with white pellicle covering the surface of the liquid medium was selected. The culture broth of the selected flask was serially diluted with 0.85% NaCl (w/v) and 0.1 mL of each dilution was spread on GEY agar, which was comprised of 2.0% D-glucose, 1.0% yeast extract, 5% ethanol and 0.3% $CaCO_3$. The agar plates were incubated at 30°C until colonies were formed. The colonies with a clear zone around were selected and transferred to vials containing 5 mL of HS medium and then incubated at 30°C for 3-7 days. Subsequently, only the vials with white pellicle on the surface were collected for further purification. The pellicles were confirmed by boiling with 0.5N NaOH for 15 min., since they might not be cellulose.

Selection of *Gluconacetobacter* Isolates

The BC-producing isolates with the highest and the lowest yields were selected from each fruit on the basis of BC thickness, yield and appearance. A single colony of each BC-producing isolate was transferred into 5 mL of HS medium in a vial and incubated statically at 30°C for 7 days. The resulting pellicle was harvested and washed three times with distilled water. Subsequently, BC appearance was observed by the naked eye and the thickness was measured with a vernier. The pellicle was then purified by heating with 2% NaOH at 121°C for 15 min. to remove bacterial contaminants and other residues. Finally, the purified cellulose was dried at 80°C in a hot air oven to constant weight.

Identification of *Gluconacetobacter* Strains

Morphological, physiological and biochemical characteristics of the selected isolates were determined using the method described by Asai et al. [15], Sokollek et al. [16] and Tortora et al. [17]. All the selected cellulose-producing bacteria were examined for 16S rRNA gene sequence analysis according to the method described by Yukphan et al. [18]. A specific fragment for 16S rRNA gene-coding regions was amplified using PCR amplification. Two primers, 20F (5'-GAG TTT GAT CCT GGC TCA G-3'; positions 9-27) and 1500R (5'-GTT ACC TTG TTA CGA CTT-3'; positions 1509-1492) were used. The positions in the rRNA gene fragment were based on the *Escherichia coli* numbering system (accession number V00348 [19]). The purified 16S rRNA genes from positions 9 to 1509 (approximately 1,500 bases) were sequenced by using four primers, 27F (5'-AGA GTT TGA TCM TGG CTC AG-3'; positions 27-46), 800R (5'-TAC CAG GGT ATC TAA TCC-3'; position 800-783), 518F (5'- CCA GCA GCC GCG GTA ATA CG-3'; position 518-537) and 1492R (5'- TAC GGY TAC CTT GTT ACG ACT T-3'; position 1492-1471). A phylogenetic tree for 1,280 bases was constructed by the neighbour-joining method of Saitou and Nei [20] using MEGA programme (version 4.0) [21] after multiple alignments of the sequences obtained with CLUSTAL W [22]. The distance matrices for the aligned sequences were calculated by the two-parameter method of Kimura [23]. The bootstrap values at branching points in the phylogenetic tree were calculated with 1,000 replications [24]. A 16S rRNA gene sequence similarity between the type strain of *Gluconacetobacter* species and an isolate was calculated for 1,390 bases.

BC Production by *Gluconacetobacter* Strains

To investigate BC-producing capacity, one loop of a cellulose-producing isolate was transferred to 100 mL of HS medium in a 250-mL flask and incubated at 30°C for 48 hr as starter culture. Ten millilitres of the culture was then added to 90 ml of HS medium in a 250-mL flask and incubated at 30°C for 7 days. The resulting pellicle was harvested, washed three times with distilled water and purified by heating with 2% NaOH at 121°C for 15 min. The purified cellulose pellicle was dried at 80°C in a hot air oven to constant weight.

RESULTS AND DISCUSSION

Identification of *Gluconacetobacter* Strains

From the 48 rotten fruits collected, 2,500 bacterial isolates were obtained as BC-producing candidates. They were then examined for BC production using a modified HS medium. As a result, 204 isolates from 16 fruits were BC-producing bacteria (Table 1). The most efficient isolates were from the governor's plum (*Flacourtia indica*) with 25 isolates, approximately 1.00% of the total 2,500 isolates and the least was from lady finger's banana (*Musa acuminata*) with one isolate, approximately 0.04% of the total isolates.

Table 1. BC-producing bacterial isolates

Isolation source and code	BC-producing isolate (%[a])	Selected isolate	Subgroup
Beleric myrobalan (*Terminalia bellerica*), BEL	3 (0.12)	BEL1	III (*G. hansenii*)
		BEL2	III (*G. hansenii*)
Fetid passion flower (*Passiflora foetida*), FET	15 (0.60)	FET4	III (*G. hansenii*)
		FET8	V (*G. sucrofermentans*)
Governor's plum (*Flacourtia indica*), GOV	25 (1.00)	GOV9	I (*G. oboediens*)
		GOV15	I (*G. oboediens*)
Grape (*Vitis vinifera*), GRA	11 (0.45)	GRA2	VIb (unidentified)
		GRA8	VIb (unidentified)
Java plum (*Syzygium cumini*), JAV	3 (0.12)	JAV1	VIb (unidentified)
		JAV3	VIb (unidentified)
Lady's finger banana (*Musa acuminata*), LAD	1 (0.04)	LAD1	III (*G. hansenii*)
Lychee (*Litchi chinensis*), LYC	15 (0.60)	LYC7	V (*G. sucrofermentans*)
		LYC8	III (*G. hansenii*)
Mamao (*Antidesma thwaiteaianum*), MAM	4 (0.16)	MAM2	VIb (unidentified)
		MAM4	I (*G. oboediens*)
Mangosteen (*Garcinia mangostana*), MAG	23 (0.92)	MAG6	VIa (unidentified)
		MAG15	VIb (unidentified)
Papaya (*Carrica papaya*), PAP	2 (0.08)	PAP1	VIb (unidentified)
Rambutan (*Nephelium lappaceum*), RAM	20 (0.80)	RAM1	II (*G. rhaeticus*)
		RAM4	VIb (unidentified)
Sapodilla (*Manikara achras*), SPO	23 (0.92)	SPO4	I (*G. oboediens*)
		SPO15	IV (*G. swingsii*)
Star fruit (*Averrhoa carambola*), STA	21 (0.85)	STA5	III (*G. hansenii*)
Sugar apple (*Annona squamosa*), SUG	20 (0.80)	SUG5	VIa (unidentified)
		SUG8	VIa (unidentified)
Water melon (*Citrullus lanatus*), WAT	15 (0.60)	WAT11	I (*G. oboediens*)
		WAT14	IV (*G. swingsii*)
Wild lemon (unknown species), WIL	3 (0.12)	WIL2	III (*G. hansenii*)
		WIL3	VIb (unidentified)
Total	204 (8.16)		

[a]Percentage of BC-producing bacteria from a total of 2,500 isolates

From the 204 BC-producing isolates, 29 isolates were selected as representative BC-producing strains and divided into seven subgroups based on morphological, physiological, biochemical characteristics and 16S rRNA gene sequences (Table 2 and Figure 1). Colonies of the 29 isolates on HS agar plates after 48-hr growth were pale yellow, smooth, viscous, convex, dense, with circular or irregular shape and entire or undulating margin. All the isolates were Gram-negative, rod-shaped or short rod and occurred singly or in pairs. The morphological results obtained are congruent with Dellaglio et al. [25], who isolated *Gluconacetobacter* strains from Italian apple fruit.

All the BC-producing isolates showed catalase-positive reactions and growth at pH 3.0-7.0. They grew slowly at pH 3.0, 3.5 and 4.0, but the growth was better at pH 4.5-7.0. Growing in different carbon sources indicated that all the isolates could not grow on sorbitol or methanol medium but grew well on glucose or sucrose medium (data not shown). Testing for acid production in different carbon sources indicated that all the isolates produced acid from D-glucose and D-sorbitol, but 9 out of 29 isolates also produced acid from D-arabinose, L-rhamnose and L-sorbose. From the different phenotypic characteristics obtained, the isolates were grouped into seven subgroups (Table 2).

Subgroup I contains five isolates, GOV9, GOV15, MAM4, SPO4 and WAT11, and is not identified as *G. intermedius* but as *G. oboediens*. The calculated 16S rRNA gene sequence similarities of these isolates are in the range of 99.6-99.7% of the type strain. According to Lisdiyanti et al. [29], *G. intermedius* is a later subjective synonym of *G. oboediens*, although the isolates first constituted a cluster along with the type strain of *G. intermedius* (Figure 1). They were isolated from governor's plum, mamao and water melon.

Subgroup II contains only one isolate, RAM1, and is identified as *G. rhaeticus*. The calculated 16S rRNA gene sequence similarity of the isolate is 99.9% of the type strain. It was isolated from rambutan.

Subgroup III contains seven isolates, BEL1, BEL2, FET4, LAD1, STA5, WIL2 and LYC8, and is identified as *G. hansenii*. The calculated 16S rRNA gene sequence similarities of these isolates are in the range of 99.6-99.8% of the type strain. They were isolated from beleric myrobalan, fetid passionflower, lady's finger banana, star fruit, wild lemon and lychee. Although isolate LYC8 is located in the cluster of *G. kombuchae* KG3^T (AY4688433), the isolate is identified as *G. hansenii*, as suggested by Cleenwerck et al. [30], who reported that *G. kombuchae* is a later subjective synonym of *G. hansenii*.

Subgroup IV contains two isolates, SPO15 and WAT14, which are located within the same cluster as *G. swingsii* and *G. europaeus* in the phylogenetic tree (Figure 1). On the basis of the growth on 30% D-glucose (w/v) with/without 0.2% acetic acid (v/v) [31], the isolates are identified as *G. swingsii*, not as *G. europaeus*, since they show the same results as the former but not as the latter (Table 2). The two isolates have 99.9% 16S rRNA gene sequence similarity to the type strain of *G. swingsii* and were isolated from sapodilla and water melon.

Subgroup V contains two isolates, LYC7 and FET8, and are identified as *G. sucrofermentans*, to the type strain of which the calculated 16S rRNA gene sequence are 100% similar. They grew on all the different carbon sources tested and were isolated from lychee and fetid passion flower.

Subgroup VI is divided into two subgroups, VIa and VIb. Subgroup VIa contains three isolates, MAG6, SUG5 and SUG8, and subgroup VIb contains nine isolates, GRA2, GRA8, JAV1, JAV3, MAG15, MAM2, PAP1, RAM4 and WIL3, all of which are located in different phylogenetic positions from any other known species of the genus *Gluconacetobacter* in the 16S rRNA gene sequence phylogenetic tree and assumed to constitute new species. They were isolated from grape, java plum, mangosteen, mamao, papaya, rambutan, sugar apple and wild lemon.

Table 2. Different phenotypic characteristics of selected isolates

Characteristic	Subgroup I: GOV9	GOV15	MAM4	SPO4	WAT11	*G. oboediens* LMG 18849[Ta]	Subgroup II: RAM1	*G. rhaeticus* LMG 22126[Tb]
Growth on 30% D-glucose	+	+	+	+	+	+	+	+
Growth without acetic acid	+	+	+	+	+	+	+	+
Acid production from								
D -glucose	+	+	+	+	+	nr	+	nr
D -arabinose	-	-	-	-	-	nr	+	nr
D -sorbitol	+	+	+	+	+	nr	+	nr
L-rhamnose	-	-	-	-	-	nr	-	nr
L-sorbose	-	-	-	-	-	nr	-	nr
Growth on different carbon								
ethanol	+	+	-	+	+	-	+	+
sucrose	+	+	+	+	+	+	+	+
sorbitol	+	+	+	+	+	-	+	-
D-mannitol	+	+	+	+	+	-	+	+

Characteristic	Subgroup III: BEL1	BEL2	FET4	LAD1	LYC8	STA5	WIL2	*G. hansenii* NBRC 14820[Tc]	Subgroup IV: SPO15	WAT14	*G. swingsii* LMG 22125[Tb]	*G. europaeus* LMG 18890[Td]
Growth on 30% D-glucose	+	+	+	+	+	+	+	-	+	+	+	-
Growth without acetic acid	+	+	+	+	+	+	+	+	+	+	+	-
Acid production from												
D -glucose	+	+	+	+	+	+	+	+	+	+	nr	nr
D -arabinose	-	+	-	-	-	-	-	nr	-	-	nr	nr
D -sorbitol	+	+	+	+	+	+	+	-	+	+	nr	nr
L-rhamnose	+	+	-	+	-	+	+	nr	+	+	nr	nr
L-sorbose	-	+	-	-	-	-	-	-	-	-	nr	nr
Growth on different carbon												
ethanol	+	+	-	+	+	+	-	-	-	+	+	-
sucrose	+	+	-	-	+	+	+	-	+	+	+	-
sorbitol	+	+	-	+	+	+	+	v	+	+	+	-
D-mannitol	+	+	+	+	+	+	+	-	+	+	+	-

Characteristic	Subgroup V: LYC7	FET8	*G. sucrofermentans* BPR2001[Te]	Subgroup VIa: MAG6	SUG5	SUG8	Subgroup VIb: GRA2	GRA8	JAV1	JAV3	MAG15	MAM2	PAP1	RAM4	WIL3
Growth on 30% D-glucose	+	+	nr	+	+	+	+	+	+	+	+	+	+	+	+
Growth without acetic acid	+	+	nr	+	+	+	+	+	+	+	+	+	+	+	+
Acid production from															
D -glucose	+	w	+	+	+	+	+	+	+	+	+	+	+	+	+
D -arabinose	-	-	nr	-	-	-	-	+	-	-	-	-	-	-	-
D -sorbitol	+	+	nr	+	+	+	+	+	+	+	+	+	+	+	+
L-rhamnose	-	-	nr	-	-	-	-	-	-	+	-	-	+	-	-
L-sorbose	-	-	nr	-	-	-	-	+	-	-	-	-	+	-	+
Growth on different carbon															
ethanol	+	+	+	-	-	+	-	+	-	-	-	-	+	+	-
sucrose	+	w	+	+	+	+	+	+	+	+	+	+	+	+	-
sorbitol	+	w	nr	+	+	+	+	+	+	+	+	+	+	+	-
D-mannitol	+	w	nr	+	+	+	+	+	+	+	+	+	+	+	+

+ = positive; - = negative; w = weakly positive; v = very weakly positive; nr = not reported

The data of the reference strains were cited from [a,d]Sokollek et al. [16], [b]Dellaglio et al. [25], [c]Gosselé et al. [26] and Navarro et al. [27] and [e]Toyosaki et al. [28]

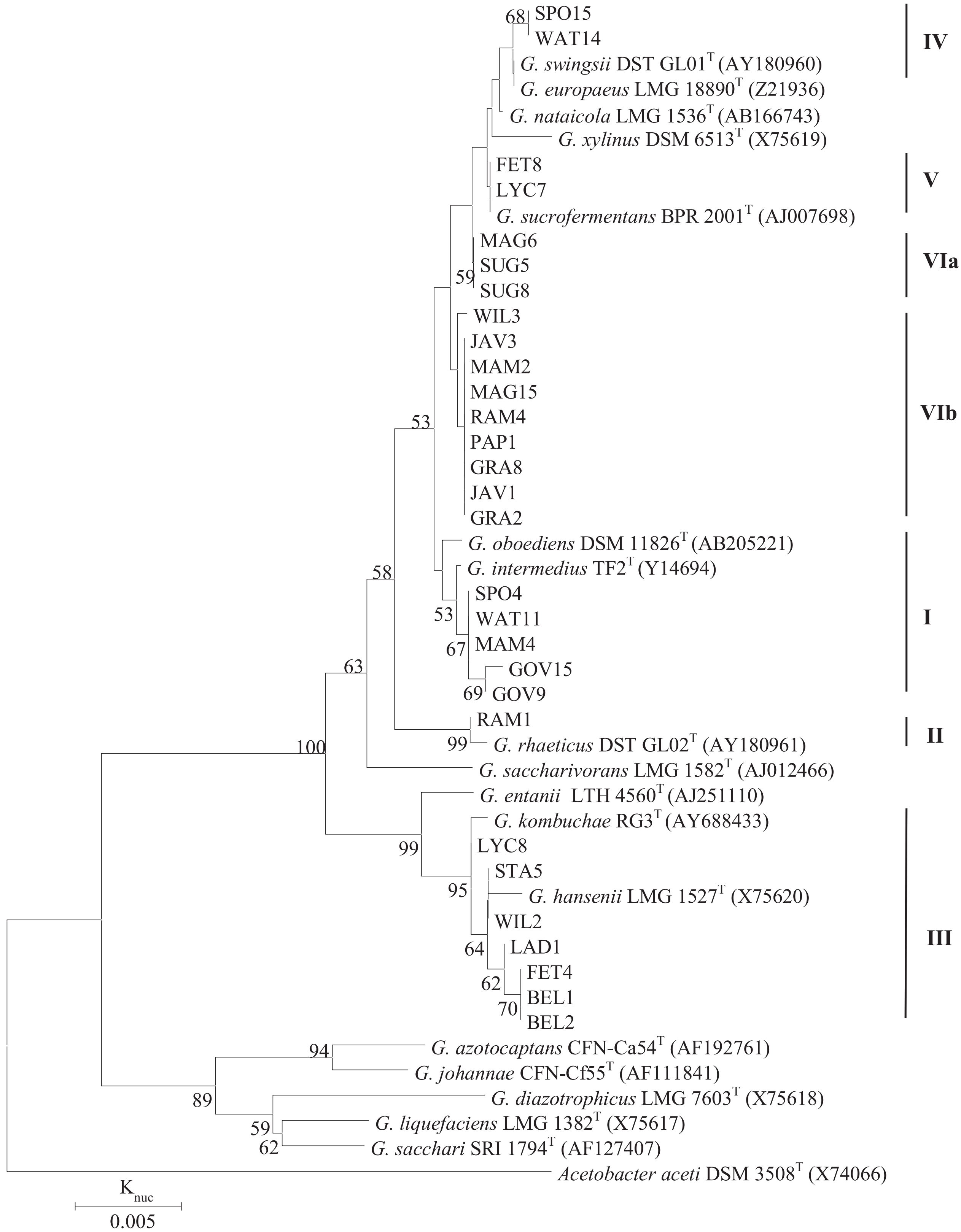

Figure 1. Phylogenetic relationships of BC-producing isolates. The numerals at the branching points indicate bootstrap values (%) derived from 1,000 replications. Only values greater than 50% are indicated.

BC Production by BC-Producing Isolates

All 29 isolates were cultivated in the standard HS medium under static condition with D-glucose as sole carbon source. After 48 hr, all isolates produced white gelatinous sheet at the air-liquid interface position of the medium. The results obtained are the same as those of Jagannath et al. [32]. The level of BC production ranged from 0.5 to 1.15 g/L, when the isolates were incubated statically at 30°C for 7 days (Figure 2). The lowest yield of 0.50 g/L was found in isolate SPO15 obtained from sapodilla and identified as *G. swingsii*. The highest yield of 1.15 g/L was found in isolate PAP1, isolated from papaya, and grouped into subgroup VIb and unidentified. The pH of the culture filtrates was 3.2-4.3.

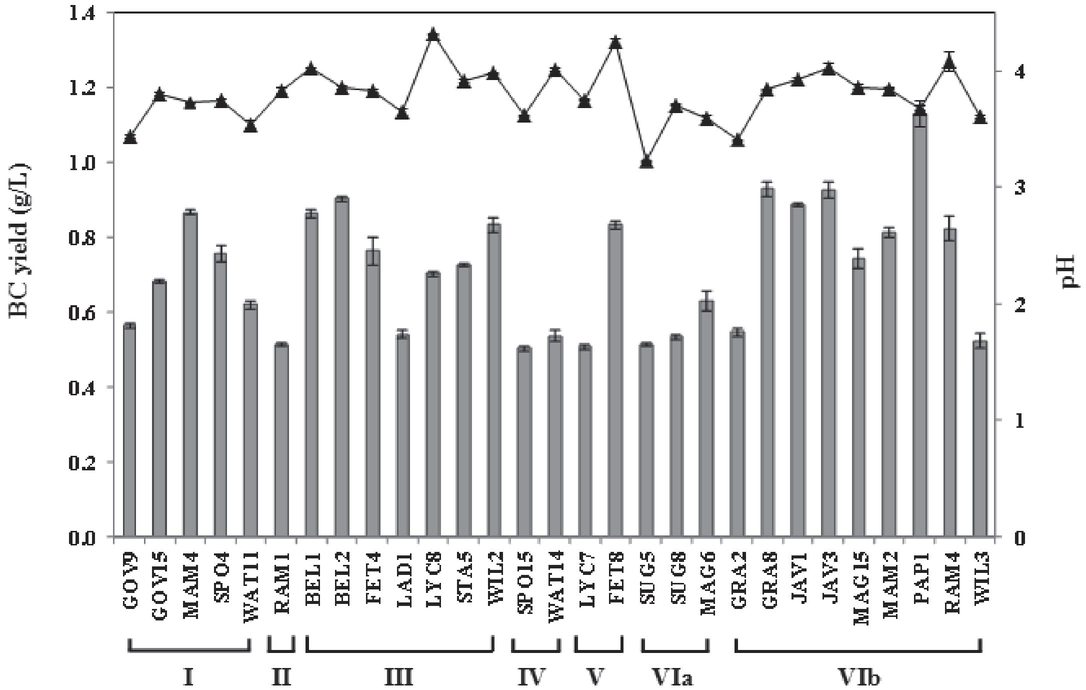

Figure 2. BC production by selected BC-producing isolates (▲ = pH). All data are means ± 1 SD of triplicate analyses.

Isolate PAP1 with the highest BC-production capability was selected and examined for viable cell count, BC production and pH change during cultivation in standard HS medium at 30°C for 10 days. As shown in Figure 3, the viable cells of isolate PAP1 increase exponentially after a 2-day lag period. The total viable cells increase rather slowly in the first and second days and then increase rapidly from the third day. The production of BC also increases rapidly from the third day, indicating that BC production by isolate PAP1 is growth-associated.

To investigate the effect of carbon sources on BC production, isolate PAP1 was incubated in standard HS medium, in which D-glucose, the original carbon source, was replaced by different carbon sources, i.e. D-fructose, D-mannitol, D-sorbitol, glycerol, ethanol, maltose, lactose and sucrose, at the concentration of 2.0% (w/v or v/v) (Figure 4). When D-mannitol is used as carbon source, isolate PAP1 produces BC with the highest yield of 3.5 g/L.

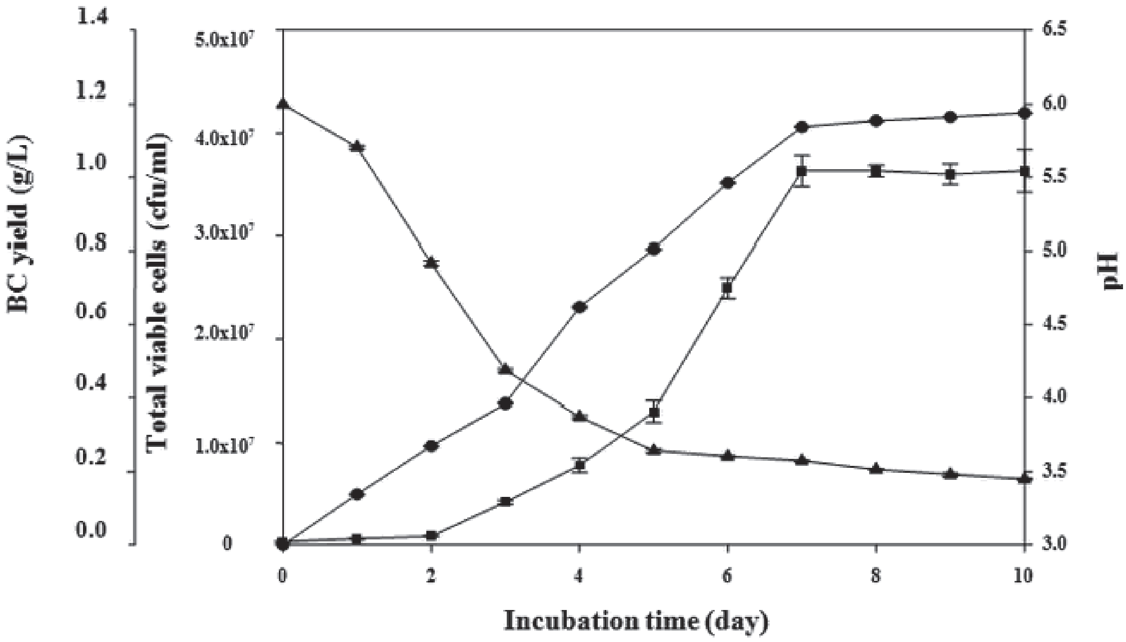

Figure 3. BC production by isolate PAP1: –●– = BC yield (g/L); –▲– = pH; –■– = total viable cells (cfu/mL). All data are means ± 1 SD of triplicate analyses.

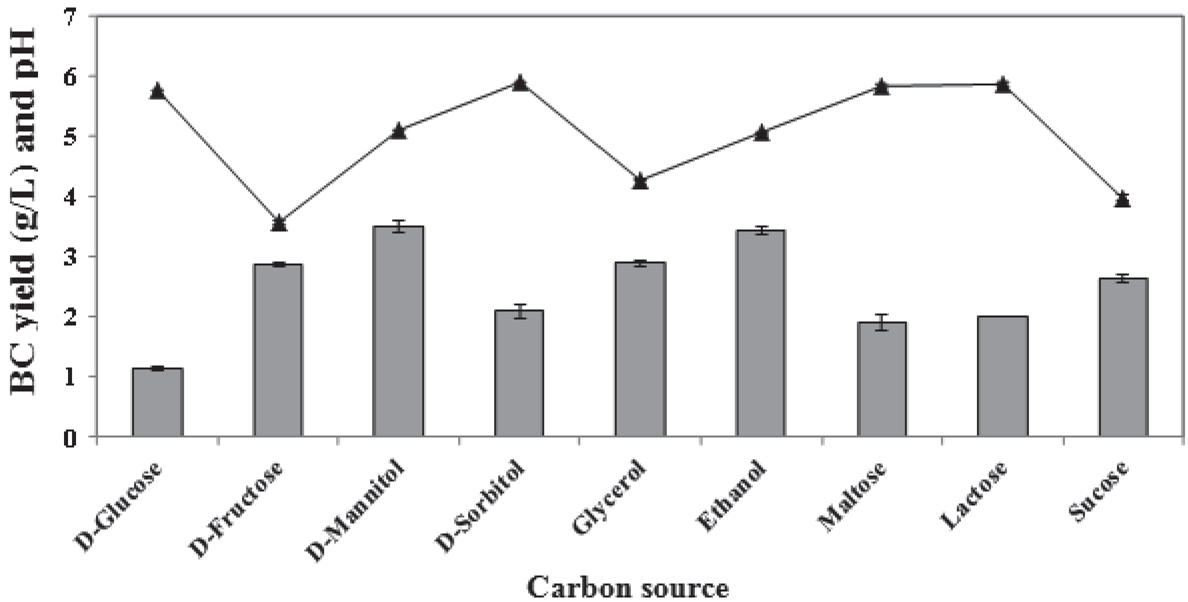

Figure 4. Effect of different carbon sources on BC production by isolate PAP1 (–▲– = pH). All data are means ± 1 SD of triplicate analyses.

A number of BC production studies have been reported. Keshk and Sameshima [33] mentioned that *Acetobacter xylinum* (= *G. xylinus*) ATCC 10245 gave 1.15 g/L of BC when cultivated in HS medium under static condition for 7 days. The amounts of BC produced in the present study appear to correspond to their results. Nguyen et al. [34] characterised the cellulose production by a *G. xylinus* strain isolated from Kombucha and found that this bacterium produced 0.28 ± 0.01 g/L of BC in HS medium when statically incubated at 30°C for 7 days. Under the same condition, Park et al. [12] also reported that 0.35 g/L cellulose was produced by a *G. hansenii* strain isolated from rotten apple. In the present study, isolate PAP1, which was isolated from rotten papaya, produces a large amount of BC (1.15 g/L) in HS medium.

It is well known that *G. xylinus*, a Gram-negative acetic acid bacterium, has long been used as a model organism for the study of BC biosynthesis, since it can utilise a wide range of substrates such as 5- or 6-carbon monosaccharides (e.g. D-glucose, D-fructose and D-xylose), oligosaccharides (e.g. sucrose), polysaccharides (e.g. starch), sugar alcohols (e.g. glycerol, D-mannitol and D-sorbitol), aliphatic alcohol (e.g. glycerol and ethanol), and industrial wastes including sugar cane molasses, coconut water, pineapple water and hydrolysed konjac powder to generate high amounts of cellulose [33-37].

In the present study, isolate PAP1 shows the capability of utilising a wide variety of carbon sources for BC production and D-mannitol seems to be the most suitable carbon source. D-Mannitol is probably transformed to D-fructose and then metabolised to BC. Under the experimental condition, D-gluconic acid was not produced during fermentation, so the pH remained stable [38]. Non-production of D-gluconic acid is assumed to give an optimal condition in cell growth and BC production. These results are in good agreement with previous reports that BC production by *Gluconacetobacter* strains and *G. xylinus* isolated from Kombucha culture produce the highest yields in a medium containing D-mannitol [34]. However, the capability of certain carbon source for BC production also seems to depend on the bacterial strain concerned. For example, *G. xylinus* ATCC 10245 and *Gluconacetobacter* sp. RKY5 isolated from persimmon vinegar give the highest BC yields (1.33 g/L and 2.45 g/L respectively) in glycerol [39, 40], and *G. sacchari* isolated from Kombucha gives the highest production (2.70 g/L) of BC in D-glucose [41]. The results obtained therefore seem to demonstrate that the factors affecting BC production are bacterial strain and carbon source.

Phylogenetic analysis based on 16S rRNA gene sequences shows that all the 29 BC-producing isolates belong to the *G. xylinus* group but not to the *G. liquefaciens* group, and are divided into seven subgroups (Figure 1). In the present study, the BC-producing bacterial isolates are identified as *G. oboediens* (subgroup I), the type strain of which does not produce BC; *G. rhaeticus* (subgroup II) and *G. hansenii* (subgroup III), the type strain of which does not produce BC; *G. swingsii* (subgroup IV) and *G. sucrofermentans* (subgroup V). However, it is remarkable in the present study that any strains assigned to *G. xylinus* were not isolated from tropical fruits collected in Thailand, suggesting that the species distribution might be rare in a tropical country. This phenomenon is in good accord with previous work on the diversity of acetic acid bacteria in Indonesia, Thailand and Philippines, where no *G. xylinus* strains are isolated from tropical fruits or flowers [42].

The isolates in the remaining subgroups VIa and VIb, are not identified. From the phylogenetic data obtained, it is obvious that these isolates constitute new species, which will be presented elsewhere.

CONCLUSIONS

The present study has demonstrated that tropical fruits collected in Thailand are a rich source of BC producers and isolate PAP1 of subgroup VIb is the most effective BC-producing *Gluconacetobacter* strain with the highest BC yield of 1.15 g/L in standard HS medium at static condition. In addition, D-mannitol is the most suitable carbon source for BC production by isolate

PAP1 with 3.5 g/L of BC. To reduce the production cost, however, optimisation of the culture condition and use of alternative cheaper carbon sources such as by-products or wastes from agricultural industry are desirable.

ACKNOWLEDGEMENTS

The authors are grateful to the National Science and Technology Development Agency, Pathumthani, Thailand for supporting this work and also to Sakaerat Environmental Research Station, Sakaerat Biosphere Reserves, Nakhon Ratchasima, Thailand for providing tropical fruit samples.

REFERENCES

1. P. Ross, R. Mayer and M. Benziman, "Cellulose biosynthesis and function in bacteria", *Microbiol. Mol. Biol. Rev.*, **1991**, *55*, 35-58.
2. J. Shah and R. M. Brown, "Towards electronic paper displays made from microbial cellulose", *Appl. Microbiol. Biotechnol*., **2005**, *66*, 352-355.
3. M. Shoda and Y. Sugano, "Recent advances in bacterial cellulose production", *Biotechnol. Bioproc. Eng.*, **2005**, *10*, 1-8.
4. A. Svensson, E. Nicklasson, T. Harrah, B. Panilaitis, D. L. Kaplan, M. Brittberg and P. Gatenholm, "Bacterial cellulose as a potential scaffold for tissue engineering of cartilage", *Biomaterials*, **2005**, *26*, 419-431.
5. D. Klemm, D. Schumann, U. Udhardt and S. Marsch, "Bacterial synthesized cellulose-artificial blood vessels for microsurgery", *Prog. Polym. Sci.*, **2001**, *26*, 1561-1603.
6. M. Iguchi, S. Yamanaka and A. Budhiono, "Bacterial cellulose-a masterpiece of nature's arts", *J. Mater. Sci.*, **2000**, *35*, 261-270.
7. E. J. Vandamme, S. De Baets, A. Vanbaelen, K. Joris and P. De Wulf, "Improved production of bacterial cellulose and its application potential", *Polym. Degrad. Stabil.*, **1998**, *59*, 93-99.
8. A. N. Nakagaito, M. Nogi and H. Yano, "Displays from transparent films of natural nanofibers", *Mater. Res. Soc. Bull.*, **2010**, *35*, 214-218.
9. Y. Yamada and P. Yukphan, "Genera and species in acetic acid bacteria", *Int. J. Food. Microbiol*., **2008**, *125*, 15-24.
10. T. Tsuchida and F. Yoshinaga, "Production of bacterial cellulose by agitation culture systems", *Pure Appl. Chem.*, **1997**, *69*, 2453-2458.
11. A. Seto, Y. Kojima, N. Tonouchi, T. Tsuchida and F. Yoshinaga, "Screening of bacterial cellulose-producing *Acetobacter* strains suitable for sucrose as a carbon source", *Biosci. Biotechnol. Biochem.*, **1997**, *61*, 735-736.
12. J. K. Park, Y. H. Park and J. Y. Jung, "Production of bacterial cellulose by *Gluconacetobacter hansenii* PJK isolated from rotten apple", *Biotechnol. Bioproc. Eng.*, **2003**, *8*, 83-88.
13. S. Valla and J. Kjosbakken, "Isolation and characterization of a new extracellular polysaccharide from a cellulose-negative strain of *Acetobacter xylinum*", *Can. J. Microbiol.*, **1981**, *27*, 599-603.
14. B. Hestrin and M. Schramm, "Synthesis of cellulose by *Acetobacter xylinum*. 2. Preparation of freeze-dried cells capable of polymerizing glucose to cellulose", *Biochem. J.*, **1954**, *58*, 345-352.

15. T. Asai, H. Iizuka and K. Komagata, "The flagellation and taxonomy of the genera *Gluconobacter* and *Acetobacter* with reference to the existence of intermediate strains", *J. Gen. Appl. Microbiol.*, **1964**, *10*, 95-126.
16. S. J. Sokollek, C. Hertel and W. P. Hammes, "Description of *Acetobacter oboediens* sp. nov. and *Acetobacter pomorum* sp. nov., two new species isolated from industrial vinegar fermentations", *Int. J. Syst. Bacteriol.*, **1998**, *48*, 935-940.
17. G. J. Tortora, B. R. Funke and C. L. Case, "Microbiology: An Introduction", 7th Edn., Benjamin Cummings Publishing, San Francisco, **2001**, pp.69-70.
18. P. Yukphan, T. Malimas, M. Takahashi, W. Potacharoen, T. Busabun, S. Tanasupawat, Y. Nakagawa, M. Tanticharoen and Y. Yamada, "Re-identification of *Gluconobacter* strains based on the restriction analysis of 16S-23S rDNA internal transcribed spacer regions", *J. Gen. Appl. Microbiol.*, **2004**, *50*, 189-195.
19. J. Brosius, T. J. Dull, D. D. Sleeter and H. F. Noller, "Gene organization and primary structure of a ribosomal RNA operon from *Escherichia coli*", *J. Mol. Biol.*, **1981**, *148*, 107-127.
20. N. Saitou and M. Nei, "The neighbor-joining method: A new method for reconstructing phylogenetic trees", *Mol. Bio. Evol.*, **1987**, *4*, 406-425.
21. K. Tamura, J. Dudley, M. Nei and S. Kumar, "MEGA4: Molecular evolutionary genetics analysis (MEGA) software version 4.0", *Mol. Biol. Evol.*, **2007**, *24*, 1596-1599.
22. J. D. Thomson, D. G. Higgins and T. J. Gibson, "CLUSTAL W: Improving the sensitivity of progressive multiple sequence alignment through sequence weighting, position-specific gap penalties and weight matrix choice", *Nucleic Acids Res.*, **1994**, *22*, 4673-4680.
23. M. Kimura, "A simple method for estimating evolutionary rates of base substitutions through comparative studies of nucleotide sequences", *J. Mol. Evol.*, **1980**, *16*, 111-120.
24. J. Felsenstein, "Confidence limits on phylogenies: An approach using the bootstrap", *Evolution*, **1985**, *39*, 783-791.
25. F. Dellaglio, I. Cleenwerck, G. E. Felis, K. Engelbeen, D. Janssens and M. Marzotto, "Description of *Gluconacetobacter swingsii* sp. nov. and *Gluconacetobacter rhaeticus* sp. nov., isolated from Italian apple fruit", *Int. J. Syst. Evol. Microbiol.*, **2005**, *55*, 2365-2370.
26. F. Gosselé, J. Swings, K. Kersters, P. Pauwels and J. De Ley, "Numerical analysis of phenotypic features and protein gel electrophoregrams of a wide variety of *Acetobacter* strains. Proposal for the improvement of the taxonomy of the genus *Acetobacter* Beijerinck 1898, 215^{AL}", *Syst. Appl. Microbiol.*, **1983**, *4*, 338-368.
27. R. R. Navarro, T. Uchimura and K. Komagata, "Taxonomic heterogeneity of strains comprising *Gluconacetobacter hansenii*", *J. Gen. Appl. Microbiol.*, **1999**, *45*, 295-300.
28. H. Toyosaki, Y. Kojima, T. Tsuchida, K. I. Hoshino, Y. Yamada and F. Yoshinaga, "The characterization of an acetic acid bacterium useful for producing bacterial cellulose in agitation cultures: The proposal of *Acetobacter xylinum* subsp. *sucrofermentans* subsp. nov.", *J. Gen. Appl. Microbiol.*, **1995**, *41*, 307-314.
29. P. Lisdiyanti, R. R. Navarro, T. Uchimura and K. Komagata, "Reclassification of *Gluconacetobacter hansenii* strains and proposals of *Gluconacetobacter saccharivorans* sp. nov. and *Gluconacetobacter nataicola* sp. nov.", *Int. J. Syst. Evol. Microbiol.*, **2006**, *56*, 2101-2111.
30. I. Cleenwerck, M. De Wachter, Á. González, L. De Vuyst and P. De Vos, "Differentiation of species of the family *Acetobacteraceae* by AFLP DNA fingerprinting: *Gluconacetobacter*

kombuchae is a later heterotypic synonym of *Gluconacetobacter hansenii*", *Int. J. Syst. Evol. Microbiol.*, **2009**, *59*, 1771-1786.

31. D. Dutta and R. Gachhui, "Nitrogen-fixing and cellulose-producing *Gluconacetobacter kombuchae* sp. nov., isolated from Kombucha tea", *Int. J. Syst. Evol. Microbiol.*, **2007**, *57*, 353-357.
32. A. Jagannath, A. Kalaiselvan, S. S. Manjunath, P. S. Raju and A. S. Bawa, "The effect of pH, sucrose and ammonium sulphate concentrations on the production of bacterial cellulose (Nata-de-coco) by *Acetobacter xylinum*", *World J. Microbiol. Biotechnol.,* **2008**, *24*, 2593-2599.
33. S. Keshk and K. Sameshima, "The utilization of sugar cane molasses with/without the presence of lignosulfonate for the production of bacterial cellulose", *Appl. Microbiol. Biotechnol.*, **2006**, *72*, 291-296.
34. V. T. Nguyen, B. Flanagan, M. J. Gidley and G. A. Dykes, "Characterization of cellulose production by a *Gluconacetobacter xylinus* strain from Kombucha", *Curr. Microbiol.*, **2008**, *57*, 449-453.
35. P. R. Chawla, I. B. Bajaj, S. A. Survase and R. S. Singhal, "Microbial cellulose: Fermentative production and applications", *Food. Technol. Biotechnol.*, **2009**, *47*, 107-124.
36. S. Kongruang, "Bacterial cellulose production by *Acetobacter xylinum* strains from agricultural waste products", *Appl. Biochem. Biotechnol.*, **2008**, *148*, 245-256.
37. F. Hong and K. Qiu, "An alternative carbon source from konjac powder for enhancing production of bacterial cellulose in static cultures by a model strain *Acetobacter aceti* subsp. *xylinus* ATCC 23770", *Carbohydr. Polym.*, **2008**, *72*, 545-549.
38. R. Jonas and L. F. Farah, "Production and application of microbial cellulose", *Polym. Degrad. Stabil.*, **1998**, *59*, 101-106.
39. S. M. A. S. Keshk and K. Sameshima, "Evaluation of different carbon sources for bacterial cellulose production", *Afr. J. Biotechnol.*, **2005**, *4*, 478-482.
40. S. Y. Kim, J. N. Kim, Y. J. Wee, D. H. Park and H. W. Ryu, "Production of bacterial cellulose by *Gluconacetobacter* sp. RKY5 isolated from persimmon vinegar", *Appl. Biochem. Biotechnol.*, **2006**, *131*, 705-715.
41. E. Trovatti, L. S. Serafim, C. S. R. Freire, A. J. D. Silvestre and C. P. Neto, "*Gluconacetobacter sacchari*. An efficient bacterial cellulose cell-factory", *Carbohydr. Polym.*, **2011**, *86*, 1417-1420.
42. P. Lisdiyanti, K. Katsura, W. Potacharoen, R. R. Navarro, Y. Yamada, T. Uchimura and K. Komagata, "Diversity of acetic acid bacteria in Indonesia, Thailand, and the Philippines", *Microbiol. Cult. Coll.*, **2003**, *19*, 91-99.

Maejo Int. J. Sci. Technol. **2013**, *7*(01), 83-93

Maejo International
Journal of Science and Technology

ISSN 1905-7873
Available online at www.mijst.mju.ac.th

Report

Essential oil composition of sixteen elite cultivars of *Mentha* from western Himalayan region, India

Rajendra C. Padalia[1,*], Ram S. Verma[1], Amit Chauhan[1], Velusamy Sundaresan[2] and Chandan S. Chanotiya[2]

[1] CSIR-Central Institute of Medicinal and Aromatic Plants (CIMAP), Research Centre, Pantnagar-263 149, Uttarakhand, India

[2] CSIR-Central Institute of Medicinal and Aromatic Plants (CIMAP), Lucknow-226 015, Uttar Pradesh, India

* Corresponding author, e-mail: padaliarc@rediffmail.com; tel: +91 5944 234445; fax: +91 5944 234712

Received: 12 October 2011 / Accepted: 1 February 2013 / Published: 4 February 2013

Abstract: The hydrodistilled essential oils of 16 cultivars of *Mentha*, viz. *M. arvensis* L., *M. spicata* L. and *M. citrata* Ehrh., were analysed and compared by gas chromatography and gas chromatography-mass spectrometry. Fifty-seven constituents representing 92.8-99.8% of the total essential oil composition were identified. Monoterpenoids (88.1-98.6%) are the major constituents of the essential oils. The major constituents of the oils in 9 cultivars of *M. arvensis* are menthol (73.7-85.8%), menthone (1.5-11.0%), menthyl acetate (0.5-5.3%), isomenthone (2.1-3.9%), limonene (1.2-3.3%) and neomenthol (1.9-2.5%). Carvone (51.3-65.1%), limonene (15.1-25.2%), β-pinene (1.3-3.2%) and 1,8-cineole (≤0.1-3.6%) are the major constituents in 5 cultivars of *M. spicata*, while in one cultivar (Ganga) of *M. spicata* the major constituents are piperitenone oxide (76.7%), α-terpineol (4.9%) and limonene (4.7%). Linalool (59.7%), linalyl acetate (18.4%), nerol (2.0%), *trans*-p-menth-1-en-2-ol (1.8%), α-terpineol (1.5%) and limonene (1.1%) are the major constituents of *M. citrata*.

Keywords: *Mentha arvensis*, *Mentha spicata*, *Mentha citrata*, essential oils, western Himalayan region

---

INTRODUCTION

Mentha species (commonly known as mint), belonging to family Lamiaceae, constitute one of the most popular essential oil crops. They are widely distributed and cultivated in the temperate and subtemperate regions of the world [1]. Among them, *Mentha arvensis* (corn mint), *M. piperita* (peppermint), *M. citrata* (bergamot mint) and *M. spicata* (spearmint) are the main species cultivated in the temperate, Mediterranean and subtropical regions [2-4]. These species show considerable chemical diversity in the essential oil composition and are considered industrial crops as they produce a number of commercially valuable essential oils containing a complex mixture of monoterpenoids which are extensively used in pharmaceutical, food, flavour, cosmetics, beverages and allied industries [5-23]. Earlier reports on the chemical composition of oils from *Mentha* species from Himalayan region showed menthol (61.92-89.30%) and carvone (59.62-76.65%) as major constituents of oils from *M. arvensis* and *M. spicata* respectively [16-20]. Menthol (30.3-47.8%), menthone (4.5-48.6%), menthyl acetate (1.0-9.5%), menthofuran (0.1-14.6%), 1,8-cineole (4.1-8.9%), neomenthol (1.5-4.9%) and isomenthone (1.2-3.9%) were reported as major constituents of oils from *M. piperita* cultivars grown in mid- and foothills of Uttarakhand, India [21]. Piperitone, piperitenone oxide and piperitone epoxides were reported as the major oil constituents of *M. longifolia* [22]. However, another report on oil of *M. longifolia* from Himalayan region showed carvone (61.12-78.70%), dihydrocarveol (0.40-9.45%), *cis*-carvyl acetate (0.16-6.43%) and germacrene D (1.25-5.73%) as major constituents [23]. In oil of *M. citrata*, linalool (32.86-46.31%), linalyl acetate (19.27-37.72%) and α-terpineol (2.90-4.61%) were reported as major constituents at different crop stages [17]. India fulfills over 80% of the total global demand with production of more than 16,000 ton of mint oil, spreading mainly over the Indo-Gangetic plains and north-west India [21, 24, 25]. The essential oil composition of various mint species shows remarkable variation due to their hybrid nature and existence of various chemotypes, along with common climatic and geographical variations. The present study aims to assess the yield and quality performance of oils from prevalent commercial cultivars of *Mentha*. The essential oil composition of 16 cultivars of *Mentha* species, viz. *M. arvensis* L., *M. spicata* L. and *M. citrata* Ehrh., from the foothills of western Himalayas, are compared in detail.

MATERIALS AND METHODS

Plant Materials and Isolation of Essential Oils

Fresh aerial parts of different cultivars of *Mentha* species were collected from the experimental field of Research Centre, Central Institute of Medicinal and Aromatic Plants, Pantnagar, Uttarakhand. The experimental site is located at the latitude of 29°N and longitude of 79.38°E, at an altitude of 243.84 metres at the foothills of the Himalayas with a hot summer and chilled winter climate. The maximum temperature ranges between 35-45°C and the minimum between 2-5°C with average rainfall of 1350 mm during the year. The soil was clay loam in texture with neutral reaction (pH 7.1). The monsoon usually breaks in mid June and continues up to September. Botanical authentication of the plant materials was carried out at the taxonomy department of CIMAP Research Centre, Pantnagar. All cultivars were planted in the month of February by their vegetative propagules (suckers and runners) at inter-row space of 50 cm and raised by following normal agricultural practices. The origins of all the cultivars studied are given in Table 1.

Table 1. Genetic origin of commercially grown elite cultivars of *Mentha*

Plant	Cultivar	Abbreviation	Origin/ Development	Reference
Mentha arvensis L. (Japanese mint)	Shivalik	I	Introduction from China	26
	Himalaya	II	Hybrid of Gomti and Kalka	26
	MAS-I	III	Somatic variant of the MA-3 accession from Thailand	26
	Damroo	IV	Selection in OPSPs* of the variety Shivalik	19
	Kalka	V	Cross-hybridisation	19
	Gomti	VI	Seedling variant of Shivalik	27
	Kushal	VII	In vitro somaclonal selection	28
	Saksham	VIII	Clonal selection	29
	Kosi	IX	Half-sib progeny selection in cv. Kalka	30
Mentha spicata L. (Spearmint)	MSS-5	X	Clonal selection	31
	Neera	XI	Induced mutagenesis	31
	Arka	XII	Induced mutagenesis	31
	Neerkalka	XIII	Interspecific hybridisation of *M. arvensis* cv. Kalka and *M. spicata* cv. Neera	32
	Supriya	XIV	Selection of superior strain in a northern Himalayan accession	33
	Ganga	XV	Clonal selection	34
Mentha citrata L. (Bergamot mint)	Kiran	XVI	Induced mutagenesis	35

* Open Pollinated Seed Progenies

Freshly harvested samples (100 g each) were hydrodistilled in a Clevenger apparatus for 3 hr. The oils were collected, dehydrated by anhydrous sodium sulphate, stored in amber vials and put in a cool and dark place prior to analysis. The extraction yield was calculated in mL of oil per 100 g of samples.

Gas Chromatographic (GC) Analysis

GC analysis of the essential oil samples was carried out on a Nucon gas chromatograph model 5765 equipped with a flame ionisation detector (FID) and CP Wax-52 CB (30 m × 0.32 i.d., 0.25 μm film thickness) fused silica capillary column. Hydrogen was used as carrier gas at 1.0 mL/min. Temperature programming was done between 70-230°C at 4°C/min. with final hold time of 10 min. Injector and detector temperatures were 210°C and 220°C respectively. Injection volume was 0.02 μL neat and split ratio was 1:40. The percentage of the individual constituent was calculated by electronic integration of the FID peak areas without response factor correction. GC analysis of a few oil samples was also carried out for cross identification of constituents by retention index (RI) on a Varian CP-3800 GC apparatus using a DB-5 column (30 m x 0.25 mm i.d., film thickness 0.25 μm) equipped with an FID. The column temperature (60-240°C) was programmed at 3°C/min. with final hold time of 10 min. using nitrogen as carrier gas at 1 mL/min.

Analysis by Gas Chromatography-Mass Spectrometry (GC-MS)

GC-MS analysis of the essential oils was performed with a Perkin-Elmer turbomass quadrupole mass spectrometer fitted with an Equity-5 fused silica capillary column (60 m × 0.32 mm i.d., film thickness 0.25 μm). The oven column temperature was 70-250°C, programmed at 3°C/min. with initial and final hold time of 2 min., using helium as carrier gas at constant pressure (10 psi). The injection volume was 0.02 μL neat with split ratio of 1:30. The injector and ion source temperature was 250^{o}C. The ionisation energy was 70 eV (EI) with a mass scan range of 40-400 amu.

Identification of Constituents

Identification of constituents was done on the basis of retention time, RI (determined with reference to homologous series of *n*-alkanes (C_9-C_{24}) under identical experimental condition in both polar and non polar columns), coinjection with standards, mass spectra library search (NIST/EPA/NIH version 2.1 and Wiley registry of mass spectral data, 7th edition), and by comparing RI and mass spectral data with literature [36, 37]. For quantification, the relative area percentage obtained for each constituent from the GC/FID analysis of the oils was used to calculate the mean values without using correction factors.

RESULTS AND DISCUSSION

Analysis results of the hydrodistilled essential oil of *Mentha* cultivars as well as oil yields are presented Table 2 in order of their elution on CP Wax 52 CB (0.30 m × 0.32 mm) capillary column. Fifty-seven compounds are identified, representing 92.8-99.8% of the total oil composition, which is mainly dominated by monoterpenoids (88.1-98.6%). Thirty-three constituents are identified in the essential oils of nine cultivars of *M. arvensis* accounting for 98.8-99.8% of oil composition. The major constituents of oils are monoterpenoids (97.7-98.6%), represented by 92.1-94.9% of oxygenated monoterpenes and 3.5-5.8% of hydrocarbons. Menthol (73.7-85.8%), menthone (1.5-11.0%), menthyl acetate (0.5-5.3%), isomenthone (2.1-3.9%), limonene (1.2-3.3%) and neomenthol (1.9-2.5%) are the major identified constituents. All the cultivars are rich in menthol (73.7%-85.8%) and the highest menthol content is found in MAS-1 (85.8%) followed by Kosi (78.7%), Shivalik (78.1%) and Damroo (78.0%). The menthone content varies between 1.5-11.0%, with the highest in Gomti (11.0%) followed by Kalka (7.6%), while MAS-1 contains a relatively low amount (1.5%).

Although the major characteristic constituents in all oils are the same, there are considerable variations in the quantitative make-up of the constituents of the essential oils. Earlier, menthol (61.9-82.1%), menthone (3.4-19.3%), isomenthone (2.3-6.1%), limonene (0.2-4.7%), menthyl acetate (0.5-4.4%) and neomenthol (1.3-2.4%) were reported as major constituents in different crop stages of *M. arvensis* from the mid-hills of Uttrakhand [16], while *M. arvensis* grown in foothill conditions showed high menthol content (77.5-89.3%), along with menthone, iso-menthone, menthyl acetate, neo menthol and limonene as other major constituents [19]. *M. arvensis* cv. Shivalik grown in the tropical climate of India shows menthol (53.2-82.3%), menthone (5.2-30.2%), isomenthone (2.1-3.5%) and neomenthol (0.9-2.0%) as major constituents from its flowering whole herb, flowers, leaves and stem [38]. In the present analysis menthol (73.7-85.8%) is also the major constituent in all cultivars of *M. arvensis*, with slight qualitative and quantitative variations in other individual oil constituents.

Table 2. Comparative oil yield and chemical composition of commercially grown elite cultivars of *Mentha*

Compound[*]	RI[a]	RI[b]	% (FID)															
			I	*II*	*III*	*IV*	*V*	*VI*	*VII*	*VIII*	*IX*	*X*	*XI*	*XII*	*XIII*	*XIV*	*XV*	*XVI*
α-Pinene	1026	939	0.5	0.7	0.5	0.7	0.5	0.7	0.7	0.6	t	0.9	1.6	1.6	0.8	0.8	0.4	0.8
α-Thujene	1028	928	t	t	t	1.0	-	-	t	-	t	-	-	0.2	1.4	-	0.6	-
β-Pinene	1104	982	0.9	1.1	0.2	t	0.7	1.0	0.9	1.0	0.9	1.4	3.2	2.0	2.4	1.3	t	0.8
Sabinene	1116	978	t	t	t	t	-	-	t	t	t	-	-	t	-	-	t	0.3
β-Myrcene	1158	994	0.5	0.6	0.5	0.6	0.6	0.6	0.6	0.6	0.6	2.3	0.2	2.8	t	1.0	0.8	0.3
α-Terpinene	1177	1022	-	-	-	-	-	-	-	-	-	t	t	0.2	-	-	t	-
Limonene	1195	1034	1.6	3.3	2.5	2.2	3.0	1.2	2.9	3.2	2.3	15.1	19.3	20.5	16.5	25.2	4.7	1.1
1,8-Cineole	1199	1038	t	t	t	t	t	0.4	-	t	-	3.0	t	3.6	3.0	t	0.4	0.9
(*Z*)-β-Ocimene	1230	1042	t	0.1	-	-	t	0.1	t	t	t	0.2	0.4	-	0.2	t	t	0.1
γ-Terpinene	1244	1065	t	t	-	-	t	t	t	t	t	0.2	-	0.5	0.2	0.2	t	0.2
(*E*)-β-Ocimene	1245	1051	-	-	-	-	-	-	-	-	-	-	-	-	-	0.2	t	0.2
p-Cymene	1271	1029	t	t	t	t	-	-	-	t	-	0.1	0.6	0.2	0.1	0.1	t	-
Terpinolene	1278	1089	-	-	-	-	-	-	-	-	-	t	0.3	t	t	t	t	0.2
3-Octyl acetate	1286	1261	-	-	-	-	-	-	-	-	-	0.2	1.0	0.4	0.2	0.9	-	-
(*Z*)-3-Hexenol	1391	841	0.1	0.2	t	0.1	0.1	t	0.1	0.1	0.1	-	-	-	-	-	-	-
3-Octanal	1428	994	0.0	0.3	0.6	0.7	0.2	1.2	0.2	0.3	0.7	0.5	1.9	0.6	0.5	0.1	0.2	-
trans-Linalool oxide	1450	1093	-	-	-	-	-	-	-	-	-	-	-	-	-	-	-	0.3
α-Cubebene	1458	1357	-	-	-	-	-	-	-	-	-	t	0.8	t	t	0.6	-	-
Menthone	1460	1155	5.5	5.8	1.5	5.0	7.6	11.0	5.0	6.5	5.6	-	-	-	1.7	0.9	-	-
trans-Sabinene hydrate	1463	1069	t	-	t	t	-	t	t	-	t	1.7	1.1	1.5	t	0.4	0.2	-
cis-Linalool oxide	1478	1074	-	-	-	-	-	-	-	-	-	-	-	-	-	-	-	0.6
Isomenthone	1488	1165	3.2	3.9	2.1	2.9	3.4	3.2	3.4	3.6	3.3	-	t	0.1	t	-	-	-
β-Bourbonene	1508	1386	-	-	-	-	-	-	-	-	-	t	0.8	t	t	0.2	0.3	0.9
Linalool	1535	1101	-	t	-	t	-	t	0.1	-	-	-	0.7	0.1	1.7	1.1	1.6	59.7
Linalyl acetate	1540	1256	-	-	-	-	-	-	-	-	-	-	-	-	-	-	-	18.4
trans-p-Menth-1-en-2-ol	1558	1140	-	-	-	-	-	-	-	-	-	t	0.9	0.5	0.1	t	-	1.8
Menthyl acetate	1560	1296	3.7	2.1	0.5	3.7	1.5	2.3	5.3	1.8	2.2	-	t	-	0.5	-	-	-
iso-Pulegol	1574	1158	0.6	0.9	0.4	0.5	0.8	0.4	0.8	0.8	0.6	-	-	-	-	-	-	-
β-Caryophyllene	1590	1420	t	t	0.5	t	0.1	0.2	0.1	0.1	0.1	1.0	1.8	1.6	1.0	0.3	0.9	t
Neomenthol	1595	1165	2.4	2.0	2.1	2.4	2.2	1.9	2.3	2.2	2.5	-	-	-	t	-	-	-
Terpinen-4-ol	1606	1180	-	t	0.1	0.1	t	0.1	t	-	-	t	0.3	0.0	t	0.7	0.7	t
(*Z*)-Dihydro carvone	1624	1193	-	-	-	-	-	-	-	-	-	0.2	1.2	0.6	0.2	0.8	-	-
Pulegone	1646	1238	0.3	0.3	0.5	0.3	0.2	0.1	0.4	0.2	0.3	-	-	-	-	0.1	-	-
Menthol	1650	1176	78.1	76.4	85.8	78.0	77.1	73.7	75.4	77.3	78.7	-	-	-	0.7	-	-	-

Table 2. (Continued)

Compound[*]	RI[a]	RI[b]	% (FID)															
			I	*II*	*III*	*IV*	*V*	*VI*	*VII*	*VIII*	*IX*	*X*	*XI*	*XII*	*XIII*	*XIV*	*XV*	*XVI*
(*E*)-β-Farnesene	1670	1188	0.4	0.1	0.1	0.2	t	0.3	t	t	0.2	0.7	t	0.1	-	0.7	t	t
Isomenthol	1673	1459	0.1	0.4	0.3	0.2	0.4	0.4	0.4	0.3	0.2	-	-	-	-	-	-	-
α-Humulene	1675	1454	-	-	-	-	-	-	-	-	-	t	0.4	0.6	-	t	t	0.2
α-Terpineol	1682	1192	0.2	0.2	0.3	0.2	0.2	0.2	0.2	0.2	0.2	t	0.7	0.1	t	0.1	4.9	1.5
Germacrene D	1701	1481	0.1	0.1	0.2	0.1	0.1	0.1	0.1	0.1	0.1	1.1	t	0.2	1.1	0.2	0.4	0.1
Piperitone	1748	1255	0.5	0.4	0.6	0.5	0.5	0.5	0.5	0.5	0.5	-	-	0.2	t	0.1	0.5	-
Carvone	1755	1242	t	t	0.1	0.1	t	t	0.1	t	t	64.8	54.0	51.3	65.1	58.3	t	-
Bicyclogermacrene	1756	1495	-	-	-	-	-	-	-	-	-	0.3	0.2	0.3	t	0.4	-	-
Geranyl acetate	1765	1380	-	-	-	-	-	-	-	-	-	-	-	-	-	-	-	0.7
Citronellol	1772	1225	-	-	-	-	-	-	-	-	-	-	-	-	-	-	-	0.2
Nerol	1804	1226	-	-	-	-	-	-	-	-	-	-	-	-	-	-	-	2.0
trans-Carveol	1845	1218	-	-	-	-	-	-	-	-	-	0.9	1.0	0.1	0.1	0.4	-	-
Geraniol	1857	1254	-	-	-	-	-	-	-	-	-	-	-	-	-	-	-	t
cis-Carveol	1882	1230	-	-	-	-	-	-	-	-	-	0.3	1.4	0.3	0.9	1.1	-	-
Myrtanol	1889	1194	-	-	-	-	-	-	-	-	-	-	-	-	-	-	0.7	-
cis-Dihydrocarveol	1912	1190	-	-	-	-	-	-	-	-	-	0.2	0.9	0.4	0.1	0.3	-	-
cis-Carvyl acetate	1930	1360	-	-	-	-	-	-	-	-	-	0.1	0.8	1.1	0.2	0.2	-	-
Piperitenone oxide	1984	1363	-	-	-	-	-	-	-	-	-	t	0.6	0.2	0.1	t	76.7	-
Caryophyllene oxide	1989	1584	t	t	-	t	t	t	t	-	-	0.3	0.8	0.4	0.3	0.2	t	0.9
Germacrene D-4-ol	2069	1578	0.1	0.1	0.4	0.1	t	t	0.1	0.1	0.1	-	-	-	-	t	t	-
Viridiflorol	2104	1592	-	-	-	-	-	-	-	-	-	-	-	-	-	0.1	0.2	-
Spathulenol	2143	1579	t	0.1	-	t	0.1	0.1	0.1	0.1	t	t	0.1	0.7	-	0.6	t	0.3
β-Eudesmol	2154	1650	-	-	-	-	-	-	-	-	-	t	0.2	0.2	-	0.1	t	0.3
Aliphatic compounds			0.1	0.5	0.6	0.8	0.3	1.2	0.3	0.4	0.8	0.7	2.9	1.0	0.7	1.0	0.2	-
Monoterpene hydrocarbons			3.5	5.8	3.7	4.5	4.8	3.6	5.1	5.4	3.8	20.2	25.6	28.0	21.6	28.8	6.5	4.0
Oxygenated monoterpenes			94.9	92.1	94.1	93.9	93.5	94.1	93.5	93.1	94.1	71.2	64.4	60.1	74.4	64.5	85.7	86.1
Sesquiterpene hydrocarbons			0.2	0.5	1.0	0.3	0.6	0.7	0.6	0.5	0.4	3.1	3.2	2.8	2.1	1.8	1.6	1.2
Oxygenated sesquiterpenes			0.1	0.2	0.4	0.1	0.1	0.1	0.2	0.2	0.1	0.3	1.1	1.3	0.3	1.0	0.2	1.5
Total identified			98.8	99.1	99.8	99.6	99.3	99.7	99.7	99.6	99.2	95.5	97.2	93.2	99.1	97.7	94.2	92.8
Oil yield (%, v/w)			1.0	0.9	0.8	1.1	1.0	1.2	1.1	0.9	1.3	0.8	0.6	0.7	0.7	0.5	0.4	0.6

[*]Mode of identification: retention index (RI), coinjection with standard/peak enrichment with known oil constituent, MS (GC-MS), [a]RI: retention ind CP Wax 52 CB (30 m × 0.32 mm); [b]RI: retention index on DB-5 fused silica capillary column (30 m × 0.25 mm); t = trace (<0.1%), (-) = not detected plant abbreviations (I-XVI), see Table 1.

Of the 6 cultivars of *M. spicata* (spearmint), carvone (51.3-65.1%) is the main constituent in 5 cultivars followed by limonene (15.1-25.2%), 1,8-cineole (≤0.1-3.6%), β-pinene (1.3-3.2%), β-myrcene (≤0.1-2.8%) and β-caryophyllene (0.3-1.8%). The oil of Neerkalka contains the highest concentration of carvone (65.1%) followed by MSS-5 (64.8%), Supriya (58.3%), Neera (54.0%) and Arka (51.3%). Neerkalka also contains menthone (1.7%), menthol (0.7%) and menthyl acetate (0.5%), which are not noticed in other cultivars of *M. spicata* except Supriya (0.9% menthone). The presence of lower concentrations of menthone, menthyl acetate and menthol in cv. Neerkalka is due to the hybrid nature of this cultivar [32]. In contrast, cv. Ganga of *M. spicata* has a different oil composition characterised by piperitenone oxide (76.7%), α-terpineol (4.9%), limonene (4.7%) and linalool (1.6%) as major constituents.

Carvone-rich spearmint has been investigated earlier in India as well as other countries. Earlier study showed carvone (59.6-72.4%) and limonene (10.7-24.8%) as major constituents of oil of *M. spicata* from the mid-hills of Himalayan region of India at different crop stages [17], while *M. spicata* collected from different subtropical and temperate zones of north-west Himalayan region of India showed carvone (49.6-76.6%) followed by limonene (9.5-22.3%), 1,8-cineole (1.3-2.6%) and *trans*-carveol (0.3-1.5%) in its oils [20]. In north Indian plains carvone content varies between 45.9-77.1% [18]. The percentage of carvone also varies in oil of spearmint grown in different countries, e.g. Egypt (46.4-68.5%) [39-40], Canada (59.0-74.0%) [41], Turkey (78.3-82.2%) [42, 43] and China (55.4-74.6%) [44]. *M. spicata* grown in other countries also contains carvone as one of the major constituents of its essential oil, e.g. Bangladesh (73.2 %) [45], Algeria (59.4%) [46] and Morocco (29.0%) [47]. Spearmint grown in Iran was found to contain less amount of carvone (22.4%) [48]. However, the essential oil of *M. spicata* chemotype from Tunisia shows a entirely different oil composition with menthone (32.7%) and pulegone (26.6%) as major constituents [49]. Linalool-rich (82.8%) chemotype of *M. spicata* was also reported from Turkey [43]. In another report on *M. spicata* grown in Iran, α-terpinene (19.7%), piperitenone oxide (19.3%), isomenthone (10.3%) and β-caryophyllene (7.6%) were reported as major constituents [50].

In the oil of *M. citrata* cv. Kiran, 28 components are identified, representing about 92.8% of the whole oil. The major constituents are linalool (59.7%), linalyl acetate (18.4%), nerol (2.0%), *trans*-p-menth-1-en-2-ol (1.8%), α-terpineol (1.5%) and limonene (1.1%). Nerol (2.0%), geranyl acetate (0.7%), citronellol (0.2%) and geraniol (≤0.1%) are the characteristic constituents which have not been reported in other cultivars of *Mentha* species.

CONCLUSIONS

The essential oil profile of 16 cultivars of *Mentha* are useful for commercial purpose as they possess a range of aroma chemicals used in perfumery, flavour, pharmaceutical and other allied industries. Moreover, the major/marker constituents in their essential oils may be utilised as an important tool in oil authentication. All the cultivars of *M. arvensis* yield oils rich in menthol (73.7-85.8%) while the five cultivars of *M. spicata* are a very good source of carvone (51.6-65.1%) and cultivar Ganga of *M. spicata* is a good source of piperitenone oxide (76.7%). The essential oil of cultivar Kiran of *M. citrata* is an excellent source of linalool and linalyl acetate.

ACKNOWLEDGEMENTS

The authors are thankful to the Director of CSIR-Central Institute of Medicinal and Aromatic, Lucknow, Uttar Pradesh for providing facilities.

REFERENCES

1. H. J. Dorman, M. Kosar, K. Kahlos, Y. Holm and R. Hiltunen, "Antioxidant properties and composition of aqueous extracts from *Mentha* species, hybrids, varieties, and cultivars", *J. Agric. Food Chem.*, **2003**, *51*, 4563-4569.
2. K. S. Krishnan Marg, "The Wealth of India, Raw Materials*",* Publication and Information Directorate (CSIR), New Delhi, **1988**, p.440.
3. B. M. Lawrence, "A planting scheme to evaluate new aromatic plants for the flavor and fragrance industries", in "New Crops" (Ed. J. Janick and J. E. Simom), John Wiley, New York, **1993**, pp. 620-627.
4. B. M. Lawrence, "Mint: The Genus Mentha", CRC Press, Boca Raton, **2007**, p.170.
5. S. D. Bharadwaj and L. J. Srivastava, "Harvesting management on *Mentha citrata* Ehrh. in mid-hill condition of Himachal Pradesh", *Indian Perfum.*, **1984**, *28*, 38-41.
6. S. Kokkini, R. Karousou and T. Lanaras, "Essential oils of spearmint (carvone-rich) plants from the island of Crete (Greece)", *Biochem. Syst. Ecol.*, **1995**, *23*, 425-430.
7. B. R. R. Rao, A. K. Bhattacharya, K. Singh, P. N. Kaul and G. R. Mallavarapu, "Comparative composition of cornmint oils produced in north and south India", *J. Essent. Oil Res.*, **1999**, *11*, 54-56.
8. J. Rohloff, "Monoterpene composition of essential oil from peppermint (*Mentha piperita* L.) with regard to leaf position using solid-phase microextraction and gas chromatography/mass spectrometry analysis", *J. Agric. Food Chem.*, **1999**, *47*, 3782-3786.
9. G. Kofidis, A. M. Bosabalidis and S. Kokkini, "Seasonal variation of essential oils in a linalool-rich chemotype of *Mentha spicata* grown wild in Greece", *J. Essent. Oil Res.*, **2004**, *16*, 469-472.
10. V. Parcha, J. Kaur and S. Ubaid, "Composition and antimicrobial studies on essential oil from *Mentha spicata*", *Indian Perfum.*, **2007**, *51*, 45-47.
11. M. D. Sokovic, J. Vukojevic, P. D. Marin, D. D. Brkic, V. Vajs and L. J. L. D. Van Griensven, "Chemical composition of essential oils of *Thymus* and *Mentha* species and their antifungal activities", *Molecules,* **2009**, *14*, 238-249.
12. A. I. Hussain, F. Anwar, P. S. Nigam, M. Ashraf and A. H. Gilani, "Seasonal variation in content, chemical composition and antimicrobial and cytotoxic activities of essential oils from four *Mentha* species", *J. Sci. Food Agric.*, **2010**, *90*, 1827-1836.
13. F. S. Sharopov, V. A. Sulaimonova and W. N. Setzer, "Essential oil composition of *Mentha longifolia* from wild populations growing in Tajikistan", *J. Med. Active Plants*, **2012**, *1*, 76-84.
14. M. Govendrajan, R. Sivakumar, M. Rajeswari and K. Yogalakshami, "Chemical composition and larvicidal activity of essential oil from *Mentha spicata* (Linn.) against three mosquito species", *Parasitol. Res.*, **2012,** *110*, 2023-2032.
15. D. Segev, N. Nitzan, D. Chaimovitsh, A. Eshel and N. Dudai, "Chemical and morphological diversity in wild populations of *Mentha longifolia* in Israel", *Chem. Biodiv*ers., **2012,** *9*, 577-588.
16. R. S. Verma, L. Rahman, R. K. Verma, A. Chauhan, A. K. Yadav and A. Singh, "Essential oil composition of menthol mint (*Mentha arvensis*) and peppermint (*Mentha piperita*) cultivars at different stages of plant growth from Kumaon region of western Himalaya", *Open Acc. J. Med. Arom. Plants*, **2010**, *1*, 13-18.

17. R. S. Verma, R. C. Padalia and A. Chauhan, "Chemical profiling of *Mentha spicata* L. var. 'viridis' and *Mentha citrata* L. cultivars at different stages from the Kumaon region of western Himalaya", *Med. Arom. Plant Sci. Biotechnol.*, **2010**, *4,* 73-76.
18. J. R. Bahl, R. P. Bansal, S. N. Garg, A. A. Naqvi, R. Luthra, A. K. Kukreja and S. Kumar, "Qualitative evaluation of the essential oils of the prevalent cultivars of commercial mint species *Mentha arvensis*, *M. spicata*, *M. piperita*, *M. cardiaca*, *M. citrata* and *M. viridis* cultivated in indo-gangetic plains", *J. Med. Arom. Plant Sci.*, **2000**, *22*, 787-797.
19. A. K. Singh, V. K. Raina, A. A. Naqvi, N. K. Patra, B. Kumar, P. Ram and S. P. S. Khanuja, "Essential oil composition and chemoarrays of menthol mint (*Mentha arvensis* L. f. *piperascens* Malinvaud ex. Holmes) cultivars", *Flavour Fragr. J.*, **2005**, *20*, 302-305.
20. R. S. Chauhan, M. K. Kaul, A. K. Shahi, A. Kumar, G. Ram and A. Tawa, "Chemical composition of essential oils in *Mentha spicata* L. accession [IIIM(J)26] from north-west Himalayan region, India", *Indust. Crops Prod.*, **2009**, *29*, 654-656.
21. R. C. Padalia, R. S. Verma and C. S. Chanotiya, "Variability in volatile terpenoid compositions of peppermint cultivars and some of the wild accession from northern India", *J. Essent. Oil Res.*, **2011**, *23*, 29-31.
22. H. Kharkwal, G. C. Shah, C. S. Mathela and R. Laurent, "Variation in the terpenoid composition of *Mentha longifolia* subsp. *himalayansis*", *Indian Perfum.*, **1994**, *38*, 29-32.
23. C. S. Mathela, R. C. Padalia, C. S. Chanotiya and A. Tiwari, "Carvone rich *Mentha longifolia* (Linn.): Chemical variation and commercial potential" *J. Essent. Oil Bear. Plants*, **2005**, *8*, 132-134.
24. S. P. S. Khanuja, "Employ contract farming to boost area under cultivation for essential oil bearing crops", *Chemical Weekly*, December 25, **2007**, pp.180-181.
25. L. K. Dashora, A. Dashora and S. S. Lakhawat, "Mint (Pudina)", in "Production Technology of Plantation Crops, Spices, Aromatic and Medicinal Plants" (Ed. S. S. Lakhawat, L. K. Dashora, A. Dashora and L. K. Dashora), Agrotech Publication Academy, Udaipur (India), **2006**, Ch.31.
26. S. Kumar, J. R. Bahl, R. P. Bansal, A. K. Kukreja, S. N. Garg, A. A. Naqui, R. Luthra and S. Sharma, "Profiles of the essential oils of Indian menthol mint *Mentha arvensis* cultivars at different stages of crop growth in northern plains", *J. Med. Arom. Plant Sci.*, **2000**, *22*, 774-786.
27. S. Kumar, A. Sharma, R. Tiwari and A. Kumar, "Gomti: A new improved variety of Japanese mint developed", *CIMAP Newslett.*, **1994**, *21*, 2-3.
28. Anonymous, "Menthol mint variety 'Kushal' released for late transplanting", *CIMAP Newslett.*, **2003**, *1,* 3-4.
29. S. P. S. Khanuja, S. Kumar, A. K. Shasany, S. Dhawan, M. P. Darokar, A. A. Naqvi, D. P. Dhawan, A. K. Singh, N. K. Patra, J. R. Bahl and R. P. Bansal, "A menthol tolerant variety 'Saksham' of *Mentha arvensis* yielding high menthol", *J. Med. Arom. Plant Sci.*, **2001**, *23*, 110-112.
30. S. Kumar, S. Sharma and V. S. Kumar, "High yielding variety Kosi of menthol mint developed", *CIMAP Newslett.*, **1998**, *25*, 2-3.
31. N. K. Patra and B. Kumar, "Improved varieties and genetic research in medicinal and aromatic plants (MAPs)", Proceedings of 2nd National Interactive Meeting (NIM) on Medicinal and Aromatic Plants, **2005**, Lucknow, India, pp.53-61.

32. N. K. Patra, H. Tanveer, S. P. S. Khanuja, A. K. Shasany, H. P. Singh, V. R. Singh and S. Kumar, "A unique interspecific hybrid spearmint clone with growth properties of *Mentha arvensis* L. and oil qualities of *Mentha spicata* L", *Theor. Appl. Genet.*, **2001**, *102*, 471-476.
33. O. P. Virmani, A. K. Gauniyal and V. S. Kumar, "A high yielding superior strain of *Mentha viridis*-Supriya developed", *CIMAP Newslett.*, **1988**, *14*, 2-3.
34. S. P. S. Khanuja, S. Kumar, A. K. Shasany, S. Dhawan, M. P. Darokar, A. K. Tripathy, S. Satapathy, T. R. S. Kumar, V. K. Gupta, S. Awasthi, V. Prajapati, A. A. Naqvi, K. K. Agrawal, J. R. Bahl, A. Ahmed, R. P. Bansal, A. Krishna and D. Saikia, "Multiutility plant 'Ganga' of *Mentha spicata* var. *viridis*", *J. Med. Arom. Plant Sci.*, **2001**, *23,* 113-116.
35. O. P. Virmani, A. K. Gauniyal and V. S. Kumar, "A high yielding variety of *Mentha citrata*-Kiran developed", *CIMAP Newslett.*, **1988**, *15*, 1-2.
36. N. W. Davies, "Gas chromatographic retention indices of monoterpenes and sesquiterpenes on methyl silicon and carbowax 20M phases", *J. Chromatogr. A*, **1990**, *503*, 1-24.
37. R. P. Adams, "Identification of Essential Oil Components by Gas Chromatography/Quadrupole Mass Spectroscopy", Allured Publishing Corporation, Carol Stream (IL), **2001**.
38. B. R. R. Rao, P. N. Kaul, G. R. Mallavarapu and S. Ramesh, "Comparative composition of whole herb, flowers, leaves and stem oils of cornmint (*Mentha arvensis* L.f. *piperascens* Malinvaud ex Holmes)", *J. Essent. Oil Res.*, **2000**, *12*, 357-359.
39. M. A. A. El-Wahab, "Evaluation of spearmint (*Mentha spicata* L.) productivity grown in different locations under upper Egypt conditions", *Res. J. Agric. Biol. Sci.*, **2009**, *5*, 250-254.
40. M. I. Foda, M. A. El-Sayed, A. A. Hassan, N. M. Rasmy and M. M. El-Moghazy, "Effect of spearmint essential oil on chemical composition and sensory properties of white cheese", *J. Am. Sci.*, **2010**, *6*, 272-279.
41. V. D. Zheljazkov, C. L. Cantrell and T. Astatkies, "Yield and composition of oil from Japanese cornmint fresh and dry material harvested successively", *Agron. J.*, **2010**, *102*, 1652-1656.
42. I. Telci and N. Sahbaz, "Variations in yield, essential oil and carvone contents in clones selected from Carvone-scented landraces of Turkish *Mentha* species", *J. Agron.*, **2005**, *4*, 96-102.
43. I. Telci, N. Sahbaz, G. Yilmaz and M. E Tugay, "Agronomical and chemical characterization of spearmint (*Mentha spicata* L.) originating in Turkey", *Econ. Bot.*, **2004**, *58*, 721-728.
44. C. X. Hua, G. R. Wang and Y. Lei, "Evaluation of essential oil composition and DNA diversity of mint resources from China", *Afri. J. Biotechnol.*, **2011**, *10*, 16740-16745.
45. J. U. Chowdhury, N. C. Nandi, M. Uddin and M. Rahman, "Chemical constituents of essential oils from two types of spearmint (*Mentha spicata* L. and *M. cardiaca* L.) introduced in Bangladesh", *Bangladesh J. Sci. Ind. Res.*, **2007**, *42*, 79-82.
46. H. Boukhebti, A. N. Chaker, H. Belhadj, F. Sahli, M. Ramdhani, H. Laouer and D. Harzallah, "Chemical composition and antibacterial activity of *Mentha pulegium* L. and *Mentha spicata* L. essential oils", *Der Pharm. Lett.*, **2011**, *3,* 267-275**.**
47. M. Znini, M. Bouklah, L. Majidi, S. Kharchouf, A. Aouniti, A. Bouyanzer, B. Hammouti, J. Costa and S. S. Al-Deyab, "Chemical composition and inhibitory effect of *Mentha spicata* essential oil on the corrosion of steel in molar hydrochloric acid", *Int. J. Electrochem. Sci.*, **2011**, *6*, 691-704.
48. A. Hadjiakhoondi, N. Aghel, N. Zamanizadech-Nadgar and H. Vatandoost, "Chemical and biological study of *Mentha spicata* L. essential oil from Iran", *DARU J. Pharm. Sci.*, **2000**, *8*, 19-21.

49. W. Dhifi, N. Jelali, W. Mnif, M. Litaiem and N. Hamdi, "Chemical composition of the essential oil of *Mentha spicata* L. from Tunisia and its biological activities", *J. Food Biochem.*, **2012**, DOI: 10.1111/j.1745-4514.2012.00656.x.

50. I. Rasooli, L. Gachkar, D. Yadegarinia, M. R. Bagher and S. D. Alipoor Astaneh, "Antibacterial and antioxidative characterization of essential oils from *Mentha piperita* and *Mentha spicata* grown in Iran", *Acta Aliment.*, **2008**, *37*, 41-52.

Maejo Int. J. Sci. Technol. **2013**, *7*(01), 94-106

Maejo International Journal of Science and Technology

ISSN 1905-7873
Available online at www.mijst.mju.ac.th

Full Paper

A case study on estimating the flood severity using flood hydrographs for small ungauged catchments in Korea

Eung Seok Kim [1] and Hyun Il Choi [2,*]

[1] Department of Civil Engineering, Sunmoon University, 100, Kalsan-ri, Tangjeong-myeon, Asan-si, Chungnam-do, 336-708, Korea
[2] Department of Civil Engineering, Yeungnam University, 214-1, Dae-dong, Gyeongsan-si, Gyeongbuk-do, 712-749, Korea

* Corresponding author, e-mail: hichoi@ynu.ac.kr

Received: 17 January 2012 / Accepted: 20 February 2013 / Published: 20 February 2013

Abstract: Local floods with rapid run-off and debris flow have posed a great potential threat of danger to life and property in recent years. Previous studies have examined the flash flood index determined by the characteristics of observed flood hydrographs such as rising limb, peak discharge and time to peak. To estimate the flood severity for small watersheds in Korea where the observed hydrograph is usually not available, this study proposes a flood hazard index (FHI) based on hydrographs generated from a rainfall run-off model for the annual maximum rainfall series of long-term observed data. The FHI is obtained by summing the relative severity factors measured by the ratios of characteristics of each flood to the highest recorded maximum value and implemented for two selected small ungauged basins in Korea. This study also presents regression equations between FHI and rainfall characteristics to predict the severity of flooding in small catchments. A stronger relation between FHI and maximum rainfall over a short interval demonstrates that heavy or excessive rainfall in a short period of time can cause a serious local flood in small watersheds.

Keywords: flood hazard index, flood severity, run-off hydrograph, rainfall run-off model

---

INTRODUCTION

In recent years, heavy rainfall in a short period of time over a small area often caused sudden local flooding leading to significant loss of life and property. Most watersheds in the Korean Peninsula are exposed to flood hazards due to both climatic and geomorphic vulnerability by convective storms of short duration and high intensity over small, steep slope regions. As a result, the rapid run-off associated with debris flow inundated some watershed areas and caused bank erosion and bridge collapse as reported by the Korea National Emergency Management Agency (KNEMA) [1]. Although such flood damage is a common natural disaster in Korea, it is considered almost infeasible to cope with flash flooding rising quite quickly with little or no advance flood warning in small watersheds. The present flood forecasting systems based on a rainfall run-off model places a limit on predicting flash flooding in small watersheds with short flood response time [2-4].

While flash floods were considered mainly from a climatological perspective with special focus on the temporal and spatial characteristics of rainfall [5-7], Kyiamah [8] initially characterised flash floods from a run-off perspective using run-off hydrographs. To distinguish flash floods from other floods, Bhaskar et al. [9] presented a flash flood index using run-off hydrograph characteristics such as rising curve gradient, flood magnitude ratio and flood response time, evaluated directly from observed run-off hydrographs of 30 flood events from four watersheds in eastern Kentucky. Jung [10] estimated the flash flood index for several flood events of the Bo-chung River basin in the Korean Peninsula following Bhaskar et al. [9]. In these studies, the flash flood index was determined by the sum of three relative severity factors using each different ordinal scale where class intervals were to some extent arbitrary. Although each relative severity factor was applied systematically to all flood events, the flash flood index was often subjected to a certain factor with a greater scale value than other factors. Kim and Kim [3] estimated the flash flood index to investigate the relative severity of flash floods in the Han River basin with 101 flood events and quantified the flash flood severity for some flood events caused by heavy rainfall in July of 2006.

In previous studies the flash flood index was computed directly from the observed flood hydrographs. Since most small watersheds in Korea usually do not have a local flood observation and warning system, in this study the flash flood index by Bhaskar et al. [9] is modified and a flood hazard index (FHI) is presented, which is determined by summing each relative severity factor such as the rising curve gradient, flood magnitude ratio and flood response time measured at different scales and units, normalised to the highest recorded maximum value. The FHI can be used to estimate the relative severity of flood hazards for a flood event to the highest recorded maximum flood level. However, the FHI based on the characteristics of flood run-off hydrographs does not incorporate any vulnerability feature. Although a flood disaster is the result of a flood hazard, the resulting loss depends on the ability of the affected population to resist the hazard. Thus, the proposed flood index is designated as FHI. In order to understand the hydrologic behaviour of local flooding in small ungauged catchments, FHI is obtained by quantifying the characteristics of flood run-off hydrographs generated from a rainfall run-off model, viz. the hydrologic engineering centre-hydrologic modelling system (HEC-HMS), for the annual maximum rainfall series of long-term observed data. FHI is implemented in two selected small ungauged basins in the Korean Peninsula: the Oui-mi River basin (OM) located in a mountainous region and the Mae-gok River basin (MG) with a relatively flat drainage area. This study also examines the relationship between FHI and rainfall characteristics in the two basins in order to provide a basic database for forecasting a local flood directly from rainfall pattern.

STUDY CATCHMENTS

OM and MG, selected as the study catchments, are surrounded by rainfall gauge stations from which long-term hourly rainfall data are collected. A hilly 16.74 km² natural basin 7.52 km long, OM is located between 128°10′35″-128°11′37″E and 37°14′39″-37°15′29″N [11]. The annual maximum rainfall series during 1973-2008 was collected for OM from the Jae-chun gauge station managed by KNEMA. The annual mean rainfall volume was 1,322.5 mm over the same period and the highest recorded maximum depth of a single rainfall event was 228.5 mm on September 11, 1990. MG has a flat natural drainage area of 35.48 km² and a basin length of 11.25 km. It is located between 127°01′56″-127°07′29″E and 36°46′44″-36°51′48″N [12]. The annual maximum rainfall series during 1973-2008 was collected for MG from Chun-an gauge station managed by KNEMA. The annual mean rainfall volume was 1,235.9 mm over the same period and the recorded maximum depth of a single rainfall event was 262.5 mm on August 9, 1995. Figure 1 depicts the basin maps and Table 1 summarizes the basin characteristics of the two catchments under study.

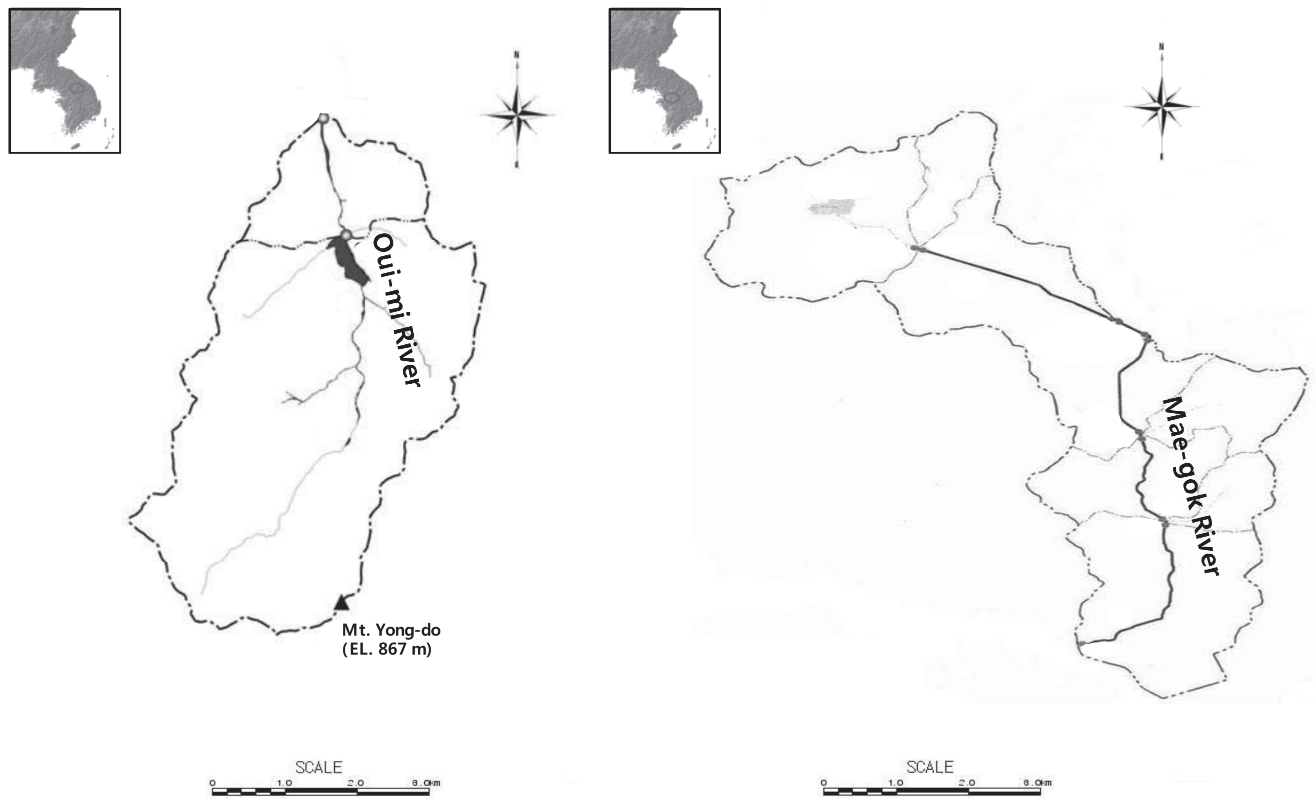

(a) (b)

Figure 1. Basin maps for (a) the Oui-mi River (OM) and (b) the Mae-gok River (MG)

Table 1. Characteristics of the two study basins

Basin	Basin area: A(km²)	Basin length: L(km)	Basin width: A/L(km)	Shape factor: A/L²	Average elevation (m)	Average slope (%)
OM	16.74	7.52	2.23	0.30	544.9	53.4
MG	35.48	11.25	3.15	0.28	65.0	9.6

RUN-OFF SIMULATIONS

Flood Run-off Hydrographs

Flood run-off hydrographs were generated from the rainfall run-off model, i.e. HEC-HMS [13], using the annual maximum precipitation series of the Jae-chun gauge station for OM and the Chun-an gauge station for MG for 36 years from 1973-2008. The Natural Resources Conservation Service curve number method [14] was used for the loss rate and the Clark unit hydrograph [15] was used as the transform method. Table 2 shows parameter values required for HEC-HMS run-off simulations in the two basins. All parameter values suggested in the basic plan reports [11, 12] were used for OM and MG. The 36-year annual maximum flood run-off simulation results are summarised in Tables 4 and 5 for OM and MG respectively.

Table 2. Parameter values for the flood run-off generation by HEC-HMS in the two basins

Basin	NRCS curve number	Storage coefficient (hr)
OM	70.10	1.18
MG	87.92	2.02

Long-term Run-off Simulations

As shown in Table 3, the basic plan reports for OM [11] and MG [12] maintenance works have presented the monthly run-off simulated by the Kajiyama equation and the daily watershed streamflow model respectively, the latter being a daily streamflow model based on soil water storage [16].

Table 3. Simulated monthly run-off in the two basins

Basin	Monthly run-off (m^3/sec)												
	Jan	Feb	Mar	Apr	May	Jun	Jul	Aug	Sep	Oct	Nov	Dec	Mean
OM	0.07	0.09	0.12	0.29	0.22	0.43	1.31	1.10	0.55	0.17	0.11	0.08	0.40
MG	0.19	0.20	0.25	0.38	0.41	0.70	1.74	2.46	1.19	0.38	0.24	0.24	0.70

ESTIMATION OF FLOOD HAZARD INDEX (FHI)

This study quantifies the severity of floods in small ungauged catchments by estimating FHI from flood hydrographs simulated by a rainfall run-off model for the annual maximum precipitation series of long-term observations. Bhaskar et al. [9] characterised the flash flood severity by defining a flash flood index *RF* evaluated from the observed flood hydrograph characteristics such as the rising curve gradient *K*, flood magnitude ratio M and flood response time *T*. These characteristics were quantified by the relative severity factors at each different ordinal scale of assignment, where the choice of class intervals was to some extent arbitrary. The flash flood index *RF* determined by the sum of the three severity factors is often subjected to a certain factor among the three with a greater scale of measurement than other factors. Hence this study presents FHI integrated from each relative severity factor normalised to the highest recorded maximum value.

Rising Curve Gradient

The rising limb of hydrographs can be described by an exponential function as Equation (1) and then the rising curve gradient *K* can be computed by Equation (2):

$$Q_t = Q_0 e^{Kt} \tag{1}$$

$$K = \frac{\ln(Q_t / Q_0)}{t} \tag{2}$$

where Q_0 is the specified initial discharge, and Q_t and K_t are the discharge and the rising curve gradient respectively, at a later time *t* close to the time to peak. Because the rising curve gradient represents the steepness of the rising limb of a flood hydrograph, a large value of parameter *K* can be associated with a rapid local flood. The rising curve gradient *K* ranges between 3.79-24.67/day for OM as shown in column 4 of Table 4, and between 3.17-36.81/day for MG as shown in column 4 of Table 5. To quantify the relative severity for the rising curve gradient *K* as a dimensionless index *RK*, the ratio of K_i of each flood to the highest recorded maximum value K_{max} is computed from the 36-year long-term flood data:

$$RK = \frac{K_i}{K_{\max}} \tag{3}$$

Flood Magnitude Ratio

The flood magnitude ratio *M* means a ratio of the peak flood discharge to the long-term average discharge, as defined in Equation (4):

$$M = Q_p / Q_a \tag{4}$$

where Q_p is the flood peak discharge and Q_a is the long-term average discharge (0.4m^3/s for OM and 0.7m^3/s for MG) as shown in Table 3. The flood magnitude ratio *M* varies between 36.17-458.15 for OM as shown in column 5 of Table 4, and between 46.60-504.04 for MG as shown in column 5 of Table 5. The relative severity factor *RM* is also computed by the ratio of each flood event's M_i to the highest recorded maximum value M_{max} from the 36-year long-term flood data:

$$RM = \frac{M_i}{M_{\max}} \tag{5}$$

Flood Response Time

The flood response time T is defined as the time duration between the start of a flood event and the time of peak flow, which can be measured directly from flood hydrographs. T varies between 3-24 hr for OM as shown in column 6 of Table 4, and between 3-25 hr for MG as shown in column 6 of Table 5. Because a low T is readily associated to a high run-off velocity causing sudden local flooding, the relative severity factor RT is computed by the ratio of the inverse value of T_i of each flood event to the inverse value of the recorded minimum value T_{min} from the 36-year long-term flood data:

$$RT = \frac{T_{min}}{T_i} \tag{6}$$

Flood Hazard Index (FHI)

We can define more relative severity factors RS_j representing the flood hydrograph characteristics, aside from the rising curve gradient K, the flood magnitude ratio M and the flash flood response time T mentioned above. These relative severity factors need to be summed for an overall value to evaluate the flood severity for each flood event. If the number of relative severity factors is n, the relative flood severity RF_n is given in the general form as:

$$RF_n = \sum_{j=1}^{n} RS_j \tag{7}$$

where the relative severity factors RS_j may comprise RK, RM, RT and any other possible severity factors. A high value of RF_n is expected to indicate a sudden local flood of great volume. While Bhaskar et al. [9] presented RF_3, which is the sum of the three relative severity factors on different scale values such as RK = 1-7, RM = 1-16, and RT = 1-10, RF_3 from the same scale relative severity factors is computed in this study.

The rising curve gradient K and the flood response time T may represent similar characteristics of a flood hydrograph because a low value of T can be associated with a high run-off velocity leading to a steep rising limb of flood hydrographs. The correlation coefficients between RK and RT are very high at 0.948 for OM and 0.973 for MG as shown in Table 6. It is therefore required to avoid double-counting of similar severity factors in the relative flood severity RF_n, the sum of relative severity factors. Therefore, this study presents another relative flood severity RF_2, the sum of the two relative severity factors, i.e. the rising curve gradient K and the flood magnitude ratio M, and then compares RF_2 with RF_3. Also, this study presents FHI_n, a ratio of each flood event $(RF_n)_i$ to the maximum $(RF_n)_{max}$ in order to evaluate the severity of each flood event relative to the extreme flood situation:

$$FHI_n = \frac{(RF_n)_i}{(RF_n)_{\max}} \times 100\ (\%) \tag{8}$$

Tables 4 and 5 show FHI_3 for RF_3 and FHI_2 for RF_2 in Equation (8), along with the rainfall characteristics for the two basins, OM and MG.

Table 4. Summary of run-off and flood hazard indexing characteristics, along with rainfall data for the Oui-mi River basin (OM)

No	Flood Run-off Characteristics					Flood Indexing Parameters								Rainfall Characteristics								
	Flood event date (1)	Flood peak discharge Q_p (m^3/s) (2)	Time to peak discharge T (hr) (3)	Rising curve gradient K (day^{-1}) (4)	Flood magnitude ratio M (5)	Flood response time T (hr) (6)	Relative severity factor RK (7)	Relative severity factor RM (8)	Relative severity factor RT (9)	Flood index RF_3[a)] (10)	Flood index FHI_3[b)] (11)	Flood index RF_2[c)] (12)	Flood index FHI_2[d)] (13)	Average rainfall intensity I_a (mm/hr) (14)	Maximum 1-hour rainfall R_{1h} (mm) (15)	Maximum 2-hour rainfall R_{2h} (mm) (16)	Maximum 3-hour rainfall R_{3h} (mm) (17)	Maximum 4-hour rainfall R_{4h} (mm) (18)	Maximum 5-hour rainfall R_{5h} (mm) (19)	Maximum 6-hour rainfall R_{6h} (mm) (20)	Total rainfall depth R_t (mm) (21)	Rainfall duration time D (hr) (22)
1	06/29/73	20.5	8.0	8.51	51.18	8.00	0.34	0.11	0.38	0.83	38.81	0.46	26.88	5.06	14	25	32	36	37.5	40	40.5	8
2	08/23/74	14.5	4.0	14.94	36.17	4.00	0.61	0.08	0.75	1.43	66.94	0.68	40.29	4.47	22.3	27.5	29.6	35.3	42.3	46.5	67	15
3	09/15/75	30.7	19.0	4.10	76.81	19.00	0.17	0.17	0.16	0.49	22.94	0.33	19.64	4.39	13	23	27	36.5	40	51	101	23
4	08/14/76	28.0	11.0	6.87	69.95	11.00	0.28	0.15	0.27	0.70	32.85	0.43	25.38	4.26	15	23.5	26	36	39	39	81	19
5	09/06/77	39.6	16.0	5.24	98.97	16.00	0.21	0.22	0.19	0.62	28.75	0.43	25.23	5.37	21.5	42	46.5	67	83.5	84.4	107.4	20
6	08/19/78	44.9	18.0	4.83	112.35	18.00	0.20	0.25	0.17	0.61	28.36	0.44	25.96	6.44	29.5	37	46	54.5	66.5	79	122.3	19
7	08/04/79	59.2	11.0	8.51	147.97	11.00	0.34	0.32	0.27	0.94	43.89	0.67	39.31	9.39	29.5	45.5	57	78	94.5	106	112.7	12
8	07/22/80	71.7	17.0	5.78	179.35	17.00	0.23	0.39	0.18	0.80	37.43	0.63	36.82	6.63	43	53.2	75.4	85.6	91.1	95.9	132.6	20
9	07/01/81	31.9	15.0	5.25	79.69	15.00	0.21	0.17	0.20	0.59	27.38	0.39	22.76	5.59	15	25.5	31	37.5	47	53	95	17
10	08/21/82	26.2	3.0	24.67	65.51	3.00	1.00	0.14	1.00	2.14	100.00	1.14	67.28	6.05	32	38	42	43.5	49.5	51.5	60.5	10
11	07/19/83	24.7	7.0	10.37	61.73	7.00	0.42	0.13	0.43	0.98	45.90	0.56	32.67	6.11	17	28.5	36.5	43.5	48.5	50.5	55	9
12	09/02/84	24.0	17.0	4.23	59.99	17.00	0.17	0.13	0.18	0.48	22.34	0.30	17.80	4.83	10.5	16	24	29	36	43	96.5	20
13	07/17/85	57.8	5.0	18.60	144.49	5.00	0.75	0.32	0.60	1.67	77.90	1.07	62.94	14.92	29	45	65	78	89	89.5	89.5	6
14	07/19/86	80.5	7.0	14.42	201.33	7.00	0.58	0.44	0.43	1.45	67.78	1.02	60.28	6.39	32	58	69	78.5	86	97	134.2	21
15	07/22/87	70.0	4.0	24.40	175.04	4.00	0.99	0.38	0.75	2.12	98.98	1.37	80.71	8.15	41.5	57.5	67.5	82	92	101.5	187.5	23
16	07/14/88	111.5	12.0	9.06	278.70	12.00	0.37	0.61	0.25	1.23	57.20	0.98	57.43	13.97	33	57	75.5	99.5	118	134	223.5	16
17	07/26/89	77.4	7.0	14.28	193.40	7.00	0.58	0.42	0.43	1.43	66.72	1.00	58.93	6.22	34	67.5	85.5	89.5	95	99	143	23
18	09/11/90	92.8	24.0	4.35	232.09	24.00	0.18	0.51	0.13	0.81	37.70	0.68	40.19	9.52	38.5	72	88	93.5	94.5	102	228.5	24
19	07/20/91	58.3	12.0	7.77	145.64	12.00	0.31	0.32	0.25	0.88	41.19	0.63	37.24	10.58	32	38	47.5	61.5	65	74	137.5	13
20	09/24/92	35.6	15.0	5.42	88.91	15.00	0.22	0.19	0.20	0.61	28.65	0.41	24.36	5.44	13.5	25.5	36.5	49	56.5	64	98	18
21	07/13/93	70.4	13.0	7.52	176.02	13.00	0.30	0.38	0.23	0.92	42.92	0.69	40.55	7.55	30.5	42	52.5	63.5	69	75	158.5	21
22	06/30/94	123.6	20.0	5.56	309.10	20.00	0.23	0.67	0.15	1.05	49.00	0.90	52.98	8.54	37	68.5	90.5	94	100	102.5	196.5	23
23	08/25/95	40.7	8.0	10.57	101.83	8.00	0.43	0.22	0.38	1.03	47.87	0.65	38.31	5.71	22.5	29	36.5	43	61.5	69.5	120	21
24	07/28/96	55.0	4.0	22.95	137.50	4.00	0.93	0.30	0.75	1.98	92.41	1.23	72.43	12.33	35	53	68.5	72.5	73.5	74	74	6
25	07/01/97	98.7	18.0	5.88	246.82	18.00	0.24	0.54	0.17	0.94	44.04	0.78	45.74	7.24	49.5	56.5	63.5	69.5	73.5	79	166.5	23
26	08/08/98	50.7	15.0	5.99	126.73	15.00	0.24	0.28	0.20	0.72	33.57	0.52	30.57	4.75	19.5	38.5	41	41.5	43	48	95	20
27	08/02/99	57.8	22.0	4.23	144.51	22.00	0.17	0.32	0.14	0.62	29.08	0.49	28.65	5.61	27.5	40.5	51	57.5	65	73.5	123.5	22
28	07/22/00	64.2	11.0	8.68	160.45	11.00	0.35	0.35	0.27	0.97	45.49	0.70	41.33	7.42	36	50	54.5	63.5	66	78.5	96.5	13
29	06/30/01	98.3	5.0	21.15	245.79	5.00	0.86	0.54	0.60	1.99	93.04	1.39	82.04	17.75	41	72	87	93.5	104	106.5	106.5	6
30	08/31/02	62.1	23.0	4.12	155.22	23.00	0.17	0.34	0.13	0.64	29.69	0.51	29.77	8.61	22.5	40.5	54	68.5	82	85.5	198	23
31	06/27/03	46.8	9.0	9.77	117.07	9.00	0.40	0.26	0.33	0.98	45.96	0.65	38.35	8.17	15	30	42.5	52	61.5	75	122.5	15
32	08/18/04	33.0	21.0	3.79	82.43	21.00	0.15	0.18	0.14	0.48	22.22	0.33	19.63	3.73	12.5	23	31	40.5	51	59.5	89.5	24
33	07/11/05	33.6	10.0	8.00	83.97	10.00	0.32	0.18	0.30	0.81	37.68	0.51	29.87	5.74	23	33	44	55	67.5	73.5	109	19
34	07/16/06	67.5	15.0	6.45	168.65	15.00	0.26	0.37	0.20	0.83	38.70	0.63	37.05	8.46	22.5	42	54.5	71	86	91	203	24
35	08/05/07	183.3	7.0	17.24	458.15	7.00	0.70	1.00	0.43	2.13	99.28	1.70	100.00	18.65	68	122.5	149	161	171.5	180.5	186.5	10
36	07/24/08	70.6	19.0	5.15	176.43	19.00	0.21	0.39	0.16	0.75	35.07	0.59	34.95	4.02	49	63	68	69.5	74	77.5	96.5	24
	average	59.9	12.6	9.68	149.72	12.56	0.39	0.33	0.33	1.05	48.83	0.72	42.34	7.72	28.52	44.70	55.43	64.72	72.79	79.16	123.76	17.50
	maximum	183.3	24.0	24.67	458.15	24.00	1.00	1.00	1.00	2.14	100.00	1.70	100.00	18.65	68.00	122.50	149.00	161.00	171.50	180.50	228.50	24.00
	minimum	14.5	3.0	3.79	36.17	3.00	0.15	0.08	0.13	0.48	22.22	0.30	17.80	3.73	10.50	16.00	24.00	29.00	36.00	39.00	40.50	6.00

Note: a) $RF_3 = RK + RM + RT$, b) $FHI_3 = \dfrac{(RF_3)_i}{(RF_3)_{\max}} \times 100$, c) $RF_2 = RK + RM$, d) $FHI_2 = \dfrac{(RF_2)_i}{(RF_2)_{\max}} \times 100$

Table 5. Summary of run-off and flood hazard indexing characteristics, along with rainfall data for the Mae-gok River basin (MG)

No	**Flood Run-off Characteristics**				**Flood Indexing Parameters**									**Rainfall Characteristics**								
	Flood event date	Flood peak discharge	Time to peak discharge	Rising curve gradient	Flood magnitude ratio	Flood response time	Relative severity factor			Flood index				Average rainfall intensity	Maximum 1-hour rainfall	Maximum 2-hour rainfall	Maximum 3-hour rainfall	Maximum 4-hour rainfall	Maximum 5-hour rainfall	Maximum 6-hour rainfall	Total rainfall depth	Rainfall duration time
		Q_p (m^3/s)	T (hr)	K (day-1)	M	T (hr)	RK	RM	RT	RF_3 [a]	FHI_3 [b]	RF_2 [c]	FHI_2 [d]	I_a (mm/hr)	R_{1h} (mm)	R_{2h} (mm)	R_{3h} (mm)	R_{4h} (mm)	R_{5h} (mm)	R_{6h} (mm)	R_t (mm)	D (hr)
	(1)	(2)	(3)	(4)	(5)	(6)	(7)	(8)	(9)	(10)	(11)	(12)	(13)	(14)	(15)	(16)	(17)	(18)	(19)	(20)	(21)	(22)
1	08/23/73	135.22	15.0	6.66	193.17	15.00	0.18	0.38	0.20	0.76	29.48	0.56	35.42	4.69	42.5	57.4	65.9	68.4	75.9	84.4	93.7	20
2	07/09/74	135.23	6.0	16.66	193.19	6.00	0.45	0.38	0.50	1.34	51.52	0.84	52.47	7.22	25	42.5	54	78.5	89.5	99.5	101.1	14
3	07/28/75	57.11	9.0	8.81	81.58	9.00	0.24	0.16	0.33	0.73	28.33	0.40	25.18	6.05	12.5	20	25.5	30	36.5	45.5	66.5	11
4	08/14/76	209.21	3.0	36.81	298.87	3.00	1.00	0.59	1.00	2.59	100.00	1.59	100.00	10.47	49.5	94.5	107.5	115.4	115.4	115.4	125.6	12
5	09/06/77	180.72	8.0	13.37	258.17	8.00	0.36	0.51	0.38	1.25	48.22	0.88	54.95	7.39	37	73.5	84.5	91	100.6	104.6	147.7	20
6	08/16/78	189.15	9.0	12.00	270.21	9.00	0.33	0.54	0.33	1.20	46.10	0.86	54.12	13.67	27.5	54	76	101.5	117	119	123	9
7	06/26/79	101.30	3.0	31.01	144.71	3.00	0.84	0.29	1.00	2.13	82.13	1.13	70.91	10.94	29.5	46	61.5	69.5	78	81.5	87.5	8
8	07/14/80	198.50	5.0	21.83	283.57	5.00	0.59	0.56	0.60	1.76	67.71	1.16	72.55	15.50	46	73	96.5	104.5	107.5	108	108.5	7
9	07/12/81	73.64	5.0	17.07	105.20	5.00	0.46	0.21	0.60	1.27	49.08	0.67	42.22	6.25	16	30.5	43.5	53.5	61.5	66	81.2	13
10	07/28/82	180.74	8.0	13.37	258.20	8.00	0.36	0.51	0.38	1.25	48.22	0.88	54.95	8.30	44.5	61	86.5	95	104	116	166	20
11	07/19/83	75.74	11.0	7.82	108.21	11.00	0.21	0.21	0.27	0.70	26.99	0.43	26.82	5.30	18	28	33.5	37	42	49	74.2	14
12	07/04/84	210.61	8.0	13.82	300.87	8.00	0.38	0.60	0.38	1.35	51.97	0.97	61.05	7.52	39.5	58	75	91	114.5	133	158	21
13	08/10/85	38.78	13.0	5.38	55.40	13.00	0.15	0.11	0.23	0.49	18.78	0.26	16.08	2.45	11	15.5	18.5	21	23	25.5	49	20
14	07/19/86	171.31	5.0	21.13	244.73	5.00	0.57	0.49	0.60	1.66	64.00	1.06	66.51	13.36	34	57	83	106	111	114	120.2	9
15	07/21/87	174.96	18.0	5.90	249.94	18.00	0.16	0.50	0.17	0.82	31.73	0.66	41.19	7.84	31.5	53.5	79.5	85.5	88.5	89	149	19
16	07/11/88	46.11	12.0	6.18	65.88	12.00	0.17	0.13	0.25	0.55	21.15	0.30	18.74	4.54	12	21	24	29	35	38	63.5	14
17	09/14/89	74.73	15.0	5.72	106.75	15.00	0.16	0.21	0.20	0.57	21.87	0.37	23.04	4.36	16.5	31	39.5	47	57.5	66	96	22
18	06/19/90	104.34	8.0	11.72	149.06	8.00	0.32	0.30	0.38	0.99	38.14	0.61	38.55	5.92	25.5	32	41	56	67	72.5	112.5	19
19	05/26/91	60.02	5.0	16.09	85.74	5.00	0.44	0.17	0.60	1.21	46.56	0.61	38.12	3.08	15.5	26	30	37.5	48	52	61.5	20
20	08/27/92	179.12	11.0	9.70	255.89	11.00	0.26	0.51	0.27	1.04	40.26	0.77	48.41	7.60	29.5	49.5	61	90.5	107.5	119.5	159.5	21
21	07/13/93	66.09	4.0	20.69	94.42	4.00	0.56	0.19	0.75	1.50	57.83	0.75	47.05	5.25	20.5	33.5	48	51	55.5	62	115.5	22
22	06/30/94	110.73	23.0	4.14	158.19	23.00	0.11	0.31	0.13	0.56	21.47	0.43	26.76	5.84	32.5	38.5	48	51	55.5	55.5	128.5	22
23	08/09/95	352.83	6.0	20.50	504.04	6.00	0.56	1.00	0.50	2.06	79.32	1.56	97.73	23.86	67.5	103.5	132.5	156.5	175.5	200.5	262.5	11
24	06/17/96	79.28	21.0	4.15	113.26	21.00	0.11	0.22	0.14	0.48	18.52	0.34	21.18	4.61	21.5	25.5	32.5	37.5	41.5	51	101.5	22
25	07/01/97	209.74	13.0	8.50	299.63	13.00	0.23	0.59	0.23	1.06	40.73	0.83	51.81	7.97	33	62.5	86	99.5	108.5	113.5	151.5	19
26	09/30/98	72.26	17.0	5.00	103.22	17.00	0.14	0.20	0.18	0.52	19.94	0.34	21.37	7.20	11.5	18	26	33	39.5	48	165.5	23
27	08/02/99	107.51	4.0	23.61	153.59	4.00	0.64	0.30	0.75	1.70	65.42	0.95	59.40	12.32	32.5	57.5	65.5	79.5	81.5	88.5	135.5	11
28	08/20/00	116.47	9.0	10.71	166.39	9.00	0.29	0.33	0.33	0.95	36.81	0.62	38.98	7.61	25	41.5	44	50	53.5	67.5	106.5	14
29	08/07/01	200.53	7.0	15.63	286.47	7.00	0.42	0.57	0.43	1.42	54.82	0.99	62.34	18.36	35.5	65.5	80.5	91	113	128	128.5	7
30	08/07/02	240.13	13.0	8.75	343.04	13.00	0.24	0.68	0.23	1.15	44.31	0.92	57.65	14.94	37.5	64	86	105	133	161	239	16
31	06/27/03	103.84	10.0	9.36	148.34	10.00	0.25	0.29	0.30	0.85	32.73	0.55	34.44	7.29	16.5	31.5	45	52.5	59.5	70.5	124	17
32	06/16/04	56.95	25.0	3.17	81.36	25.00	0.09	0.16	0.12	0.37	14.17	0.25	15.54	4.06	15.5	29.5	39.5	49.5	57	66.5	97.5	24
33	09/17/05	164.66	10.0	10.47	235.23	10.00	0.28	0.47	0.30	1.05	40.54	0.75	47.15	10.18	33.5	56.5	81	89	99.5	103	112	11
34	07/16/06	83.36	12.0	7.36	119.09	12.00	0.20	0.24	0.25	0.69	26.47	0.44	27.39	8.09	22.5	34	55.5	67	79.5	90	137.5	17
35	08/04/07	90.39	9.0	10.03	129.13	9.00	0.27	0.26	0.33	0.86	33.25	0.53	33.19	8.50	45	66.5	71	75	100.5	122	144.5	17
36	06/18/08	32.62	16.0	4.11	46.60	16.00	0.11	0.09	0.19	0.39	15.11	0.20	12.82	4.03	18.5	24	27	29.5	35.5	39	68.5	17
average		130.1	10.4	12.42	185.87	10.44	0.34	0.37	0.38	1.09	42.05	0.71	44.34	8.40	28.65	46.55	59.84	70.12	79.68	87.91	121.19	16.19
maximum		352.8	25.0	36.81	504.04	25.00	1.00	1.00	1.00	2.59	100.00	1.59	100.00	23.86	67.50	103.50	132.50	156.50	175.50	200.50	262.50	24.00
minimum		32.6	3.0	3.17	46.60	3.00	0.09	0.09	0.12	0.37	14.17	0.20	12.82	2.45	11.00	15.50	18.50	21.00	23.00	25.50	49.00	7.00

Note: a) $RF_3 = RK + RM + RT$, b) $FHI_3 = \dfrac{(RF_3)_i}{(RF_3)_{\max}} \times 100$, c) $RF_2 = RK + RM$, d) $FHI_2 = \dfrac{(RF_2)_i}{(RF_2)_{\max}} \times 100$

Table 6. Correlation coefficients between two relative severity factors

Basin	Correlation coefficient		
	RK and *RM*	*RM* and *RT*	*RK* and *RT*
OM	0.162	-0.089	0.948
MG	0.371	0.174	0.973

RESULTS AND DISCUSSION

Analysis of the relationship between rainfall and run-off is important for understanding the characteristics of sudden local flooding in a short period of time over a small area. This study examines the relationship between FHI and the rainfall characteristics of the 36-year annual maximum rainfall series in two study basins. This analysis is accomplished using regression equations and scatter plots between FHI and the rainfall characteristics, viz. the average rainfall intensity I_a, the maximum rainfall depths for 1-, 2-, 3-, 4-, 5- and 6-hour durations, R_{1h}, R_{2h}, R_{3h}, R_{4h}, R_{5h} and R_{6h} respectively, the total rainfall depth R_t and the rainfall duration D. The average rainfall intensity means the total amount of rainfall for a storm event divided by the duration of the storm. The scatter plots of FHI_3 and FHI_2 versus each rainfall data in the two basins are illustrated in Figures 2 and 3. Table 7 summarises the regression analysis results for the relations between FHI_n and rainfall data in the two basins.

FHI_2 shows a much stronger relation to some rainfall data with relatively high coefficients of determination R^2 for both basins as compared with the relationship between FHI_3 and the rainfall characteristics. This suggests that FHI_2, which prevents double-counting of relative severity factors with similar characteristics, is more suited for estimating the relative flood severity directly from rainfall patterns in small watersheds. OM has a relatively high linear relation between FHI_2 and the 2-hour maximum rainfall depth R_{2h} with coefficient of determination R^2 of 0.605, as shown in Figure 3 (a). The trend between FHI_2 and the 4-hour maximum rainfall depth R_{4h} shows the best-fit line with R^2 of 0.765 for MG, as illustrated in Figure 3 (b). This demonstrates that the flood behaviour of OM located in the mountainous region with a smaller area is strongly influenced by the excessive rainfall in a shorter period of time as compared with the result from MG, a relatively larger flat watershed. The total rainfall amount R_t and the duration D show a weak and limited relationship to FHI_3 and FHI_2 in both basins (Figures 2 and 3). This result suggests that a local flood in small watersheds is mainly caused by excessive rainfall in a short period of time rather than the total rainfall amount. Furthermore, R^2 in MG are much higher than those in OM for most of the regression equations as summarised in Table 7. This is partially due to the use of point rainfall data measured by a gauge station around the basin, which might not have adequately captured the spatial variation of rainfall over the hilly region of OM compared to a more accurate representation in the flat region of MG.

Although the current relation results between FHI and the rainfall characteristics are not conclusive and more tests are required for the damage reported from past floods of real severity in a large number of watersheds, the proposed FHI methodology is expected to provide the basic database for forecasting a local flood directly from rainfall patterns.

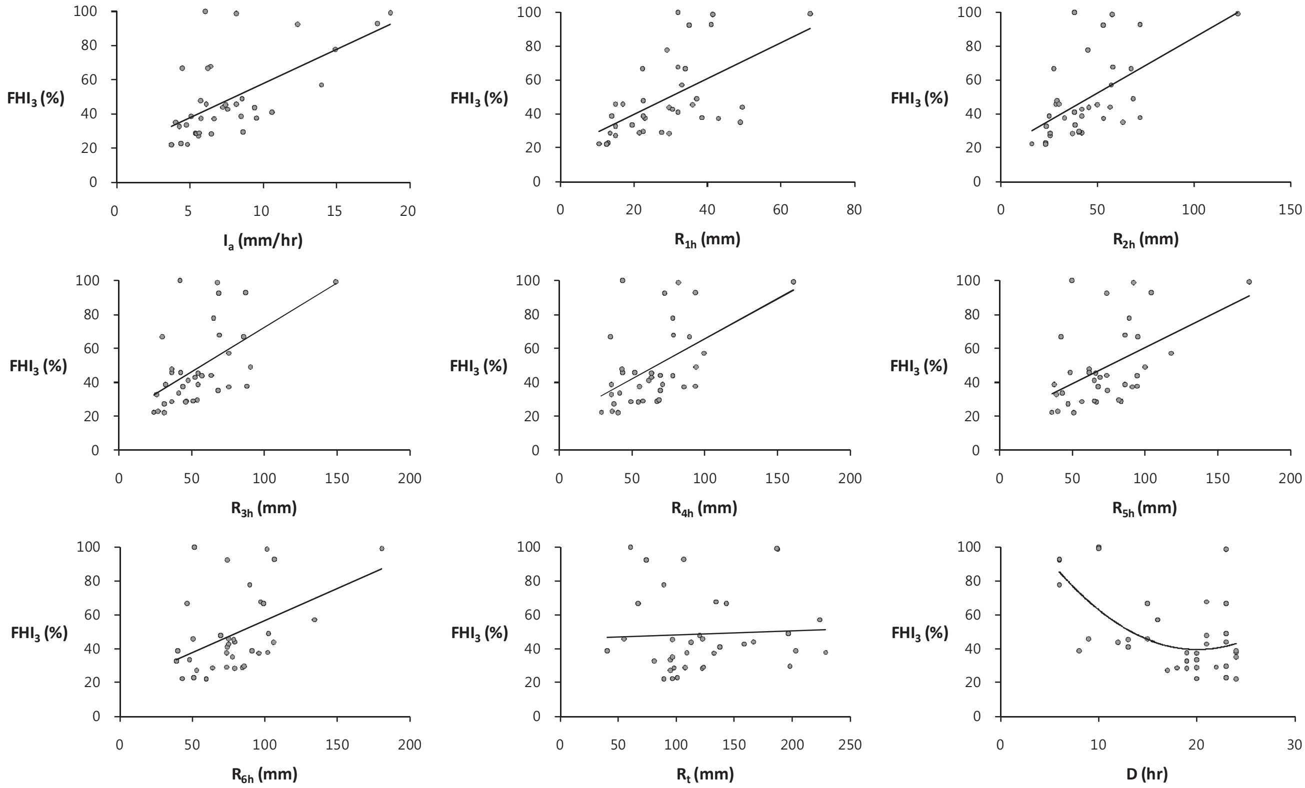

(a) Oui-mi River basin (OM)

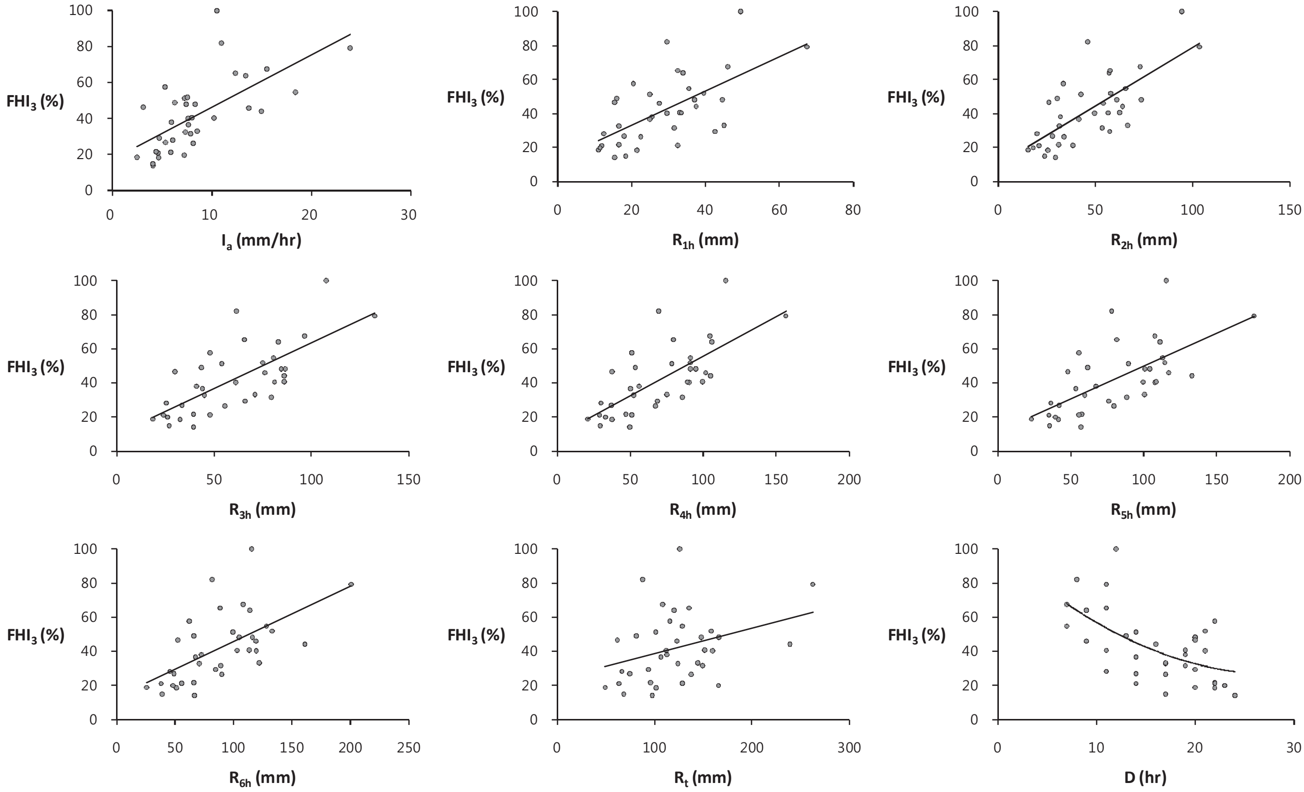

(b) Mae-gok River basin (MG)

Figure 2. Plots for trends between FHI_3 and rainfall characteristics (average rainfall intensity I_a, 1-hour maximum rainfall depth R_{1h}, 2-hour maximum rainfall depth R_{2h}, 3-hour maximum rainfall depth R_{3h}, 4-hour maximum rainfall depth R_{4h}, 5-hour maximum rainfall depth R_{5h}, 6-hour maximum rainfall depth R_{6h}, total rainfall depth R_t, and rainfall duration D) in (a) OM and (b) MG

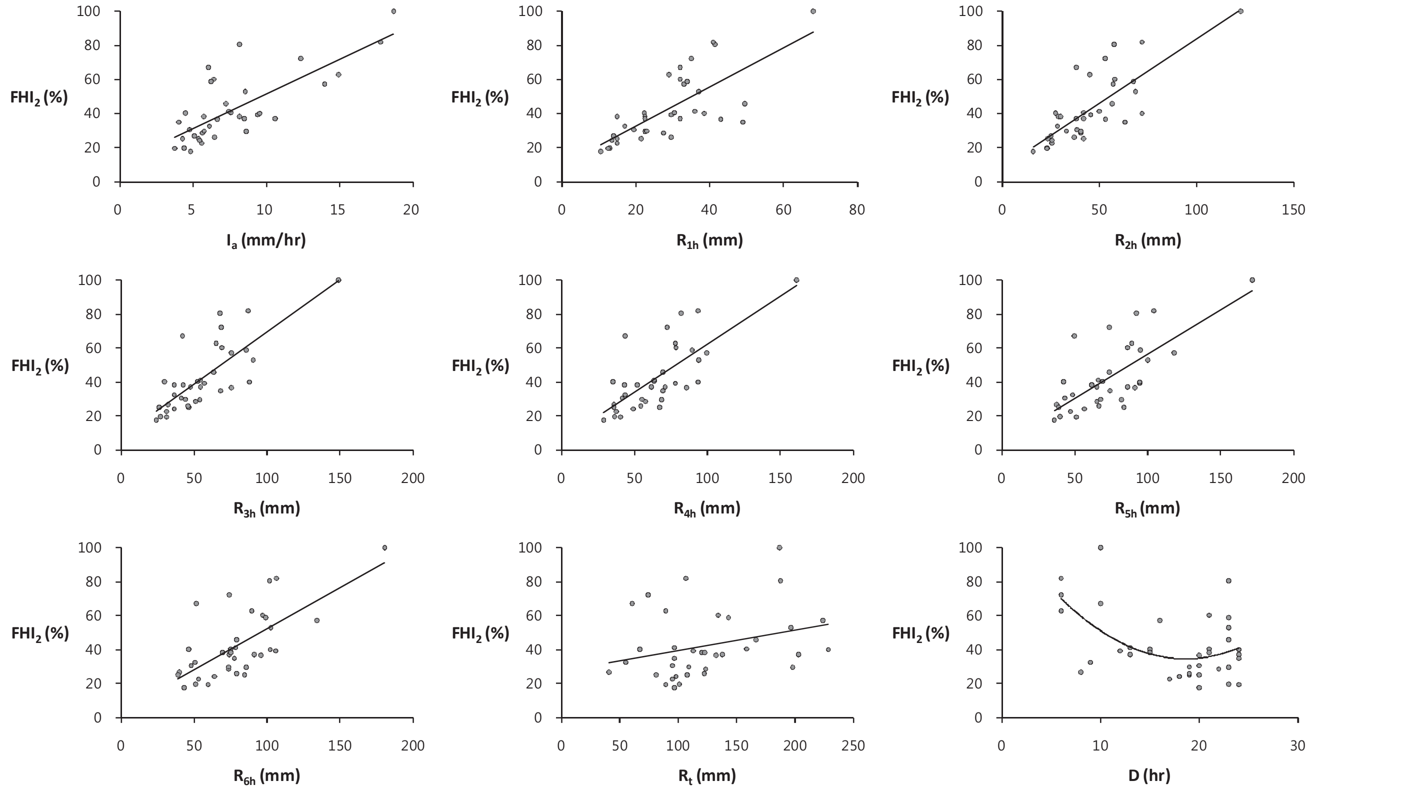

(a) Oui-mi River basin (OM)

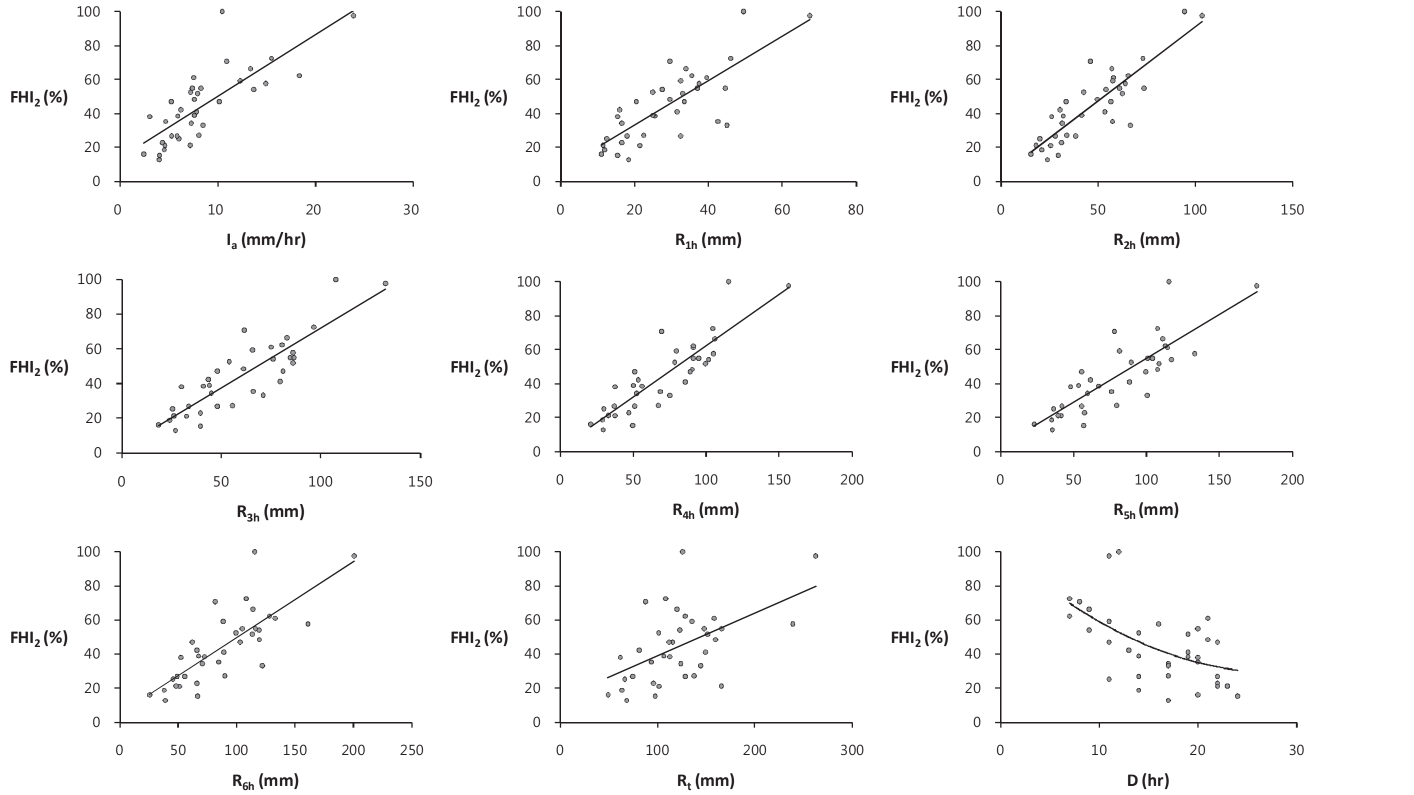

(b) Mae-gok River basin (MG)

Figure 3. Plots for trends between FHI$_2$ and rainfall characteristics (average rainfall intensity I_a, 1-hour maximum rainfall depth R_{1h}, 2-hour maximum rainfall depth R_{2h}, 3-hour maximum rainfall depth R_{3h}, 4-hour maximum rainfall depth R_{4h}, 5-hour maximum rainfall depth R_{5h}, 6-hour maximum rainfall depth R_{6h}, total rainfall depth R_t, and rainfall duration D) in (a) OM and (b) MG

Table 7. Regression analysis results for the relations between FHIn and rainfall data

Rainfall data	OM		MG	
	Regression Equation	R^2	Regression Equation	R^2
I_a	$FHI_3 = 4.000I_a + 17.928$	0.393	$FHI_3 = 2.893I_a + 17.737$	0.424
	$FHI_2 = 4.064I_a + 10.956$	0.577	$FHI_2 = 3.633I_a + 13.807$	0.601
R_{1h}	$FHI_3 = 1.058R_{1h} + 18.643$	0.321	$FHI_3 = 1.005R_{1h} + 13.238$	0.405
	$FHI_2 = 1.152R_{1h} + 9.484$	0.542	$FHI_2 = 1.311R_{1h} + 6.774$	0.619
R_{2h}	$FHI_3 = 0.659R_{2h} + 19.371$	0.325	$FHI_3 = 0.692R_{2h} + 9.854$	0.525
	$FHI_2 = 0.754R_{2h} + 8.635$	0.605	$FHI_2 = 0.871R_{2h} + 3.769$	0.750
R_{3h}	$FHI_3 = 0.528R_{3h} + 19.555$	0.311	$FHI_3 = 0.538R_{3h} + 9.855$	0.507
	$FHI_2 = 0.614R_{3h} + 8.311$	0.599	$FHI_2 = 0.692R_{3h} + 2.918$	0.754
R_{4h}	$FHI_3 = 0.473R_{4h} + 18.190$	0.272	$FHI_3 = 0.468R_{4h} + 9.257$	0.505
	$FHI_2 = 0.568R_{4h} + 5.593$	0.557	$FHI_2 = 0.607R_{4h} + 1.779$	0.765
R_{5h}	$FHI_3 = 0.429R_{5h} + 17.621$	0.247	$FHI_3 = 0.388R_{5h} + 11.156$	0.428
	$FHI_2 = 0.519R_{5h} + 4.581$	0.516	$FHI_2 = 0.519R_{5h} + 3.016$	0.688
R_{6h}	$FHI_3 = 0.382R_{6h} + 18.611$	0.211	$FHI_3 = 0.323R_{6h} + 13.634$	0.359
	$FHI_2 = 0.479R_{6h} + 4.420$	0.472	$FHI_2 = 0.445R_{6h} + 5.218$	0.612
R_t	$FHI_3 = 0.026R_t + 45.589$	0.003	$FHI_3 = 0.147R_t + 24.198$	0.107
	$FHI_2 = 0.119R_t + 27.628$	0.084	$FHI_2 = 0.253R_t + 13.739$	0.282
D	$FHI_3 = 0.232D^2 - 9.325D + 133.130$	0.360	$FHI_3 = 0.092D^2 - 5.175D + 99.582$	0.352
	$FHI_2 = 0.223D^2 - 8.304D + 111.980$	0.277	$FHI_2 = 0.091D^2 - 5.133D + 101.340$	0.309

CONCLUSIONS

This study has presented a new flood hazard index (FHI) to characterise local flooding by run-off hydrographs generated from the annual maximum rainfall series of long-term observations for small ungauged watersheds. The stronger relation between FHI and the maximum rainfall over a short interval illustrates that excessive rainfall in a short period of time mainly causes the local flooding in small watersheds. The availability of higher spatial-resolution rainfall data is expected to significantly improve the flood predictability in order to cope with the consistent threat of flood hazards in small ungauged watersheds. The conditions for effective implementation of FHI are improvements in the accuracy of rainfall run-off model predictability and precipitation forecasting. The best-fit regression equation between FHI and the rainfall data can provide the basic database for forecasting the local flood severity directly from rainfall patterns in small ungauged catchments, where the flood response time is quite short. For practical use of the regression analysis results of this study in a flash flood forecasting and warning system, further research is needed to determine a threshold of FHI to be linked with the threshold run-off in GIS-based, flash flood guidance.

ACKNOWLEDGEMENTS

This research was supported by the Yeungnam University research grant (211A380025) in 2011.

REFERENCES

1. Korea National Emergency Management Agency (KNEMA), *The Annual Natural Disaster Bulletin*, **2010**, pp.100-107.
2. H. S. Shin, H. T. Kim and M. J. Park, "The study of the fitness on calculation of the flood warning trigger rainfall using GIS and GCUH", *J. Korea Water Resour. Assoc.*, **2004**, *37*, 407-424.
3. B. S. Kim and H. S. Kim, "Estimation of the flash flood severity using runoff hydrograph and flash flood index", *J. Korea Water Resour. Assoc.*, **2008**, *41*,185-196.
4. L. Marchi, M. Borga, E. Preciso and E. Gaume, "Characterisation of selected extreme flash floods in Europe and implications for flood risk management", *J. Hydrol.*, **2010**, *394*, 118-133.
5. J. A. Smith, M. L. Baeck, Y. Zhang and C. A. Doswell, "Extreme rainfall and flooding from supercell thunderstorms", *J. Hydrometeorol.*, **2001**, *2*, 469-489.
6. J. A. Rogash and J. Racy, "Some meteorological characteristics of significant tornado events occurring in proximity to flash flooding", *Weather Forecast.*, **2002**, *17*, 155-159.
7. E. R. Vivoni, D. Entekhabi, R. L. Bras, V. Y. Ivanov, M. P. Van Horne, C. Grassott and R. N. Hoffman, "Extending the predictability of hydrometeorological flood events using radar rainfall nowcasting", *J. Hydrometeorol.*, **2006**, *7*, 660-677.
8. G. K. A. Kyiamah, "Monitoring and characterization of flash flood", *MS Thesis*, **1996**, University of Louisville, USA.
9. N. R. Bhaskar, M. N. French and G. K. Kyiamah, "Characterization of flash floods in Eastern Kentucky", *J. Hydrol. Eng.*, **2000**, *5*, 327-331.
10. J. C. Jung, "The study on estimation of the flash flood index for the Bo-chun River basin", *MS Thesis*, **2000**, Suwon University, Korea.
11. "The basic plan report for the Oui-mi River maintenance works", Wonju City, Gangwon Province, Korea, **2007**.
12. "The basic plan report for the Mae-gok River maintenance works", Chungcheongnam Province, Korea, **2004**.
13. U. S. Army Corps of Engineers, "Hydrologic Modeling System: Technical Reference Manual", Hydrologic Engineering Center, Davis (CA), **2000**.
14. Natural Resources Conservation Service (NRCS), "Urban Hydrology for Small Watersheds", Technical Release 55, U.S. Department of Agriculture, **1986**.
15. C. O. Clark, "Storage and the unit hydrograph", *Trans. ASCE*, **1945**, *110*, 1419-1446.
16. J. Noh, "A conceptual watershed model for daily streamflow based on soil water storage", *PhD Thesis*, **1991**, Seoul National University, Korea.

Maejo Int. J. Sci. Technol. **2013**, *7*(01), 107-112

Maejo International
Journal of Science and Technology

ISSN 1905-7873
Available online at www.mijst.mju.ac.th

Full Paper

p-Absolutely summable sequences of fuzzy real numbers

Ayhan Esi

Department of Mathematics, Adiyaman University, Adiyaman, Turkey

E-mail: aesi23@hotmail.com

Received: 6 April 2012 / Accepted: 8 March 2013 / Published: 13 March 2013

Abstract: In this paper the fuzzy sequence space $\left(\ell_p\right)_\lambda^F$ is introduced and some algebraic properties such as solidness, symmetricalness, convergence free and sequence algebra are studied, and some inclusion relations for the space $\left(\ell_p\right)_\lambda^F$ are provided.

Keywords: p-absolutely summable sequences, fuzzy real numbers, convergence free, sequence algebra

---

INTRODUCTION

The concept of fuzzy sets was first introduced by Zadeh [1]. Bounded and convergent sequences of fuzzy numbers were introduced by Matloka [2], who showed that every convergent sequence of fuzzy numbers is bounded. Later on sequences of fuzzy numbers were discussed by Nanda [3], Esi [4], Kaleva and Seikkala [5], Tripathy and Baruah [6-8], Tripathy and Borgogain [9,10], Tripathy and Dutta [11,12], Tripathy and Sarma [13,14], and Tripathy et al. [15]. Briefly, we recall some of the basic notations in the theory of fuzzy numbers and for more information one may refer to Matloka [2] and Diamond and Kloeden [16] for more details.

A fuzzy number X is a fuzzy subset of the real line R, i.e. a mapping $X:\mathrm{R}\to J(=[0,1])$ associating each real number t with its grade of membership $X(t)$. A fuzzy number X is *convex* if $X(t)\geq X(s)\wedge X(r)=min\{X(s),X(r)\}$, where $s<t<r$. If there exists $t_0\in\mathrm{R}$ such that $X(t_0)=1$, then the fuzzy number X is called *normal*. A fuzzy number X is said to be *upper-semi continuous* if for each $\varepsilon > 0$ and for all $a\in J$, $X^{-1}([0,a+\varepsilon))$ is open in the usual topology of R. Let $\mathrm{R}(J)$ denote the set of all fuzzy numbers which are upper semicontinuous and have compact support, i.e. if $X\in\mathrm{R}(J)$, then for any $\alpha\in[0,1]$, $[X]^\alpha$ is compact, where

$$[X]^\alpha=\{t\in\mathrm{R}:X(t)\geq\alpha,\ \text{if}\ \alpha\in[0,1]\},\ [X]^0=closure\ \ of\ \ (\{t\in\mathrm{R}:X(t)>\alpha,\ \text{if}\ \alpha=0\}).$$

The set R of real numbers can be embedded in $\mathrm{R}(J)$ if we define $\bar{r}\in\mathrm{R}(J)$ by

$$\bar{r}(t)=\begin{cases}1, \text{if} t=r\\ 0, \text{if} t\neq r\end{cases}.$$

The additive identity and multiplicative identity of $\mathsf{R}(J)$ are defined by $\bar{0}$ and $\bar{1}$ respectively. The arithmetic operations on $\mathsf{R}(J)$ are defined as follows:

$$(X\oplus Y)(t)=\sup\{X(s)\wedge Y(t-s)\}, t\in\mathsf{R},$$

$$(X\,\Theta\,Y)(t)=\sup\{X(s)\wedge Y(s-t)\}, t\in\mathsf{R},$$

$$(X\otimes Y)(t)=\sup\{X(s)\wedge Y(\frac{t}{s})\}, t\in\mathsf{R},$$

$$(\frac{X}{Y})(t)=\sup\{X(st)\wedge Y(s)\}, t\in\mathsf{R}, \text{provided } 0\notin[Y]^0.$$

Let $X,Y\in\mathsf{R}(J)$ and the $\alpha-$ level sets be $[X]^\alpha=[x_1^\alpha,x_2^\alpha],[Y]^\alpha=[y_1^\alpha,y_2^\alpha],\alpha\in[0,1]$. Then the above operations can be defined in terms of $\alpha-$level sets as follows:

$$[X\oplus Y]^\alpha=[x_1^\alpha+y_1^\alpha, x_2^\alpha+y_2^\alpha],$$

$$[X\,\Theta\,Y]^\alpha=[x_1^\alpha-y_1^\alpha, x_2^\alpha-y_2^\alpha],$$

$$[X\otimes Y]^\alpha=[\min_{i,j\in\{1,2\}} x_i^\alpha y_j^\alpha, \max_{i,j\in\{1,2\}} x_i^\alpha y_j^\alpha],$$

$$[X^{-1}]^\alpha=[(x_2^\alpha)^{-1},(x_1^\alpha)^{-1}], x_1^\alpha>0, \textit{for each } 0<\alpha\leq 1.$$

For $r\in R$ and $X\in\mathsf{R}(J)$, the product rX is defined as follows:

$$rX(t)=\begin{cases}X(r^{-1}t), \text{if} r\neq 0\\ 0, \text{if} r=0\end{cases}.$$

The absolute value , $|X|$, of $X\in\mathsf{R}(J)$ is defined [5] by

$$|X|(t)=\begin{cases}\max\{X(t),X(-t)\}, \text{if} t\geq 0\\ 0, \text{if} t<0\end{cases}.$$

A mapping $\bar{d}:\mathsf{R}(J)\times\mathsf{R}(J)\to\mathsf{R}^+\cup\{0\}$ is defined by

$$\bar{d}(X,Y)=\sup_{0\leq\alpha} d([X]^\alpha,[Y]^\alpha).$$

It is known that $(\mathsf{R}(J),\bar{d})$ is a complete metric space [5].

A metric on $\mathsf{R}(J)$ is said to be *translation invariant* if

$$\bar{d}(X+Z,Y+Z)=\bar{d}(X,Y), \textit{for } X,Y,Z\in R(J).$$

A sequence $X=(X_k)$ of fuzzy numbers is a function X from the set N of natural numbers in $L(R)$. The fuzzy number X_k denotes the value of the function at $k\in\mathsf{N}$ [2].
Let E^F denote the sequence space of fuzzy numbers.

A sequence space E^F is said to be *solid* (or *normal*) if $(Y_k)\in E^F$ whenever $(X_k)\in E^F$ and $|Y_k|\le|X_k|$ for all $k\in\mathbb{N}$.

A sequence space E^F is said to be *symmetric* if $(X_k)\in E^F$ implies $(X_{\pi(k)})\in E^F$ where π is a permutation of $\mathbb{N}$.

A sequence space E^F is said to be *sequence algebra* if $(X_k\otimes Y_k)\in E^F$ whenever $(X_k),(Y_k)\in E^F$.

A sequence space E^F is said to be *convergence free* if $(Y_k)\in E^F$ whenever $(X_k)\in E^F$ and $X_k=\bar{0}$ implies $Y_k=\bar{0}$.

A sequence space E^F is said to be *monotone* if E^F contains the canonical pre-images of all its step spaces.

Lemma. *If a sequence space E^F is normal then it is monotone*. (For the crisp set case, one may refer to Kamthan and Gupta [17]).

In this paper, we define the p-absolutely $\lambda-$summable sequence space of fuzzy real numbers $(\ell_p)_\lambda^F$ as follows: Let $\lambda=(\lambda_n)$ be a non-decreasing sequence of positive numbers such that $\lambda_{n+1}\le\lambda_n+1, \lambda_1=1, \lambda_n\to\infty$ as $n\to\infty$, $I_n=[n-\lambda_n+1,n]$ and we define:

$$(\ell_p)_\lambda^F=\left\{X=(X_k):\sum_{n=1}^{\infty}\left(\frac{1}{\lambda_n}\sum_{k\in I_n}\bar{d}(X_k,\bar{0})\right)^p<\infty\right\}$$

where $1\le p<\infty$. It is noted that $(\ell_p)_\lambda^F=Ces(p)$ for $\lambda_n=n$ for all $n\in\mathbb{N}$.

MAIN RESULTS

Theorem 1. The sequence space $(\ell_p)_\lambda^F$ is closed under addition and scalar multiplication.

Proof: Let X=(X$_k$)$\in(\ell_p)_\lambda^F$ and $\alpha\in\mathbb{R}$. Then

$$\sum_{n=1}^{\infty}\left(\frac{1}{\lambda_n}\sum_{k\in I_n}\bar{d}(X_k,\bar{0})\right)^p<\infty.$$

Then we write:

$$\sum_{n=1}^{\infty}\left(\frac{1}{\lambda_n}\sum_{k\in I_n}\bar{d}(\alpha X_k,\bar{0})\right)^p=\sum_{n=1}^{\infty}\left(\frac{1}{\lambda_n}\sum_{k\in I_n}|\alpha|\bar{d}(X_k,\bar{0})\right)^p$$

$$=|\alpha|^p\sum_{n=1}^{\infty}\left(\frac{1}{\lambda_n}\sum_{k\in I_n}\bar{d}(X_k,\bar{0})\right)^p<\infty.$$

This implies that αX=(αX$_k$)$\in(\ell_p)_\lambda^F$. Now let X=(X$_k$), Y=(Y$_k$)$\in(\ell_p)_\lambda^F$. Then

$$\sum_{n=1}^{\infty}\left(\frac{1}{\lambda_n}\sum_{k\in I_n}\bar{d}(X_k,\bar{0})\right)^p<\infty \text{ and } \sum_{n=1}^{\infty}\left(\frac{1}{\lambda_n}\sum_{k\in I_n}\bar{d}(Y_k,\bar{0})\right)^p<\infty.$$

Then we can write:

$$\sum_{n=1}^{\infty}\left(\frac{1}{\lambda_n}\sum_{k\in I_n}\bar{d}\left(X_k+Y_k,\bar{0}\right)\right)^p \le \sum_{n=1}^{\infty}\left(\frac{1}{\lambda_n}\sum_{k\in I_n}\bar{d}\left(X_k,\bar{0}\right)\right)^p + \sum_{n=1}^{\infty}\left(\frac{1}{\lambda_n}\sum_{k\in I_n}\bar{d}\left(Y_k,\bar{0}\right)\right)^p < \infty.$$

Thus X+Y=(X_k+Y_k) $\in \left(\ell_p\right)_\lambda^F$.

Theorem 2. The sequence space $\left(\ell_p\right)_\lambda^F$ is solid and hence monotone.

Proof: Let $X=\left(X_k\right)$ and $Y=\left(Y_k\right)$ be two sequences of fuzzy real numbers such that $\bar{d}\left(Y_k,\bar{0}\right)\le \bar{d}\left(X_k,\bar{0}\right)$ for all $k\in\mathbb{N}$. If X=(X_k) $\in \left(\ell_p\right)_\lambda^F$. Then

$$\sum_{n=1}^{\infty}\left(\frac{1}{\lambda_n}\sum_{k\in I_n}\bar{d}\left(X_k,\bar{0}\right)\right)^p < \infty.$$

Now, we have

$$\sum_{n=1}^{\infty}\left(\frac{1}{\lambda_n}\sum_{k\in I_n}\bar{d}\left(Y_k,\bar{0}\right)\right)^p \le \sum_{n=1}^{\infty}\left(\frac{1}{\lambda_n}\sum_{k\in I_n}\bar{d}\left(X_k,\bar{0}\right)\right)^p < \infty.$$

Hence Y=(Y_k) $\in \left(\ell_p\right)_\lambda^F$. Thus, the sequence space $\left(\ell_p\right)_\lambda^F$ is solid and hence monotone.

Theorem 3. The sequence space $\left(\ell_p\right)_\lambda^F$ is sequence algebra.

Proof: Let X=(X_k), Y=(Y_k) $\in \left(\ell_p\right)_\lambda^F$. Then

$$\sum_{n=1}^{\infty}\left(\frac{1}{\lambda_n}\sum_{k\in I_n}\bar{d}\left(X_k,\bar{0}\right)\right)^p < \infty \text{and} \sum_{n=1}^{\infty}\left(\frac{1}{\lambda_n}\sum_{k\in I_n}\bar{d}\left(Y_k,\bar{0}\right)\right)^p < \infty.$$

Thus, we can write:

$$\sum_{n=1}^{\infty}\left(\frac{1}{\lambda_n}\sum_{k\in I_n}\bar{d}\left(X_k\otimes Y_k,\bar{0}\right)\right)^p \le \sum_{n=1}^{\infty}\left(\frac{1}{\lambda_n}\sum_{k\in I_n}\bar{d}\left(X_k,\bar{0}\right).\bar{d}\left(Y_k,\bar{0}\right)\right)^p$$

$$\le \sum_{n=1}^{\infty}\left(\frac{1}{\lambda_n}\sum_{k\in I_n}\bar{d}\left(X_k,\bar{0}\right)\right)^p . \sum_{n=1}^{\infty}\left(\frac{1}{\lambda_n}\sum_{k\in I_n}\bar{d}\left(Y_k,\bar{0}\right)\right)^p < \infty.$$

Thus, ($X_k \otimes Y_k$) $\in \left(\ell_p\right)_\lambda^F$. So the sequence space $\left(\ell_p\right)_\lambda^F$ is sequence algebra.

Theorem 4. The sequence space $\left(\ell_p\right)_\lambda^F$ is not symmetric in general.

Proof: We shall prove it by the following example:

Example 1. Let $p=1$, $\lambda_n = n$ for all $n \in \mathrm{N}$. Consider the sequence $X=(X_k)$ defined by:

$$X_k(t)=\begin{cases} k^2t+1, \text{if } -k^{-2} \le t \le 0 \\ 1-k^2t, \text{if } 0 \le t \le k^{-2} \\ 0, \text{otherwise} \end{cases}.$$

Then

$$\sum_{n=1}^{\infty}\left(\frac{1}{\lambda_n}\sum_{k\in I_n}\bar{d}\left(X_k,\bar{0}\right)\right)^p = \sum_{n=1}^{\infty}\left(\frac{1}{n}\sum_{k\in I_n}k^{-2}\right) < \infty.$$

Hence X=(X$_k$)$\in \left(\ell_p\right)_\lambda^F$. Now we consider the rearrangement of $X=(X_k)$ defined as $Y=\left(Y_k\right)=\left(X_1,\bar{0},X_2,\bar{0},X_3,\bar{0},...\right)$. Then we have:

$$\sum_{n=1}^{\infty}\left(\frac{1}{\lambda_n}\sum_{k\in I_n}\bar{d}\left(Y_k,\bar{0}\right)\right)^p \to \infty.$$

Then Y=(Y$_k$)$\notin \left(\ell_p\right)_\lambda^F$. Hence the sequence space $\left(\ell_p\right)_\lambda^F$ is not symmetric in general.

Theorem 5. The sequence space $\left(\ell_p\right)_\lambda^F$ is not convergence free in general.

Proof: We shall prove it by the following example:

Example 2. Let $p=1$ and $\lambda_n = n$ for all $n \in \mathrm{N}$. Consider the sequence $X=(X_k)$ defined by:

$$X_k(t)=\begin{cases} k^2t+1, \text{if } -k^{-2} \le t \le 0 \\ 1-k^2t, \text{if } 0 \le t \le k^{-2} \\ 0, \text{otherwise} \end{cases}.$$

Then

$$\sum_{n=1}^{\infty}\left(\frac{1}{\lambda_n}\sum_{k\in I_n}\bar{d}\left(X_k,\bar{0}\right)\right)^p = \sum_{n=1}^{\infty}\left(\frac{1}{n}\sum_{k\in I_n}k^{-2}\right) < \infty.$$

Thus, $X=(X_k)\in\left(l_p\right)_\lambda^F$. Now we consider the sequence $Y=\left(Y_k\right)$ defined by:

$$Y_k(t)=\begin{cases} k^{\frac{1}{2}}t+1, \text{if } -k^{-\frac{1}{2}} \le t \le 0 \\ 1-k^{\frac{1}{2}}t, \text{if } 0 \le t \le k^{\frac{-1}{2}} \\ 0, \text{otherwise} \end{cases}.$$

Then

$$\sum_{n=1}^{\infty}\left(\frac{1}{\lambda_n}\sum_{k\in I_n}\bar{d}\left(Y_k,\bar{0}\right)\right)^p = \sum_{n=1}^{\infty}\left(\frac{1}{n}\sum_{k\in I_n}k^{-\frac{1}{2}}\right) = \infty.$$

Thus, Y=(Y$_k$)$\notin \left(\ell_p\right)_\lambda^F$. Hence the sequence space $\left(\ell_p\right)_\lambda^F$ is not convergence free in general.

Theorem 6. Let $0<p<q$. Then $\left(\ell_p\right)_\lambda^F \subset \left(\ell_q\right)_\lambda^F$.

Proof: It is clear from the following inclusion relation: for any X=(X_k)$\in \left(\ell_p\right)_\lambda^F$,

$$\sum_{n=1}^{\infty}\left(\frac{1}{\lambda_n}\sum_{k\in I_n}\bar{d}\left(X_k,\bar{0}\right)\right)^p \leq \sum_{n=1}^{\infty}\left(\frac{1}{\lambda_n}\sum_{k\in I_n}\bar{d}\left(X_k,\bar{0}\right)\right)^q.$$

REFERENCES

1. L. A. Zadeh, "Fuzzy sets", *Inform. Control*, **1965**, *8*, 338-353.
2. M. Matloka, "Sequences of fuzzy numbers", *BUSEFAL*, **1986**, *28*, 28-37.
3. S. Nanda, "On sequences of fuzzy numbers", *Fuzzy Sets Syst.*, **1989**, *33*, 123-126.
4. A. Esi, "On some new paranormed sequence spaces of fuzzy numbers defined by Orlicz functions and statistical convergence", *Math. Modell. Anal.*, **2006**, *11,* 379-388.
5. O. Kaleva and S. Seikkala, "On fuzzy metric spaces", *Fuzzy Sets Syst.*, **1984**, *12*, 215-229.
6. B. C. Tripathy and A. Baruah, "New type of difference sequence spaces of fuzzy real numbers", *Math. Modell. Anal.*, **2009**, *14,* 391-397.
7. B. C. Tripathy and A. Baruah, "Nörlund and Riesz mean of sequences of fuzzy real numbers", *Appl. Math. Lett.*, **2010**, *23*, 651-655.
8. B. C. Tripathy and A. Baruah, "Lacunary statically convergent and lacunary strongly convergent generalized difference sequences of fuzzy real numbers", *Kyungpook Math. J.*, **2010**, *50*, 565-574.
9. B. C. Tripathy and S. Borgogain, "The sequence space $m(M,\phi,\Delta_n^m,p)^F$", *Math. Modell. Anal.*, **2008**, *13*, 577-586.
10. B. C. Tripathy and S. Borgogain, "Some classes of difference sequence spaces of fuzzy real numbers defined by Orlicz function", *Adv. Fuzzy Syst.*, **2011**, *Article ID216414*.
11. B. C. Tripathy and A. J. Dutta, "On fuzzy real-valued double sequence space $_2\ell_F^p$ ", *Math. Comput. Modell.*, **2007**, *46*, 1294-1299.
12. B. C. Tripathy and A. J. Dutta, "Bounded variation double sequence space of fuzzy real numbers", *Comput. Math. Appl.*, **2010**, *59*, 1031-1037.
13. B. C. Tripathy and B. Sarma, "Sequence spaces of fuzzy real numbers defined by Orlicz functions", *Math. Slovaca*, **2008**, *58*, 621-628.
14. B. C. Tripathy and B. Sarma, "Some double sequence spaces of fuzzy numbers defined by Orlicz function", *Acta Math. Sci.*, **2011**, *31*, 134-140.
15. B. C. Tripathy, M. Sen and S. Nath, "*I*-convergence in probabilistic *n*-normed space", *Soft Comput.*, **2012,** *16*, 1021-1027.
16. P. Diamond and P. Kloeden, "Metric Spaces of Fuzzy Sets: Theory and Applications", World Scientific Publishing, Singapore, **1994**.
17. P. K. Kampthan and M. Gupta, "Sequence Spaces and Series", Marcel Dekker, New York, **1980**, p.53.

Maejo Int. J. Sci. Technol. **2013**, *7*(01), 113-132

Maejo International
Journal of Science and Technology

ISSN 1905-7873
Available online at www.mijst.mju.ac.th

Review

Thai pigs and cattle production, genetic diversity of livestock and strategies for preserving animal genetic resources

Rangsun Charoensook [1, 2], Christoph Knorr [2], Bertram Brenig [2] and Kesinee Gatphayak [3,*]

[1] Department of Agricultural Sciences, Faculty of Agriculture Natural Resources and Environment, Naresuan University, 65000 Phitsanulok, Thailand
[2] Institute of Veterinary Medicine, Georg-August University of Göttingen, Burckhardtweg 2, 37077 Göttingen, Germany
[3] Department of Animal and Aquatic Science, Faculty of Agriculture, Chiang Mai University, 50200 Chiang Mai, Thailand
* Corresponding author, e-mail: k.gat@chiangmai.ac.th

Received: 8 August 2011 / Accepted: 22 February 2013 / Published: 14 March 2013

Abstract: This paper reviews the current situation of livestock production in Thailand, genetic diversity and evaluation, as well as management strategies for animal genetic resources focusing on pigs and cattle. Sustainable conservation of indigenous livestock as a genetic resource and vital components within the agricultural biodiversity domain is a great challenge as well as an asset for the future development of livestock production in Thailand.

Keywords: animal genetic resources, genetic diversity, Thai pig and cattle breeds, livestock production

---

INTRODUCTION

Indigenous livestock has played an important role in smallholder farms and local populations for a long time. They have been raised using low input but they still generate their products and by-products to meet household needs. Moreover, in relation to biodiversity, indigenous livestock seem to be a reservoir of genes that could be an asset for future use. However, in recent years livestock production in Thailand was switched from backyard systems to industrialised husbandry [1, 2]. In parallel, exotic livestock was imported to improve the production performance and for economically important traits. Indigenous livestock were therefore gradually used for crossbreeding and were finally replaced completely by exotic commercial breeds. These breeding strategies oppose the concepts of sustainability and resource management and their long-term use threatens the loss of the genetic identity and diversity of the indigenous breeds.

CURRENT SITUATION OF LIVESTOCK PRODUCTION IN THAILAND

A major structural change in livestock production occurred in the past 20-25 years in Thailand. Private sector innovations such as improved breeds, feed technology, housing, farm management and contractual arrangements have been the prime drivers of growth and export opportunities, and rapid domestic and regional economic growth during the 1985-1995 period were the essential catalysts [1]. The livestock industries have been clustered in close proximity to Bangkok and the heavy concentration of animals is causing environmental stress. Farm sizes have become significantly large and the expansion is made possible by imported technology and increasing domestic demand. Pig and cattle development have been driven by domestic market demand and significantly affected by governmental regulations of slaughterhouses and by subsidies [1]. In this section, general information on the Thai agricultural sector and livestock production focusing on pig and cattle production is provided.

Economic Values of Agriculture and Livestock Production

According to the National Statistical Office (NSO), the population of Thailand stood at about 67,070,000 inhabitants in 2009 and the gross domestic product (GDP) was US$ 3,939 per capita [3]. Thailand is an agricultural country with around 34% of the households throughout the country working in agriculture and 93% of them located in rural areas. The two major activities in the agriculture area are the cultivation of crops (54%) and integrated crop-livestock farming (35%). Fifty-three per cent of the cultivated areas are being used for rice production [4]. The major forms of livestock in Thailand are pigs, chicken and cattle. Thailand is a major agricultural exporter to countries all over the world. Agriculture's share of the GDP in 2009 was around 9.2%. Within the agricultural sector, crops account for approximately 68% of the total output while the livestock are only a relatively small part of the overall agricultural sector, contributing 17% in 2009 [3, 4].

The agricultural sector in Thailand has undergone a substantial transformation to non-traditional crops since the past few years. It has shifted away from commodities such as rice and cassava towards more highly valued products. Para rubber, frozen chicken and shrimp products have become important, particularly for export markets. According to the Office of Agricultural Economics (OAE), the major export products in 2009 were rice (US$ 4,784 million), Para rubber (US$ 3,595 million), shrimp products (US$ 2,588 million), frozen chicken (US$ 1,304 million) and cassava products (US$ 1,296 million) [5].

For 2010, the Office of Agricultural Economics [5] recorded a decrease of 0.9% in the agricultural share of Thailand's economy. The two major contributing factors were a serious drought and the infestation of crop pests in the early months of the year 2010, which was accentuated by heavy floods later in the year. Consequently, the impact upon most of the major crops was a decline in production as the yearly crop production index fell by 2.1% compared to the year before. However, the overall prices of crops remained favourably high, especially for Para rubber, cassava and palm oil. For rice alone, even though yields were lower than in 2009, they still reached high levels contributing to a 22.8% increase in the farmers' income index. Livestock production is expected to be on the rise by 1.5% per year due to favourable price incentives coupled with the absence of serious livestock epidemic outbreak and bright export trends. Livestock produce such as dairy products and beef is an almost insignificant component of the Thai economy in terms of aggregate output despite a more than fourfold increase in the number of dairy cattle stocks and a 10 per cent increase in beef cattle stocks in 1986 and 1999 [1]. Furthermore, the growth of the fishery sector is expected to reach 1.2% due to its production expansion as a result of the growing demand for raw material supplies used in the processing facilities for export purposes. The fishery sector will therefore continue to grow [5].

Pig and Beef Cattle Husbandry in Thailand

At present, livestock production in Thailand is growing very quickly and plays an important role in food production. It has shifted from backyard animals and integrated crop-livestock farming systems to industrial livestock farming enterprises [1, 2], although the extent of this development differs among livestock species. Rapid growth has occurred in pig and poultry production. Pigs as well as broilers and layers have been produced mainly by large agribusiness companies for the export markets [1, 5, 6]. The principal challenge for pig production in Thailand is to close the wide gap between demand and production by upgrading the current production system towards that with high input and high output. In contrast to the pig production situation, the importance of beef cattle and buffaloes is still low in spite of the fact that they are mostly raised by smallholders in rural areas rather than by companies.

Pig production

The development of pig production started in the 1960s when the first group of exotic pig-breeds was imported by the Department of Livestock Development from the United Kingdom. These were Large White, Tamworth and Berkshire breeds. Later, Landrace and Duroc pigs were imported from the United States [2]. Before these exotic breeds were introduced, farmers relied on the relatively slow growing native pigs that had the desirable quality of not needing much in the way of trade inputs [1]. Since 1981 pig breeding has steadily been industrialised in Thailand. Thus, indigenous native pigs have been increasingly mated with imported breeds to improve their performance in economically important traits. Native pigs have gradually become crossbreeds and are finally replaced by European commercial breeds as the meat delivering end product in the pork industry [7].

Nowadays, like in other major swine-producing areas of the world, there has been a change from small farms to large farming enterprises. This trend will continue and is expected to lead to improved quality pork and to better meet the requirements of overseas importers. Ten large operators account for most of the increase in the current production and the outlook for development is significantly positive. Groups of agribusiness companies such as Charoen Pokphand (CP), Betagro, Laem Thong and Mittraparp are integrated and account for more than 20% of the swine production in Thailand. The operations employed by these companies are fully automated and have increased the efficiency of production, which will make them competitive in the world market.

The total commercial breeding swine population in 2009 was 991,140 animals. The boar population was 85,041 animals and the sow population was estimated at 906,099 animals. These sows wean an average of 17 pigs/sow/year [2]. The primary swine-producing area is the central region with approximately 57% (4,669,535 head) of the country's pig population (8,537,703 head). The southern part has the lowest number of pigs, possibly reflecting the higher cost of pig fattening because of a shortage of feed in this region, or the fact that the southern part of Thailand has a relatively high Muslim population that do not consume pork meat. Most of the pork produced in Thailand is consumed domestically; export markets are limited to Hong Kong, Vietnam and Singapore. Processed pork products are, however, more widely exported [1, 2].

Native pigs

Contrary to commercial pigs, Thai native pigs are predominantly raised by communities in the northern region, representing almost half of the country's native pig population (Table 1). The average number of pigs per household is 4.3 head. Smallholders in the hill tribe communities traditionally raise a few indigenous pigs following local custom and religion. Animals are sacrificed at special celebrations such as New Year and wedding [7-9]. However, small pig populations without any scrutinised breeding programme are always at risk of losing genetic diversity and identity [10, 11].

Table 1. Regional distribution of pig farming in Thailand

Region	Number		Number		Total	
	Native breeds	Farmers	Commercial breeds [a]	Farmers	Animals	Farmers
Northern	218,406	50,365	1,145,564	47,943	1,363,970	98,308
North-eastern	142,116	26,033	1,340,001	63,022	1,482,117	89,055
Central	36,910	4,671	4,632,625	19,500	4,669,535	24,171
Southern	57,459	7,933	964,622	28,322	1,022,081	36,255
Total	454,891	89,002	8,082,812	158,787	8,537,703	247,789

Source: Modified from the Department of Livestock Development [2]
[a] Breeding and fattening pigs

Thai native pigs are classified as lard-type pigs. They grow slowly and their reproduction rate is low. However, they adapt well to hot and humid climate, tolerate low-quality feed and are probably resistant to foot-and-mouth disease and internal parasites, among others [7]. The characterisation of Thai native pigs has been made by the domestic animal diversity information system of the FAO [12]. Native Thai pigs are classified into four 'breeds', viz. Raad (or Ka Done), Puang, Hailum and Kwai (Table 2 and Figure 1), according to their physical appearance and the region where they are predominant.

As pigs in northern Thailand have also been kept and bred by hill tribes, some researchers have classified them as an independent group [7]. They have a narrower head, a longer snout and a shorter body compared to Thai native pigs from the lowlands. Hill-tribe pigs can be classified into two types: the small black type (similar to Raad or Ka Done pigs) and the black-and-white type (similar to Hailum and Kwai pigs), 70% of them being of the former type. Large-eared pigs found in Thunghuachang district of Lamphun province, which are probably cross-bred from hill-tribe pigs and Chinese Meishan pigs, are more prolific than indigenous hill-tribe pigs. However, nowadays it is difficult to determine any unique characteristics that are specific for each pig breed [7, 10, 11].

Table 2. Phenotypic classification of four Thai native pigs

Name	Weight [a] (kg)	Specific phenotype	Number of teats	Litter size	Predominance in Thailand
Raad	60-70	Black hair-coat colour; short body; small head; small and erect ears; long and straight snout	9-12	5-6	Lower north-eastern
Puang	120-130	Black and wrinkled skin; large thick ears; similar to Chinese Taihu pigs	N/A [b]	6-7	Upper north-eastern
Hailum	110-120	Black-and-white hair-coat colour; black colour at head, back and rump; white at belly and legs; short and straight snout; small and erect ears; similar to Chinese Hainan pigs	10-14	7-8	Central, eastern and southern
Kwai	130-150	Black hair-coat colour; white legs; long and straight snouts; larger ears; white ring around black cornea	10-12	6-7	Northern

Source: Modified from Rattanaronchart [7] and DAD-IS [12]
[a] Average mature weight of female and male pigs
[b] Not applicable

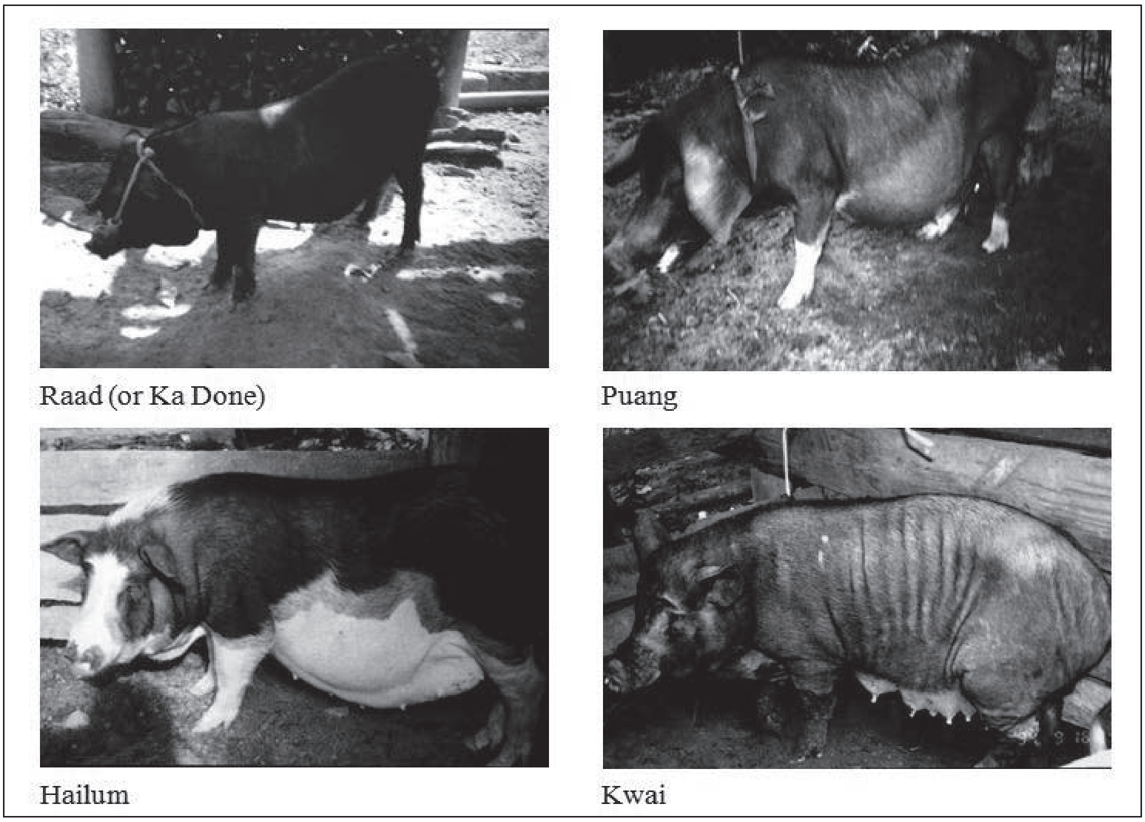

Figure 1. Four breeds of Thai native pigs [2, 7]

Beef cattle production

According to the Department of Livestock Development [2], the beef cattle stocks increased from 4,635,741 to 8,595,428 between 2000 and 2009. The increase was due to the policy of the Thai government to encourage farmers to raise beef cattle in an effort to reduce the amount of imported beef [13]. Several activities aimed at increasing beef cattle production initiated by the Thai government were initiated, such as the royal-initiated Cattle-and-Buffalo Bank project in 1978, the Beef Cattle Farm promotion in the north-eastern region in 1989 and the One-Million Beef Cattle Households promotion in 2004 [2].

In 2009 the average number of cattle per household for the whole country was just 6.2 head. This indicates that smallholders own the majority of beef cattle. The main region is the north-east where 54% of Thailand's beef cattle were found (Table 3). The number of pure-bred and cross-bred cattle was 3,153,013 head compared to 5,442,415 head of native cattle, which indicates the genetic potential of the indigenous animals. Beef cattle in Thailand are produced by extensive grazing systems rather than in confined feedlots or under controlled grazing. Village farmers who generally raise few ruminants usually use small areas beside crop fields for grazing in addition to paddy fields after the harvest [2, 14].

Table 3. Regional distribution of cattle farming in Thailand

Region	Number		Number		Total	
	Native breeds	Farmers	Exotic/cross-breeds	Farmers	Animals	Farmers
Northern	1,008,686	108,091	669,246	59,098	1,677,932	165,223
North-eastern	3,083,410	623,931	1,572,034	331,991	4,655,444	898,305
Central	710,758	58,534	785,275	58,097	1,496,033	114,228
Southern	639,561	163,357	126,458	38,936	766,019	191,962
Total	5,442,415	953,913	3,153,013	488,122	8,595,428	1,369,718

Source: Modified from the Department of Livestock Development [2]

Native cattle

Thai native cattle are classified as *Bos indicus* cattle and were predominantly used as draught animals in the past. They have accompanied Thai people for a long period of time and have now adapted well to local environments [15]. The north-eastern part of the country is also the most important area in terms of native cattle production with an average of five head per household. Thai native cattle are mainly kept under extensive grazing. During the dry season the animals graze in the forests or are fed only rice straw. Thai native bulls weigh between 300-450 kg and cows 200-300 kg on average [2]. Although Thai native cattle are small framed and display a low growth rate, they seem to have a good adaptability to low quality feed. They are also heat tolerant and resistant to parasites. The low energy requirement and the efficient utilisation of low quality roughage without protein favour their survival under severe feeding conditions [2, 14, 15].

Thai native cattle are categorised into four ecotypes, viz. the Northern ecotype (White Lamphun), the North-eastern ecotype, the Central ecotype and the Southern ecotype (Figure 2). This classification is confirmed by the study using phenotypic information of cattle kept on government research farms by their original region using a cluster analysis with a 75% coefficient of determination. However, there has been no genetic information with respect to the difference between the ecotypes [15-17].

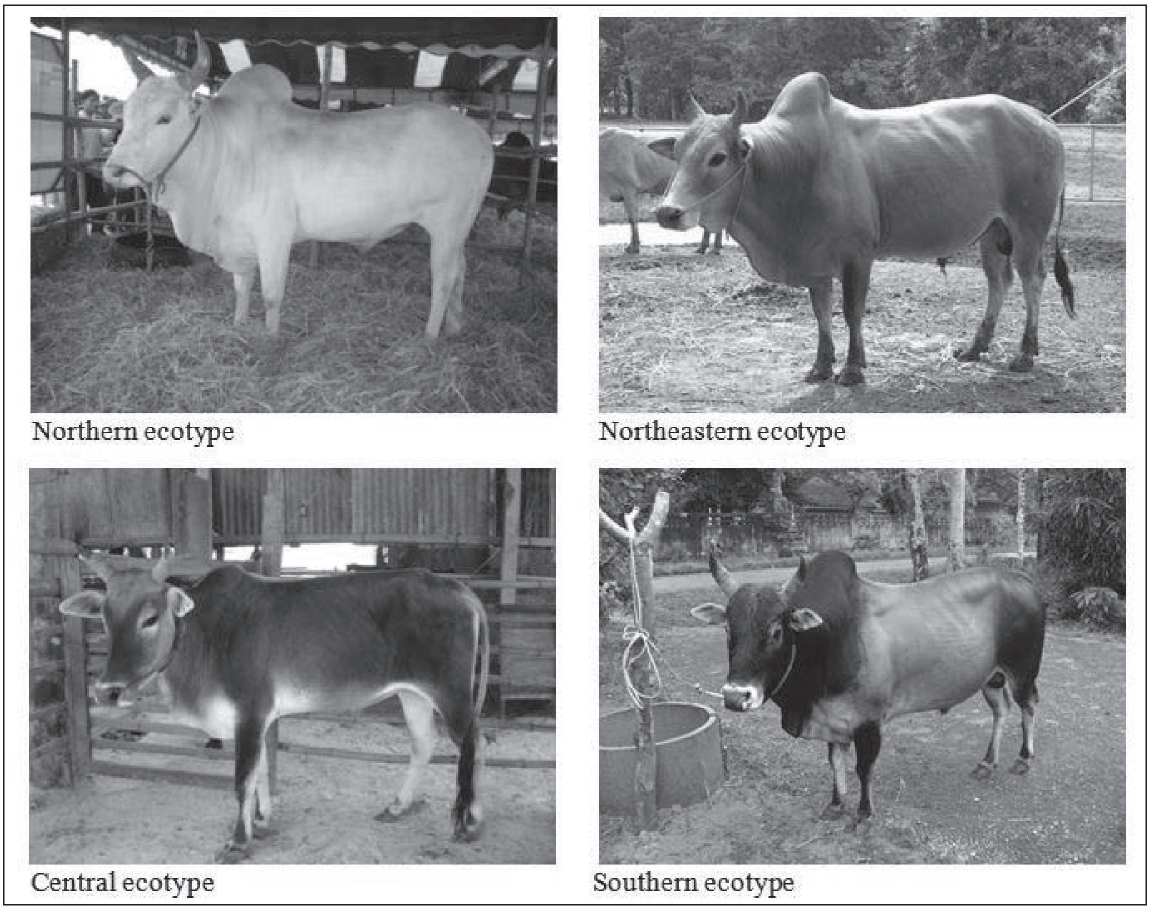

Figure 2. Four ecotypes of Thai native cattle [2, 17]

In northern Thailand, the White Lamphun and the mountain cattle are the two most widespread native cattle breeds. They show a rather high rate of fertility, are tolerant to a poor quality of natural grasses and are well adapted to internal and external parasites. They are also resistant to diseases such as Anaplasmosis. They adapt well to hot and humid climate [18]. The White Lamphun breed shows an entirely white phenotype and are pink-skinned. They are classified as an endangered-maintained breed (with probably fewer than 1,000 breeding females). Their origin is still unknown but it has been a popular breed among northern Thai populations. The name is derived from Lamphun province where the breed is prevalent [2, 18]. The mountain cattle vary in colour (red brown, white gray or black) and are probably the smallest breed (150-200 kg mature wt.) among the Thai native cattle breeds. They are mainly raised in mountainous areas [18].

The performance advantages of native Thai cattle have been overshadowed by the large body size of imported exotic breeds. Indigenous cattle have therefore been neglected and crossed with zebu cattle (*Bos indicus*) such as Brahman and several *Bos taurus* breeds [2, 19]. These were mostly imported into the native cattle population by means of frozen semen such as that of Charolais, Hereford, Simmental and Shorthorn for the purpose of crossbreeding [1, 15].

GENETIC DIVERSITY AND EVALUATION OF LIVESTOCK

Genetic diversity is generated by either mutations, frequency of different allele changes due to migration, selection, or chance. Genetic diversity of livestock represents the heritable variations within and between populations. Populations may be either the entire species or a specific collection of individuals within a species, such as a breed, a strain, a line, or even a herd/flock [20]. Genetic diversity is required for populations to evolve and to cope with environmental changes. A loss of genetic diversity is often associated with inbreeding and a reduction of reproductive fitness. Genetic diversity and the evaluation of domestic animals have attracted attention worldwide. Consequently, the International Union for Conservation of Nature (IUCN) recognises the need to conserve genetic diversity as one of the three global conservation priorities [21]. Thus, a better understanding of the mechanisms which cause genetic diversity is a necessary priority in managing livestock populations. Worldwide efforts have been undertaken to conserve livestock diversity. Monitoring the number of breeds, their population size and degree of endangerment is coordinated by the FAO on a global level. The FAO report on the state of the world's animal genetic resources shows that roughly one third of all breeds are considered to be at risk of extinction [22].

Assessment of Genetic Diversity and Phylogeny

DNA sequence variants may result in amino acid substitutions within the protein encoding the locus. Such protein variations may result in functional biochemical or morphological dissimilarities that cause differences in the reproductive rate, the survival or the behaviour of individuals. These genetic variations are spread through the population by recombination events due to sexual reproduction [21]. Genetic diversity has been measured for many different traits including continuously varying (quantitative) characters, as well as for deleterious alleles and for proteins, nuclear DNA loci, mitochondrial DNA (mtDNA) and chromosomes. Genetic diversity is typically described using parameters that reflect the amount of polymorphism, the average heterozygosity, the allelic diversity and the genetic distance (Table 4).

The data on genetic diversity has been used to reconstruct phylogenetics on the order of genome rearrangement, the so-called breakpoint phylogeny [23]. Phylogeny is the study of genetic relationships among various groups of organisms (e.g. species, population) that descend from a common ancestor. This approach can be used to compare any two existing organisms, no matter how greatly they may differ in their morphological traits [24].

The classification of the methods used to construct phylogenetic trees from molecular data can be of two types depending on the type of data used. Firstly, classification occurs according to whether the method uses discrete character states or a distance matrix of pairwise dissimilarities. Secondly, classification depends on whether the method clusters include stepwise operational taxonomic units (OTUs), resulting in only one best tree, or all theoretically possible trees are considered. Table 5 lists the state of the phylogenetic tree construction and tree analysis methods, and their classification according to the above-mentioned strategies used. Computer programmes such as PHYLIP [25], MEGA [26] and PAUP [27] can be used to construct phylogenetic trees.

Table 4. Terminology used to describe genetic diversity

Terminology	Description
Genome	The complete genetic material of a species or individual (all of the DNA, all of the chromosomes)
Locus	A segment of DNA or an individual gene
Alleles	Different forms of the same locus that differ in the DNA sequence, e.g. alleles A, a, B and b
Genotypes	The combination of parental alleles present at a locus in an individual, e.g. A/A, A/a or a/a
Haplotypes	Parental alleles at several loci on the same chromosome, e.g. A-b-c
Homozygous	An individual with two copies of the same allele at a locus, e.g. A/A or a/a
Heterozygous	An individual with two different alleles at a locus, e.g. A/a
Allele frequency	The frequency of an allele in a population
Monomorphic	Lacking genetic diversity; a locus in a population is monomorphic if it has only one allele present in the population.
Polymorphic	Having genetic diversity; a locus in a population is polymorphic if it has more than one allele present in the population.
Proportion of polymorphism (*P*)	Number of polymorphic loci / total number of loci sampled
Average heterozygosity (*H*)	Sum of proportions of heterozygotes at all loci / total number of loci sampled. Typically, expected heterozygosity (H_e) is less sensitive than observed heterozygosity (H_o). In random mating population, H_e and H_o are similar
Allelic diversity (*A*)	Average number of alleles per locus
Co-dominance	Situation where all genotypes can be distinguished from the phenotype, i.e. A/A, A/a, a/a can be phenotypically distinguished.
Genetic distance	A measure of the genetic difference between allele frequencies in population; it is based on many loci and can be used to reconstruct phylogenetic trees, e.g. Nei's genetic distance.

Source: Modified from Frankham et al.. [21]

Table 5. Phylogenetic analysis methods and their strategies

	Exhaustive search	Stepwise clustering	Software
Character state	Maximum parsimony (MP)		PAUP, MEGA, PHYLIP
	Maximum likelihood (ML)		PAUP, PHYLIP
Distance matrix	Fitch-Margoliash	UPGMA[a]	PHYLIP
		Neighbour-joining	PAUP, MEGA, PHYLIP

Source: Modified from Salemi and Vandamme [24]
[a] Unweighted pair group method with arithmetic mean

Molecular Markers of Genetic Characterisation in Livestock

The application of molecular markers to the study of genetic diversity has evolved very rapidly since the mid-1960s. The dominating protein electrophoresis approaches within the field of population genetics and evolutionary biology were replaced by DNA analyses in the late 1970s, primarily through the use of restriction enzymes. In the 1980s DNA fragment approaches and mitochondrial DNA sequence analyses became more popular. More recently, the introduction of PCR-mediated DNA genotyping or sequencing has provided the first rapid and easy access to the ultimate genetic data [20].

At present, several molecular markers have been widely used for genetic diversity and phylogenetic analyses in livestock. These are microsatellite analysis, restriction fragment length polymorphism (RFLP), random amplified polymorphic DNA (RAPD), amplified fragment length polymorphism (AFLP), single nucleotide polymorphism (SNP), direct sequencing, mitochondrial DNA (mtDNA) analysis and Y-chromosome specific markers [28, 29]. In the following section, mtDNA, microsatellite and SNP analyses focusing on pigs and cattle are discussed.

Mitochondrial DNA (mtDNA) markers

MtDNA is maternally inherited without recombination. The number of nucleotide differences between mitochondrial genomes therefore directly reflects the genetic distance that separates them. Moreover, mtDNA mutates 5-10 times more frequently than nuclear DNA, thus allowing the study of the divergence between wild and domestic populations under the short time scale of domestication [28].

In pigs the initial mtDNA studies showed that European and Chinese pigs were domesticated independently from European and Asian subspecies of wild boar [30, 31]. Later studies, however, suggested at least seven domestication events across Eurasia and East Asia [32-34]. These studies also suggested the occurrence of introgression of Asian domestic pigs into some European breeds during the 18th and 19th centuries.

Larson et al. [33] demonstrated that multiple domestication occurred at different locations on the islands of South-east Asia and Oceania. Domestic pigs of Near-Eastern ancestry were introduced to Europe during the Neolithic period. The European wild boar was also domesticated at this time. Once domesticated, European pigs rapidly replaced the introduced domestic pigs of the Near-Eastern origin throughout Europe. A recent study hypothesised five new cryptic domestication events from three geographical locations, namely India (MC1), South-east Asian peninsular (MC2, MC3, MC4) and the coast of Taiwan (MC5) [35]. Charoensook et al. [36]

further resolved porcine phylogeny in South-east Asia by analysing Thai mtDNA haplotypes (Thai native pigs and Thai wild boars). They supported a putative independent domestication event as they incorporated eight of their haplotypes into clade MC3, which represents exclusive samples that are indigenous to the Indo-Burma biodiversity hotspot, a region that includes Thailand to the Kra Isthmus.

In cattle one of the first contributions of DNA research to reconstruct the domestication was a comparison of the mtDNA of taurine and indicine cattle [37]. The divergence of their control regions implied separate domestication events, which most likely started around 8,000 years BC in South-western Asia and the Indus Valley respectively [38]. Zebus were probably imported into Africa after the Arabian invasions in the 7th century [39]. Interestingly, the discovery that African zebus carry taurine mtDNA implies that African zebus were the result of crossing zebu bulls with taurine cows [39].

Furthermore, mtDNA polymorphisms have revealed several other aspects of the early differentiation of taurine cattle. The predominance of one taurine mtDNA haplogroup (T1) in Africa [40] and a new haplogroup in Eastern Asia (T4) suggest two other regions of domestication [41, 42]. However, complete mtDNA sequences show that T1 and T4 are closely related to the major T3 haplogroup, so their predominance probably reflects founder effects in Africa and Eastern Asia respectively [43]. The T3 mtDNA haplogroup is predominant in most European and Northern Asian breeds [42] and is one of the four major haplogroups (T, T1, T2 and T3) in South-western Asia. By contrast, in the African taurine cattle haplogroup T1 is dominant, which is rare in South-western Asia. These observations are in line with the South-west Asian origin of European cattle, confirming the paleontological evidence of a gradual introduction of domestic cattle in Europe from South-western Asia [29, 38].

Microsatellite markers

There are several types of nuclear DNA markers. Microsatellites have been the markers of choice to study genetic variation in recent years. Based upon the sites on which the same short sequence is repeated multiple times, they present a high mutation rate and have a co-dominant nature. This makes them appropriate for the study of both within-breed and between-breed genetic diversity. According to the FAO and the International Society of Animal Genetics, microsatellite panels have been established for the genetic characterisation of pigs and cattle [44]. The porcine panel consists of 27 and the bovine of 30 polymorphic markers.

In a collaborative EU project (PigBioDiv1) [45] 58 European pig populations including local breeds, national varieties of international breeds, privately owned commercial populations and the Chinese Meishan breed as an out-group were genotyped for 50 microsatellite markers. The microsatellite data show that the individual breed contribution to between-breed diversity ranges from 0.04% to 3.94% of the total European between-breed diversity. The local breeds account for 56%, followed by commercial lines and international breeds [45]. The ongoing project PigBioDiv2 covers 50 Chinese breeds and investigates mtDNA and Y-chromosomal regions in addition to the microsatellite data of the European breeds [29]. Trait gene loci and markers are also to be analysed to seek insight into the functional differences between breeds. The first results of the microsatellite-based analysis using pooled DNA samples indicate that Chinese breeds, both within and between breeds, reveal a higher degree of genetic variability than the European breeds, [29, 46].

Bovine microsatellite data [47-49] and AFLP fingerprinting results [50] are in line with the endemic expansion of agriculture and the raising of cattle from South-eastern to North-western

Europe [29]. Cymbron et al. [48] observed that the correlations between genetic and geographical distances are different for the Mediterranean and Northern cattle breeds, suggesting that this reflects the separate Neolithic migrations along the Mediterranean coasts and the Danube respectively. A larger set of microsatellite data [51, 52] indeed indicates a separate position of the Mediterranean cattle, but divides the trans-alpine cattle into two different clusters of breeds: the Central-European (alpine, southern-French) one and Northern European one. Genotypes from 30 microsatellites for 69 European breeds were used to test the formal criteria of conservation [51]. The popular Weitzman method based on genetic distances favours highly inbred populations even if these have been derived recently from other populations. The ranking of conservation priorities on the basis of marker-estimated kinships is less influenced by inbreeding and favours the Mediterranean breeds. These breeds indeed display a relatively high degree of molecular diversity which, next to phenotypic uniqueness, is an obvious argument for conservation [29].

Single nucleotide polymorphism (SNP) markers

SNPs are point mutations in the genome sequence, predominantly bi-allelic and highly abundant throughout the genome. They are widely used in animal genetics and breeding because they have the potential to detect both neutral and functional genetic variations, and although most of them are located in non-coding regions, some correspond to mutation-inducing changes in the expressed genes [28, 53, 54].

Fang et al. [54] investigated genetic variations in the melanocortin receptor-1 (MC1R) gene among 15 wild and 68 domestic pigs from both Europe and Asia to address the genetic determination of coat colour, which is so much more variable in domestic animals than in their wild ancestors. They found that all mutations are silent in wild animals, suggesting a purifying selection. However, nine of ten mutations found in the domestic pigs result in altered protein sequences, suggesting that early farmers intentionally selected for novel coat colour.

Amaral et al. [53] evaluated linkage disequilibrium (LD) and haplotype block structures in 15 to 25 individuals from each of 10 European and 10 Chinese pig breeds genotyped for 1,536 SNPs in three genomic regions. The LD extends up to 2 cM in Europe and up to 0.05 cM in China. The authors suggested two possible explanations: either the European ancestral stock has a higher level of LD or modern breeding programmes have increased the extent of LD in Europe.

The haplotypic diversity using SNPs was also the focus of another study investigating the polymorphism of porcine IGF2 gene [55]. The results show that selection can be observed and analysed in the making by comparing different breeds that represent distinct stages of the selective process. Furthermore, there is no evidence that, overall, domestication reduces genetic variability in the *IGF2* region with respect to current wild ancestors of the pig (although a complete selective sweep is found in some very lean breeds such as Pietrain) [29].

The SNP data [56, 57] would reveal more about the history of European cattle. SNPs emphasise the zebu-taurine divergence and hence also the difference between Podolian and other European cattle [50]. Large-scale SNP analysis shows that in several breeds LD extends further than in humans but is hardly detectable at distances of over 200 kb [57, 58]. These data also suggest a rapid recent decrease of the effective population size of domestic cattle [42, 59].

Large numbers of SNPs, however, are required for precision; as a rule of thumb about six SNPs are equivalent to one microsatellite [28]. In addition, another critical aspect is their discovery, usually through sequencing techniques. Nevertheless, it seems that they are becoming the markers of choice because of increasing automation coupled with low costs. Several large-scale projects are currently carried out to identify SNPs in livestock. According to the National Centre of Biotechnology Information (NCBI) [60], 4,931,454 bovine and 557,135 porcine SNPs have been recorded so far (as of April 8th, 2012). In the near future, new technologies such as high throughput SNP typing or even whole-genome sequencing are likely to revolutionise our knowledge about the diversity and uniqueness of breeds with the ultimate objective of gaining a complete understanding of the molecular basis of functional diversity [29].

MANAGEMENT STRATEGIES FOR PRESERVING ANIMAL GENETIC RESOURCES IN THAILAND

The FAO defines genetic resources as those populations that show the highest genetic differences within a species and/or show unique alleles and allelic combinations [61]. The term animal genetic resources (AnGR) is used to include all animal species, breeds and strains that are of economic, scientific and cultural interest to humankind in terms of food and agricultural production for the present or the future. Another equivalent term increasingly used is livestock genetic resources. Since the past 10-12 thousand years, there have been more than 40 species of animals that are domesticated (or semi-domesticated) that contribute directly (through animal products used for food and fibre) and indirectly (through functions and products such as draft power, manure, transport and store of wealth). Common species include cattle, sheep, goats, pigs, chickens, horses and buffaloes, but many other domesticated animals such as camels, donkeys, elephants, reindeer and rabbits are important to different cultures and regions of the world [20, 22, 61]. The conservation and utilisation of indigenous AnGR has recently become concepts of greater importance. Conservation of animal genetics is now vital for sustainable management of these resources. This can be accomplished by the preservation of endangered and valuable breeds, selection programmes which will restore genetic diversity in industrial breeds, or the cryo-conservation of gametes, embryos and somatic cells of the existing gene pool [62]. The utilisation of indigenous AnGR will be a benefit to breeding programmes of high-production livestock under tropical climates.

Thailand has agreed upon the Agenda 21 of the United Nations Conferences on Environment and Development in 1992 to conserve the biological diversity and global environment. The National Environment Board of Thailand established the action plan for sustainable conservation of biological diversity in 1998. Strategies were outlined to strengthen the capacity for sustainable use of the environment and natural resources and to define and implement standard criteria for the conservation of biological resources that are applicable to the country [2]. The Department of Livestock Development under the Ministry of Agriculture and Cooperatives is responsible for livestock health and production. The activities regarding the conservation of AnGR are described in the national plans for biological diversity. The strategies are as follows: (i) to enhance capacity building, (ii) to increase the ability to conserve effectively, (iii) to create public awareness of conservation of AnGR, (iv) to conserve the diversity of breed, population and genetic resources, (v) to minimise harmful activities against biodiversity, (vi) to encourage the conservation and use of national resources including both the environment and the culture, and (vii) to encourage the cooperation between all agents both nationally and internationally. All activities focus on the indigenous AnGR [2, 63] and adequate approach is important for a management strategy of indigenous AnGR (Figure 3).

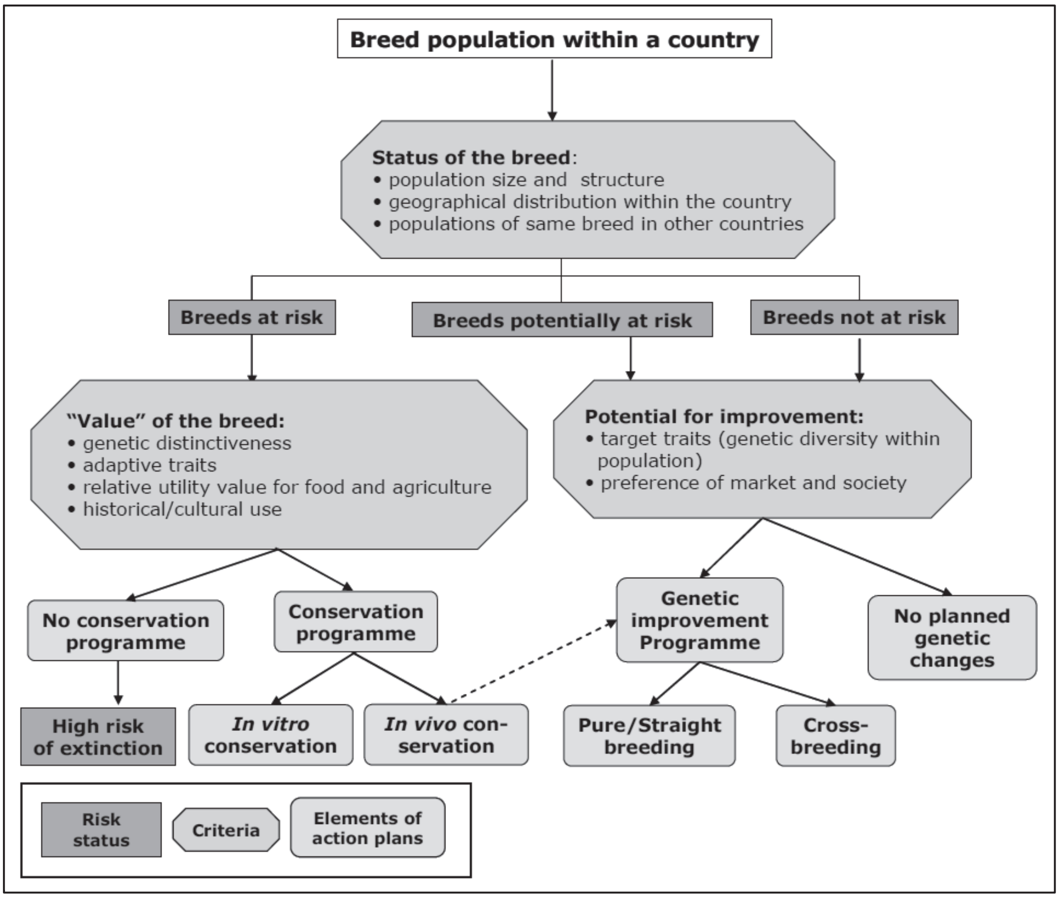

Figure 3. Design of animal genetic resources management strategies [60]

At present, however, the knowledge of indigenous species is still limited and scattered among agencies. A further collaboration among the agencies within the country is required. The livestock sector is a system which combines all the components of biological diversity, economy, social aspect and culture. The research purposes are to develop sustainable livestock in order to produce quality food, as well as to protect the safety of humans and the environment. Thus, research should emphasise the management of AnGR as an integral part of agricultural biodiversity [63, 64]. Breed improvement programmes have been initiated for some livestock species, viz. dairy cattle, beef cattle, buffalo and swine in some limited herds, although a national breeding programme is not available due to the lack of a recording system. In vitro conservation, considered as a sustainable process, has been performed through the cryopreservation of eggs, semen and embryos, and collection of seeds, tissues and cells, which can have a large impact on community participation [22, 61, 65].

CONCLUSIONS AND RECOMMENDATIONS

Livestock production in Thailand has dramatically changed from the ownership of backyard animals to an industrialised husbandry approach. Most of the animals used for food production are imported exotic breeds or their cross-breeds with indigenous animals. Although the indigenous animals have a large genetic diversity, there have been very few efforts to characterise their genetic background. Thus, sufficient information to confirm their original identity is still missing. Breed characterisation based on local names and phenotypic descriptions that have been used for a long time cannot clarify the admixture or gene introgression in populations. Well-characterised populations and appropriate breeding programmes must therefore be established to describe the uniqueness of the resources.

The need to conserve and utilise existing genetic diversity is a process in which all stakeholders should participate for future benefits to mankind. Studies on the development of economic traits, genetics and preservation of indigenous breeds are crucial to the defining and registering of genetic resources. Well-planned breeding programmes and measures for effective communication, especially between the decision-makers, are urgently needed. Sustaining conservation of indigenous livestock genetic resources as a vital component within the agricultural biodiversity domain will be a great challenge as well as a benefit for the development of livestock production in Thailand.

REFERENCES

1. P. Riethmuller and N. Chalermpao, "The Livestock Industries of Thailand", FAO Regional Office for Asia and the Pacific, Bangkok, **2002**.
2. Department of Livestock Development, Ministry of Agriculture and Cooperatives, Bangkok, http://www.dld.go.th/th/ (Accessed: 7 October 2010).
3. National Statistical Office, "Population Projections for Thailand 2000-2030", **2010,** http://web.nso.go.th/index.html (Accessed: 7 October 2010).
4. National Statistical Office, "The 2003 Agriculture Census", **2010**, http://web.nso.go.th/en/census/agricult/cen_agri03-1.html (Accessed: 7 October 2010).
5. Office of Agricultural Economics, "Agricultural Statistics", **2010,** http://www.oae.go.th/main.php?filename=index (Accessed: 7 October 2010).
6. A. Na-Chiangmai, "Current situation and development trends of beef production in Thailand", Proceedings of Australian Centre for International Agriculture Research (ACIAR), **2002,** Canberra, Australia, pp.93-97**.**
7. S. Rattanaronchart, "Present situation of Thai native pigs", *Project Report*, **1994**, Department of Animal Science, Chiang Mai University, Thailand.
8. S. Nakai, "Decision-making on the use of diverse combinations of agricultural products and natural plants in pig feed: A case study of native pig smallholder in northern Thailand", *Trop. Anim. Health Prod.*, **2008,** *40*, 201-208.
9. S. Nakai, "Reproductive performance analysis of native pig smallholders in the hillside of northern Thailand", *Trop. Anim. Health Prod.*, **2008,** *40*, 561-566.
10. R. Charoensook, B. Brenig, K. Gatphayak, S. Taesoongnern and C. Knorr, "Genetic identity of native pig breeds in northern Thailand evidenced by microsatellite markers", Proceedings of International Conference on Research for Development in Agriculture and Forestry, Food and Natural Resource Management, **2009,** Hamburg, Germany, p.281.
11. R. Charoensook, B. Brenig, K. Gatphayak and C. Knorr, "Genetic comparison of Thai, Chinese and European pig breeds using microsatellite polymorphism", Proceedings of the German Society for Animal Production (DGFZ), **2009,** Giessen, Germany. pp.98-99.

12. Domestic Animal Diversity Information System (DAD-IS) of FAO, http://dad.fao.org/ (Accessed: 7 October 2010).
13. The Government Public Relations Department, Bangkok, http://thailand.prd.go.th (Accessed: 7 October 2010).
14. T. Kawashima, "Role of native ruminants in establishment of sustainable agricultural systems in northeast Thailand", *JIRCAS Working Rep.*, **2002,** *30*, 65-67.
15. W. Intaratham, "The Thai indigenous cattle breeding improvement project", Proceedings of International Workshop on Development Strategies for Genetic Evaluation for Beef Production in Developing Countries, **2002**, Khon Kaen, Thailand, pp.124-127.
16. K. Akkahart, "Line clustering and estimation of genetic parameters for growth traits and body measurement in Thai native cattle", *Master Thesis*, **2003,** Khon Kaen University, Thailand.
17. C. Chaikong, "Comparisons of beef buffalo and beef cattle production systems in northeastern Thailand", *PhD Thesis*, **2010,** Georg-August-University of Göttingen, Germany.
18. S. Rattanaronchart, "White Lamphun cattle conservation and development project: A brief of 15 years experience", *Project Report,* **1998,** Department of Animal Science, Chiang Mai University, Thailand.
19. C. Chantalakana and P. Skunmun, "Sustainable Smallholder Animal System in the Tropics", 1st Edn., Kasetsart University Press, Bangkok, **2002**, p.302.
20. J. E. O. Rege and A. M. Okeyo, "Improving Our Knowledge of Tropical Indigenous Animal Genetic Resources", International Livestock Research Institute, Nairobi, **2006**.
21. R. Frankham, D. A. Briscoe and J. D. Ballou, "Introduction to Conservation Genetics", Cambridge University Press, Cambridge, **2002**, p.6.
22. FAO Corporate Document Repository, "The State of the World's Animal Genetic Resources for Food and Agriculture", Commission on Genetic Resources for Food and Agriculture, FAO, Rome, **2007,** p.511.
23. M. Blanchette, G. Bourque and D. Sankoff, "Breakpoint phylogenies", *Genome Inform. Ser. Workshop Genome Inform.*, **1997,** *8*, 25-34.
24. M. Salemi and A. M. Vandamme, "The Phylogenetic Handbook: A Practical Approach to DNA and Protein Phylogeny", 1st Edn., Cambridge University Press, Cambridge, **2003**.
25. J. Felsenstein, "PHYLIP: Phylogeny inference package version 3.6a", **1995**, Department of genetics, University of Washington, Seattle.
26. K. Tamura, J. Dudley, M. Nei and S. Kumar, "MEGA4: Molecular evolutionary genetics analysis (MEGA) software version 4.0", *Mol. Biol. Evol.*, **2007,** *24*, 1596-1599.
27. D. L. Swofford, "PAUP: Phylogenetic analysis using Parsimony (and other methods) 4.0", **2002**, Sinauer Associates, Sunderland (MA).
28. M. A. Toro, J. Fernandez and A. Caballero, "Molecular characterization of breeds and its use in conservation", *Livestock Sci.*, **2009**, *120*, 174-195.
29. L. F. Groeneveld, J. A. Lenstra, H. Eding, M. A. Toro, B. Scherf, D. Pilling, R. Negrini, E. K. Finlay, H. Jianlin, E. Groeneveld and S. Weigend, "Genetic diversity in farm animals - A review", *Anim. Genet.*, **2010**, *41(Suppl 1)*, 6-31.

30. E. Giuffra, J. M. Kijas, V. Amarger, O. Carlborg, J. T. Jeon and L. Andersson, "The origin of the domestic pig: Independent domestication and subsequent introgression", *Genetics*, **2000,** *154*, 1785-1791.
31. G. Larson, U. Albarella, K. Dobney, P. Rowley-Conwy, J. Schibler, A. Tresset, J. D. Vigne, C. J. Edwards, A. Schlumbaum, A. Dinu, A. Balacsescu, G. Dolman, A. Tagliacozzo, N. Manaseryan, P. Miracle, L. Van Wijngaarden-Bakker, M. Masseti, D. G. Bradley and A. Cooper, "Ancient DNA, pig domestication, and the spread of the Neolithic into Europe", *Proc. Natl. Acad. Sci. USA*, **2007,** *104*, 15276-15281.
32. G. Larson, K. Dobney, U. Albarella, M. Fang, E. Matisoo-Smith, J. Robins, S. Lowden, H. Finlayson, T. Brand, E. Willerslev, P. Rowley-Conwy, L. Andersson and A. Cooper, "Worldwide phylogeography of wild boar reveals multiple centers of pig domestication", *Science*, **2005,** *307*, 1618-1621.
33. G. Larson, T. Cucchi, M. Fujita, E. Matisoo-Smith, J. Robins, A. Anderson, B. Rolett, M. Spriggs, G. Dolman, T. H. Kim, N. T. Thuy, E. Randi, M. Doherty, R. A. Due, R. Bollt, T. Djubiantono, B. Griffin, M. Intoh, E. Keane, P. Kirch, K. T. Li, M. Morwood, L. M. Pedrina, P. J. Piper, R. J. Rabett, P. Shooter, G. Van den Bergh, E. West, S. Wickler, J. Yuan, A. Cooper and K. Dobney, "Phylogeny and ancient DNA of Sus provides insights into neolithic expansion in Island Southeast Asia and Oceania", *Proc. Natl. Acad. Sci. USA*, **2007,** *104*, 4834-4839.
34. C. Y. Wu, Y. N. Jiang, H. P. Chu, S. H. Li, Y. Wang, Y. H. Li, Y. Chang and Y. T. Ju, "The type I Lanyu pig has a maternal genetic lineage distinct from Asian and European pigs", *Anim. Genet.*, **2007,** *38*, 499-505.
35. G. Larson, R. Liu, X. Zhao, J. Yuan, D. Fuller, L. Barton, K. Dobney, Q. Fan, Z. Gu, X. H. Liu, Y. Luo, P. Lv, L. Andersson and N. Li, "Patterns of East Asian pig domestication, migration, and turnover revealed by modern and ancient DNA", *Proc. Natl. Acad. Sci. USA*, **2010,** *107*, 7686-7691.
36. R. Charoensook, B. Brenig, K. Gatphayak and C. Knorr, "Further resolution of porcine phylogeny in Southeast Asia by Thai mtDNA haplotypes", *Anim. Genet.*, **2011**, *42*, 445-450.
37. D. G. Bradley, D. E. MacHugh, P. Cunningham and R. T. Loftus, "Mitochondrial diversity and the origins of African and European cattle", *Proc. Natl. Acad. Sci. USA*, **1996,** *93*, 5131-5135.
38. M. A. Zeder, E. Emshwiller, B. D. Smith and D. G. Bradley, "Documenting domestication: The intersection of genetics and archaeology", *Trends Genet.*, **2006,** *22*, 139-155.
39. D. G. Bradley, R. T. Loftus, P. Cunningham and D. E. MacHugh, "Genetics and domestic cattle origins", *Evol. Anthropol.*, **1998**, *6*, 79-86.
40. C. S. Troy, D. E. MacHugh, J. F. Bailey, D. A. Magee, R. T. Loftus, P. Cunningham, A. T. Chamberlain, B. C. Sykes and D. G. Bradley, "Genetic evidence for Near-Eastern origins of European cattle", *Nature*, **2001,** *410*, 1088-1091.
41. H. Mannen, M. Kohno, Y. Nagata, S. Tsuji, D. G. Bradley, J. S. Yeo, D. Nyamsamba, Y. Zagdsuren, M. Yokohama, K. Nomura and T. Amano, "Independent mitochondrial origin and historical genetic differentiation in North Eastern Asian cattle", *Mol. Phylogen. Evol.*, **2004,** *32*, 539-544.

42. J. Kantanen, C. J. Edwards, D. G. Bradley, H. Viinalass, S. Thessler, Z. Ivanova, T. Kiselyova, M. Cinkulov, R. Popov, S. Stojanovic, I. Ammosov and J. Vilkki, "Maternal and paternal genealogy of Eurasian taurine cattle (*Bostaurus*)", *Heredity*, **2009,** *103*, 404-415.
43. A. Achilli, S. Bonfiglio, A. Olivieri, A. Malusa, M. Pala, B. H. Kashani, U. A. Perego, P. Ajmone-Marsan, L. Liotta, O. Semino, H. J. Bandelt, L. Ferretti and A. Torroni, "The multifaceted origin of taurine cattle reflected by the mitochondrial genome", *PLoS. One*, **2009,** *4*, e5753.
44. FAO, "Secondary guidelines for development of national farm animal genetic resources management plans, measurement of domestic animal diversity (MoDAD)", **2004,** http://dad.fao.org/cgi-bin/getblob.cgi?sid=ca53b91a6f7c80be8e7066f4a5066dc1,50006220 (Accessed: 7 October 2010).
45. L. Ollivier, L. Alderson, G. C. Gandini, J. L. Foulley, C. S. Haley, R. Joosten, A. P. Rattink, B. Harlizius, M. A. M. Groenen, Y. Amigues, M. Y. Boscher, G. Russell, A. Law, R. Davoli, V. Russo, D. Matassino, C. Desautes, E. Fimland, M. Bagga, J. V. Delgado, J. L. Vega-Pla, A. M. Martinez, A. M. Ramos, P. Glodek, J. N. Meyer, G. S. Plastow, K. W. Siggens, A. L. Archibald, D. Milan, M. San Cristobal, G. Laval, K. Hammond, R. Cardellino and C. Chevalet, "An assessment of European pig diversity using molecular markers: Partitioning of diversity among breeds", *Conserv. Genet.*, **2005,** *6*, 729-741.
46. H. J. Megens, R. Crooijmans, M. S. Cristobal, X. Hui, N. Li and M. A. M. Groenen, "Biodiversity of pig breeds from China and Europe estimated from pooled DNA samples: Differences in microsatellite variation between two areas of domestication", *Genet. Sel. Evol.*, **2008,** *40*, 103-128.
47. I. Medugorac, A. Medugorac, I. Russ, C. E. Veit-Kensch, P. Taberlet, B. Luntz, H. M. Mix and M. Forster, "Genetic diversity of European cattle breeds highlights the conservation value of traditional unselected breeds with high effective population size", *Mol. Ecol.*, **2009,** *18*, 3394-3410.
48. T. Cymbron, A. R. Freeman, M. I. Malheiro, J. D. Vigne and D. G. Bradley, "Microsatellite diversity suggests different histories for Mediterranean and Northern European cattle populations", *Proc. Royal Soc. B Biol. Sci.*, **2005,** *272*, 1837-1843.
49. M. H. Li, I. Tapio, J. Vilkki, Z. Ivanova, T. Kiselyova, N. Marzanov, M. Cinkulov, S. Stojanovic, I. Ammosov, R. Popov and J. Kantanen, "The genetic structure of cattle populations (*Bostaurus*) in northern Eurasia and the neighbouring Near Eastern regions: Implications for breeding strategies and conservation", *Mol. Ecol.*, **2007,** *16*, 3839-3853.
50. R. Negrini, I. J. Nijman, E. Milanesi, K. Moazami-Goudarzi, J. L. Williams, G. Erhardt, S. Dunner, C. Rodellar, A. Valentini, D. G. Bradley, I. Olsaker, J. Kantanen, P. Ajmone-Marsan and J. A. Lenstra, "Differentiation of European cattle by AFLP fingerprinting", *Anim. Genet.*, **2007,** *38*, 60-66.
51. European Cattle Genetic Diversity Consortium, "Marker-assisted conservation of European cattle breeds: An evaluation", *Anim. Genet.*, **2006,** *37*, 475-481.

52. J. A. Lenstra, "Metaanalysis of microsatellites data allows a molecular classification of European cattle", Proceedings of 31st International Congress on Animal Genetics, **2008,** Amsterdam, Netherlands, Poster no.5041.
53. A. J. Amaral, H. J. Megens, R. P. M. A. Crooijmans, H. C. M. Heuven and M. A. M. Groenen, "Linkage disequilibrium decay and haplotype block structure in the pig", *Genetics*, **2008,** *179*, 569-579.
54. M. Fang, G. Larson, H. S. Ribeiro, N. Li and L. Andersson, "Contrasting mode of evolution at a coat color locus in wild and domestic pigs", *PLoS Genet.*, **2009,** *5*, e1000341.
55. A. Ojeda, L. S. Huang, J. Ren, A. Angiolillo, I. C. Cho, H. Soto, C. Lemus-Flores, S. M. Makuza, J. M. Folch and M. Perez-Enciso, "Selection in the making: A worldwide survey of haplotypic diversity around a causative mutation in porcine *IGF2*", *Genetics*, **2008**, *178*, 1639-1652.
56. S. D. McKay, R. D. Schnabel, B. M. Murdoch, L. K. Matukumalli, J. Aerts, W. Coppieters, D. Crews, E. D. Neto, C. A. Gill, C. Gao, H. Mannen, Z. Q. Wang, C. P. Van Tassell, J. L. Williams, J. F. Taylor and S. S. Moore, "An assessment of population structure in eight breeds of cattle using a whole genome SNP panel", *BMC Genetics*, **2008,** *9*, 37.
57. R. A. Gibbs, J. F. Taylor, C. P. Van Tassell, W. Barendse, K. A. Eversoie, C. A. Gill, R. D. Green, D. L. Hamernik, S. M. Kappes, S. Lien, L. K. Matukumalli, J. C. McEwan, L. V. Nazareth, R. D. Schnabel, G. M. Weinstock, D. A. Wheeler, P. Ajmone-Marsan, P. J. Boettcher, A. R. Caetano, J. F. Garcia, O. Hanotte, P. Mariani, L. C. Skow, T. S. Sonstegard, J. L. Williams, B. Diallo, L. Hailemariam, M. L. Martinez, C. A. Morris, L. O. Silva, R. J. Spelman, W. Mulatu, K. Zhao, C. A. Abbey, M. Agaba, F. R. Araujo, R. J. Bunch, J. Burton, C. Gorni, H. Olivier, B. E. Harrison, B. Luff, M. A. Machado, J. Mwakaya, G. Plastow, W. Sim, T. Smith, M. B. Thomas, A. Valentini, P. Williams, J. Womack, J. A. Wooliams, Y. Liu, X. Qin, K. C. Worley, C. Gao, H. Jiang, S. S. Moore, Y. Ren, X. Z. Song, C. D. Bustamante, R. D. Hernandez, D. M. Muzny, S. Patil, A. San Lucas, Q. Fu, M. P. Kent, R. Vega, A. Matukumalli, S. McWilliam, G. Sclep, K. Bryc, J. Choi, H. Gao, J. J. Grefenstette, B. Murdoch, A. Stella, R. Villa-Angulo, M. Wright, J. Aerts, O. Jann, R. Negrini, M. E. Goddard, B. J. Hayes, D. G. Bradley, M. B. da Silva, L. P. Lau, G. E. Liu, D. J. Lynn, F. Panzitta and K. G. Dodds, "Genome-wide survey of SNP variation uncovers the genetic structure of cattle breeds", *Science*, **2009,** *324*, 528-532.
58. M. Gautier, T. Faraut, K. Moazami-Goudarzi, V. Navratil, M. Fogfio, C. Grohs, A. Boland, J. G. Garnier, D. Boichard, G. M. Lathrop, I. G. Gut and A. Eggen, "Genetic and haplotypic structure in 14 European and African cattle breeds", *Genetics*, **2007,** *177*, 1059-1070.
59. C. Ginja, L. T. da Gama and M. C. Penedo, "Y Chromosome haplotype analysis in Portuguese cattle breeds using SNPs and STRs", *J. Hered.*, **2009,** *100*, 148-157.
60. National Center of Biotechnology Information (NCBI), http://www.ncbi.nlm.nih.gov/ (Accessed: 8 April 2012).
61. FAO, "A Strategic Approach for Conservation and Continued Use of Animal Genetic Resource", Commission on Genetic Resources for Food and Agriculture,Rome, FAO, Rome, **2006**.

62. P. Ajmone-Marsan, "A global view of livestock biodiversity and conservation-GLOBALDIV", *Anim. Genet.*, **2010,** *41(Suppl 1)*, 1-5.
63. V. Khumnirdpetch, "State of Thai animal genetic resources", Proceedings of 7th World Congress on Genetics Applied to Livestock Production, **2002,** Montpellier, France, pp.1-4.
64. V. Khumnirdpetch, "Detection of GMOs in the broilers that utilized genetically modified SBM as a feed ingredient", Proceedings of Plant and Animal Genome Conference IX, **2001,** San Diego, USA, p.207.
65. FAO Corporate Document Repository, "Global Plan of Action for Animal Genetic Resources and the Interlaken Declaration", Commission on Genetic Resuources for Food and Agriculture, FAO, Rome, **2007,** p.38.

Maejo Int. J. Sci. Technol. **2013**, *7*(01), 133-144

Maejo International Journal of Science and Technology

ISSN 1905-7873
Available online at www.mijst.mju.ac.th

Full Paper

Symmetries and exact solutions of Einstein field equations for perfect fluid distribution and pure radiation fields

Lakhveer Kaur * and Rajesh Kumar Gupta

School of Mathematics and Computer Applications, Thapar University, Patiala-147004, Punjab, India

* Corresponding author, e-mail: lakhveer712@gmail.com

Received: 29 September 2011 / Accepted: 20 March 2013 / Published: 1 April 2013

Abstract: Lie group formalism is applied to Einstein field equations for perfect fluid distribution and pure radiation fields in the investigation of symmetries and exact solutions. The similarity reductions are obtained by determining the complete sets of point symmetries of these equations. The reduced ordinary differential equations are further studied and some non-trivial exact solutions are successfully furnished.

Keywords: Lie classical method, Einstein field equations, perfect fluid distribution, pure radiation fields

---

INTRODUCTION

It is well known that complex physical phenomena are related to non-linear partial differential equations, which are involved in many fields of science, especially in optical fibres, chemical kinematics, chemical physics and general relativity. Further, the investigation of exact solutions of non-linear partial differential equations has an important role in the study of non-linear physical phenomena. The literature abounds with many different techniques that have been invoked in an effort to obtain new exact solutions for different configurations of matter.

Lie group analysis method [1-3], also called the symmetry method, is one of the most effective methods for determining solutions of non-linear partial differential equations. Since the second half of the 19th century and about 200 years after Leibniz and Newton introduced the concept of the derivative, solving ordinary differential equations (ODEs) has been one of the most important problems in applied mathematics. Sophus Lie (1842-1899) became interested in this problem and with inspiration from Galois's theory [1] for solving algebraic equations discovered what is known today as Lie group analysis. Lie showed that the majority of known methods of integration of ordinary differential equations, which until then had seemed artificial, could be derived in a unified manner using his theory of continuous transformation groups [3]. Recently there have been considerable developments in finding exact solutions of non-linear differential equations, as evident by a number of research work [4-6]. For many years after Einstein proposed his general theory of relativity, only a few exact solutions were known. Today the situation is completely different and we now have a vast number of solutions of Einstein field equations for various fields [7]. However, very few are well understood in the sense that they can be clearly interpreted as the fields of real physical sources. The obvious exceptions are the Schwarzschild [8] and Kerr solutions [9], which have been very thoroughly analysed and which clearly describe the gravitational fields surrounding static and rotating black holes respectively.

Thus, the study of exact solutions to Einstein field equations for various fields is an important part of the theory of general relativity. Einstein field equations, which play a central role in Einstein theory of general relativity, have symmetry consideration as one of the most important mathematical properties apart from applications and implications in astrophysics. The heart of the classification schemes for the solutions of these equations is the symmetry methods based on the Lie group. Einstein field equations were studied by various authors [6, 10, 11, 12] to establish exact solutions by using Lie group analysis.

In this paper, we study the exact solutions of Einstein field equations for perfect fluid distribution and pure radiation fields. Lie symmetry method is used to generate various symmetries of the equations and then an optimal system comprising basic vector fields is identified, and finally the reduced systems of ODEs and their exact solutions are presented. The exact solutions thus obtained can be utilised for checking the validity of numerical and approximation techniques and programmes of the theory of general relativity.

EINSTEIN FIELD EQUATIONS FOR PERFECT FLUID DISTRIBUTION

The possibility of the existence of gravitational waves propagated with the speed of light was first pointed out by Einstein in the case of weak gravitational field [13]. The usual procedure in Cartesian coordinates is to start with a field:

$$g_{ik} = \eta_{ik} + h_{ik} \qquad i,k = 1,2,3,4, \tag{1}$$

where η_{ik} is the Galilean metric and h_{ik} describes the modifications due to a weak gravitational field. In view of the linearised field equations $R_{ik} = 0$ coupled with a set of coordinates conditions, h_{ik} satisfies the wave equation. In particular, when h_{ik} depends on t and x only, there exists a coordinate system [14] in which one can take all the components h_{ik} to vanish except

$$h_{22} = -h_{33} \neq 0, \quad h_{23} = -h_{32} \neq 0 \tag{2}$$

where the non-vanishing components are arbitrary functions of the argument $(t-x)$. Since general relativity is essentially a non-linear theory, its intrinsic consequences cannot be based on a weak field approximation and there must be certain reservations about the conclusions drawn from the linearised field. Bondi et al. [15] demonstrated the existence of plane gravitational waves described by an exact solution of Einstein field equations for empty space-time. In the present paper, we consider the exact gravitational field equations:

$$R_{ik} = -8\pi\left(T_{ik} - \frac{1}{2}g_{ik}T\right) \tag{3}$$

for a line element:

$$ds^2 = dt^2 - dx^2 - (1-u)dy^2 - (1+u)dz^2 + 2vdydz \tag{4}$$

where u and v are functions of t and x only.

In the case of the line element (4), the non-zero components of the curvature tensor and the Ricci tensor are given as follows:

$$\begin{aligned}
R_{yzyz} &= \frac{u_x{}^2 - u_t{}^2 + v_x{}^2 - v_t{}^2}{4} \\
R_{z\mu z\nu} &= \frac{2Pu_{\mu\nu} - (1-u)u_\mu u_\nu - (1+u)v_\mu v_\nu + v(u_\mu v_\nu + v_\mu u_\nu)}{4P} \\
R_{y\mu y\nu} &= \frac{-(2Pu_{\mu\nu} + (1+u)u_\mu u_\nu + (1-u)v_\mu v_\nu + v(u_\mu v_\nu + v_\mu u_\nu))}{4P} \\
R_{y\mu z\nu} &= \frac{-(2Pu_{\mu\nu} - (1-u)u_\mu u_\nu + (1+u)v_\mu v_\nu - v(u_\mu v_\nu - v_\mu u_\nu))}{4P} \\
R_{yztx} &= \frac{(u_t v_x - v_t u_x)}{2P} \\
R_{\mu\nu} &= \frac{-(2P(uu_{\mu\nu} + vv_{\mu\nu}) + (1+u^2-v^2)u_\mu u_\nu + (1-u^2+v^2)v_\mu v_\nu + 2uv(u_\mu v_\nu + v_\mu u_\nu))}{2P^2} \\
R_{yy} + R_{zz} &= \frac{u_x{}^2 - u_t{}^2 + v_x{}^2 - v_t{}^2}{P} \\
R_{yy} - R_{zz} &= \frac{P(u_{xx} - u_{tt}) - u(v_x{}^2 - v_t{}^2) + v(u_x v_x - v_t u_t)}{P} \\
R_{yz} = R_{zy} &= \frac{P(v_{xx} - v_{tt}) - v(u_x{}^2 - u_t{}^2) + u(u_x v_x - v_t u_t)}{P}
\end{aligned} \tag{5}$$

where μ and ν take the values t and x only, and $u_i \equiv \frac{\partial u}{\partial x^i}$, $u_{ik} \equiv \frac{\partial u}{\partial x^i \partial x^k}$,... etc., and $\left(x^1, x^2, x^3, x^4\right) = (t, y, z, x)$ and $P = (1-u^2-v^2)$.

The Perfect Fluid Distribution

We examine the compatibility of the perfect fluid distribution of matter defined by the field equations:

$$R_{ik} = -8\pi[(p+\rho)v_i v_k - \frac{1}{2}g_{ik}(\rho - p)],\ g^{ik}v_i v_k = 1, \tag{6}$$

where p and ρ are the proper pressure and proper density respectively and v_i is the flow vector. In view of (5) and (6), we have the following four relations:

$$\begin{aligned}
&(1-u)^{-1}R_{yy} = (1+u)^{-1}R_{zz} = -v^{-1}R_{yz} \\
&((1-u)R_{tt} - R_{yy})((1-u)R_{xx} + R_{yy}) = (1-u)^2 R_{tx}{}^2.
\end{aligned} \tag{7}$$

Two of the relations, contained in the first set of the above equations, give:

$$P(u_{xx}-u_{tt})+u(u_x{}^2-u_t{}^2)+u(u_xv_x-u_tv_t)=0$$
$$P(v_{xx}-v_{tt})+v(v_x{}^2-v_t{}^2)+u(u_xv_x-u_tv_t)=0. \tag{8}$$

A perfect fluid distribution of matter is possible if $u=v$.

Thus these relations are compatible with the perfect fluid distribution of matter if $u=v$ and the resulting single equation is as follows:

$$(1-2u^2)(u_{tt}-u_{xx})+2u(u_t{}^2-u_x{}^2)=0, \tag{9}$$

Lie Symmetry Analysis

Lie point symmetry of a differential equation is an invertible transformation of the dependent and independent variables that leaves the equation unchanged. The technique has earlier been used to obtain exact solutions of various non-linear partial differential equations [4-6, 10, 11]; hence there is no need to discuss the method in detail. In this section, we obtain the symmetry groups of equation (9) using the Lie classical method. The symmetry group of equation (9) is generated by a vector field of the form:

$$V=\xi(x,t,u)\frac{\partial}{\partial x}+\tau(x,t,u)\frac{\partial}{\partial t}+\eta(x,t,u)\frac{\partial}{\partial u} \tag{10}$$

where ξ, τ and η are functions of x, t and u. Assuming that the system of equation (9) is invariant, we find that the coefficient functions ξ, τ and η must satisfy the symmetry condition:

$$-4\eta u(u_{tt}-u_{xx})+(1-2u^2)(\eta^{tt}-\eta^{xx})+2\eta(u_t{}^2-u_x{}^2)+4u(u_t\eta^t-u_x\eta^x)=0 \tag{11}$$

where η^x, η^t, η^{xx} and η^{tt} are extended (prolonged) infinitesimals acting on an enlarged space that includes derivatives of the dependent variables u_x, u_t, u_{xx} and u_{tt} respectively. After some straightforward albeit tedious and lengthy calculations, we derive the following forms of the infinitesimal elements ξ, τ and η:

$$\xi=F_1(t+x)-F_2(t-x)$$
$$\tau=F_1(t+x)+F_2(t-x) \tag{12}$$
$$\eta=0$$

where $F_1(t+x)$ and $F_2(t-x)$ are arbitrary functions. Thus, equation (9) admits a set of Lie algebra of infinite dimensions.

For the symmetries described in (12), the similarity variable $\zeta=\zeta(x,t)$ and the corresponding form of u as a function of the new independent variable ζ are as follows:

$$\zeta=\int\frac{F_1(t+x)+F_2(t-x)}{F_1(t+x)F_2(t-x)}dx+\int\frac{-F_1(t+x)+F_2(t-x)}{F_1(t+x)F_2(t-x)}dt$$
$$u(x,t)=F(\zeta). \tag{13}$$

In the above set of equations (13), the function F is a function of ζ and is determined by substituting (13) in (9) and solving the resulting non-linear ODE, which is:

$$2F'(\zeta)^2F(\zeta)+F''(\zeta)-2F(\zeta)^2F''(\zeta)=0, \tag{14}$$

where prime (') denotes the differentiation with respect to variable ζ . Solving equation (14) and reverting back to the original variables, we obtain the following group-invariant solutions of equation (9):

Solutions in terms of cos () function

$$(i)\ u(x,t)=\pm\frac{\sqrt{2}}{2}\cos\left(c_1+c_2\left(\int\frac{F_1(t+x)+F_2(t-x)}{F_1(t+x)F_2(t-x)}dx+\int\frac{-F_1(t+x)+F_2(t-x)}{F_1(t+x)F_2(t-x)}dt\right)\right)$$

$$(ii)\ u(x,t)=\pm\frac{\sqrt{2}}{2}\mp\sqrt{2}\cos\left(c_1+c_2\left(\int\frac{F_1(t+x)+F_2(t-x)}{F_1(t+x)F_2(t-x)}dx+\int\frac{-F_1(t+x)+F_2(t-x)}{F_1(t+x)F_2(t-x)}dt\right)\right)^2 \quad (15)$$

$$(iii)\ u(x,t)=\pm\frac{3\sqrt{2}}{2}\cos\left(c_1+c_2\left(\int\frac{F_1(t+x)+F_2(t-x)}{F_1(t+x)F_2(t-x)}dx+\int\frac{-F_1(t+x)+F_2(t-x)}{F_1(t+x)F_2(t-x)}dt\right)\right)$$
$$\mp 2\sqrt{2}\cos\left(c_1+c_2\left(\int\frac{F_1(t+x)+F_2(t-x)}{F_1(t+x)F_2(t-x)}dx+\int\frac{-F_1(t+x)+F_2(t-x)}{F_1(t+x)F_2(t-x)}dt\right)\right)^3,$$

where c_1 and c_2 are arbitrary constants.

Solutions in terms of sin () function

$$(i)\ u(x,t)=\pm\frac{\sqrt{2}}{2}\sin\left(c_1+c_2\left(\int\frac{F_1(t+x)+F_2(t-x)}{F_1(t+x)F_2(t-x)}dx+\int\frac{-F_1(t+x)+F_2(t-x)}{F_1(t+x)F_2(t-x)}dt\right)\right)$$

$$(ii)\ u(x,t)=\pm\frac{\sqrt{2}}{2}\mp\sqrt{2}\sin\left(c_1+c_2\left(\int\frac{F_1(t+x)+F_2(t-x)}{F_1(t+x)F_2(t-x)}dx+\int\frac{-F_1(t+x)+F_2(t-x)}{F_1(t+x)F_2(t-x)}dt\right)\right)^2 \quad (16)$$

$$(iii)\ u(x,t)=\pm\frac{3\sqrt{2}}{2}\sin\left(c_1+c_2\left(\int\frac{F_1(t+x)+F_2(t-x)}{F_1(t+x)F_2(t-x)}dx+\int\frac{-F_1(t+x)+F_2(t-x)}{F_1(t+x)F_2(t-x)}dt\right)\right)$$
$$\mp 2\sqrt{2}\sin\left(c_1+c_2\left(\int\frac{F_1(t+x)+F_2(t-x)}{F_1(t+x)F_2(t-x)}dx+\int\frac{-F_1(t+x)+F_2(t-x)}{F_1(t+x)F_2(t-x)}dt\right)\right)^3,$$

where c_1 and c_2 are arbitrary constants.

EINSTEIN FIELD EQUATIONS FOR PURE RADIATION FIELDS

From the beginning of the theory of general relativity, there has been a sustained search for the new exact solutions of Einstein equations for various fields. The exact solutions of Einstein field equations play very important roles in the discussion of physical problems. The Riemann curvature tensor plays the most fundamental role in Einstein theory of gravitation. The algebraic and differential properties of this tensor have characterised wave fields in general relativity in great detail. The problem of pure radiation fields has been discussed by several authors [16-22].

The field equations corresponding to the pure radiation fields are:

$$R_i^{\ j}=\kappa\omega_i\omega^j, \qquad (17)$$

where κ is a scalar. When $\kappa=0$, one gets pure gravitational radiation. The more general waves given by (17) ($\kappa\neq 0$) are distinct from pure gravitational waves. We will derive some of the exact solutions of the Einstein-Rosen [23] cylindrically symmetric space-time corresponding to pure radiation fields.

Metric Form and Field Equations

Consider Einstein-Rosen metric [23] in cylindrical polar coordinates r, ϕ, z and time t as:

$$ds^2 = e^{(2v-2u)}(dt^2 - dr^2) - r^2 e^{(-2u)} d\phi^2 - e^{(2u)} dz^2 , \tag{18}$$

where u and v are functions of r and t only. The non-zero components of curvature tensor obtained from (18) are:

$$\begin{aligned}
R_r^r &= e^{(2u-2v)}\left(-v_{rr} + v_{tt} + u_{rr} - u_{tt} - 2u_r^2 + \frac{v_r + u_r}{r}\right) \\
R_\phi^\phi &= -R_z^z = e^{(2u-2v)}\left(u_{rr} - u_{tt} + \frac{u_r}{r}\right) \\
R_t^t &= e^{(2u-2v)}\left(-v_{rr} + v_{tt} + u_{rr} - u_{tt} + 2u_t^2 + \frac{u_r - v_r}{r}\right) \\
R_r^t &= -R_t^r = e^{(2u-2v)}\left(2u_r u_t - \frac{v_t}{r}\right).
\end{aligned} \tag{19}$$

Pure radiation fields with null vector ω^i such that $\omega^r = 1, \omega^\phi = 0, \omega^z = 0$ and $\omega^t = 1,$ for the metric (18) by using (17), obey the field equations:

$$\begin{aligned}
R_r^r + R_t^t &= 0 \\
R_r^r + R_t^r &= 0 \\
R_\phi^\phi + R_z^z &= 0.
\end{aligned} \tag{20}$$

Making use of expressions for R_i^i given in (19), the relations (20) give the system of partial differential equations:

$$\begin{aligned}
u_{rr} + \frac{u_r}{r} - u_{tt} &= 0 \\
v_r + v_t - r(u_r + u_t)^2 &= 0 \\
v_{rr} - v_{tt} + u_r^2 - u_t^2 &= 0.
\end{aligned} \tag{21}$$

So we have three equations for the determination of two unknowns, u and v, and one can easily verify that these three equations are all consistent. Therefore, we drop the third equation in system (21) and solve the remaining two equations for u and v. Hence we get a system of partial differential equations:

$$\begin{aligned}
u_{rr} + \frac{u_r}{r} - u_{tt} &= 0 \\
v_r + v_t - r(u_r + u_t)^2 &= 0.
\end{aligned} \tag{22}$$

Lie symmetry method is utilised to obtain the group invariant solutions of the non-linear system (22). A number of cases arise depending on the nature of the Lie symmetry generator. We derive various symmetries of system (22) by using Lie group method and then an optimal system comprising basic vector fields is identified. Further, the reduced systems of ODEs and some of the exact solutions of equation (22) are presented. The Lie algebra associated with system (22) consists of the following six vector fields:

$$X_1 = u\frac{\partial}{\partial u} + 2v\frac{\partial}{\partial v},\ X_2 = \log(r)\frac{\partial}{\partial u} + 2u\frac{\partial}{\partial v},\ X_3 = \frac{\partial}{\partial v},\ X_4 = \frac{\partial}{\partial u},\ X_5 = r\frac{\partial}{\partial r} + t\frac{\partial}{\partial t},\ X_6 = \frac{\partial}{\partial t}. \quad (23)$$

In general, there is an infinite number of sub-algebras of this Lie algebra formed from any linear combination of generators $X_i,\ i = 1,2,3,4,5,6$. However, two algebras are similar if they are connected to each other by a transformation from the symmetry group; then their corresponding invariant solutions are connected to each other by the same transformation. Therefore, it is sufficient to put all similar sub-algebras into one class; the set of all these representatives is called an optimal system [1, 2], which consists of the following six basic vector fields:

$$(i)\ X_1 + \mu X_5,\ \ (ii)\ X_2 + \mu X_5,\ \ (iii)\ X_3 + \mu X_5,\ \ (iv)\ X_4 + \mu X_5,\ \ (v)\ X_5,\ \ (vi)\ X_6. \quad (24)$$

Symmetry Reductions and Exact Solutions

Now the primary focus is on the reductions associated with the vector fields in the optimal system and the attempt to furnish exact solutions.

$(i)\ \ X_1 + \mu X_5$

Corresponding to this vector field, the form of the similarity variable and similarity solution is:

$$\zeta = \frac{r}{t},\ u(r,t) = t^{\frac{1}{\mu}}F(\zeta),\ v(r,t) = t^{\frac{2}{\mu}}G(\zeta).$$

On using these in system (22) , the reduced system of ODEs is:

$$\begin{aligned} &F''(\zeta)(1-\zeta^2) + \frac{2\zeta F'(\zeta)}{\mu} + \frac{F'(\zeta)}{\mu} - 2F'(\zeta)\zeta - \frac{F(\zeta)}{\mu^2} + \frac{F(\zeta)}{\mu} = 0 \\ &G''(\zeta) + \frac{2G(\zeta)}{\mu} - G'(\zeta)\zeta - \zeta\left(\frac{F(\zeta)}{\mu} - \zeta F'(\zeta) + F'(\zeta)\right)^2 = 0 \end{aligned} \quad (25)$$

The solution of the reduced system of ODEs (25) is:

$$\begin{aligned} F(\zeta) &= c_1 hypergeom\left(\left[\frac{-1}{2\mu}, \frac{\mu-1}{2\mu}\right], \left[\frac{\mu-2}{2\mu}\right], 1-\zeta^2\right) \\ &\quad + c_2(-1+\zeta^2)^{\frac{2+\mu}{2\mu}} hypergeom\left(\left[\frac{1+2\mu}{2\mu}, \frac{\mu+1}{2\mu}\right], \left[\frac{3\mu+2}{2\mu}\right], 1-\zeta^2\right) \end{aligned} \quad (26)$$

$$G(\zeta) = \left(\int \frac{-\zeta(F'(\zeta)\zeta\mu - F(\zeta) - F'(\zeta)\mu)^2(-1+\zeta)^{\frac{-\mu-2}{2}}}{\mu} d\zeta + c_1\right)(-1+\zeta^2)^{\frac{2}{\mu}}.$$

Hence, the solution of system (22) is:

$$
\begin{aligned}
u(r,t) &= \left(c_1 hypergeom\left(\left[\frac{-1}{2\mu}, \frac{\mu-1}{2\mu} \right], \left[\frac{\mu-2}{2\mu} \right], \left(1 - \left(\frac{r}{t} \right)^2 \right) \right) \right) t^{\frac{1}{\mu}} \\
&+ \left(c_2 \left(-1 + \left(\frac{r}{t} \right)^2 \right)^{\frac{2+\mu}{2\mu}} hypergeom\left(\left[\frac{1+2\mu}{2\mu}, \frac{\mu+1}{2\mu} \right], \left[\frac{3\mu+2}{2\mu} \right], \left(1 - \left(\frac{r}{t} \right)^2 \right) \right) \right) t^{\frac{1}{\mu}} \\
v(r,t) &= \left(\left(\int \frac{-\zeta (F'(\zeta)\zeta\mu - F(\zeta) - F'(\zeta)\mu)^2 (-1+\zeta)^{\frac{-\mu-2}{2}}}{\mu} d\zeta + c_1 \right) (-1+\zeta^2)^{\frac{2}{\mu}} \right) t^{\frac{2}{\mu}}.
\end{aligned} \tag{27}
$$

where c_1 and c_2 are arbitrary constants and *hypergeom* stands for hypergeometric function.

(ii) $X_2 + \mu X_5$

For this vector field, the form of the similarity variable and similarity solution is:

$$
\zeta = \frac{r}{t},\ u(r,t) = \frac{(\log(r))^2}{2\mu} + F(\zeta),\ v(r,t) = \frac{(\log(r))^3}{3\mu^2} + \frac{2F(\zeta)\log(r)}{\mu} + G(\zeta).
$$

On using these in system (22), the following system of reduced ODEs is obtained:

$$
\begin{aligned}
& F''(\zeta)\mu\zeta^2(1-\zeta^2) - 2\mu\zeta^3 F'(\zeta) + \mu F'(\zeta)\zeta + 1 = 0 \\
& \mu\zeta^2 G'(\zeta) - \mu\zeta G'(\zeta) + (F(\zeta))^2\zeta^4\mu - 2(F'(\zeta))^2\zeta^3\mu + (F'(\zeta))^2\zeta^2\mu - 2(F(\zeta)) = 0.
\end{aligned} \tag{28}
$$

The solution of system (28) is given by:

$$
\begin{aligned}
F(\zeta) &= \int \frac{-\arctan\left(\frac{1}{\sqrt{(-1+\zeta^2)}} \right) \sqrt{(-1+\zeta^2)} + c_2\mu\sqrt{(-1+\zeta^2)}}{(\zeta^2-1)\zeta\mu} d\zeta + c_3 \\
G(\zeta) &= \int \frac{-(F(\zeta))^2\zeta^4\mu + 2(F'(\zeta))^2\zeta^3\mu - (F'(\zeta))^2\zeta^2\mu + 2(F(\zeta))}{\mu\zeta(\zeta-1)} d\zeta + c_1.
\end{aligned} \tag{29}
$$

where c_1, c_2 and c_3 are arbitrary constants. Thus, we get the following solution of system (22) by using (29):

$$
\begin{aligned}
u(r,t) &= \frac{(\log(r))^2}{2\mu} + F(\zeta) \\
v(r,t) &= \frac{(\log(r))^3}{3\mu^2} + \frac{2F(\zeta)\log(r)}{\mu} + G(\zeta).
\end{aligned} \tag{30}
$$

(iii) $X_3 + \mu X_5$

For this vector field, the form of the similarity variable and similarity solution is:

$$
\zeta = \frac{r}{t},\ u(r,t) = F(\zeta),\ v(r,t) = \frac{\log(t)}{\mu} + G(\zeta).
$$

Using these substitutions, system (22) reduces to:

$$F''(\zeta)(1-\zeta^2)-2\zeta F'(\zeta)+\frac{F'(\zeta)}{\zeta}=0$$
$$G'(\zeta)(1-\zeta)-\zeta(-\zeta F'(\zeta)+F'(\zeta))^2+\frac{1}{\mu}=0. \tag{31}$$

The solution of the reduced system of ODEs (31) is obtained and the solution of system (22) is:

$$u(r,t)=\arctan\left(\frac{t}{\sqrt{(r^2-t^2)}}\right)c_2+c_1$$
$$v(r,t)=-c_2^2\log(r)+c_2^2\log(r+t)+\frac{1}{\mu}\log(r-t)+c_3, \tag{32}$$

where c_1, c_2 and c_3 are arbitrary constants.

(*iv*) $X_4+\mu X_5$

In this case the form of the similarity variable and similarity solution is:

$$\zeta=\frac{r}{t},\ u(r,t)=F(\zeta)+\frac{\log(r)}{\mu},\ v(r,t)=G(\zeta).$$

Using these substitutions in system (22), we get the following reduced system of ODEs:

$$F''(\zeta)(1-\zeta^2)-2\zeta F'(\zeta)+\frac{F'(\zeta)}{\zeta}+\frac{1}{\mu}=0$$
$$G'(\zeta)(1-\zeta)-\zeta\left(-\zeta F'(\zeta)+F'(\zeta)+\frac{1}{\mu}\right)^2=0. \tag{33}$$

The solution of reduced ODEs (33) is obtained and hence the solution of system (22) is:

$$u(r,t)=\frac{\log(r)}{\mu}-c_1\arctan\left(\frac{t}{\sqrt{(r^2-t^2)}}\right)+c_2$$
$$v(r,t)=-\frac{\log(r-t)}{\mu^2}+\frac{\log(r)}{\mu^2}-c_1^2\log(r)+c_1^2\log(r+t)-\frac{2c_1\arctan\left(\frac{t}{\sqrt{(r^2-t^2)}}\right)}{\mu}+c_3, \tag{34}$$

where c_1, c_2 and c_3 are arbitrary constants.

(*v*) X_5

For this vector field, the form of the similarity variable and similarity solution is:

$$\zeta=\frac{r}{t},\ u(r,t)=F(\zeta),\ v(r,t)=G(\zeta).$$

Using these substitutions, system (22) reduces to:

$$F''(\zeta)(1-\zeta^2)-2\zeta F'(\zeta)+\frac{F'(\zeta)}{\zeta}=0$$
$$G'(\zeta)(1-\zeta)-\zeta(-\zeta F'(\zeta)+F'(\zeta))^2=0. \tag{35}$$

The solution of reduced ODEs (35) is furnished and the solution of system (22) is:

$$\begin{aligned} u(r,t) &= c_1 \arctan\left(\frac{t}{\sqrt{(r^2-t^2)}}\right) + c_2 \\ v(r,t) &= -c_1^2 \log(r) + c_1^2 \log(r+t) + c_3, \end{aligned} \tag{36}$$

where c_1, c_2 and c_3 are arbitrary constants.

(vi) X_6

Corresponding to this vector field, the form of the similarity variable and similarity solution is:

$\zeta = r,\ u(r,t) = F(\zeta),\ v(r,t) = G(\zeta).$

On using these in system (22), the system of reduced ODEs is given by:

$$\begin{aligned} &\zeta F''(\zeta) + F'(\zeta) = 0 \\ &G'(\zeta) - \zeta(F'(\zeta))^2 = 0. \end{aligned} \tag{37}$$

The solution of reduced ODEs (37) is obtained and the solution of system (22) is deduced as:

$$\begin{aligned} u(r,t) &= c_1 + c_3 \log(r) \\ v(r,t) &= c_2 + c_3^2 \log(r), \end{aligned} \tag{38}$$

where c_1, c_2 and c_3 are arbitrary constants.

Since, after reduction to ODEs, further attempt to apply Lie group analysis to ODEs has been made, but no further physically important non-trivial symmetries come out, hence the solutions of ODEs are obtained directly. After attaining the reductions and exact solutions corresponding to essential vector fields of the optimal system, we observe that in each of physically relevant case, the similarity variable is of the form r/t . Since reductions can be obtained from any linear combination of basic vector fields (23), we can consider other linear combinations for physically significant reductions and exact solutions.

For example, we consider linear combination $X_1 + \mu X_2 + \lambda X_6$ of vector fields. For this vector field, the form of the similarity variable and similarity solution is:

$$\zeta = r,\ u(r,t) = e^{\frac{t}{\lambda}} F(\zeta) - \mu \log(\zeta),\ v(r,t) = -2\mu e^{\frac{t}{\lambda}} F(\zeta) + \mu^2 \log(\zeta) + e^{\frac{2t}{\lambda}} G(\zeta).$$

On using these in system (22), the reduced system of ODEs is:

$$\begin{aligned} &-F''(\zeta)\zeta\lambda^2 + F(\zeta)\zeta - \lambda^2 F'(\zeta) = 0 \\ &-G'(\zeta)\lambda^2 - 2G(\zeta)\lambda + F(\zeta)^2\zeta + 2F(\zeta)F'(\zeta)\zeta\lambda + F'(\zeta)^2\lambda^2\zeta = 0. \end{aligned} \tag{39}$$

The solution of reduced ODEs is obtained and the solution of system (22) is deduced as:

$$u(r,t) = \left(c_2 J_0\left(\frac{r}{\lambda}\right) + c_3 Y_0\left(\frac{r}{\lambda}\right)\right) e^{\frac{t}{\lambda}} - \mu \log(r)$$

$$v(r,t) = \left(\int r e^{\left(\frac{2r}{\lambda}\right)} \left(c_2 J_1\left(\frac{r}{\lambda}\right) - c_3 Y_1\left(\frac{r}{\lambda}\right) + c_2 J_0\left(\frac{r}{\lambda}\right) - c_3 Y_0\left(\frac{r}{\lambda}\right)\right)^2 dr + c_1 \lambda^2 \right) \frac{e^{\left(\frac{-2r}{\lambda}\right)} e^{\left(\frac{2t}{\lambda}\right)}}{\lambda^2} \tag{40}$$
$$+ \mu^2 \log(r) - 2\mu e^{\left(\frac{t}{\lambda}\right)} \left(c_2 J_0\left(\frac{r}{\lambda}\right) + c_3 Y_0\left(\frac{r}{\lambda}\right)\right),$$

where $J_\ell(x)$ and $Y_\ell(x)$ are the modified Bessel functions of the first and second kinds respectively. They satisfy the modified Bessel equation:

$$x^2 Y'' + xY' - (x^2 + \ell^2)Y = 0,$$

where c_1, c_2 and c_3 are arbitrary constants.

CONCLUSIONS

In this work, we have studied Einstein field equations for perfect fluid distribution and the system of partial differential equations corresponding to Einstein-Rosen cylindrically symmetric space-time for pure radiation fields by using Lie symmetry analysis method. Especially, all similarity reductions and exact solutions based on the Lie group method are obtained by generating the group infinitesimals. The partial differential equations are reduced to ordinary differential equations, which are further studied with the aim of deriving certain exact solutions. It is worth mentioning here that the authenticity of all the solutions has been checked with the aid of software Maple. Thus, we have found new exact solutions that might prove to be interesting for further applications.

ACKNOWLEDGEMENTS

The authors express their sincere thanks to the referees for their useful and constructive suggestions.

REFERENCES

1. L. V. Ovsiannikov, "Group Analysis of Differential Equations", Academic Press, New York, **1982**.
2. P. J. Olver, "Applications of Lie Groups to Differential Equations", Springer Verlag, New York, **1993**.
3. G. W. Bluman and S. C. Anco, "Symmetry and Integration Methods for Differential Equations", 2nd Edn., Springer-Verlag, New York, **2002**.
4. C. M. Khalique and K. R. Adem, "Exact solutions of the (2+1)-dimensional Zakharov-Kuznetsov modified equal width equation using Lie group analysis", *Math. Comput. Model.*, **2011**, *54*, 184-189.
5. K. Singh, R. K. Gupta and S. Kumar, "Benjamin-Bona-Mahony (BBM) equation with variable coefficients: Similarity reductions and Painlevé analysis", *Appl. Math. Comput.*, **2011**, *217*, 7021-7027.

6. R. K. Gupta and K. Singh, "Symmetry analysis and some exact solutions of cylindrically symmetric null fields in general relativity", *Commun. Nonlinear Sci. Numer. Simul.*, **2011**, *16*, 4189-4196.
7. H. Stephani, D. Kramer, M. MacCallum, C. Hoenselaers and E. Herlt, "Exact Solutions of Einstein's Field Equations", 2nd Edn., Cambridge University Press, Cambridge, **2003**.
8. K. Schwarzschild, "On the gravitational field of a mass point according to Einstein's theory", *Sitzungsber. Dtsch. Akad. Wiss. Berl. Kl. Math. Phys. Technol.*, **1916**, *3*, 189-196.
9. R. P. Kerr, "Gravitational field of a spinning mass as an example of algebraically special metrics", *Phys. Rev. Lett.*, **1963**, *11*, 237-238.
10. L. Marchildon, "Lie symmetries of Einstein's vacuum equations in N dimensions", *J. Nonlinear Math. Phys.*, **1998**, *5*, 68-81.
11. A. T. Ali, "New exact solutions of the Einstein vacuum equations for rotating axially symmetric fields", *Phys. Scrip.*, **2009**, *79*, 035006.
12. M. Kumar and Y. K. Gupta, "Some invariant solutions for non-conformal perfect fluid plates in 5-flat form in general relativity", *Pramana J. Phys.*, **2010**, *74*, 883-893.
13. A. Einstein, "Comment on Schrodinger's note: On a system of solutions for the generally covariant gravitational field equations' ", *Physik. Z.*, **1918,** *7*, 33-36.
14. P. G. Bergmann, "Introduction to the Theory of Relativity", Dover Publications, New York, **1976**.
15. H. Bondi, F. A. E. Pirani and I. Robinson, "Gravitational waves in general relativity III. Exact plane waves", *Proc. Roy. Soc. Lond.*, **1959**, *251*, 519-533.
16. R. P. Akabari, U. K. Dave and L. K. Patel, "Some pure radiation fields in general relativity", *J. Aust. Math. Soc. (Series B)*, **1980**, *21*, 464-473.
17. P. Wils, "Homogeneous and conformally Ricci flat pure radiation fields", *Class. Quantum Grav.*, **1989**, *6*, 1243-1251.
18. J. Lewandowski, P. Nurowski and J. Tafel, "Algebraically special solutions of the Einstein equations with pure radiation fields", *Class. Quantum Grav.*, **1991**, *8*, 493-501.
19. A. M. Grundland and J. Tafel, "Group invariant solutions to the Einstein equations with pure radiation fields", *Class. Quantum Grav.*, **1993**, *10*, 2337-2345.
20. D. Kramer and U. Hähner, "A rotating pure radiation field", *Class. Quantum Grav.*, **1995**, *12*, 2287-2296.
21. U. von der Gönna and D. Kramer, "Pure and gravitational radiation", *Class. Quantum Grav.*, **1998**, *15*, 215-223.
22. D. Radojevic, "Two examples of pure radiation fields", *Theor. Appl. Mech.*, **2001**, *26*, 83-89.
23. A. Einstein and N. Rosen, "On gravitational waves", *J. Franklin Inst.*, **1937**, *223*, 43-54.

Maejo Int. J. Sci. Technol. **2013**, *7*(01), 145-154

Maejo International Journal of Science and Technology

ISSN 1905-7873
Available online at www.mijst.mju.ac.th

Full Paper

Second-order duality for minimax fractional programming involving generalised Type-I functions

Anurag Jayswal [1,*] and Dilip Kumar [2]

[1] Department of Applied Mathematics, Indian School of Mines, Dhanbad-826004, India
[2] Department of Applied Mathematics, Birla Institute of Technology, Mesra, Ranchi-835215, India
[*] Corresponding author, e-mail: anurag_jais123@yahoo.com

Received: 17 January 2012 / Accepted: 10 April 2013 / Published: 17 April 2013

Abstract: A class of minimax fractional programming problem and its two types of second-order dual models are considered with an establishment of weak, strong and strict converse duality theorems from a view point of generalised convexity. Some previously known results in the framework of generalised convexity are naturally unified and extended.

Keywords: minimax fractional programming, second-order duality, Type-I functions, generalised convexity

---

INTRODUCTION

Optimisation is a mathematical technique for obtaining the greatest or least possible value of a function with one or several variables. This becomes more difficult in the presence of certain constraints imposed on the variables. Optimisation techniques are needed in various disciplines of science and engineering. In fact they are being applied to every sphere of human activity which can be modelled in a mathematical form.

Optimisation problems in which both a minimisation and maximisation process of fractional objectives are performed are usually referred to in the optimisation literature as generalised minimax fractional programming problems. These problems have arisen in multi-objective programming [1], game theory [2], goal programming [3], minimum risk problems [4] and economics [5, 6]. Stancu-Minasian [7] gave a survey on fractional programming which covers applications as well as major theoretical and algorithmic developments.

In this paper, we consider the following minimax fractional programming problem:

(P) Minimise $\psi(\mathrm{x}) = \sup_{y \in Y} \dfrac{f(x, y)}{h(x, y)}$

subject to $g(x) \le 0, \; x \in R^n$,

where Y is a compact subset of R^l , $f, h : R^n \times R^l \to R$ are C^2 functions on $R^n \times R^l$, and $g : R^n \to R^m$ is a C^2 function on R^n. It is assumed that for each $(x, y) \in R^n \times R^l$, $f(x, y) \geq 0$ and $h(x, y) > 0$.

In the study of optimality conditions and duality results for minimax programming problems, Yadav and Mukherjee [8] established the optimality conditions to construct two dual problems and derived duality theorems for differentiable fractional minimax programming. Chandra and Kumar [9] pointed out that the formulation of Yadav and Mukherjee [8] has some omissions and inconsistencies and constructed two modified dual problems and proved duality theorems for (convex) differentiable fractional minimax programming. To relax convexity assumptions involved in sufficient optimality conditions and duality theorems, various generalised convexity notions have been proposed. Focusing on the minimax fractional programming problem, Yang and Hou [10] established the sufficient optimality conditions and derived a number of duality results. Many other authors were involved in developing the optimality conditions and deriving the duality results for minimax programming problems [11-23].

Mangasarian [24] first formulated the second-order dual for a non-linear programming problem and established the duality results under somewhat involved assumptions. Mond [25] reproved second-order duality results involving simpler assumptions and showed that the second-order dual has computational advantages over the first-order dual. In order to generalise the notion of convexity to the second and higher orders and extend the validity of results to larger classes of optimisation problems, Ahmad and Husain [26] introduced a class of second-order (F, α, ρ, d)-convex functions and established duality theorems for a second-order Mond-Weir type multi-objective dual problem. Husain et al. [27] considered two types of second-order dual model for a minimax fractional programming problem and adopted the concept of η-bonvexity/generalised η-bonvexity to discuss appropriate duality theorems.

In this paper after some preliminaries and definitions are given, the weak, strong and strict converse duality theorems for two types of dual models to the minimax fractional programming problem (P) under the second-order Type-I assumptions are discussed.

NOTATIONS AND PRELIMINARIES

Let $S = \{x \in R^n : g(x) \leq 0\}$ denote a set of all feasible solutions of problem (P). For each $(x,\ y) \in R^n \times R^l$, we define:

$$J(x) = \{j \in M : g_j(x) = 0\} \quad \text{where } M = \{1, 2, ..., m\},$$

$$Y(x) = \left\{ y \in Y : f(x, y) + \left(x^T Bx\right)^{1/2} = \sup_{z \in Y} f(x, z) + \left(x^T Bx\right)^{1/2} \right\}, \text{ and}$$

$$K(x) = \Big\{(s, t, \bar{y}) \in N \times R_+^s \times R^{ls} : 1 \leq s \leq n+1,\ t = (t_1, t_2, ..., t_s) \in R_+^s$$
$$\text{with } \sum_{i=1}^{s} t_i = 1 \text{ and } \bar{y} = (\bar{y}_1, \bar{y}_2, ..., \bar{y}_s) \text{ and } \bar{y}_i \in Y(x), i = 1,2,...,s\Big\}.$$

In the sequel the following result [9] is needed:

Theorem 1 (Necessary conditions). *If* x^* *is a solution (local or global) of problem* (P) *and* $\nabla g_j(x^*), j \in J(x^*)$ *are linearly independent, then there exist* $(s^*, t^*, \bar{y}^*) \in K(x^*)$, $\lambda^* \in R_+$, *and* $\mu \in R_+^m$ *such that*

$$\nabla \sum_{i=1}^{s^*} t_i^* \left(f(x^*, \bar{y}_i^*) - \lambda^* h(x^*, \bar{y}_i^*) \right) + \nabla \sum_{j=1}^{m} \mu_j^* g_j(x^*),$$

$$f(x^*, \bar{y}_i^*) - \lambda^* h(x^*, \bar{y}_i^*) = 0, \quad i = 1,2,\ldots,s^*,$$

$$\sum_{j=1}^{m} \mu_j^* g_j(x^*) = 0,$$

$$t_i^* \geq 0, \quad \sum_{i=1}^{s^*} t_i^* = 1, \quad \bar{y}_i^* \in Y(x^*), \quad i = 1,2,\ldots,s^*.$$

In order to consider the second-order duality for problem (P), we define the following second order Type I and related functions:

Definition 1. *The pair* (f, g) *is said to be second order Type I at* $\bar{x} \in X$ *with respect to* η *if there exists a vector function* $\eta : X \times X \to R^n$ *such that for all* $x \in X, p \in R^n, y_i \in Y(x)$, $i = 1,2,\ldots,s, j = 1,2,\ldots,m,$

$$f(x, y_i) - f(\bar{x}, y_i) + \frac{1}{2} p^T \nabla^2 f(\bar{x}, y_i) p \geq \eta^T(x, \bar{x}) \left[\nabla f(\bar{x}, y_i) + \nabla^2 f(\bar{x}, y_i) p \right]$$

$$-g_j(\bar{x}) + \frac{1}{2} p^T \nabla^2 g_j(\bar{x}) p \geq \eta^T(x, \bar{x}) \left[\nabla g_j(\bar{x}) + \nabla^2 g_j(\bar{x}) p \right].$$

In the above definition, if the inequalities appear as strict inequalities, then we say that (f, g) is strictly second order Type I at $\bar{x} \in X$.

Definition 2. *The pair* (f, g) *is said to be second order pseudoquasi Type I at* $\bar{x} \in X$ *with respect to* η *if there exists a vector function* $\eta : X \times X \to R^n$ *such that for all* $x \in X, p \in R^n, y_i \in Y(x)$, $i = 1,2,\ldots,s, j = 1,2,\ldots,m,$

$$f(x, y_i) - f(\bar{x}, y_i) + \frac{1}{2} p^T \nabla^2 f(\bar{x}, y_i) p < 0$$

$$\Rightarrow \eta^T(x, \bar{x}) \left[\nabla f(\bar{x}, y_i) + \nabla^2 f(\bar{x}, y_i) p \right] < 0,$$

$$-g_j(\bar{x}) + \frac{1}{2} p^T \nabla^2 g_j(\bar{x}) p \leq 0$$

$$\Rightarrow \eta^T(x, \bar{x}) \left[\nabla g_j(\bar{x}) + \nabla^2 g_j(\bar{x}) p \right] \leq 0.$$

If the second inequality is strict, then (f, g) is said to be second-order strictly pseudoquasi Type I at $\bar{x} \in X$.

FIRST DUALITY MODEL

In relation to (P), we consider the following dual problem:

$$\textbf{(MD)} \qquad \max_{(s,t,\bar{y}) \in K(z)} \quad \sup_{(z,\mu,\lambda,p) \in H_1(s,t,\bar{y})} \lambda,$$

where $H_1(s,t,\bar{y})$ denotes the set of all $(z,\mu,\lambda,p)\in R^n\times R_+^m\times R_+\times R^n$ satisfying

$$\nabla\sum_{i=1}^{s}t_i\big(f(z,\bar{y}_i)-\lambda h(z,\bar{y}_i)\big)+\nabla^2\sum_{i=1}^{s}t_i\big(f(z,\bar{y}_i)-\lambda h(z,\bar{y}_i)\big)p$$
$$+\nabla\sum_{j=1}^{m}\mu_j g_j(z)+\nabla^2\sum_{j=1}^{m}\mu_j g_j(z)p=0, \tag{1}$$

$$\sum_{i=1}^{s}t_i\big(f(z,\bar{y}_i)-\lambda h(z,\bar{y}_i)\big)-\frac{1}{2}p^T\nabla^2\sum_{i=1}^{s}t_i\big(f(z,\bar{y}_i)-\lambda h(z,\bar{y}_i)\big)p\geq 0, \tag{2}$$

$$\sum_{j=1}^{m}\mu_j g_j(z)-\frac{1}{2}p^T\nabla^2\sum_{j=1}^{m}\mu_j g_j(z)p\geq 0. \tag{3}$$

If, for a triplet $(s,t,\bar{y})\in K(z)$, the set $H_1(s,t,\bar{y})=\phi$, then we define the supremum over it to be $-\infty$.

Remark 1. If $p=0$, then (MD) becomes the dual given in Liu and Wu [28].

Theorem 2 (Weak duality). *Let x and $(z,\mu,\lambda,s,t,\bar{y},p)$ be the feasible solutions of* (P) *and* (MD) *respectively. Assume that* $\left[\sum_{i=1}^{s}t_i\big(f(\cdot,\bar{y}_i)-\lambda h(\cdot,\bar{y}_i)\big),\sum_{j=1}^{m}\mu_j g_j(\cdot)\right]$ *is second order Type I at z with $\eta(x,z)>0$. Then* $\sup_{y\in Y}\dfrac{f(x,y)}{h(x,y)}\geq\lambda$.

Proof. Suppose it is contrary to the result that $\sup_{y\in Y}\dfrac{f(x,y)}{h(x,y)}<\lambda$.

Thus, we have $f(x,\bar{y}_i)-\lambda h(x,\bar{y}_i)<0$ for all $\bar{y}_i\in Y(x),\ i=1,2,...,s.$

It follows from $t_i\geq 0,\ i=1,2,...,s$ that $t_i\big(f(x,\bar{y}_i)-\lambda h(x,\bar{y}_i)\big)\leq 0$, with at least one strict inequality since $t=(t_1,t_2,...,t_s)\neq 0.$ Taking summation over i and using $\sum_{i=1}^{s}t_i=1$, we have by (2):

$$\sum_{i=1}^{s}t_i\big(f(x,\bar{y}_i)-\lambda h(x,\bar{y}_i)\big)<0\leq\sum_{i=1}^{s}t_i\big(f(z,\bar{y}_i)-\lambda h(z,\bar{y}_i)\big)\ -\frac{1}{2}p^T\nabla^2\sum_{i=1}^{s}t_i\big(f(z,\bar{y}_i)-\lambda h(z,\bar{y}_i)\big)p.$$

The above inequality, together with (3), implies:

$$\sum_{i=1}^{s}t_i\big(f(x,\bar{y}_i)-\lambda h(x,\bar{y}_i)\big)-\sum_{i=1}^{s}t_i\big(f(z,\bar{y}_i)-\lambda h(z,\bar{y}_i)\big)-\sum_{j=1}^{m}\mu_j g_j(z)$$
$$+\frac{1}{2}p^T\nabla^2\sum_{i=1}^{s}t_i\big(f(z,\bar{y}_i)-\lambda h(z,\bar{y}_i)\big)p+\frac{1}{2}p^T\nabla^2\sum_{j=1}^{m}\mu_j g_j(z)p<0. \tag{4}$$

Now the second-order Type-I assumption on $\left[\sum_{i=1}^{s}t_i\big(f(\cdot,\bar{y}_i)-\lambda h(\cdot,\bar{y}_i)\big),\sum_{j=1}^{m}\mu_j g_j(\cdot)\right]$ at z gives:

$$\sum_{i=1}^{s}t_i\big(f(x,\bar{y}_i)-\lambda h(x,\bar{y}_i)\big)-\sum_{i=1}^{s}t_i\big(f(z,\bar{y}_i)-\lambda h(z,\bar{y}_i)\big)+\frac{1}{2}p^T\nabla^2\sum_{i=1}^{s}t_i\big(f(z,\bar{y}_i)-\lambda h(z,\bar{y}_i)\big)p$$
$$\geq\eta^T(x,z)\left[\nabla\sum_{i=1}^{s}t_i\big(f(z,\bar{y}_i)-\lambda h(z,\bar{y}_i)\big)+\nabla^2\sum_{i=1}^{s}t_i\big(f(z,\bar{y}_i)-\lambda h(z,\bar{y}_i)\big)p\right],$$

$$-\sum_{j=1}^{m}\mu_j g_j(z)+\frac{1}{2}p^T\nabla^2\sum_{j=1}^{m}\mu_j g_j(z)p\geq\eta^T(x,z)\left[\nabla\sum_{j=1}^{m}\mu_j g_j(z)+\nabla^2\sum_{j=1}^{m}\mu_j g_j(z)p\right].$$

Combining the above two inequalities, we get:

$$\sum_{i=1}^{s} t_i\left(f(x,\bar{y}_i)-\lambda h(x,\bar{y}_i)\right)-\sum_{i=1}^{s} t_i\left(f(z,\bar{y}_i)-\lambda h(z,\bar{y}_i)\right)-\sum_{j=1}^{m}\mu_j g_j(z)$$
$$+\frac{1}{2}p^T\nabla^2\sum_{i=1}^{s} t_i\left(f(z,\bar{y}_i)-\lambda h(z,\bar{y}_i)\right)p+\frac{1}{2}p^T\nabla^2\sum_{j=1}^{m}\mu_j g_j(z)p$$
$$\geq \eta^T(x,z)\left[\nabla\sum_{i=1}^{s} t_i\left(f(z,\bar{y}_i)-\lambda h(z,\bar{y}_i)\right)+\nabla^2\sum_{i=1}^{s} t_i\left(f(z,\bar{y}_i)-\lambda h(z,\bar{y}_i)\right)p\right.$$
$$\left.+\nabla\sum_{j=1}^{m}\mu_j g_j(z)+\nabla^2\sum_{j=1}^{m}\mu_j g_j(z)p\right],$$

which, along with (4) and $\eta(x,z)>0$, implies:

$$\nabla\sum_{i=1}^{s} t_i\left(f(z,\bar{y}_i)-\lambda h(z,\bar{y}_i)\right)+\nabla^2\sum_{i=1}^{s} t_i\left(f(z,\bar{y}_i)-\lambda h(z,\bar{y}_i)\right)p$$
$$+\nabla\sum_{j=1}^{m}\mu_j g_j(z)+\nabla^2\sum_{j=1}^{m}\mu_j g_j(z)p<0,$$

which contradicts (1). This completes the proof.

Theorem 3 (Strong duality). *Assume that* x^* *is an optimal solution of* (P) *and* $\nabla g_j(x^*),\ j\in J(x^*)$ *are linearly independent. Then there exist* $(s^*,t^*,\bar{y}^*)\in K(x^*)$ *and* $(x^*,\mu^*,\lambda^*,p^*=0)\in H_1(s^*,t^*,\bar{y}^*)$ *such that* $(x^*,\ \mu^*,\lambda^*,s^*,t^*,\bar{y}^*,p^*=0)$ *is a feasible solution of* (MD) *and the two objectives have the same values. Further, if the hypothesis of Theorem 2 (weak duality) holds for all feasible solutions* $(z,\mu,\lambda,s,t,\bar{y},p)$ *of* (MD)*, then* $(x^*,\ \mu^*,\lambda^*,s^*,t^*,\bar{y}^*,p^*=0)$ *is an optimal solution of* (MD).

Proof. Since x^* is an optimal solution of (P) and $\nabla g_j(x^*),\ j\in J(x^*)$ are linearly independent, then by Theorem 1, there exist $(s^*,t^*,\bar{y}^*)\in K(x^*)$ and $(x^*,\mu^*,\lambda^*,p^*=0)\in H_1(s^*,t^*,\bar{y}^*)$ such that $(x^*,\mu^*,\lambda^*,s^*,t^*,\bar{y}^*,p^*=0)$ is a feasible solution of (MD) and the two objectives have the same values. The optimality of $(x^*,\mu^*,\lambda^*,s^*,t^*,\bar{y}^*,p^*=0)$ for (MD) thus follows from weak duality Theorem 2.

Theorem 4 (Strict converse duality). *Let* x^* *and* $(z^*,\mu^*,\lambda^*,s^*,t^*,\bar{y}^*,p^*=0)$ *be the optimal of* (P) *and* (MD) *respectively. Suppose that* $\left[\sum_{i=1}^{s^*} t_i^*\left(f(\cdot,\bar{y}_i^*)-\lambda^* h(\cdot,\bar{y}_i^*)\right),\sum_{j=1}^{m}\mu_j^* g_j(\cdot)\right]$ *is strictly second order Type I at* z^**, and* $\nabla g_j(x^*),\ j\in J(x^*)$ *are linearly independent. Then* $z^*=x^*$*, i.e.* z^* *is an optimal solution of* (P).

Proof. Suppose it is contrary to the result that $z^*\neq x^*$. Since x^* and $(z^*,\mu^*,\lambda^*,s^*,t^*,\bar{y}^*,p^*)$ are the optimal of (P) and (MD) respectively, and $\nabla g_j(x^*),\ j\in J(x^*)$ are linearly independent, from the Strong Duality Theorem 3, therefore, we reach: $\sup_{y^*\in Y}\frac{f(x^*,y^*)}{h(x^*,y^*)}=\lambda^*$

Thus, we have $f\left(x^*, \bar{y}_i^*\right) - \lambda^* h\left(x^*, \bar{y}_i^*\right) \le 0$ for all $\bar{y}_i^* \in Y\left(x^*\right)$, $i = 1,2,\ldots,s^*$.
Now proceeding as in Theorem 2, we get:

$$\sum_{i=1}^{s^*} t_i^*\left(f\left(x^*, \bar{y}_i^*\right) - \lambda^* h\left(x^*, \bar{y}_i^*\right)\right) - \sum_{i=1}^{s^*} t_i^*\left(f\left(z^*, \bar{y}_i^*\right) - \lambda^* h\left(z^*, \bar{y}_i^*\right)\right) - \sum_{j=1}^{m} \mu_j^* g_j\left(z^*\right)$$
$$+\frac{1}{2} p^{*T} \nabla^2 \sum_{i=1}^{s^*} t_i^*\left(f\left(z^*, \bar{y}_i^*\right) - \lambda^* h\left(z^*, \bar{y}_i^*\right)\right) p^* + \frac{1}{2} p^{*T} \nabla^2 \sum_{j=1}^{m} \mu_j^* g_j\left(z^*\right) p^* \le 0. \tag{5}$$

The strictly second-order Type-I assumption on $\left[\sum_{i=1}^{s^*} t_i^*\left(f\left(\cdot, \bar{y}_i^*\right) - \lambda^* h\left(\cdot, \bar{y}_i^*\right)\right), \sum_{j=1}^{m} \mu_j^* g_j(\cdot)\right]$ at z gives:

$$\sum_{i=1}^{s^*} t_i^*\left(f\left(x^*, \bar{y}_i^*\right) - \lambda^* h\left(x^*, \bar{y}_i^*\right)\right) - \sum_{i=1}^{s^*} t_i^*\left(f\left(z^*, \bar{y}_i^*\right) - \lambda^* h\left(z^*, \bar{y}_i^*\right)\right)$$
$$+\frac{1}{2} p^{*T} \nabla^2 \sum_{i=1}^{s^*} t_i^*\left(f\left(z^*, \bar{y}_i^*\right) - \lambda^* h\left(z^*, \bar{y}_i^*\right)\right) p^*$$
$$> \eta^T\left(x^*, z^*\right)\left[\nabla \sum_{i=1}^{s^*} t_i^*\left(f\left(z^*, \bar{y}_i^*\right) - \lambda^* h\left(z^*, \bar{y}_i^*\right)\right) + \nabla^2 \sum_{i=1}^{s^*} t_i^*\left(f\left(z^*, \bar{y}_i^*\right) - \lambda^* h\left(z^*, \bar{y}_i^*\right)\right) p^*\right],$$
$$-\sum_{j=1}^{m} \mu_j^* g_j\left(z^*\right) + \frac{1}{2} p^{*T} \nabla^2 \sum_{j=1}^{m} \mu_j^* g_j\left(z^*\right) p^* > \eta^T\left(x^*, z^*\right)\left[\nabla \sum_{j=1}^{m} \mu_j^* g_j\left(z^*\right) + \nabla^2 \sum_{j=1}^{m} \mu_j^* g_j\left(z^*\right) p^*\right].$$

Combining the above two inequalities, we get:

$$\sum_{i=1}^{s^*} t_i^*\left(f\left(x^*, \bar{y}_i^*\right) - \lambda^* h\left(x^*, \bar{y}_i^*\right)\right) - \sum_{i=1}^{s^*} t_i^*\left(f\left(z^*, \bar{y}_i^*\right) - \lambda^* h\left(z^*, \bar{y}_i^*\right)\right) - \sum_{j=1}^{m} \mu_j^* g_j\left(z^*\right)$$
$$+\frac{1}{2} p^{*T} \nabla^2 \sum_{i=1}^{s^*} t_i^*\left(f\left(z^*, \bar{y}_i^*\right) - \lambda^* h\left(z^*, \bar{y}_i^*\right)\right) p^* + \frac{1}{2} p^{*T} \nabla^2 \sum_{j=1}^{m} \mu_j^* g_j\left(z^*\right) p^*$$
$$> \eta^T\left(x^*, z^*\right)\left[\nabla \sum_{i=1}^{s^*} t_i^*\left(f\left(z^*, \bar{y}_i^*\right) - \lambda^* h\left(z^*, \bar{y}_i^*\right)\right) + \nabla^2 \sum_{i=1}^{s^*} t_i^*\left(f\left(z^*, \bar{y}_i^*\right) - \lambda^* h\left(z^*, \bar{y}_i^*\right)\right) p^*\right.$$
$$\left. + \nabla \sum_{j=1}^{m} \mu_j^* g_j\left(z^*\right) + \nabla^2 \sum_{j=1}^{m} \mu_j^* g_j\left(z^*\right) p^*\right],$$

which along with (1), implies:

$$\sum_{i=1}^{s^*} t_i^*\left(f\left(x^*, \bar{y}_i^*\right) - \lambda^* h\left(x^*, \bar{y}_i^*\right)\right) - \sum_{i=1}^{s^*} t_i^*\left(f\left(z^*, \bar{y}_i^*\right) - \lambda^* h\left(z^*, \bar{y}_i^*\right)\right) - \sum_{j=1}^{m} \mu_j^* g_j\left(z^*\right)$$
$$+\frac{1}{2} p^{*T} \nabla^2 \sum_{i=1}^{s^*} t_i^*\left(f\left(z^*, \bar{y}_i^*\right) - \lambda^* h\left(z^*, \bar{y}_i^*\right)\right) p^* + \frac{1}{2} p^{*T} \nabla^2 \sum_{j=1}^{m} \mu_j^* g_j\left(z^*\right) p^* > 0$$

which contradicts (5). Hence $z^* = x^*$.

SECOND DUALITY MODEL

Now, we consider the following dual for (P) and establish weak, strong and strict converse duality theorems:

$$\textbf{(GMD)} \qquad \max_{(s,t,\bar{y})\in K(z)} \quad \sup_{(z,\mu,\lambda,p)\in H_2(s,t,\bar{y})} \lambda,$$

where $H_2(s,t,\bar{y})$ denotes the set of all $(z,\mu,\lambda,p)\in R^n\times R^m_+\times R_+\times R^n$ satisfying:

$$\nabla\sum_{i=1}^{s}t_i\big(f(z,\bar{y}_i)-\lambda h(z,\bar{y}_i)\big)+\nabla^2\sum_{i=1}^{s}t_i\big(f(z,\bar{y}_i)-\lambda h(z,\bar{y}_i)\big)p$$
$$+\nabla\sum_{j=1}^{m}\mu_j g_j(z)+\nabla^2\sum_{j=1}^{m}\mu_j g_j(z)p=0, \tag{6}$$

$$\sum_{i=1}^{s}t_i\big(f(z,\bar{y}_i)-\lambda h(z,\bar{y}_i)\big)+\sum_{j\in J_0}\mu_j g_j(z)$$
$$-\frac{1}{2}p^T\nabla^2\left[\sum_{i=1}^{s}t_i\big(f(z,\bar{y}_i)-\lambda h(z,\bar{y}_i)\big)+\sum_{j\in J_0}\mu_j g_j(z)\right]p\geq 0, \tag{7}$$

$$\sum_{j\in J_\alpha}\mu_j g_j(z)-\frac{1}{2}p^T\nabla^2\sum_{j\in J_\alpha}\mu_j g_j(z)p\geq 0,\quad \alpha=1,2,\dots,r, \tag{8}$$

where $J_\alpha\subseteq M$, $\alpha=0,1,2,\dots,r$, with $\bigcup_{\alpha=0}^{r}J_\alpha=M$ and $J_\alpha\cap J_\beta=\phi$ if $\alpha\neq\beta$. If, for a triplet $(s,t,\bar{y})\in K(z)$, the set $H_2(s,t,\bar{y})=\phi$, then we define the supremum over it to be -∞.

Theorem 5 (Weak duality). *Let* x *and* $(z,\mu,\lambda,s,t,\bar{y},p)$ *be the feasible solutions of* (P) *and* (GMD) *respectively. Assume that* $\left[\sum_{i=1}^{s}t_i\big(f(\cdot,\bar{y}_i)-\lambda h(\cdot,\bar{y}_i)\big)+\sum_{j\in J_0}\mu_j g_j(\cdot),\ \sum_{j\in J_\alpha}\mu_j g_j(\cdot),\ \alpha=1,2,\dots,r\right]$ *is second order pseudoquasi Type I at* z*, with* $\eta(x,z)>0$*. Then*

$$\sup_{y\in Y}\frac{f(x,y)}{h(x,y)}\geq\lambda.$$

Proof. Suppose it is contrary to the result that $\sup_{y\in Y}\dfrac{f(x,y)}{h(x,y)}<\lambda$.

Thus, we have $f(x,\bar{y}_i)-\lambda h(x,\bar{y}_i)<0$ for all $\bar{y}_i\in Y(x),\ i=1,2,\dots,s.$

It follows from $t_i\geq 0,\ i=1,2,\dots,s,$ that $t_i\big(f(x,\bar{y}_i)-\lambda h(x,\bar{y}_i)\big)\leq 0$,

with at least one strict inequality since $t=(t_1,t_2,\dots,t_s)\neq 0$. Taking summation over i and using $\sum_{i=1}^{s}t_i=1$, we have: $\sum_{i=1}^{s}t_i\big(f(x,\bar{y}_i)-\lambda h(x,\bar{y}_i)\big)<0$.

The above inequality, together with the feasibility of x for (P), $\mu\geq 0$ and (7), implies:

$$\sum_{i=1}^{s}t_i\big(f(x,\bar{y}_i)-\lambda h(x,\bar{y}_i)\big)+\sum_{j\in J_0}\mu_j g_j(x)<0\leq\sum_{i=1}^{s}t_i\big(f(z,\bar{y}_i)-\lambda h(z,\bar{y}_i)\big)+\sum_{j\in J_0}\mu_j g_j(z)$$
$$-\frac{1}{2}p^T\nabla^2\left[\sum_{i=1}^{s}t_i\big(f(z,\bar{y}_i)-\lambda h(z,\bar{y}_i)\big)+\sum_{j\in J_0}\mu_j g_j(z)\right]p. \tag{9}$$

Also from (8), we have:

$$-\sum_{j\in J_0}\mu_j g_j(z)+\frac{1}{2}p^T\nabla^2\sum_{j\in J_0}\mu_j g_j(z)p\leq 0,\quad \alpha=1,2,\dots,r. \tag{10}$$

The inequalities (9), (10) and the second order pseudoquasi Type I assumption on $\left[\sum_{i=1}^{s} t_i\left(f(\cdot,\bar{y}_i)-\lambda h(\cdot,\bar{y}_i)\right)+\sum_{j\in J_0}\mu_j g_j(\cdot),\ \sum_{j\in J_\alpha}\mu_j g_j(\cdot),\ \alpha=1,2,\dots,r\right]$ at z implies:

$$\eta^T(x,z)\left[\nabla\sum_{i=1}^{s} t_i\left(f(z,\bar{y}_i)-\lambda h(z,\bar{y}_i)\right)+\nabla^2\sum_{i=1}^{s} t_i\left(f(z,\bar{y}_i)-\lambda h(z,\bar{y}_i)\right)p\right.$$
$$\left.+\nabla\sum_{j\in J_0}\mu_j g_j(z)+\nabla^2\sum_{j\in J_0}\mu_j g_j(z)p\right]<0,$$

$$\eta^T(x,z)\left[\nabla\sum_{j\in J_\alpha}\mu_j g_j(z)+\nabla^2\sum_{j\in J_\alpha}\mu_j g_j(z)p\right]\le 0,\quad \alpha=1,2,\dots,r.$$

Combining these inequalities with $\eta(x,z)>0$, we get:

$$\nabla\sum_{i=1}^{s} t_i\left(f(z,\bar{y}_i)-\lambda h(z,\bar{y}_i)\right)+\nabla^2\sum_{i=1}^{s} t_i\left(f(z,\bar{y}_i)-\lambda h(z,\bar{y}_i)\right)p$$
$$+\nabla\sum_{j=1}^{m}\mu_j g_j(z)+\nabla^2\sum_{j=1}^{m}\mu_j g_j(z)p<0,$$

which contradicts (6). This completes the proof.

Theorem 6 (Strong duality). *Assume that x^* is an optimal solution of* (P) *and $\nabla g_j(x^*)$, $j\in J(x^*)$ are linearly independent. Then there exist $(s^*,t^*,\bar{y}^*)\in K(x^*)$ and $(x^*,\mu^*,\lambda^*,p^*=0)\in H_2(s^*,t^*,\bar{y}^*)$ such that $(x^*,\ \mu^*,\lambda^*,s^*,t^*,\bar{y}^*,p^*=0)$ is a feasible solution of* (GMD) *and the two objectives have the same values. Further, if the hypothesis of Theorem 5 (weak duality) holds for all feasible solutions $(z,\mu,\lambda,s,t,\bar{y},p)$ of* (GMD), *then $(x^*,\ \mu^*,\lambda^*,s^*,t^*,\bar{y}^*,p^*=0)$ is an optimal solution of* (GMD).

Proof: The proof of the above theorem is similar to that of Theorem 3 and hence omitted.

Theorem 7 (Strict converse duality). *Let x^* and $(z^*,\mu^*,\lambda^*,s^*,t^*,\bar{y}^*,p^*)$ be the optimal of* (P) *and* (GMD) *respectively. Suppose that $\left[\sum_{i=1}^{s^*} t_i^*\left(f(\cdot,\bar{y}_i^*)-\lambda^* h(\cdot,\bar{y}_i^*)\right)+\sum_{j\in J_0}\mu_j^* g_j(\cdot),\ \sum_{j\in J_\alpha}\mu_j^* g_j(\cdot),\quad \alpha=1,2,\dots,r\right]$ is second order strictly pseudoquasi Type I at z^*, and $\nabla g_j(x^*)$, $j\in J(x^*)$ are linearly independent. Then $z^*=x^*$, i.e. z^* is an optimal solution of* (P).

Proof: It can be proved by a contradiction, applying Theorem 6.

CONCLUSIONS

We have established weak, strong and strict converse duality theorems for a class of generalised fractional minimax programming problems possessing some second-order Type-I invexity property. This paper extends earlier work in which duality results were obtained for a generalised fractional optimisation problem by applying a convexity assumption.

ACKNOWLEDGEMENTS

The authors are thankful to the referees whose comments improve the quality of the paper. The research of the first author was partially supported by the Indian School of Mines, Dhanbad, India under FRS (17)/2010-2011/AM.

REFERENCES

1. T. Weir, "A dual for multiobjective fractional programming problem", *J. Infor. Optim. Sci.*, **1986**, *7*, 261-269.
2. S. Chandra, B. D. Craven and B. Mond, "Generalized fractional programming duality: A ratio game approach", *J. Aust. Math. Soc. Ser. B*, **1986**, *28*, 170-180.
3. A. Charnes and W. W. Copper, "Goal programming and multiple objective optimization: Part I", *Eur. J. Oper. Res.*, **1977**, *1*, 39-54.
4. I. M. Stancu-Minasian and S. Tigan, "On some fractional programming models occurring in minimum-risk problems", *Lect. Notes Econ. Math. Syst.*, **1990**, *345*, 295-324.
5. A. Cambini, E. Castagnoli, L. Martein, P. Mazzoleni and S. Schaible (Eds.), "Generalized convexity and fractional programming with economics applications", Proceedings of International Workshop on Generalized Concavity, Fractional Programming and Economics Applications, **1988**, Pisa, Italy.
6. J. V. Neumann, "A model of general economic equilibrium", *Rev. Econ. Stud.*, **1945**, *13*, 1-9.
7. I. M. Stancu-Minasian, "Fractional Programming: Theory, Methods and Applications", Springer Publishing, New York, **1997**.
8. S. R. Yadav and R. N. Mukherjee, "Duality for fractional minimax programming problems", *J. Aust. Math. Soc. Ser. B*, **1990**, *31*, 484-492.
9. S. Chandra and V. Kumar, "Duality in fractional minimax programming", *J. Aust. Math. Soc. Ser. A*, **1995**, *58*, 376-386.
10. X. M. Yang and S. H. Hou, "On minimax fractional optimality and duality with generalized convexity", *J. Global Optim.*, **2005**, *31*, 235-252.
11. I. Ahmad and Z. Husain, "Duality in nondifferentiable minimax fractional programming with generalized convexity", *Appl. Math. Comput.*, **2006**, *176*, 545-551.
12. I. Ahmad, Z. Husain and S. Sharma, "Second order duality in nondifferentiable minimax programming involving type I functions", *J. Comput. Appl. Math.*, **2008**, *215*, 91-102.
13. I. Ahmad, Z. Husain and S. Sharma, "Higher-order duality in nondifferentiable minimax programming with generalized type I functions", *J. Optim. Theory Appl.*, **2009**, *141*, 1-12.
14. I. Ahmad, "On second-order duality for minimax fractional programming problems with generalized convexity", *Abstr. Appl. Anal.*, **2011**, Article no. 563924.
15. I. Ahmad, S. K. Gupta, N. Kailey and R. P. Agarwal, "Duality in nondifferentiable minimax fractional programming with *B*-(*p*, *r*)-invexity", *J. Inequal. Appl.*, **2011**, *2011*, 75.
16. C. R. Bector, S. Chandra and I. Hussain, "Second order duality for a minimax programming problem", *Opsearch*, **1991**, *28*, 249-263.
17. I. Husain, M. A. Hanson and Z. Jabeen, "On nondifferentiable fractional minimax programming", *Eur. J. Oper. Res.*, **2005**, *160*, 202-217.

18. Q. Hu, Y. Chen and J. Jian, "Second-order duality for non-differentiable minimax fractional programming", *Int. J. Comp. Math.*, **2012**, *89*, 11-16.
19. A. Jayswal, "Non-differentiable minimax fractional programming with generalized α -univexity", *J. Comput. Appl. Math.*, **2008**, *214*, 121-135.
20. H. C. Lai, J. C. Liu and K. Tanaka, "Necessary and sufficient conditions for minimax fractional programming", *J. Math. Anal. Appl.*, **1999**, *230*, 311-328.
21. H. C. Lai and J. C. Lee, "On duality theorems for a nondifferentiable minimax fractional programming", *J. Comput. Appl. Math.*, **2002**, *146*, 115-126.
22. J. C. Liu, "Second order duality for minimax programming", *Util. Math.*, **1999**, *56*, 53-63.
23. S. Sharma and T. R. Gulati, "Second order duality in minmax fractional programming with generalized univexity", *J. Global Optim.*, **2012**, *52*, 161-169.
24. O. L. Mangasarian, "Second- and higher-order duality in nonlinear programming", *J. Math. Anal. Appl.*, **1975**, *51*, 607-620.
25. B. Mond, "Second order duality for nonlinear programs", *Opsearch*, **1974**, *11*, 90-99.
26. I. Ahmad and Z. Husain, "Second order $\left(F,\alpha,\rho,d\right)$-convexity and duality in multiobjective programming", *Inform. Sci.*, **2006**, *176*, 3094-3103.
27. Z. Husain, I. Ahmad and S. Sharma, "Second order duality for minimax fractional programming", *Optim. Lett.*, **2009**, *3*, 277-286.
28. J. C. Liu and C. S. Wu, "On minimax fractional optimality conditions with invexity", *J. Math. Anal. Appl.*, **1998**, *219*, 21-35.

Maejo Int. J. Sci. Technol. **2013**, *7*(01), 155-165

Maejo International Journal of Science and Technology

ISSN 1905-7873
Available online at www.mijst.mju.ac.th

Communication

Factors influencing dietary supplement consumption: A case study in Chiang Mai, Thailand

Wiwat Wangcharoen [1,*], Doungporn Amornlerdpison [2] and Kriangsak Mengumphan [2]

[1] Faculty of Engineering and Agricultural Industry, Maejo University, Chiang Mai 50290, Thailand
[2] Faculty of Fisheries Technology and Aquatic Resources, Maejo University, Chiang Mai 50290, Thailand
* Corresponding author, e-mail: wiwat@mju.ac.th

Received: 30 October 2011 / Accepted: 20 April 2013 / Published: 26 April 2013

Abstract: A consumer survey on dietary supplement consumption was carried out on 494 consumers aged 20 years and older in Chiang Mai province. The percentage of consumers who regularly consumed dietary supplements was 38.5%. Vitamins and minerals were the most consumed products, followed by functional drinks, functional foods, protein extracts, dietary fibre, cod liver oil, phytochemicals, algae products, fat absorbers, fish oils and bee products in that order. Females and participants who had recommended waistlines, had higher income, usually felt stressed or sick, and who preferred eating fruits/vegetables or routinely drank water tended to have a higher rate of consumption of dietary supplements. Participants gave priority over a product with guaranteed quality when they made decision to purchase dietary supplements, but their purchase was also influenced by the attractiveness of the product and advertisement for it.

Key words: dietary supplement, consumption of dietary supplements, consumer survey

---

INTRODUCTION

Good health is what many consumers desire. The cost of health care is continuing to rise and as a consequence consumers are more and more interested in their health and in seeking alternative forms of medicine [1-3]. This trend is reflected in an increase in dietary supplement and herbal product consumption [4]. International sales of dietary supplements were forecasted to reach USD 24.22 billion in 2011 and USD 29.75 billion by 2015 [5]. Dietary supplement sales in Thailand in 2011 were estimated at 27,000 million Baht with a 10-12% annual rate of growth [6]. About 80% of the products are marketed through the method of direct sale [7].

Dietary supplement consumption may be associated with demographic factors [8-9], health-related characteristics [8-10], psychological factors [11] and an incidence of disease [12]. The prevalence of dietary supplement consumption varies with any given population, the definition of supplements, the definition of what constitutes regular supplement usage [3], the time period of the survey and the changing demographics in the period [13]. Those who are female, have an education beyond high school, earn higher levels of income, are older, are self-employed, have a lower body mass index, participate in physical activities, consume greater fruits and/or vegetables, eat less fat, take less prepared foods, like to eat out, have higher stress levels, are a non-smoker, and consume moderate or no amount of alcohol tend to be faithful users of supplements [8-10] though not in all cases [3]. In addition, although supplement users tend to be more educated, no correlation is found between supplement consumption and nutritional knowledge [13].

In Thailand, dietary supplement products are controlled by the Notifications of Ministry of Public Health No. 293 [14] and No. 309 [15]. They are defined as products that are taken or consumed in addition to conventional foods, and which contain nutrients or other substances as ingredients and are in the forms of tablet, capsule, powder, flake, liquid or others, but which are not considered conventional foods, being for consumers who expect benefits of health promotion [14]. Moreover, there must be clear wording on the product label stating that 'individuals should regularly take a varied diet that includes the 5 essential nutrients in appropriate portions' and that 'there is no guarantee of the prevention or cure of diseases' [15].

Since most dietary supplement products in Thailand are marketed by direct sales, the most important factor influencing dietary supplement consumption is the direct selling strategy, especially face-to-face selling and network marketing [16]. Face-to-face selling allows the salespeople to build a relationship with the customers, earn their trust, judge their response and tailor their sales pitch to suit each individual customer [17]. Network marketing lets the salespeople persuade customers into becoming their downstream agents, who will be awarded with bonuses according to the number of people in their own downstream and the sale performance of their entire network [18].

The purpose of this survey-based study is to identify consumer characteristics which are associated with dietary supplement consumption and also the factors influencing the purchase of dietary supplements by consumers who are aged 20 years or older in Chiang Mai, using some multivariate statistics, namely binary logistic regression, principal component analysis and discriminant analysis.

MATERIALS AND METHODS

Participants and Survey Instrument

The participants consisted of adults aged 20 years or older residing in Chiang Mai province. They were divided into 4 age groups: 20-29, 30-39, 40-49 and 50 years or older, and each age group contained at least 50 males and 50 females.

A questionnaire was designed to collect data on demographics, dietary supplement consumption, behaviour related to health and factors influencing dietary supplement purchase. A pretest was conducted using 12 volunteers to evaluate the clarity of the survey queries. The improved questionnaire and 8 trained interviewers were used to collect data from 494 participants between July-August 2011.

Statistical Analysis

Collected data were first analysed by descriptive statistics including frequency, percentage, mean and standard deviation. Some multivariate statistics were also used. Binary logistic regression was used to identify demographic factors associated with dietary supplement consumption. Principal component analysis was employed to group behaviour related to health and factors influencing dietary supplement purchasing. Differentiation of users and non-users of dietary supplements was made by discriminant analysis using the same behaviours and factors. All analysis was done by SPSS 16.0 Family.

RESULTS AND DISCUSSION

According to the survey on the participants' demographics and data on dietary supplement use (Table 1), almost 40% of the participants had a higher body mass index than is considered appropriate (18.5-22.9 kg/m^2) and about 30% of them had longer waistlines than the recommended values ($\leq$ 90 cm for males and $\leq$ 80 cm for females). These results agree with a report of the Bureau of Policy and Strategy, Office of the Permanent Secretary, which states that 1 in 3 people have a risk of visceral obesity [19]. Its concern is related to the fact that excess abdominal fat is associated with chronic non-communicable diseases such as diabetes, hypertension, vascular and heart diseases, and cancer. In this survey, hypertension was found to be the most common congenital disease.

In this survey 38.5% of the participants reported that they regularly consumed dietary supplements. In two previous surveys that were conducted in 2008, a year well within the period of the Thai economic crisis [20], the first, conducted in Nakhon Ratchasima, reported that only 14.2% of the participants, including those under 20 years old, consumed dietary supplements [21]. The second study was an online survey which showed that 66% of the Thai participants consumed dietary supplements [22], although there were only 34.6% of participants in this study who used the internet, and most of them were aged between 20-29 (51.8%) and 30-39 (24.7%) and held a Bachelor's degree or higher (86.5%). The differences between the three surveys can probably be attributed to differences in the participants who were recruited for the respective studies, if the period of time between studies is neglected.

In this study, about 80% of dietary supplement users purchased products for themselves with an average monthly purchase of 1,046.8 Baht. Vitamins and minerals were the most consumed dietary supplements, which matches the study in Nakon Ratchasima [21]. The following items were found to be the next most commonly consumed dietary supplements: functional drinks, functional foods, protein extracts, dietary fibre, cod liver oil, phytochemicals, algae products, fat absorbers, fish oils and bee products in that order. The reasons given by non-users for not consuming dietary supplements were: the products are unnecessary and have a high price tag; the claims (benefits) made for the products are incredible and thus undesirable; the products are not palatable; and the products are not in an interesting form.

Table 1. Abridged characteristics and dietary supplement consumption of consumers

Characteristic	Description	Frequency	Per cent
Gender	Male	246	49.8
	Female	248	50.2
Age (years)	20 - 29	131	26.5
	30 - 39	123	24.9
	40 - 49	120	24.3
	50 and over	120	24.3
Marital status	Single	231	46.8
	Married	258	52.2
	Others	5	1.0
Body mass index (kg/m^2)	18.5 or less	63	12.8
	18.5 - 22.9	235	47.6
	23.0 - 24.9	70	14.2
	25.0 - 29.9	105	21.3
	30 or more	21	4.3
Waistline (cm)	Male $\leq$ 90, Female $\leq$ 80	343	69.4
	Male > 90, Female > 80	151	30.6
Education	Primary education	82	16.6
	Secondary education	87	17.6
	Diploma / certificate	49	9.9
	Bachelor degree	239	48.4
	Master degree or higher	31	6.3
	Others	6	1.2
Monthly income (Baht)	5,000 or less	110	22.3
	5,001 - 10,000	197	39.9
	10,001 - 15,000	85	17.2
	15,001 - 20,000	49	9.9
	20,001 or more	53	10.7
Congenital disease	Yes	104	21.1
	No	327	66.2
	Do not know	63	12.7
Congenital disease list (per cent based on 104)	Hypertension	38	36.5
	Allergy	26	25
	Gastrointestinal problem	20	19.2
	Diabetes	17	16.3
	Respiratory problem	8	7.7
	Coronary heart disease	5	4.8
	Others	6	5.8

Table 1. (continued)

Characteristic	Description	Frequency	Per cent
Dietary supplement consumption	Yes	190	38.5
	No	304	61.5
Dietary supplement list (per cent based on 190)	Vitamins and minerals	78	41.1
	Functional drinks	62	32.6
	Functional foods	56	29.5
	Protein extracts	41	21.6
	Dietary fibre	35	18.4
	Cod liver oil	34	17.9
	Phytochemicals	30	15.8
	Algae products	20	10.5
	Fat absorbers	18	9.5
	Fish oil	18	9.5
	Bee products	12	6.3
Dietary supplement purchase by oneself (per cent based on 190)	Yes	155	81.6
	No	35	18.4
Monthly purchase of dietary supplement (Baht) (per cent based on 155) Mean = 1,046.8	500 or less	60	38.7
	501 - 1,000	40	25.8
	1,001 - 1,500	25	16.1
	1,501 - 2,000	19	12.3
	2,001 - 3,000	5	3.2
	3,001 or more	6	3.9
Reasons for not consuming dietary supplement (per cent based on 304)	Not necessary	127	41.8
	High price	86	28.3
	Undesirable product	63	20.7
	Incredible health benefit	55	18.1
	Unpalatable	26	8.6
	Uninteresting product form	22	7.2

In binary logistic regression, dietary supplement consumption is used as dependent variable and demographic factors (gender, age, marital status, body mass index, waistline, education, monthly income and congenital disease) are used as independent predictors. Gender, waistline and income are found to be significantly different ($p \leq 0.10$). Females, participants who have recommended waistline and those with higher income tend to have higher consumption of dietary supplements as shown by the odds ratios in Table 2. The odds ratio is a way of determining whether the probability of a certain event is the same for two groups, i.e. reference and compared groups. An odds ratio of 1 implies that the event is equally likely in both groups, while an odds ratio greater than one implies that the event is more likely in the reference group, and an odds ratio less than one implies that the event is less likely in the reference group [23].

Table 2. Demographic factors associated with dietary supplement consumption (n = 494)

Factor	Odds ratio*	95% Confident interval	P value
Gender			0.000
Male	1.00		
Female	1.95	1.35 – 2.82	
Waistline (cm)			0.096
Male < 90, Female < 80	1.41	0.94 – 2.11	
Male > 90, Female > 80	1.00		
Monthly income (Baht)			0.026
5,000 or less	1.00		
5,001 - 10,000	1.62	0.97 – 2.71	
10,001 - 15,000	2.15	1.17 – 3.93	
15,001 - 20,000	3.08	1.52 – 6.23	
20,001 or more	3.31	1.45 – 7.55	

* Odds ratio greater than one implies that the consumption is more likely in the reference group (1.00)

Consumer behaviours related to health are expressed in Table 3 and are analysed by principal component analysis. Twelve measurements of behaviour can be reduced to 5 independent principal components (PCs) that explain 60.0% of the variance. The numbers in each PC column in Table 3 are the PC loadings, i.e. the regression correlations between behaviour and PC, and they are used together with the participants' data to compute the PC score of each participant [24]. Thus, 3 meals a day, exercise and sport, sufficient sleep and annual health checkup are all highly related to PC1. Feeling stressed and being sick are highly related to PC2. Consumption of fruits/vegetables and drinking of water are highly related to PC3. Drinking of alcoholic beverages and smoking are highly related to PC4, and consumption of spicy and instant or processed foods are highly related to PC5. Since all high factor loadings are positive numbers, this means that participants have the same pattern for all forms of behaviour which are highly related to each PC. For example, participants who have 3 meals a day tend to get exercise or play sports, have sufficient sleep and have annual health checkup (PC1).

To differentiate users and non-users of dietary supplements, the PC scores of all participants are used as independent predictors and the dietary supplement consumption is used as dependent variable in the discriminant analysis. A significant discriminant function ($p \leq 0.05$) for predicting dietary supplement consumption of the participants with 59.7% of correct classification is found and the mean scores of users and non-users are 0.272 and -0.173 respectively. The following equation is the discriminant function:

$$\text{Discriminant score} = 0.007 - 0.085\ PC1 + 0.748\ PC2 + 0.626\ PC3 - 0.134\ PC4 - 0.267\ PC5$$

Table 3. Consumer self-rating on their own behaviours related to health and the results of grouping by principal component analysis (n = 494)

Behaviour	Mean[a] ± S.D.	PC1[b] (13.9%)	PC2[b] (11.9%)	PC3[b] (11.8%)	PC4[b] (11.3%)	PC5[b] (11.1%)
Have 3 meals a day (breakfast, lunch, dinner)	3.77±1.07	0.663	-0.190	-0.116	-0.047	0.308
Prefer spicy foods	3.16±1.08	-0.147	-0.022	0.165	0.193	0.759
Prefer instant or processed foods	2.57±0.93	0.015	0.313	0.042	0.006	0.676
Prefer fruits/vegetables	3.80±0.91	0.147	0.108	0.798	-0.127	0.105
Prefer drinking water to other drinks	3.75±0.97	0.252	-0.163	0.748	-0.026	0.015
Drink alcoholic beverage	2.30±1.12	-0.057	0.136	0.051	0.844	0.039
Smoke	1.53±1.02	0.115	0.014	-0.024	0.790	-0.019
Get exercise and play sport	2.74±0.97	0.593	0.194	0.199	0.077	-0.120
Have sufficient sleep	3.37±0.90	0.703	-0.094	0.226	0.108	0.079
Feel stressed	2.90±1.00	-0.124	0.789	0.144	0.152	0.114
Be sick	2.31±0.85	0.189	0.784	-0.204	0.019	0.082
Have annual health checkup	2.40±1.21	0.554	0.259	0.290	-0.154	-0.083

[a] 5 = very much or always, 4 = much, 3 = moderate, 2 = little, 1 = very little or never
[b] Numbers in each PC column are the correlation coefficients between behaviours and PCs; each PC accounts for its strong correlated behaviours (>|0.5|), and the PC percentage is the explained variance (13.9+11.9+11.8+11.3+11.1 = 60%).

Since good predictors tend to have a large discriminant coefficient [25], PC2 and PC3 may be considered good predictors. This means that behaviours which are highly related to PC2 and PC3 may also be considered as good predictors. Thus, participants who feel stressed and are sick and who prefer fruits/vegetables and drinking of water tend to be users of dietary supplements. Correctly classified cases for this discriminant function are found to be only 59.7%, because there are other factors that influence dietary supplement consumption, such as demographic characteristics, some of which are found in the binary logistic regression.

Factors influencing dietary supplement purchasing in Table 4 are analysed by principal component analysis. Ten factors are reduced to 2 independent PCs, which explain 58.3% of the variance and PC loadings for each original factor are shown in Table 4. Health benefits of product, Thai FDA sign, well-known manufacturer/brand, type and quantity of active ingredients and supporting research are highly related to PC1, while attractive advertising, attractive product/packaging, palatability, and ease of consuming and carrying are highly related to PC2. Thus, PC1 represents guarantee of product quality and PC2 represents product attractiveness and advertising. From this analysis, it seems that price is less correlated with dietary supplement purchasing than product quality and product attractiveness and advertising. Acceptable price might be a variable of many factors since it was not highly related with any PC by principal component analysis [24].

Table 4. Factors influencing dietary supplement purchase and results of grouping by principal component analysis (n = 494)

Factor	Mean[a] $\pm$ S.D.	PC1[b] (30.7%)	PC2[b] (27.6%)
Health benefits of product	4.01$\pm$0.87	0.859	0.070
Thai FDA sign	4.17$\pm$0.85	0.841	0.083
Well-known manufacturer/brand	3.84$\pm$0.93	0.599	0.427
Attractive advertising	3.41$\pm$0.94	0.192	0.724
Attractive product/packaging	3.41$\pm$0.91	0.133	0.793
Palatability	3.40$\pm$1.04	0.151	0.719
Ease of consuming and carrying	3.61$\pm$0.97	0.309	0.690
Type and quantity of active ingredients	3.96$\pm$0.96	0.723	0.377
Supporting research	3.89$\pm$0.92	0.656	0.403
Price	3.67$\pm$0.97	0.372	0.349

[a] 5 = extremely important, 4 = very important, 3 = moderately important, 2 = slightly important, 1 = not important
[b] Numbers in each PC column are the correlation coefficients between factors and PCs; each PC accounts for its strong correlating factors (> $|0.5|$), and the PC percentage is the explained variance (30.7+27.6 = 58.3%).

In the discriminant analysis the PC scores for all participants computed from PC loadings in Table 4 are used as independent predictors and dietary supplement consumption is used as dependent variable. A non-significant discriminant function ($p>0.05$) for predicting dietary supplement consumption of the participants is found and the mean scores of users and non-users are 0.089 and -0.057 respectively. This result means that there is no significant difference between users and non-users regarding factors influencing dietary supplement purchase. This discriminant function is expressed by the following equation:

Discriminant score = -0.003 + 0.882 PC1 + 0.470 PC2

Although this discriminant analysis cannot distinguish between dietary supplement users and non-users, the large discriminant coefficients for both PCs show that both the product quality and product attractiveness can be good predictors, although the weight of the former is greater. This means that participants concentrate on the quality of dietary supplement rather than its attractiveness. As with previous studies of Bower et al. [26], Walker et al. [27] and Khongjeamsiri et al. [28], the purchase intention of functional foods significantly increases ($p\leq0.05$) when consumers become aware of special health benefits of the products. However, consumer awareness could come from the advertisement for a product or from other sources without a scientific proof. In addition, the Thai FDA logo, which is used to guarantee the quality and safety of a product [29], could make some consumers believe in its health benefits. Kim et al. [13] showed that there was no correlation between dietary supplement consumption and nutritional knowledge, and Aungapipatra et al. reported that there were misunderstandings regarding dietary supplement products [21].

CONCLUSIONS

From this survey, 30-40% of the participants aged 20 years or older could be considered overweight with excess abdominal fat indicated by the waistline and body mass index, and 38.5% of the participants consumed dietary supplements. Multivariate statistics can provide more and easier-to-understand information on consumers considered to be dietary supplement users and on the factors influencing their dietary supplement purchase. The following have been shown to be the characteristics of dietary supplement consumers: being female, people with recommended waistlines and those who have higher income, while their behaviours include feeling stress or sick, routinely taking fruits/vegetables or routinely drinking water. In making decision to purchase dietary supplements, consumers concentrate on product quality rather than attractiveness and advertisement, whilst an acceptable price of product seems to be influenced by many factors.

ACKNOWLEDGEMENTS

The authors are grateful to the National Research Council of Thailand (NRCT) for the funding of this project and sincerely thank all participants in this survey as well as the Faculty of Engineering and Agricultural Industry and the Faculty of Fisheries Technology and Aquatic Resources, Maejo University for providing some of the facilities required.

REFERENCES

1. D. M. Eisenberg, R. B. Davis, S. L. Ettner, S. Appel, S. Wilkey, M. Van Rompay and R. C. Kessler, "Trends in alternative medicine use in the United States, 1990-1997: Results of a follow-up national survey", *J. Am. Med. Assoc.*, **1998**, *280*, 1569-1575.
2. L. Gilbert, "HealthFocus Trend Report: 1999", HealthFocus, DesMoines (IA), **1999**.
3. J. L. Greger, "Dietary supplement use: Consumer characteristics and interests", *J. Nutr.*, **2001**, *131*, 1339s-1343s.
4. Nutraceuticals World, "Dietary supplements 2010: Despite globalization issues, scientific validation concerns, potentially restrictive regulations, rocky economics and an uneasy healthcare system, the dietary supplement market continues to grow", **2010**, http://www.nutraceuticalsworld.com/issues/2010-04/view_features/dietary-supplements-2010/ (Accessed: October 2010).
5. P. Lertwilai, "NIA supports the innovation of dietary supplement" (in Thai), **2011**, http://eureka.bangkokbiznews.com/detail/409241 (Accessed: October 2011).
6. K. Ritteerawee, "Dietary supplement market reaches 27,000 million baht" (in Thai), **2011**, http://www.posttoday.com/ธุรกิจ/ตลาด-1091102อาหรเสริมโต/-7หมื่นล. (Accessed: October 2011).
7. Food Intelligence Center, "Dietary supplement" (in Thai), **2009**, http://fic.nfi.or.th/th/thaifood/product52-dietary.asp. (Accessed: September 2011).
8. M. J. Slesinski, A. F. Subar and L. L. Kahle, "Trends in use of vitamin and mineral supplements in the United States: The 1987 and 1992 national health interview surveys", *J. Am. Diet. Assoc.*, **1995**, *95*, 921-923.

9. B. J. Lyle, J. A. Mares-Perlman, B. E. Klein, R. Klein and J. L. Greger, "Supplement users differ from non users in demographic, lifestyle, dietary and health characteristics", *J. Nutr.*, **1998**, *128*, 2355-2362.
10. R. E. Patterson, M. L. Neuhouser, E. White, J. R. Hunt and A. R. Kristal, "Cancer-related behavior of vitamin supplement users", *Cancer Epidemiol. Biomark. Prev.*, **1998**, *7*, 79-81.
11. M. A. Read, R. L. Burnner, G. Miller, S. T. St Jero, B. Scott and T. P. Carmody, "Relationship of vitamin/mineral supplementation to certain psychologic factors", *J. Am. Diet. Assoc.*, **1991**, *91*, 1429-1431.
12. J. Ishihara, T. Sobue, S. Yamamoto, S. Sasaki and S. Tsugane, "Demographics, lifestyles, health characteristics, and dietary intake among dietary supplement users in Japan", *Int. J. Epidemiol.*, **2003**, *32*, 546-553.
13. E. H. Kim, K. M. Schroeder, R. F. Houser and J. T. Dwyer, "Two small surveys, 25 years apart, investigating motivations of dietary choice in 2 groups of vegetarians in the Boston area", *J. Am. Diet. Assoc.*, **1999**, *99*, 598-601.
14. Notification of Ministry of Public Health No. 293 (B.E. 2548) Re. Food Supplements, **2005**, http://iodinethailand.fda.moph.go.th/fda/new/images/cms/top_upload/1169706519_no.293.pdf (Accessed: October 2011).
15. Notification of Ministry of Public Health No. 309 (B.E. 2550) Re. Food Supplements (2nd edition), **2007**, http://iodinethailand.fda.moph.go.th/fda/new/images/cms/top_upload/1224646506_Notification309.pdf (Accessed: October 2011).
16. Y. Tantipidok, P. Kasikum, R. Auttasita, O. Chetthakul and P. Suksuthi, "Alternative health system development in Thailand: Knowledge synthesis on health system reform" (in Thai), Research Report, Health System Research Institute, Nonthaburi**, 2000**.
17. K. O'Lone, "The importance of face to face selling", **2007**, http://www.helium.com/items/253979-the-importance-of-face-to-face-selling (Accessed: October 2011).
18. J. Y. Yen, M. L. Chen and Y. C. Chen, "The study of direct selling management strategies: An example of the Avon cosmetics company in Taiwan", *J. Int. Manag. Studies*, **2008**, *3*, 214-227.
19. Bureau of Policy and Strategy, Office of Permanent Secretary, "Health fact sheet: Hot issue of this week" (in Thai), **2010**, http://www.moph.go.th/ops/thp/images/stories/Report_pics/Thai_Report/HighLight/Y54/Issue_2.pdf (Accessed: October 2011).
20. J. Walsh, "Thai Khem Kaeng: An inadequate response by the Thai State to the impact of the 2008 economic crisis", *J. Econ. Behav. Studies*, **2010**, *1*, 1-8.
21. L. Aungapipatra, P. Limworawan and P. Panuwatsuk, "Consumption behaviour and understanding on dietary supplements of Thai people in the north-east part" (in Thai), *J. Bureau Alternat. Med.*,, **2008**, *1*, 37-45.
22. Bangkokbiznews, "Thai dietary supplement market is the first order ranked" (in Thai), **2009**, http://www.bangkokbiznews.com/home/detail/business/research/20090316/25027/81.html (Accessed: October 2011).
23. S. Simon, "What is an odds ratio?", **2008**, http://www.childrensmercy.org/stats/definitions/or.htm (Accessed: October 2011).
24. SAS, "Principal component analysis", (no date), http://support.sas.com/publishing/pubcat/chaps/55129.pdf (Accessed: October 2011).

25. SAGE Publication, "Chapter 25 Discriminant analysis", (no date), http://www.uk.sagepub.com/burns/website%20material/Chapter%2025%20-%20Discriminant%20Analysis.pdf (Accessed: October 2011).
26. J. A. Bower, M. A. Saadat and C. Whitten, "Effect of liking, information and consumer characteristics on purchase intention and willingness to pay more for a fat spread with a proven health benefit", *Food Qual. Prefer.*, **2003**, *14*, 65-74.
27. J. Walker, C. A. Boeneke, S. Sriwattana, J. A. Herrera-Corredor and W. Prinyawiwatkul, "Consumer acceptance and purchase intent of a novel low-fat sugar-free sherbet containing soy protein", *J. Food Qual.*, **2010**, *33*, 27-41.
28. W. Khongjeamsiri, W. Wangcharoen, S. Pimpilai and W. Daengprok, "Development of Job's tears ice cream recipes with carrot juice and pumpkin paste", *Maejo Int. J. Sci. Technol.*, **2011**, *5*, 390-400.
29. Food and Drug Administration Thailand, "Food control in Thailand", (no date), http://www.fda.moph. go.th/eng/food/details/foodControl.htm (Accessed: December, 2012).

Maejo Int. J. Sci. Technol. **2013**, *7*(01), 166-180

Maejo International Journal of Science and Technology

ISSN 1905-7873
Available online at www.mijst.mju.ac.th

Full Paper

Detecting drought stress in longan tree using thermal imaging

Winai Wiriya-Alongkorn[1,*], Wolfram Spreer[2,3], Somchai Ongprasert[4], Klaus Spohrer[2], Tanachai Pankasemsuk[1] and Joachim Müller[2]

[1] Department of Plant Science and Natural Resources, Chiang Mai University, Faculty of Agriculture, Chiang Mai 50200, Thailand

[2] Institute of Agricultural Engineering, Universität Hohenheim, 70593 Stuttgart, Germany

[3] Science and Technology Research Institute, Chiang Mai University, Chiang Mai 50200, Thailand

[4] Department of Soil Resources and Environment, Faculty of Agriculture, Mae Jo University, Chiang Mai 50290, Thailand

[*] Corresponding author, e-mail: cmuwinai54@hotmail.com; winai.w@mju.ac.th; tel.: +66 91-636-4456

Received: 6 July 2012 / Accepted: 24 April 2013 / Published: 29 April 2013

Abstract: Thailand is the world's number-one producer of longan fruit. In general, longan production takes place during the dry season under irrigation. Recently, more attention has been given to water-efficient irrigation. Water stress detection by thermal imaging, which is a non-invasive and rapid assessment method, may be an interesting tool for improved irrigation planning. In this study, four potted longan trees were subjected to water stress. Stress responses in terms of stomatal resistance (r_s) and leaf water potential (LWP) were monitored and compared with a non-stressed control. Based on thermal imaging, the crop water stress index (CWSI) was determined throughout the experiment for all trees and correlations with classical parameters were investigated. A field experiment was also carried out with 20 field-grown longan trees, either subjected to water stress treatment or serving as controls; trees were monitored for r_s, LWP and CWSI. Under controlled conditions there was a high correlation between CWSI and both r_s and LWP during the entire experimental period. In the field experiment it was found that CWSI was best correlated with r_s when images were taken from the shaded side of the leaves. A threshold value of 0.7 for CWSI is proposed to distinguish between stressed and non-stressed longan trees.

Keywords: *Dimocarpus longan*, irrigation, crop water stress index, stomatal resistance, leaf water potential, thermal imaging, drought stress, longan tree

---

INTRODUCTION

Longan (*Dimocarpus longan* Lour.) is a perennial subtropical fruit tree indigenous to Southeast Asia. Together with lychee (*Litchi chinensis* Sonn.), it is the most popular member of the Sapindaceae family, which has over 2,000 species and 150 genera [1]. Even though longan flowering can reliably be induced through the application of potassium chlorate and thus production is possible all year round [2], presently about 80% of longan fruit is produced during the 'on-season', which starts with flowering in February and with fruits mainly harvested in July.

Longan trees are particularly sensitive to drought during the flowering and early fruit development stages [3]. Thus, irrigation management is crucial in growing regions which have a distinctly summer rainfall pattern [4]. As on-season flowering and fruit development coincides with the dry season in Thailand, high fruit yields can only be obtained using irrigation. Irrigation water requirements are calculated using a crop coefficient (k_c) of 0.83, based on empirical data from Diczbalis [5], or 0.85 as determined by Spohrer et al. [6] based on physiological measurements of lychee trees, assuming low evaporation (k_e = 0.05) as achieved by micro-irrigation. Since limited water resources create an obstacle for increased longan production, deficit irrigation strategies have recently been investigated. They are summarised in the following paragraph.

Experiments in commercial orchards in Thailand have shown that partial root-zone drying (PRD) with a replenishment by irrigation of 66% of the calculated evapotranspiration (ET_c) does not cause a significant reduction in yield or fruit quality as compared to a 100%-watered control [7]. As a result, under conditions of extreme drought, deficit irrigation can help to ensure stable yields, and lower irrigation water use can reduce electricity costs for water pumping even when water is cost-free [8]. In a previous study, PRD under controlled conditions (with 60% of ET_c) was applied to three-year-old longan trees grown under a plastic shelter. The trees subjected to PRD showed stunted vegetative growth without noticeable foliar wilt. During 28 weeks of the experiment, the control trees gave two flushes while those subjected to PRD gave only one flush but with a higher number of leaves and shorter shoots than those developed in the control during the first flush [9]. Furthermore, reduced concentrations of phosphorus and potassium were found in the leaf tissues of PRD-irrigated longan trees [10]. These findings on reduced biomass formation may indicate similar long-term effects in longan as have been reported for other tree species, such as the lower crown volume found in almonds [11], and the reduced root-biomass growth shown in peach trees [12]. However, other studies of mango under similar climatic conditions to those found in Thailand, which has an intensive rainy season, have not revealed any long-term negative impact on yields [13]. In the light of this, there is a need for more research on the response of longan trees to drought stress.

Plants under water stress close their stomata to reduce transpiration. The leaf temperature thus increases as a result of a lower evaporative cooling, which can be detected by infrared thermometry. To quantify the level of water stress by infrared thermometry, several methods have been reported. Idso et al. [14] proposed that the accumulated difference between air temperature (T_a) and canopy temperature (T_c) be considered for calculating stress degree days. This, however, does not take into account the vapour pressure deficit (VPD), net radiation or wind speed. Therefore, the 'crop water stress index' (CWSI) was introduced. The CWSI correlates canopy temperature to the upper (dry) and lower (wet) reference temperatures. It is inversely correlated with leaf water potential (LWP) [15]. Alternatively, the 'I_G-index' [16] can be calculated based on the same references. It is proportional to the stomatal conductance.

The introduction of thermal imaging has added new possibilities to stress detection by IR thermometry. Generally, the advantage of thermography is that a semi-automatic stress analysis of large areas of a canopy can be achieved with much more effective replication than when using porometry, thus providing great benefits for comparative studies such as screening activities [17]. As a consequence, the effective use of thermography for breeding purposes has been demonstrated under laboratory conditions for the identification of mutants [18], as well as for the phenotyping of rice under field conditions [19]. Results of greenhouse experiments with different ornamentals suggest that there is a potential use of thermal imaging for scheduling the deficit irrigation of hardy nursery stock [20].

Another promising application of thermal imaging in agriculture is in the development of precision irrigation as this process facilitates the mapping of water status variability [21]. As a result, variability maps can be developed from ground-based thermal imaging using, for example, cameras mounted on irrigation machines, which can then be correlated with aerial images [22, 23]. Due to the high costs and logistical requirements involved, the use of this technology has so far been restricted to industrialised countries. The practical application of thermal imaging in the field depends on obtaining reference data, which is crop-specific. Most studies on the application of thermal imaging so far have been carried out on grapevine [24, 25]. Further information is available on its use for annual crops such as wheat [26, 27], rice [19], maize [28] and cotton [22]. As for fruit trees, apple, peach [29] and olive [23, 30] have already been investigated using thermal imaging.

Longan, as a drought-sensitive plant, is expected to show a pronounced increase in leaf temperature as a result of stomatal closure, which could be reliably detected. The aim of this study is to ascertain the CWSI threshold appropriate for determining the presence of water stress, as well as the time of day and the level of image exposure most suitable for drought stress monitoring for longan trees.

MATERIALS AND METHODS

Plant Material and Irrigation Treatment

Pot experiment

One part of the experiment was carried out using potted longan trees kept under a transparent plastic shelter at Maejo University in San Sai district, Chiang Mai province, Thailand (18° 53’ N 99° 00’ E, 320 m above m.s.l.), from the 12^{th}-18^{th} of February 2009 during the dry season with a clear sky during the entire period of observation. Eight longan trees had been cultivated in sand culture for three years prior to the experiment. For the study, pots with a diameter of 35 cm were drained and the trees irrigated daily until drainage water was visible. A modified Hoagland solution [31] was applied as liquid fertiliser once a week. At the start of the experiment, the trees were subdivided into two groups: S_{dry} and S_{irri}. Irrigation was completely stopped for S_{dry} while S_{irri} served as a control and were continuously irrigated as prior to the experiment. No fertiliser was applied during the experimental period. The pots were positioned in one row in an east-west direction, alternating between treatment and control. To the south of the pots, a 3-m space enabled the taking of digital and thermal images, while to the north a black plastic sheet was hung at a distance of 50 cm behind the trees to serve as contrast.

Field experiment

The field experiments were carried out at Maejo University experimental station (18° 55' N, 99° 02' E, 380 m above m.s.l.), where the soil is a loamy sand and has an average content of 67.8% sand, 25.8% silt and 6.4% clay. The soil can be classified as orthic acrisol, which is derived from sandstone and phyllite and has an approximate depth of 50 cm. The stone content is high (>35%), and the field capacity ranges between 10.89-12.78%. The permanent wilting point is between 5.77-6.45%. Five-year-old longan trees were planted in a 6×6 m pattern. The canopies had an average diameter of 3 m. Prior to the experiment, all the trees were irrigated in order to obtain a uniform soil water potential (SWP) of −200 mbar. The experiment started on March 5, 2010 during the dry season with a clear sky and was stopped on March 19 as some clouds appeared followed by rain. During the period of the experiment the longan trees flowered. In total, 20 trees divided into two groups were arranged in four rows, alternating between the treated and control trees within each row. Irrigation was completely stopped for 10 trees in the F_{dry} group while 10 trees in the control group (F_{irri}) were irrigated once per week with 22 mm of water.

Monitoring of Soil Water Content and Drought Stress Responses

Volumetric water content was determined by time-domain reflectometry using a Tektronix 1502B cable tester (Tektronix, USA) and a self-built probe everyday for each pot and every three days at three depths for one tree per treatment in the field experiment. The SWP was determined through the use of a tensiometer set (Rain Drop, Thailand) at 30-cm soil depth for each treatment. Pre-dawn LWP was determined by use of a Scholander-type pressure chamber (PMS Instrument, USA). Measurements took place everyday for the pot experiment on three randomly picked leaves from each tree, and every third day for the field experiment on ten leaves per treatment. Each time a thermal image was taken, the respective stomatal resistance (r_s) to water vapour of three randomly selected leaves was determined within 10 min. using an SC-1 diffusion porometer (Decagon Devices, USA). For all the experiments, temperature (T), relative humidity (RH), wind speed (u) and air pressure (p) were monitored by a portable weather station (PCE-FWS 20, PCE Group, Germany), which was installed at the experimental site. In addition, the solar radiation data were made available from an IrriWise™ irrigation control unit (Netafim, Israel) set at a 500-m distance from the experimental plots. The VPD was calculated as the difference between the saturated vapour pressure at temperature T ($e^0(T)$) and the actual vapour pressure (e_a), where $e^0(T) = 0.6108 \ln (17.27T/T+237.3)$ and $e_a = e^0(T)*(RH/100)$ [32].

Thermal Images

Image acquisition

For the pot experiment, thermal images of each tree were taken at noon by a thermo-camera (VarioCAM, InfraTec, Germany) and two adjacent trees were captured per image. One leaf on each tree was covered with petroleum jelly to serve as a dry reference. The ceramic head of a tensiometer was filled with water to serve as wet reference. This artificial reference surface (ARS), set up as described by Zia et al. [25], was hung between each pair of trees. For the field experiment, images were taken everyday at 2 p.m. using a thermo-camera (InfraCAM SD, FLIR Systems Inc., Sweden) set at a distance of 5 m from both the sunlit side and the shaded side. Once per week, images were taken every hour throughout the day. One leaf from each tree was sprayed with water 10 sec. prior to thermal image acquisition to serve as a wet reference, and another leaf was covered with petroleum jelly to serve as a dry reference. After every thermal image, a digital photo of the same set-up was taken with a digital camera (Cybershot, Canon, Japan).

Data processing

The images obtained for the pot experiment were evaluated using IRBIS 2.2 software. A polygon was fitted around the canopy of the respective trees and the canopy temperature (T_c) determined as an average value for the polygon. In addition, a rectangle was placed around both the ARS and the coated leaf in such a way that the minimum and maximum temperatures within the rectangle represented the wet (T_w) and dry (T_d) reference temperatures respectively. Images taken from the field experiment were evaluated using ThermaCAM Researcher Professional version 2.1 software. Photographs taken of the sunlit and shaded sides were analysed separately by fitting a polygon around the canopy in order to determine T_c. A rectangle was fitted around the sprayed and the coated leaves; T_w and T_d were represented by the minimum and maximum temperatures of the rectangle respectively. For both the sunlit sides and the shaded sides, the CWSI was determined according to Idso et al. [14] as: CWSI = $(T_c-T_w)/(T_d-T_w)$. Higher values of CWSI represent higher stress. The theoretical maximum of CWSI is 1.0 if $T_c = T_d$, which indicates complete stomatal closure. Differences between treatments were analysed for significance by one-way ANOVA using Origin 5.1 computer code (Microcal Software, USA). The significance of correlation between two factors was tested using SPSS software version 11.5 (SPSS, USA).

RESULTS

Pot Experiment

After stopping irrigation for the S_{dry} group, the substrate (growing medium) moisture content decreased quickly within the first four days (Figure 1A) and this resulted in a subsequent significant decrease in LWP. Beginning on the fifth day of the experiment, water stress became severe and the LWP doubled in plants under non-irrigated treatment (Figure 1B). From the fourth day onward, stomatal resistance significantly increased as compared to the control (Figure 1C). From the second day, the CWSI value was lower in the S_{irri} than the S_{dry} treatment, but this difference became statistically significant only when drought stress was severe (Figure 1D). Throughout the experiment the CWSI averaged below 0.8 for S_{irri} and above 0.8 for S_{dry}. A positive correlation was found between CWSI and stomatal resistance with a coefficient of determination (R^2) of 0.55, while a high negative correlation was found between CWSI and pre-dawn leaf water potential ($R^2 = 0.62$). Furthermore, a high correlation found between CWSI and substrate moisture ($R^2 = 0.55$) indicates that drought stress was the driving factor that increased CWSI in the trees subjected to stress treatment (Figure 2).

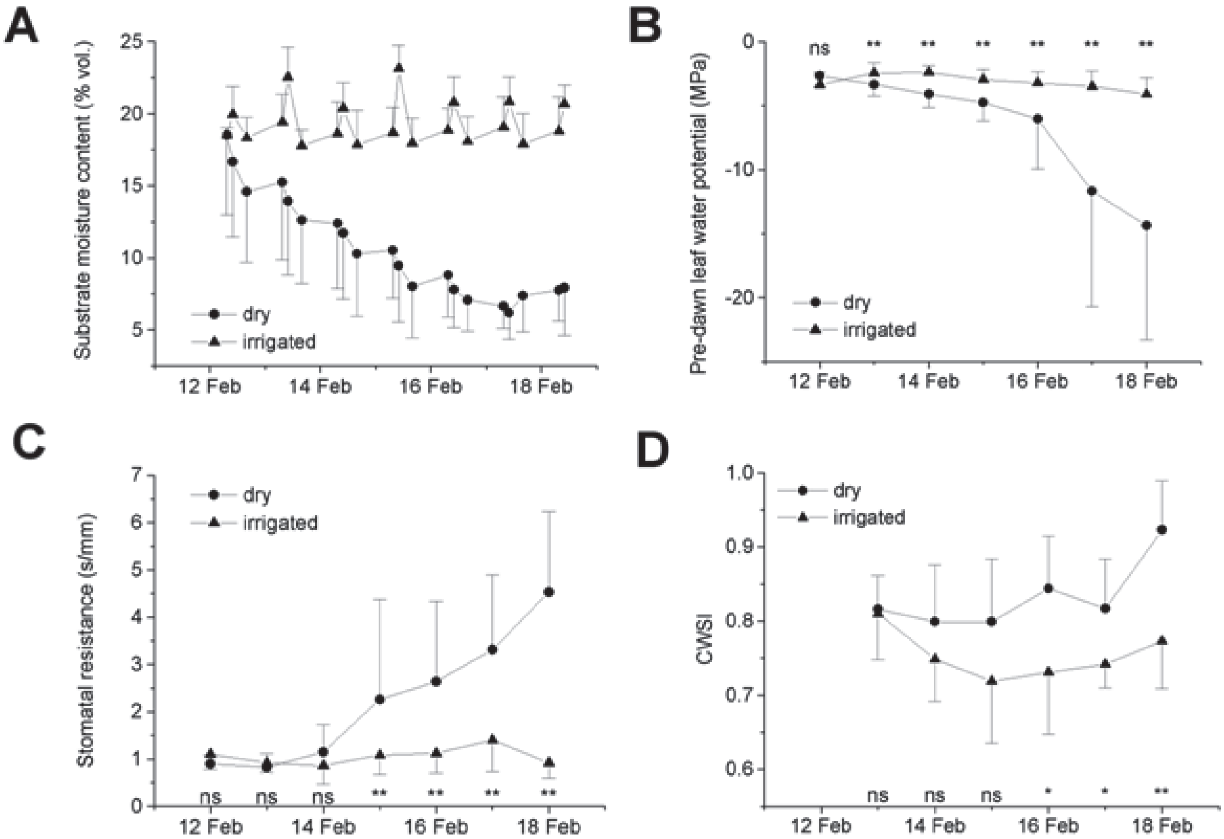

Figure 1. A: Volumetric moisture content of the substrate in pots containing irrigated and non-irrigated longan trees. **B:** Pre-dawn leaf water potential of irrigated and non-irrigated potted longan trees. Data points are the average of 12 leaves. **C:** Stomatal resistance of irrigated and non-irrigated potted longan trees. Data points are the average of 20 leaves. **D:** Crop water stress index (CWSI) for irrigated and non-irrigated potted longan trees. Data points are the average of four trees. Error bars represent ± SD. Data points marked with * and ** differ significantly from the control at α = 0.05 and 0.01 resprectively. Non-significant differences are marked with 'ns'.

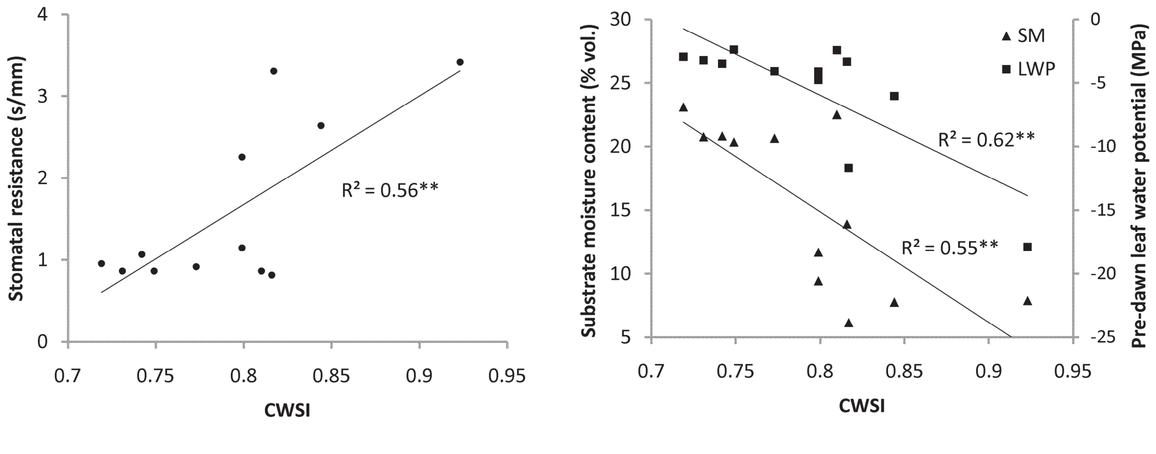

Figure 2. Correlation between crop water stress index (CWSI) and stomatal resistance (left) and between CWSI and pre-dawn leaf water potential (LWP) and substrate moisture (SM) (right) in potted longan trees. Correlations marked with ** are significant at α = 0.01.

Field Experiment

The overall amount of water available in the soil was very low due to a high stone content, but the trend for the irrigated trees (F_{irri}) was clearly different from that of the non-irrigated trees (F_{dry}). Three days after the start of the experiment, the soil in the F_{dry} treatment had dried out, and at the end of each period between one irrigation and the other, a decreased SWP was observed in the control group, although the values were in a range where no water stress would be expected. Meanwhile, the soil in F_{dry} group dried out quickly, reaching SWP values below −800 mbar; tensiometer readings were obtained by refilling the tensiometer daily. This method underestimates the real SWP. Therefore, SWP values are estimated based on water retention curve and volumetric soil moisture values obtained by the time-domain reflectometry readings (Figure 3).

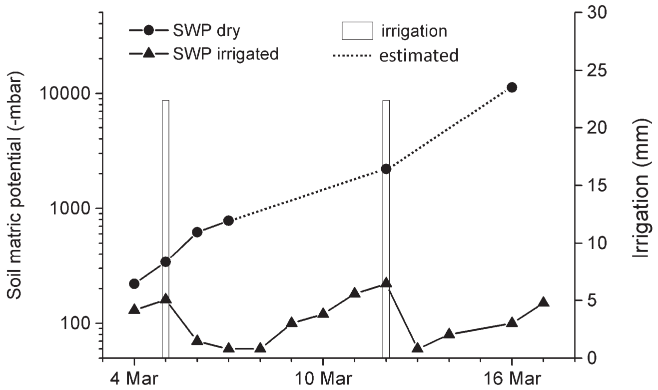

Figure 3. Soil water potential (SWP) and irrigation water application during the field experiment. The dotted line represents estimated values for SWP_{dry} below the measurement range of the tensiometer, based on soil moisture determination.

LWP measurements show stress responses of the non-irrigated trees; after only a few days of the experiment, differences between the treated and control trees become apparent (Figure 4A). A strong correlation between SWP and pre-dawn LWP (data not shown) is inherent in the nature of the measurement as before the start of transpiration there is an equilibrium between both potentials. The monitoring of r_s indicates increased resistance values in the F_{dry} treatment immediately after the start of the experiment with significant differences appearing after one week compared with control trees (Figure 4B).

An analysis shows differences in CWSI between the shaded and sunlit sides of the canopy. Due to a higher temperature on the reference surface, CWSI on the sunlit side was lower than on the shaded side even though the absolute canopy temperature was high because of the influence of radiation. One week after the start of the experiment, the average canopy temperature on the sunlit side of the F_{dry} group was higher than that of the control group, although differences in CWSI were not significant (Figure 4C). At the same time, based on thermal images of the shaded side, the CWSI was significantly higher in F_{dry} treatment as compared to control. While CWSI of the control averaged below 0.7, that of the trees under stress treatment was above 0.7 on average (Figure 4D). A low positive correlation between CWSI and r_s is found on the shaded side ($R^2 = 0.34$) while there is no correlation between the CWSI and r_s on the sunlit side ($R^2 = 0.09$) (Figure 5). By analogy, CWSI and SWP are correlated ($R^2 = 0.39$) on the shaded side, but not on the sunlit side ($R^2 = 0.29$) (Figure 6)

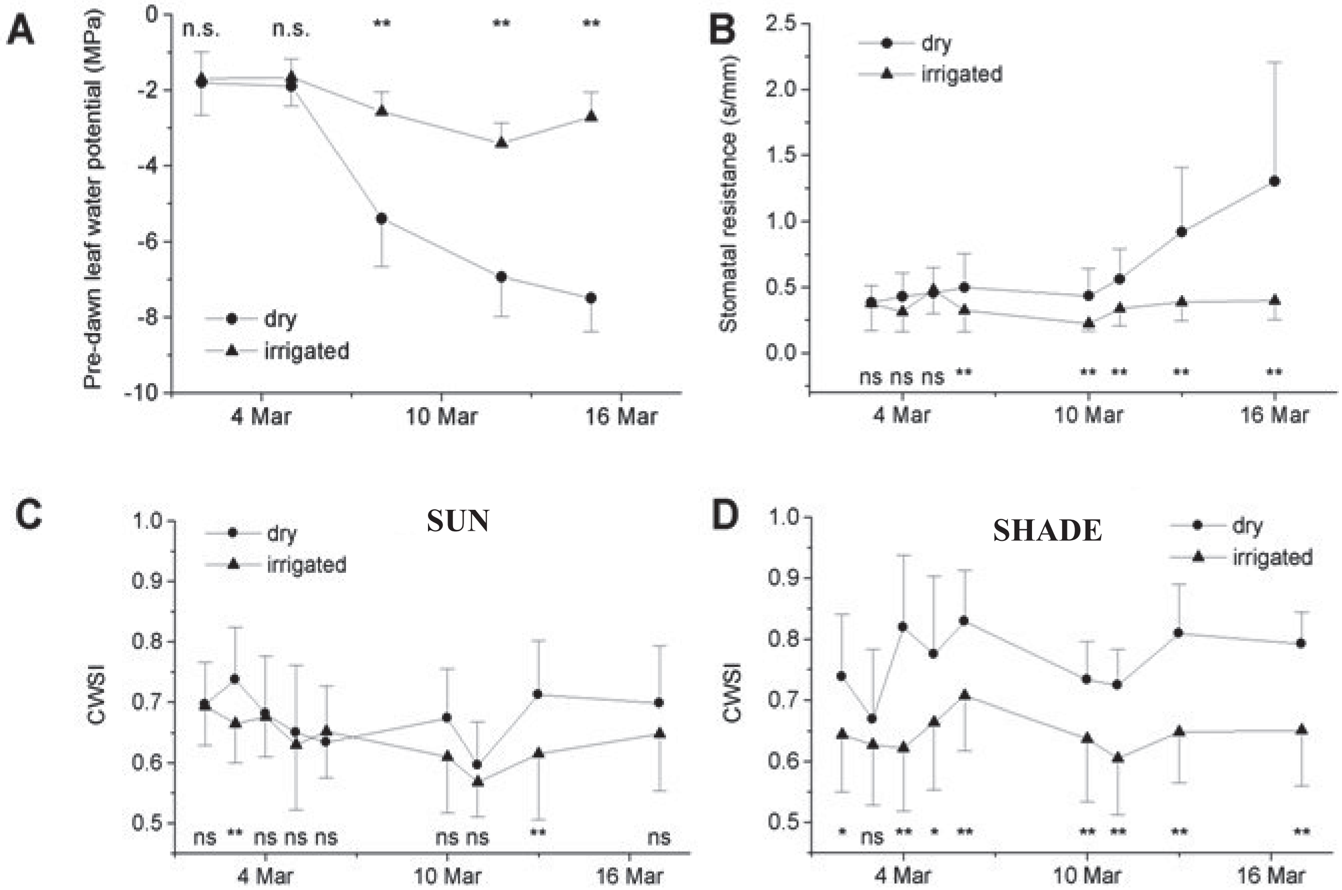

Figure 4. A: Pre-dawn leaf water potential (LWP) of irrigated and non-irrigated field-grown longan trees. Data points are the average of 10 leaves. **B:** Stomatal resistance of irrigated and non-irrigated field-grown longan trees. Data points are the average of 20 leaves. **C, D:** CWSI determined from sunlit and shaded sides of the canopy respectively. Data points are the average of 10 trees. Error bars represent ± SD. Data points marked with * and ** differ significantly from the control at $\alpha = 0.05$ and $\alpha = 0.01$ respectively. Non-significant differences are marked with 'ns'.

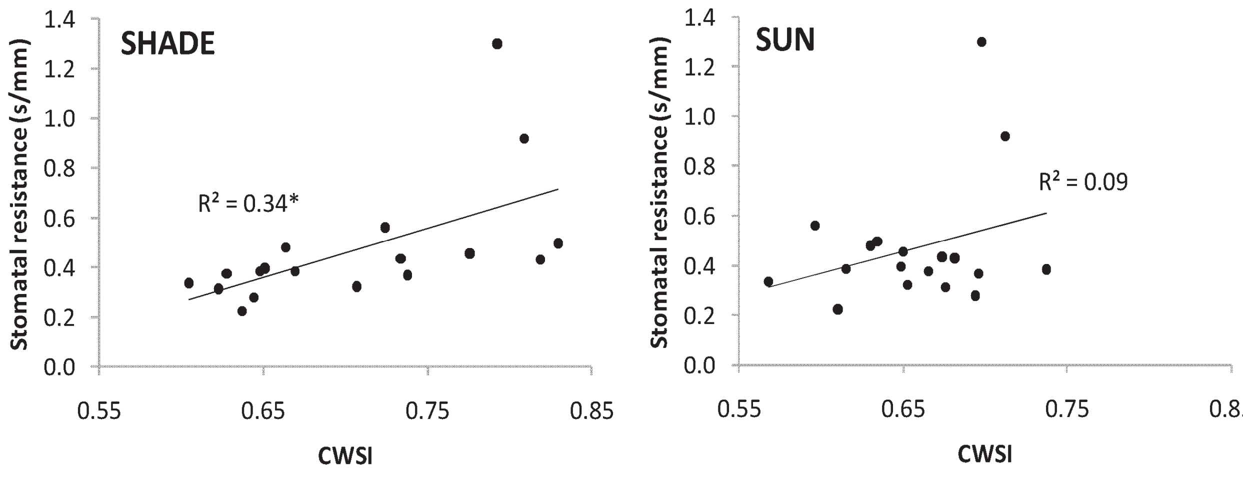

Figure 5. Correlation between stomatal resistance and CWSI in the shade (left) and on the sunlit side of the canopy (right). Correlation marked with * is significant at $\alpha = 0.05$.

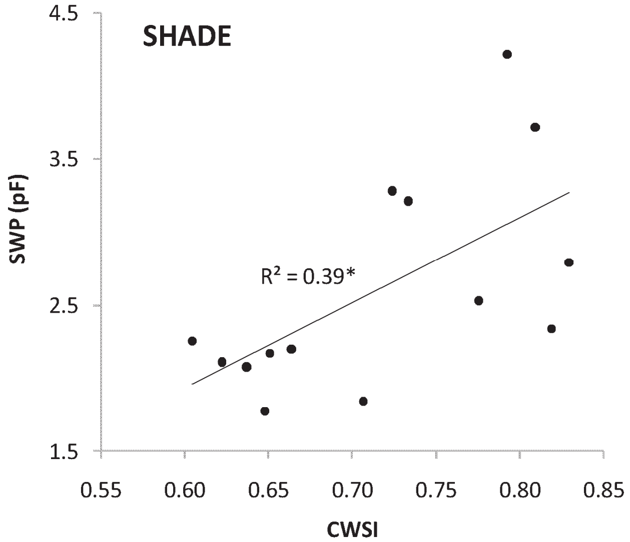

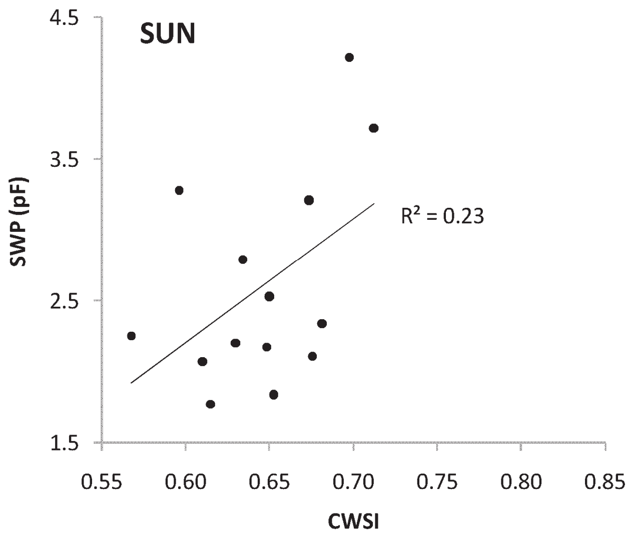

Figure 6. Correlation between soil water potential (SWP) and CWSI in the shade (left) and on the sunlit side of the canopy (right). Correlation marked with * is significant at $\alpha = 0.05$.

Figures 7A and 7B show the development of stomatal resistance during the course of a day. A typical pattern of rather low resistance in the morning together with a low VPD followed by a peak in the afternoon was observed for trees undergoing stress treatment. The stomatal resistance of control trees was lower in general and with a less pronounced increase during the day.

Differences in stomatal aperture during the morning hours were small and minor differences were observed in the CWSI before noon. However, between noon and 3 p.m., differences in CWSI were at their highest. In the shaded part of the canopy, differences between the stressed and non-stressed trees were more pronounced than in the sunlit area. Between 4 p.m. and sunset, differences in CWSI decreased as the effect of evaporative cooling in the non-stressed leaves decreased and canopy temperature converged to the dry reference temperature in both treatments (Figures 7 C-F).

DISCUSSION

The soil water potential (SWP) is the most important variable for estimating the plant water status under prevailing conditions. It is commonly measured in millibars (mbar) or pF (log mbar) and indicates how strongly the water is bound to the soil. If SWP is at approximately -100 mbar (pF 2.0), the soil has reached field capacity and the plants are well supplied with water. The start of water stress is crop dependent; while stress in vegetables may start at SWP = -400 mbar (pF 2.6), most trees do not suffer from water stress above -700 mbar (pF 2.8). When the permanent wilting point is reached at approximately -15,000 mbar (pF 4.2), no plant growth is possible. The leaf water potential (LWP) indicates how strongly water is bound to the plant tissue. Before the start of photosynthesis SWP and LWP should be in equilibrium; that is why the pre-dawn LWP is a good indicator of plant stress. With the start of photosynthesis in the morning hours, stomata open and the size of the stomatal aperture is regulated by the plant. With a reduced stomatal aperture the conductance decreases and the stomatal resistance to water vapour (r_s) increases. As a consequence, gas exchange is reduced. The determination of r_s as inverse value of stomatal conductance is an indicator of plant stress. The amount of transpiration is further influenced by the vapour pressure deficit (VPD), which is a measure of the evaporative demand of the air under prevailing air temperature and relative humidity.

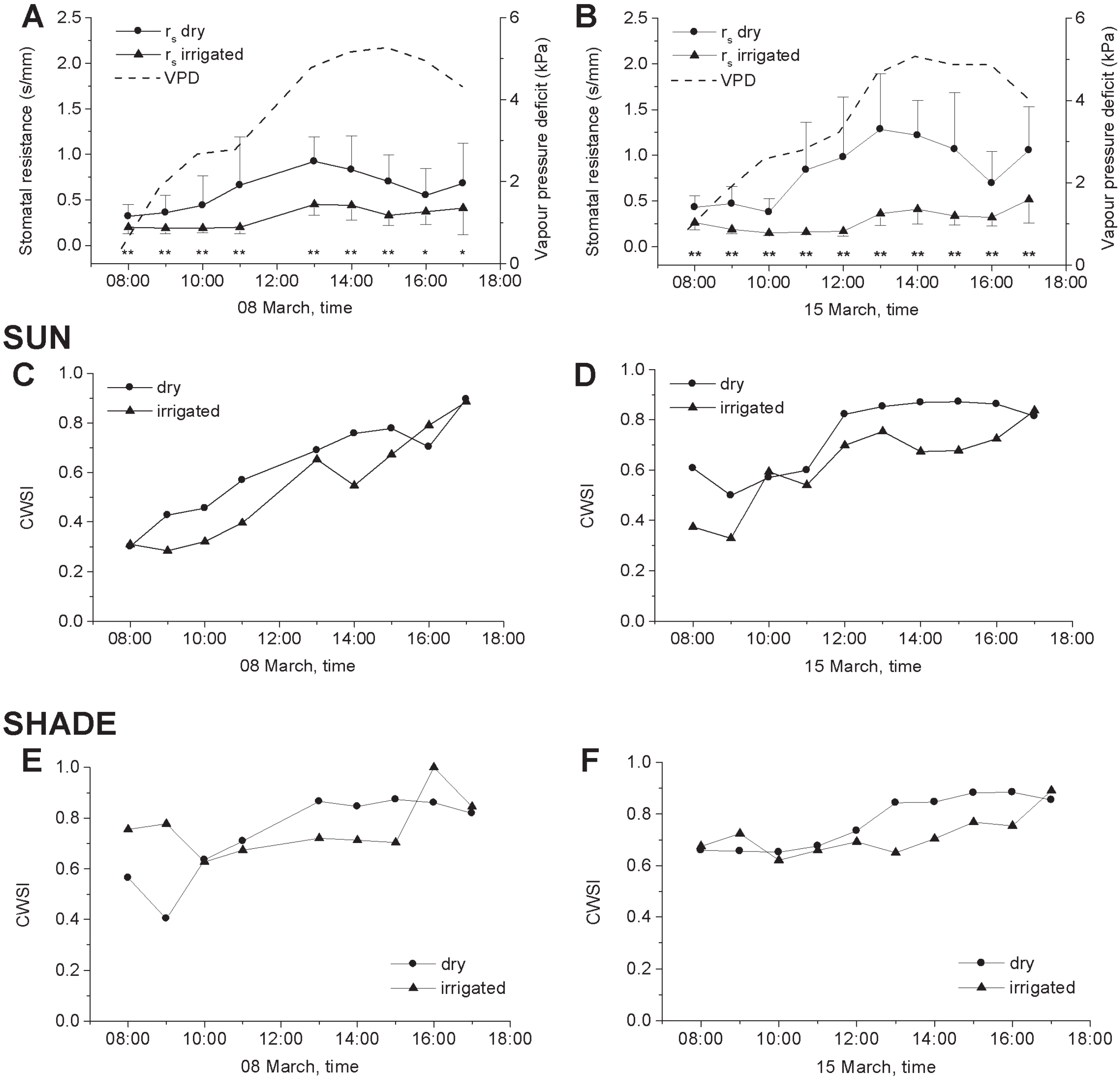

Figure 7. A, B: Vapour pressure deficit (VPD) and stomatal resistance of irrigated and non-irrigated field-grown longan trees 7 days (left) and 14 days (right) after the start of treatment. **C, D:** CWSI in the sun after 7 and 14 days. **E, F:** CWSI in the shade after 7 and 14 days. Data points of stomatal resistance are the average of 5 leaves; error bars represent ± SD. Data points marked with * and ** differ significantly from the control at $\alpha = 0.05$ and $\alpha = 0.01$ respectively. Data points of CWSI represent one analysed picture.

In this study the determination of pre-dawn LWP is shown to be the most reliable method for early detection of water stress since under controlled conditions both in pots and in the field, the LWP decreases quickly as drought is imposed on the longan trees. There is a good correlation between pre-dawn LWP and CWSI under controlled condition, similar to an earlier report in which the CWSI was correlated with the midday LWP [21]. Pre-dawn LWP is closely correlated with SWP, so the differences between well-watered and drought-stressed plants can be visible at a very early stage. Similar to soil moisture, LWP is an indirect stress variable, one which is not necessarily expressed through the plant's reaction such as stomatal closure or decrease in photosynthesis. From the values of r_s, stomatal closure seems to start later and show a greater variation, which indicates that plants, especially field-grown longan trees which differ considerably in size and root development, react differently to the same environmental conditions.

The r_s produces reliable data on plant water stress reactions, and the increase in r_s observed after two weeks under field conditions suggests that once-per-week irrigation is adequate to avoid plant drought stress, although a longer interval may be applied if water availability or water conveyance infrastructure is limited. Direct application of r_s monitoring for irrigation is, however, hampered by spatial and temporal variability in the field as it requires a large number of observations within a narrow time slot. As in previous studies [16, 17, 33], thermal imaging is successfully correlated with r_s (Figures 5 and 7**)**.

Even though the correlation coefficients (R^2) found in this study are lower than those previously reported by Jones [16], the overall trend shows CWSI to be a reliable water-stress indicator. Under controlled conditions as in the field, there is a higher correlation between CWSI and the classic stress parameters. Small trees generally show less variability in terms of stomatal closure. Pot experiments offer a better view with fewer discontinuities in the determination of the average temperature by thermal imaging, while in the field apart from weather conditions, the canopy architecture, namely leaf angle, can influence the measurements. This is also an observation which has been reported earlier [24]. It has been found that a combined thermal and visible imaging can improve the accuracy of remote drought stress detection [25, 34]. Where this is not possible, for example when using a simple thermal camera without simultaneous digital image acquisition, it has been shown that averaging temperatures over several leaves per canopy, as performed in this study, can compensate for differences in leaf angle [24].

However, if the canopy temperature is determined as mere average, thermal images must be taken on the shaded side of the canopy. If images are taken on the sunlit side, it is not possible to establish a meaningful correlation between CWSI and r_s. This observation is supported by Fuchs [35], who found greater differences in leaf temperature between stressed and unstressed plants in the shade than on the sunlit part of the canopy; and by Jones et al. [17], who suggested that CWSI is less varied in a shaded canopy compared with a sunlit one. With advanced image analysis, it is possible to discriminate between the shaded and sunlit parts of a row crop such as vine [36]. However, the influence of radiation on a heterogeneous canopy of the longan tree is greater than on the canopy of a row of grapevines. Apart from the increased complexity of the apparent temperature composition due to canopy architecture, there is also a greater variability of stomatal aperture under the influence of direct radiation. Thus, the monitoring of the sunlit side of the canopy is not directly applicable to longan trees.

The choice of reference surface influences the order of magnitude of the CWSI, and so if values are to be communicated, the kind of reference surface used has to be taken into account. In this study, as in most previous studies, petroleum-jelly-coated leaves were used throughout the measurements. This method is convenient as coated leaves remain on the plant and do not require preparation for each measurement, and since they are in continuous thermal exchange with the surrounding environment, they give a reliable value of the temperature of non-transpiring leaves. Water-sprayed leaves, as a lower reference, involve a more time-consuming process as water has to be sprayed prior to acquisition of each thermal image. This method also requires that an exact timing and precise working procedure be used. The time between the spraying of the wet reference leaf and the taking of the image must be standardised; all plants and references must be subjected to a similar radiation environment and the imager must be allowed to equilibrate before each measurement [37]. Thus, in this study the porous cup of a tensiometer was additionally used as an artificial reference surface (ARS) in order to represent the lower reference temperature. Porous tensiometer cups were used as ARS in an earlier study [25] while ARS in another study consisted of a textile material soaked in water [22]. It may also be possible to use an evaposensor for both the wet and dry references as introduced in an earlier study on irrigation scheduling [38].

In the present study, by using both types of references, water stress monitoring is possible. Based on the results, we consider the CWSI of 0.7 as an appropriate threshold for detecting the occurrence of water stress when using a sprayed leaf as wet reference. This value would be higher if an ARS had been used. Since an ARS had not been applied in the field, a threshold value of 0.7 for CWSI should be communicated for field-grown longan trees.

In general, under the influence of a high VPD (high air temperature and low relative humidity), the stomata close to prevent the tree from experiencing excessive water loss. From CWSI measurements taken during the course of day, it can be inferred that the best time to determine the CWSI is between noon and early afternoon. Coinciding with the highest level of VPD, stressed longan trees have already closed a greater part of their stomata at this time while unstressed trees still show high levels of stomatal conductance. During the daily maximum of radiation and air temperature, stressed leaves heat up to a greater extent than unstressed leaves, but from about 4 p.m. onwards, even the unstressed leaves start to close their stomata, and as a result the CWSI no longer differs between stressed and unstressed leaves.

CONCLUSIONS

Thermal imaging can be used for drought stress detection in longan trees based on image processing and by averaging a randomly selected part of the canopy. Differences between stressed and unstressed longan trees can be detected before the appearance of visible signs such as changes in leaf angle and leaf rolling. In contrast to other stress-monitoring methods, no destructive or invasive measurements are undertaken, which paves the way to remote sensing, although this technique has not yet been considered as a part of this study. It was found that measurements necessary to calculate CWSI should ideally be taken during the early afternoon in the absence of wind and clouds, and preferably on the shaded side of the tree. Under these conditions, it is possible to distinguish between drought-stressed and well-watered trees on the same plot. However, for a reliable stress determination, temperature measurements by thermal imaging should be conducted over several days as the CWSI may change due to heterogeneous climatic conditions. This problem was also encountered when determining stomatal conductance. The use of thermal imaging for stress detection in practice requires robust references–those which can be correlated with the occurrence or even the intensity of stress. Based on a proposed CWSI threshold value of 0.7 for field-grown longan trees, thermal imaging can be used for irrigation scheduling, although more research is needed on the level of irrigation intensity to be used before a practical application is possible.

ACKNOWLEDGEMENTS

This work was financed by Deutsche Forschungsgemeinschaft (DFG) within the collaborative research programme on "Sustainable land use and rural development in mountainous regions of South-east Asia" (SFB 564), and co-financed by the National Research Council of Thailand (NRCT). Special thanks are due to Asst. Prof. Dr. Nopporn Boonplod of Maejo University for facilitation of research space, and to Gary Morrison and Dr. Christopher Salisbury for English language proofreading.

REFERENCES

1. C. M. Menzel and D. R. Simpson, "Lychee cultivars around the world", in "Australian Lychee Yearbook" (Ed. M. B. Smith), Australian Lychee Growers Association, Queensland, Australia, **1991**, pp.30-34.
2. P. Manochai, P. Sruamsiri, W. Wiriya-alongkorn, D. Naphrom, M. Hegele and F. Bangerth, "Year around off season flower induction in longan (*Dimocarpus longan*, Lour.) trees by $KClO_3$ applications: Potentials and problems", *Sci. Hortic.*, **2005**, *104*, 379-390.
3. C. Menzel and G. K. Waite, "Litchi and Longan: Botany, Production and Uses", CABI Publishing, Wallingford (UK), **2005**.
4. Y. Diczbalis, B. Nicholls, I. Groves and K. Lake, "Sapindaceae production and research in Australia", *Acta Hortic.*, **2010**, *863*, 49-58.
5. Y. Diczbalis, "Longan: Improving Yield and Quality", Rural Industries Research and Development Corporation (Australia), Barton ACT, **2002**, p.22.
6. K. Spohrer, C. Jantschke, L. Herrmann, M. Engelhardt, S. Pinmanee and K. Stahr, "Lychee tree parameters for water balance modeling", *Plant Soil*, **2006**, *284*, 59-72.
7. S. Ongprasert, W. Spreer, W. Wiriya-Alongkorn, S. Ussahatanonta and K. Köller, "Alternative techniques for water-saving irrigation and optimised fertigation in fruit production in Northern Thailand", in "Sustainable Land Use in Mountainous Regions of Southeast Asia: Meeting the Challenges of Ecological, Socio-Economic and Cultural Diversity" (Ed. F. J. Heidhues, L. Herrmann, A. Neef, S. Niedhart, J. Pape, P. Sruamsiri, D. C. Thu and A. Vallé Zarate), Springer, Berlin, **2007**, pp.120-133.
8. K. Satienperakul, W. Spreer, W. Wiriya-Alongkorn, S. Ongprasert and J. Müller, "Economic assessment of water saving irrigation methods in longan production in Northern Thailand", Proceedings of Tropentag, Conference on International Research for Development, **2006**, Bonn, Germany, pp.1-8.
9. S. Ongprasert and W. Wiriya-Alongkorn, "Yield and vegetative growth of longan subjected to partial root-zone drying irrigation", *J. Agric. Res. Extension*, **2009**, *26*, 8-17.
10. U. Srikasetsarakul, W. Spreer, S. Ongprasert, W. Wiriya-Alongkorn, K. Sringarm, P. Sruamsiri and J. Müller, "Biomass formation and nutrient partitioning in potted longan trees under partial rootzone drying", *Acta Hortic.*, **2011**, *889*, 587-592.
11. G. Egea, P. A. Nortes, M. M. González-Real, A. Baille and R. Domingo, "Agronomic response and water productivity of almond trees under contrasted deficit irrigation regimes", *Agric. Water Manage.*, **2010**, *97*, 171-181.

12. J. M. Abrisqueta, O. Mounzer, S. Alvarez, W. Conejero, Y. Garcia-Orellana, L. M. Tapia, J. Vera, I. Abrisqueta and M. C. Ruiz-Sánchez, "Root dynamics of peach trees submitted to partial rootzone drying and continuous deficit irrigation", *Agric. Water Manage.*, **2008**, *95*, 959-967.
13. W. Spreer, S. Ongprasert, M. Hegele, J. N. Wünsche and J. Müller, "Yield and fruit development in mango (*Mangifera indica* L. cv. Chok Anan) under different irrigation regimes", *Agric. Water Manage.*, **2009**, *96*, 574-584.
14. S. B. Idso, R. D. Jackson, P. J. Pinter, R. J. Reginato and J. L. Hatfield, "Normalizing the stress-degree-day parameter for environmental variability", *Agric. Meteorol.*, **1981**, *24*, 45-55.
15. G. Yuan, Y. Luo, X. Sun and D. Tang, "Evaluation of a crop water stress index for detecting water stress in winter wheat in the North China Plain", *Agric. Water Manage.*, **2004**, *64*, 29-40.
16. H. G. Jones, "Use of infrared thermometry for estimation of stomatal conductance as a possible aid to irrigation scheduling", *Agric. Forest Meteorol.*, **1999**, *95*, 139-149.
17. H. G. Jones, M. Stoll, T. Santos, C. de Sousa, M. M. Chaves and O. M. Grant, "Use of infrared thermography for monitoring stomatal closure in the field: Application to grapevine" *J. Exp. Bot.*, **2002**, *53*, 2249-2260.
18. S. Merlot, A. C. Mustilli, B. Genty, H. North, V. Lefebvre, B. Sotta, A. Vavasseur and J. Giraudat, "Use of infrared thermal imaging to isolate Arabidopsis mutants defective in stomatal regulation", *Plant J.*, **2002**, *30*, 601-609.
19. H. G. Jones, R. Serraj, B. R. Loveys, L. Xiong, A. Wheaton and A. H. Price, "Thermal infrared imaging of crop canopies for the remote diagnosis and quantification of plant responses to water stress in the field", *Func. Plant Biol.*, **2009**, *36*, 978-989.
20. O. M. Grant, M. J. Davies, H. Longbottom, R. Harrison-Murray and A. Herrero, "Application of deficit irrigation to controlling growth of hardy nursery stock", *Acta Hortic.*, **2011**, *889*, 409-416.
21. Y. Cohen, V. Alchanatis, M. Meron, Y. Saraga and J. Tsipris, "Estimation of leaf water potential by thermal imagery and spatial analysis", *J. Exp. Bot.*, **2005**, *56*, 1843-1852.
22. V. Alchanatis, Y. Cohen, S. Cohen, M. Moller, M. Sprinstin, M. Meron, J. Tsipris, Y. Saraga and E. Sela, "Evaluation of different approaches for estimating and mapping crop water status in cotton with themal imaging", *Precis. Agric.*, **2010**, *11*, 27-41.
23. J. A. J. Berni, P. J. Zarco-Tejada, G. Supulcre-Cantó, E. Fereres and F. Villalobos, "Mapping canopy conductance and CWSI in olive orchards using high resolution thermal remote sensing imagery", *Remote Sens. Environ.*, **2009**, *113*, 2380-2388.
24. O. M. Grant, L. Tronina, H. G. Jones and M. M. Chaves, "Exploring thermal imaging variables for the detection of stress responses in grapevine under different irrigation regimes", *J. Exp. Bot.*, **2007**, *58*, 815-825.
25. S. Zia, K. Spohrer, N. Merkt, D. Wenyong, H. Xiongkui and J. Müller, "Non-invasive water status detection in grapevine (*Vitis vinifera* L.) by thermography", *Int. J. Agric. Biol. Eng.*, **2009**, *2*, 46-54.
26. N. K. Gontia and K. N. Tiwari, "Development of crop water stress index of wheat crop for scheduling irrigation using infrared thermometry", *Agric. Water Manage.*, **2008**, *95*, 1144-1152.
27. S. Zia, D. Wenyong, W. Spreer, K. Spohrer, H. Xiongkui and J. Müller, "Assessing crop water stress of winter wheat by thermography under different irrigation regimes in North China Plain", *Int. J. Agric. Biol. Eng.*, **2012**, *5*, 24-34.

28. G. Romano, S. Zia, W. Spreer, C. Sanchez, J. Cairns, J. L. Araus and J. Müller, "Use of thermography for high throughput phenotyping of tropical maize adaptation in water stress", *Comput. Electron. Agric.*, **2011**, *79*, 67-74.
29. R. Giuliani, E. Magnanini and J. A. Flore, "Potential use of infrared thermometry for the detection of water deficit in apple and peach orchards", *Acta Hortic.*, **2001**, *557*, 399-405.
30. G. Sepulcre-Cantó, P. J. Zarco-Tejada, J. C. Jiménez-Munoz, J. A. Sobrino, E. de Miguel and F. J. Villalobos, "Detection of water stress in an olive orchard with thermal remote sensing imagery", *Agric. Forest Meteorol.*, **2006**, *136*, 31-44.
31. D. R. Hoagland and D. I. Arnon, "The Water-Culture Method for Growing Plants without Soil", University of California Agricultural Experiment Station, Berkeley (CA), **1950**.
32. D. Raes, "The ET_0 Calculator, Reference Manual Version 3.1", Food and Agricultural Organization of the United Nations (FAO), Rome, **2009**.
33. I. Leinonen, O. M. Grant, C. P. P. Tagliavia, M. M. Chaves and H. G. Jones, "Estimating stomatal conductance with thermal imagery", *Plant Cell Environ.*, **2006**, *29*, 1508-1518.
34. M. Möller, V. Alchanatis, Y. Cohen, M. Meron, J. Tsipris, A. Naor, V. Ostrovsky, M. Sprinstin and S. Cohen, "Use of thermal and visible imagery for estimating crop water status of irrigated grapevine", *J. Exp. Bot.*, **2007**, *58*, 827-838.
35 M. Fuchs, "Infrared measurement of canopy temperature and detection of plant water stress" *Theor. Appl. Climatol.*, **1990**, *42*, 253-261.
36. I. Leinonen and H. G. Jones, "Combining thermal and visible imagery for estimating canopy temperature and identifying plant stress", *J. Exp. Bot.*, **2004**, *55*, 1423-1431.
37. O. M. Grant, M. M. Chaves and H. G. Jones, "Optimizing thermal imaging as a technique for detecting stomatal closure induced by drought stress under greenhouse conditions", *Physiol. Plant.*, **2006**, *127*, 507-518.
38. O. M. Grant, M. J. Davies, H. Longbottom and C. J. Atkinson, "Irrigation scheduling and irrigation systems: Optimising irrigation efficiency for container ornamental shrubs", *Irrig. Sci.*, **2009**, *27*, 139-153.